An investigation into the roles of p53, Nodal/ Activin and fibroblast growth factor signalling in early heart development

Sarah K Black

Cardiff University

PhD, 2016

Summary

The work presented in this thesis is an investigation into the roles of p53, Nodal/ Activin and fibroblast growth factor (FGF) signalling in early heart development in the model organism *Xenopus laevis*. The first step of heart development is the specification of cardiac tissue. However, the timing of cardiac specification and the signals which control it are largely unknown. The Nodal/ Activin and FGF signalling pathways have been implicated in cardiac specification but there is little evidence demonstrating a direct role for these pathways. Using soluble molecular inhibitors of the Nodal/ Activin and FGF signalling pathways at different stages of development, the effects of time-controlled inhibition on cardiac progenitor cells and differentiated cardiac tissue were observed. Nodal/ Activin signalling was found to be required for cardiac specification during a 2-3 hour time window following midblastula transition. It was shown that FGF signalling is not required prior to gastrulation for cardiac specification, but is required later for normal heart development. It was hypothesised that p53 may be involved in cardiac specification by mediating crosstalk between the Nodal/ Activin and FGF signalling pathways, in a similar manner to its previously suggested role in mesoderm induction. Using a combination of p53 antisense morpholino oligonucleotides and a dominant negative p53 protein, the effects of p53 downregulation on cardiac progenitor cells and differentiated cardiac tissue were examined. A novel role for p53 in early heart development was found. These findings contribute to an understanding of how p53, Nodal/ Activin and FGF signalling orchestrate numerous developmental events in the early embryo. This knowledge will be useful to advance our understanding of congenital heart diseases and for the development of improved directed differentiation protocols for cardiac regenerative medicine.

Declaration statement

This thesis is being submitted for the qualification of PhD. The contents are the result of my own independent work and investigations, except where otherwise stated or referenced, and the views expressed are my own. This work has not, and is not, being submitted to this University or any other University for any other degree or qualification. I give consent for my thesis to be available online in the University's Open Access repository, and for the title and summary to be made available to outside organisations, after expiry of a bar on access previously approved by the Academic Standards & Quality Committee.

Signed ……..... Date ……..

Acknowledgements

First and foremost I would like to thank my supervisor, Dr Branko Latinkic, for taking me on as his PhD student and for his guidance throughout. In addition I would like to thank my advisor, Professor Trevor Dale, whose advice has been much appreciated.

I am especially grateful to my fellow lab member and friend Simon Fellgett, who provided great company, excellent scientific discussions and always made time to give helpful guidance. In addition my fellow scientists and friends Janet Harwood and Helen Woodfield have provided much needed advice, proofreading and lunch breaks. The friendship and support of Simon, Helen and Janet has been invaluable during my PhD and I am very grateful for their company.

I would like to thank my family and friends for their support, but mostly for their eagerness to distract me with numerous weekend adventures.

A special thank you goes to my wonderful husband Paul, who has supplied constant love, support and encouragement.

Thanks also goes to the British Heart foundation for funding the project.

List of abbreviations

A83	A-83-01
AC	Animal cap
ALK	Activin receptor-like kinase
APB	Alkaline Phosphate Buffer
APS	Ammonium persulfate
ATP	Adenosine triphosphate
BiFC	Bimolecular fluorescence complementation
BSA	Bovine Serum Albumin
CA	Constitutively active
CA-GFP	Cardiac actin-green fluorescent protein
$Ca(NO_3)_2$	Calcium nitrate
CHD	Congenital heart diseases
CMFM	Calcium magnesium free medium
ddH_2O	Double distilled water
DEX	Dexamethasone
DMSO	Dimethyl sulfoxide
DN	dominant negative
E	*Mouse* embryonic day
EDTA	Ethylenediaminetetraacetic acid
ESC	Embryonic stem cells
FGF	Fibroblast Growth Factor
FGFR	Fibroblast Growth Factor Receptor
Fohx1	Forkhead Activin Signal Transducer
GDF	Growth differentiation factors
GR	Glucocorticoid receptor
gsc	*goosecoid*
HA	Human influenza hemagglutinin
HCG	Human Chorionic Gonadotropin
HH	Hamburger Hamilton (staging in chick)

H_2O_2	Hydrogen peroxide
Hpf	Hours post fertilisation
IC_{50}	Half maximal inhibitory concentration
IHC	Immunohistochemistry
iPSC	induced pluripotent stem cells
isl1	*ISL LIM homeobox 1*
IVF	*In vitro* fertilisation
KCl	Potassium chloride
KH_2PO_4	Potassium phosphate
LRP	Leukocyte common antigen-related phosphatase
MAPK	Mitogen-activated protein kinase
MEK	mitogen-or-extracellular-signal-regulated-protein-kinase
$MgCl_2$	Magnesium chloride
$MgSO_4$	Magnesium sulphate
MO	Antisense Morpholino Oligonucleotide
mpo	*myeloperoxidase*
mRNA	Messenger ribonucleic acid
myl7	*myosin light chain 7*
myh6	*myosin heavy chain 6*
NaCl	Sodium chloride
$NaHCO_3$	Sodium bicarbonate
Na_2HPO_4	Sodium phosphate
NAM	Normal Amphibian Medium
Na_3PO_4	Sodium phosphate
NCS	New-born calf serum
nkx2.5	NK2 homeobox 5
odc1	*ornithine decarboxylase 1*
PCR	Polymerase Chain Reaction
PD	PD0325901
p-ERK	Phosphorylated ERK
PLCγ	phospholipase-C gamma

p-p53	Phosphorylated p53
p-Smad2	Phosphorylated Smad2
PVDF	Polyvinylidene fluoride
RNA	ribonucleic acid
R-Smads	Receptor regulated Smads
RT	Room temperature
-RT	Without reverse transcription
SB	SB505124
SDS	Sodium dodecyl sulphate
Sef	Similar-expression-to-fgf-genes
sgRNA	Short guide RNA
STAT	Signal transducer and activator of transcription
SU	SU5402
SV40	Simian Vacuilating Virus 40
t	*brachyury*
Tal1	T-cell acute lymphocytic leukemia 1
TBSTw	Tris buffered saline with Tween
TEMED	Tetramethylethylenediamine
TF	Transcription factors
TGF-beta	Transforming Growth Factor Beta
tnni3	*cardiac troponin*
UTR	Untranslated region
VCS2	Venus C terminal –Smad2
VNS4	Venus N terminal –Smad4
WB	Western Blot
WE	Whole Embryo
WMISH	Whole mount *in situ* hybridisation

Table of Contents

1 Introduction

1.1 Overview

The heart is a vital organ for the health and survival of an organism. Defects in heart development, or diseases which cause damage to the mature heart, can be life changing and potentially fatal (Bruneau, 2008; Roger, 2013). The human heart has limited potential to repair itself, and is therefore a target of ongoing medical research to devise new therapies for cardiac repair (Xin et al., 2013). Understanding the signalling pathways which regulate heart development is fundamental to comprehend the causes of heart diseases, and to develop new therapies to treat damaged cardiac tissue through the use of regenerative medicine. Although many factors which influence cardiogenesis have been uncovered, the signals which initiate the very first stages of heart development, the specification of cells into the cardiac lineage, are largely unresolved. Previous research highlights the potential involvement of the Nodal/ Activin and fibroblast growth factor (FGF) signalling pathways in the specification of cardiac cells (Noseda et al., 2011). However, previous analysis does not clearly separate the roles of these signalling pathways from their broader functions in embryonic development, questioning the specificity of their involvement in cardiac lineage specification. In addition, the time at which the Nodal/ Activin and FGF signalling pathways may be required for cardiac specification is largely unknown. Experiments contained within this thesis demonstrate the manipulation of the Nodal/ Activin and FGF signalling pathways in a spatiotemporal manner, primarily using a pharmacological approach, complimented with protein expression control, to specifically question the requirement and timing of Nodal/ Activin and FGF signalling in cardiac specification. The Nodal/ Activin and FGF signalling pathways have previously been demonstrated to integrate, with pathway crosstalk mediated by the tumour suppressor protein p53 (Cordenonsi et al., 2007, 2003). New functions for p53 in embryonic development are continuously being discovered (Danilova et al., 2008; Molchadsky et al., 2010) and work presented in this thesis questions a novel role for p53 in cardiac development.

1.2 Embryonic development

During embryonic development, a fertilised egg cell divides and begins to proliferate. Initially, cells are pluripotent, meaning that they can give rise to any cell type. In mammalian organisms such as mouse or human, only cells of the inner cell mass are pluripotent, with the outer cells contributing towards extra-embryonic tissues (Bedzhov et al., 2014; Paranjpe and Veenstra, 2015). Proliferating pluripotent cells are influenced by signals within the embryo, in strictly defined time windows, which instruct the cells to develop into a particular type of cell. This process is known as specification. Specified cells are capable of changing lineage, if exposed to the appropriate influences, before terminal differentiation from a progenitor cell into a mature cell (Graf and Enver, 2009; Slack, 1991). Specified groups of cells, known as fields, undergo morphological movements, patterning, differentiation and morphogenesis events to form a complexity of interconnected organs which constitutes a functioning organism (Gilbert, 2000; Heasman, 2006). Remarkably, these processes are controlled by a relatively small number of signalling molecules which work in pathways to oversee embryonic development and regulate cellular homeostasis (Perrimon et al., 2012). The heart is an organ which develops from pluripotent cells in the early embryo. Specified cardiac cells receive numerous inductive and inhibitory signalling inputs throughout cardiogenesis to ultimately form a correctly located and fully functioning heart (Brand, 2003). A key question for developmental biology is how a relatively small number of regulatory signalling pathways modulate a diverse array of processes (Gilbert, 2000). An understanding of the mechanisms which govern cardiogenesis will likely be translatable, enabling a better understanding of numerous aspects of development, ageing, homeostasis and cancer. Furthermore, this knowledge will be indispensable in the development of new technologies to combat cardiac damage and diseases.

1.3 The vertebrate heart

The heart is a muscular organ which pumps blood through the blood vessels of an organism. The heart, blood and blood vessels make up the circulatory system. All

organs within an organism rely on the circulatory system to supply them with vital nutrients and oxygen and to remove metabolic waste. The vertebrate heart is a chambered organ consisting of myocardium, enclosed by epicardium and endocardium connective tissue, complete with valves and a coronary circulatory and conductive system. The vertebrate heart is unique amongst metazoans and is more complex than the myoepithelial pumping tubes found in invertebrates (Pérez-Pomares et al., 2009). The heart is the first organ to become fully functional during embryogenesis and is often required for further development of the organism (Brand, 2003). Cardiac damage and disease therefore can be fatal due to the limited ability of the heart to repair itself (Nadal-Ginard et al., 2003; Xin et al., 2013). During the past decades there has been a large amount of research focusing on both the anatomical and molecular aspects of heart development. The processes which lead to successful heart formation and functioning are gradually being uncovered (Moorman et al., 2003). However, a more comprehensive understanding of the molecular pathways which underlie heart development will aid the improvement of treatments for cardiac malfunctions.

The formation of the vertebrate heart involves the coordination of precisely regulated molecular and morphogenetic processes, which are conserved across many species (Olson and Srivastava, 1996). The vertebrate heart has evolved from a primitive linear pump in ancestral metazoan through the addition of new structures, due to demands from organisms' increasing size, activity and developing metabolic needs (Pérez-Pomares et al., 2009). This has transformed the vertebrate heart into a multichambered structure, complete with valves and a complex conductive and circulatory system (Fishman and Olson, 1997). Throughout evolution, although the morphology of the heart has been dramatically transformed, the gene regulatory networks directing development have been largely conserved (Olson, 2006; Pérez-Pomares et al., 2009). This conservation between vast phylogenetic distances allows cardiac development to be investigated in a range of organisms including flies, fish, amphibians, chick and mammals (Zaffran and Frasch, 2002).

In all embryos, the first step in heart development is for cells to be specified to become cardiac cells. This process is known as cardiac specification. The early embryo contains three primary germ layers; endoderm, which forms the digestive and respiratory tracts; mesoderm, which forms connective tissues, cardiovascular system and muscle; and ectoderm, which gives rise to the nervous system and epidermis (Kiecker et al., 2015; Kimelman, 2006; Noseda et al., 2011). Cardiac cell precursors are thought to arise as bilaterally symmetrical clusters of mesoderm (Foley et al., 2006; Jacobson and Sater, 1988). Cardiac precursors originate a significant distance from their final location within an organism; therefore they must migrate through the embryo during early development to relocate (Foley et al., 2006; Keller, 2002; Mohun et al., 2003; Parameswaran and Tam, 1995; Yang et al., 2002). The mass of migrating cardiac precursor cells are patterned into areas known as the primary and secondary heart fields. The primary heart field differentiates first and contributes to the majority of cardiac structures. The secondary heart field forms the outflow tract and, in organisms with a four chambered heart, the right ventricle (Dyer and Kirby, 2009; Harvey, 2002). In addition, a subset of neural crest cells contribute to cardiac structures, such as the connective tissue separating the major cardiac vessels (Hutson and Kirby, 2007). Once migrating cardiac cells reach their final location within a developing organism a linear heart tube is formed, which subsequently loops and undergoes morphogenesis to form the cardiac chambers. The timing of cardiogenesis varies between different organisms in accordance with their rate of growth and development. In humans, the heart commences beating in the third week of gestation, with blood circulating by week four (Manner et al., 2010; Sissman, 1970). The primitive heart starts beating at Hamburger Hamilton (HH) stage 10 (33 hours) in chick, embryonic day 8 (E8) in mouse and stage 36 (50 hours) in the African clawed frog *Xenopus laevis* (Sissman, 1970). In addition, the number of cardiac chambers varies between organisms. For example, amphibians have a three chambered heart consisting of a single thick walled ventricle which receives blood from two smaller atria (Mohun et al., 2003), whereas amniotes have a four chambered heart (Harvey, 2002). Despite differences in the rate of heart development and chamber number, the genetic programs and stages of development incorporating specification,

migration, heart tube looping, morphogenesis and chamber formation are highly conserved between organisms. This allows information gained in one model system to be compared with the developmentally relevant stage in another organisms.

1.4 Model organisms for investigating heart development

Information gained from different model organism has been used to develop an understanding of cardiogenesis. Each model system has advantages and disadvantages for uncovering the molecular mechanisms involved in heart development. The fruit fly, *Drosophila melanogaster,* has proved extremely useful for investigating the cardiac gene regulatory network, due to its relative lack of functional redundancy (Olson, 2006; Wolf and Rockman, 2008). The simplicity of the linear dorsal vessel does, however, limit the usefulness of this model in gaining a complete understanding of the compliment of mechanisms involved in mammalian heart development. Likewise zebrafish, *Danio rerio*, is a useful model to study basic genetics as well as the molecular and cellular mechanisms of early heart development, however, their more primitive two chambered hearts makes it harder to explore all aspects of higher vertebrate cardiogenesis (Liu and Stainier, 2012). Experimental techniques including transplantation experiments and gene expression manipulation in *Xenopus* have generated information about cell fates and molecular signalling in heart development (Samuel and Latinkić, 2009; Warkman and Krieg, 2007). Until recently there has been a lack of comprehensive genetic tools for routine genetic manipulation *Xenopus* (Artmann et al., 2010). However, with advances in gene editing techniques, such as clustered regularly interspaced short palindromic repeats (CRISPR) and transcription activator-like effector nucleases (TALENs), gene editing technologies are becoming routine in *Xenopus* (Lei et al., 2012; Nakayama et al., 2013). The mouse provides an accessible mammalian model, and is often used to investigate genetic principles through the use of transgenic lines (Rossant, 1996). Nonetheless, mouse embryos require a beating heart for continued development rendering experimental manipulations which adversely affect heart function lethal, genetic manipulations are difficult to control in a spatiotemporal manner and studies

are often costly and time consuming (Artmann et al., 2010). Cell culture allows the investigation of human cardiomyocyte development (Burridge et al., 2014, 2012; Vliet et al., 2012). Unfortunately, technologies have not advanced to a stage where cultured cells can generate mature chambered hearts, thus cell culture has limited use in understanding the complete cardiac developmental processes. *Xenopus laevis* embryos provide an easily accessible, readily available, manipulatable, high-throughput model for investigating early heart development and shall be used throughout the work encompassed in this thesis.

1.5 *Xenopus laevis* as a model organism for studying heart development

Xenopus is commonly known as the African clawed frog and there are two species which are frequently used to study vertebrate development; the tetraploid *Xenopus laevis* and the diploid *Xenopus tropicalis* (Amaya et al., 1998). *Xenopus laevis* were first used in a UK laboratory environment in the 1930s as a pregnancy test, and have been the favoured amphibian model system used throughout the last century to study various aspects of embryogenesis (Amaya et al., 1998; Lohr and Yost, 2000). More recently, *Xenopus tropicalis* are being used for studies involving genetic manipulations, as the species is better suited to the application than *Xenopus laevis* due to its simpler diploid genome (Amaya et al., 1998; Grainger, 2012). Humans and *Xenopus* share a remarkably large number of genetic and anatomical features, allowing molecular and cellular pathways uncovered in *Xenopus laevis* to be related to higher vertebrate development (Hellsten et al., 2010; Kaltenbrun et al., 2011). *Xenopus laevis* has numerous characteristics that makes it an excellent model for biomedical research. For example, adult *Xenopus laevis* can be induced to lay and fertilise eggs all year round, with typically 500-5000 rapidly developing embryos being produced per mating, allowing for high-throughput experiments (Warkman and Krieg, 2007). The eggs are laid, fertilised and then develop externally allowing non-invasive viewing using light or fluorescence microscopy (Kaltenbrun et al., 2011; Warkman and Krieg, 2007). Embryos are relatively large, 0.7-1.3 mm in diameter, and they are robust enough to withstand microinjections and microsurgery.

Microinjections can be used to introduce messenger ribonucleic acid (mRNA) or antisense morpholino oligonucleotides (MO) to regulate the expression of a protein of interest. Microinjections may also be used to introduce other nucleic acids, proteins, dyes or even whole nuclei (Kaltenbrun et al., 2011; Tandon et al., 2012). Soluble pharmacological inhibitors and activators added to *Xenopus laevis* embryo culture medium will readily diffuse to take effect throughout the embryo (Myers et al., 2014; Skirkanich et al., 2011). The manipulation of gene expression and signalling pathways can be controlled in a spatiotemporal and reversible manner by approaches including targeted microinjections and pharmacological reagents. Tissue explants excised during microsurgery can be cultured externally or grafted back into an alternate location within an embryo, and will continue developing. These and other reputable techniques allow defined regions, genes or signalling pathways to be dissected and manipulated, allowing insight into their roles during development. There are many resources available in research studies due to the popularity of *Xenopus laevis* as a model organism. For example, early embryonic cell fates have been mapped, allowing identification of particular blastomeres only 3 hours after fertilisation that will eventually give rise to the heart two days later (Kaltenbrun et al., 2011; Moody, 1987). Unlike in mammals such as mouse, early embryonic development in *Xenopus laevis* can proceed in the absence of a functioning circulatory system, allowing extensive analysis of cardiac defects in live embryos at later stages of development (Kaltenbrun et al., 2011). For these reasons, *Xenopus laevis* was the model organism chosen to work with in this study.

1.6 An overview of *Xenopus laevis* development

Following fertilisation, the *Xenopus laevis* embryo undergoes 12 rounds of synchronised cell divisions, at approximately 20-30 minute intervals, to form a 4,096 cell sphere, enclosing a fluid-filled blastocoel cavity (Heasman, 2006). The majority of zygotic transcription begins, accompanied by maternal mRNA degradation, from the 4,096 cell stage at a time point known as midblastula transition (MBT), although a small subset of zygotic transcripts are activated earlier (Tadros and Lipshitz, 2009).

Prior to midblastula transition, the embryo is largely patterned by localised maternal factors. For example, a component of the canonical Wnt signalling pathway, predicted to be Wnt 11, is relocated from a vegetal position by cortical rotation dictated by the sperm entry site, establishing the future dorsal side of the embryo (Figure 1:1 A) (Heasman, 2006). A signalling centre known as the Nieuwkoop centre is established in dorsal vegetal cells where dorsal Wnt and vegetally localised maternal VegT intersect (Figure 1:1 B) (De Robertis and Kuroda, 2004; Moon and Kimelman, 1998; Vincent and Gerhart, 1987; Zhang et al., 1998). The Nieuwkoop centre secretes Nodal related proteins in a gradient across the dorsal - ventral axis to establish and pattern the mesoderm and induce the Spemann's Organiser (Figure 1:1 C). The Spemann's Organiser is an organising centre which secretes proteins, including Nodal-related proteins and BMP antagonists, and is vital for further patterning of the embryonic germ layers (De Robertis et al., 2000; De Robertis and Kuroda, 2004; Joubin and Stern, 2001). By midblastula transition, the three germ layers - ectoderm, mesoderm and endoderm - are established (Heasman et al., 1984). Following midblastula transition, the cell cycles lengthen and becomes asynchronous and the germ layers are patterned by numerous signalling inputs. At least four major signalling pathways are believed to be essential for development, including Nodal/ Activin, bone morphogenetic protein (BMP), Wnt and FGF. Early work suggests that ligand gradients pattern the animal-vegetal and dorsal-ventral axis in the blastula stage embryo. More recent work has shown that there are numerous intracellular and extracellular pathway regulators, which are themselves localised within the embryo (Heasman, 2006). The challenge is to comprehend the signalling context at each location in the embryo to understand how different cellular fates are specified. Localised combinations of active signalling pathways are likely integrated by pathway crosstalk to result in particular cellular outcomes, allowing a relatively small number of factors to pattern the embryo. At approximately 10 hours post-fertilisation, gastrulation begins, where morphogenetic movements relocate and reorganise cells to form a three-layered structure (Sharpe and Mason, 2009). The vegetal mass ingresses in the animal direction, causing an increase in the blastocoel floor area, which will eventually form the gut. This drives the involution of the mesoderm

(starting at the dorsal side) through the blastopore, followed by further active migration animally and positioning between the ectodermal and endodermal layers. The ectoderm undergoes epiboly, where cells spread vegetally to cover the embryonic exterior (Gilbert, 2000; Heasman, 2006; Shook et al., 2004). Following gastrulation, neurulation encompasses the formation of the neural tube along the anterior-posterior axis of the embryo, accompanied by continued development of specified tissues (Gilbert, 2000). Development continues throughout the tailbud and tadpole stages with organogenesis occurring during the late tadpole stages.

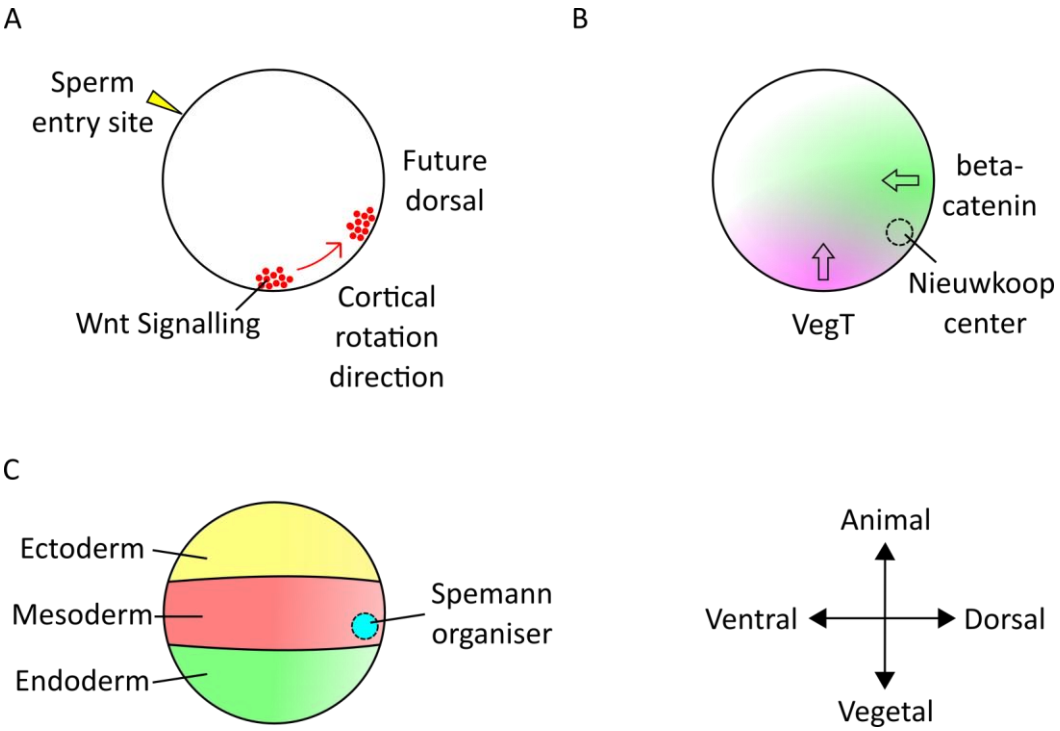

Figure 1:1 Characteristics of early *Xenopus laevis* embryonic development

(A) Cortical rotation, dictated by the sperm entry site, drives the movement of vegetally localised dorsal determinants (red) to establish the future dorsal axis. (B) Gradients of beta-catenin originating from the dorsal side of the embryo (green) and VegT originating vegetally (purple) converge to establish the Nieuwkoop centre. (C) The Nieuwkoop centre is involved in establishing the Spemann organiser, which contributes towards patterning the embryo.

1.7 The origin, migration and morphogenesis of cardiac tissue

Cardiac progenitors arise as two bilaterally symmetrical patches of dorsal lateral plate mesoderm in the early embryo of model organisms studied, including mouse, chick, amphibians, zebrafish, *Drosophila* and *Xenopus* (Figure 1:2 A shows this in *Xenopus*) (Foley et al., 2006; Jacobson and Sater, 1988; Zaffran and Frasch, 2002). During gastrulation, as a result of convergent extension movements, cardiac mesoderm ingresses through the blastopore in *Xenopus*, also known as the primitive streak in birds, reptiles and mammals (Vliet et al., 2012). Cardiac mesoderm ingression occurs at the dorsal side of the blastopore in *Xenopus* and at the rostral end of the primitive streak in organisms such as chick (Martinsen, 2005; Schoenwolf et al., 1992). The cardiac mesoderm migrates towards the future dorsal-anterior side of the embryo by late gastrulation (Figure 1:2 B shows this in *Xenopus*) (Garcia-Martinez and Schoenwolf, 1993; Keller et al., 2000; Parameswaran and Tam, 1995). The bilateral regions of cardiac mesoderm move ventrally to meet and fuse on the ventral midline during neurula stages in all organisms (Figure 1:2 C, D shows this in *Xenopus*) (Martinsen, 2005; Mohun et al., 2003). In mammals and birds, the anterior margins of the bilateral cardiac fields first merge to form the characteristic cardiac crescents in the anterior lateral region of the embryo (Harvey, 2002; Zaffran and Frasch, 2002). Cardiac tissue remains in an anterior-ventral position throughout the remainder of development and in adult life (Figure 1:2 E shows this in *Xenopus*), but undergoes morphological remodelling to form a functioning heart (Mohun et al., 2003). Upon cardiac primordia fusion, a linear heart tube is formed, orientated along the anterior-posterior axis. The heart tube is a temporary structure consisting of a tubular inner endothelial layer surrounded by a myocardial layer (Buckingham et al., 2005; Harvey, 2002; Mohun et al., 2003; Stalsberg and DeHaan, 1969). Heart tube elongation commences with the tube spiralling rightwards, in a process known as cardiac looping, with the posterior end moving in an anterior and dorsal direction (Al Naieb et al., 2013; Kolker et al., 2000; Latinkić et al., 2004; Martinsen, 2005; Mohun et al., 2000). Following this, ventricular and atrial myocardial regions become distinct, valve precursors are formed, and the heart remodels into a multi-chambered organ,

which can commence beating (Al Naieb et al., 2013; Buckingham et al., 2005; Harvey, 2002; Martinsen, 2005).

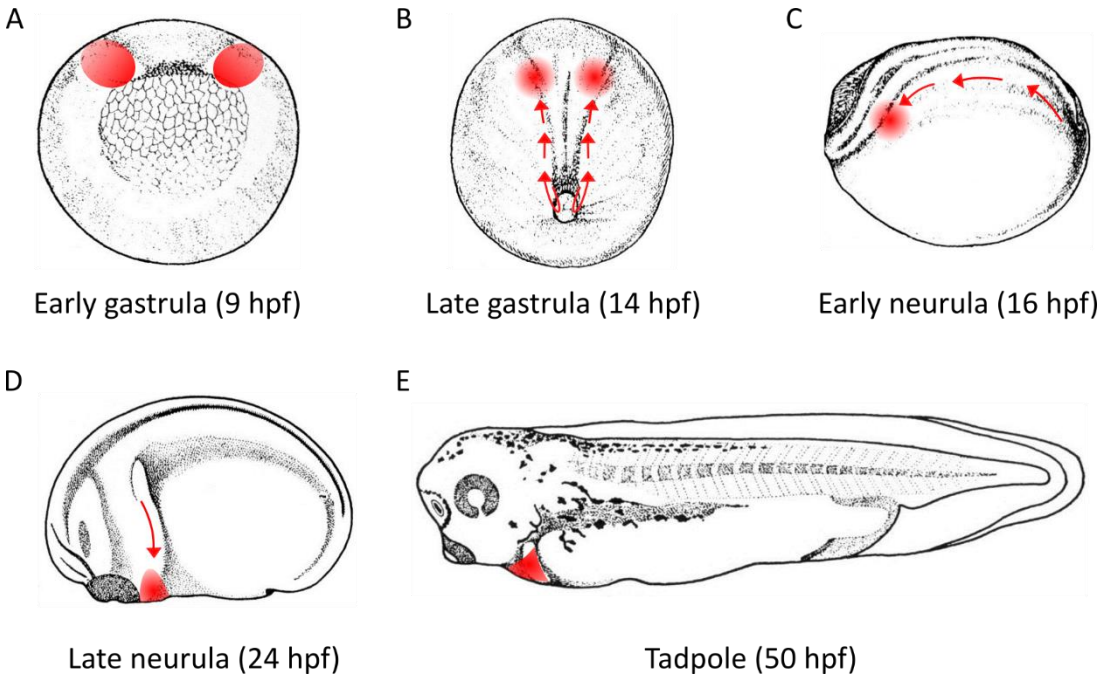

Figure 1:2 Cardiac tissue migration during *Xenopus laevis* embryogenesis

(A) A vegetal view of an early gastrula embryo. Cardiac tissue (red) is present as two bilaterally symmetrical fields of mesoderm at the dorsal side of the embryo. (B) During gastrulation, cardiac mesoderm migrates towards the dorsal-anterior end of the embryo. A posterior-dorsal view is shown. (C) During early neurula stages the two cardiac fields migrate ventrally to (D) meet on the ventral midline. A lateral view is shown. (E) Cardiomyocytes remain at this anterior ventral location, where they undergo morphological movements during tadpole stages to remodel as a three chambered beating heart. A lateral view is shown. (Foley et al., 2006; Mohun et al., 2003). Illustrations adapted from Nieuwkoop and Faber, 1994, via www.xenbase.org. hpf = hours post fertilisation.

1.8 Molecular signals of cardiac specification

Cardiac mesoderm has been shown to arise due to inductive interactions with neighbouring tissues in the early embryo. However, the precise timing and nature of this inductive signalling is largely unknown. Four major signalling pathways have been implicated in the induction of cardiac tissue: Nodal/ Activin, FGFs, BMPs and Wnts (Noseda et al., 2011). However, these signalling pathways have multiple roles in the developing embryo around the time of cardiac specification, making their precise function in cardiac specification difficult to define.

1.8.1 Nodal/ Activin

1.8.1.1 Nodal/ Activin family

Nodal and Activin belong to the transforming growth factor beta (TGF-beta) superfamily which comprises over 30 members. The TGF-beta family regulates a diverse range of processes, including cellular growth, migration, apoptosis, adhesion and differentiation (Roberts and Sporn, 1993; Wu and Hill, 2009). TGF-beta ligands include Nodals, Activins, TGF-betas, BMPs and growth differentiation factors (GDFs). These ligands and their downstream effectors are highly conserved across evolution (Wu and Hill, 2009). The TGF-beta ligands bind a range of receptors, activating different downstream effectors and eliciting a variety of cellular responses. There are two main branches of TGF-beta signalling. One branch primarily contains Nodal, Activin, Inhibin and TGF-beta ligands, and signals utilising Smad2/3 via Activin receptor-like kinases (ALK) 4, 5 and 7 (Shen, 2007; Shi and Massague, 2003). This signalling branch is often referred to as Nodal/ Activin or ALK4/5/7 signalling. The alternate branch transduces BMP, GDF and TGF-beta ligand signalling via ALK1, 2, 3 and 6, and Smad1, 5 and 8 (Shi and Massague, 2003). In early embryonic development, the *Xenopus* Nodal related factors have been shown to have roles in mesoderm induction and patterning, including cardiac specification (Luxardi et al., 2010; Osada and Wright, 1999; Reissmann et al., 2001; Samuel and Latinkić, 2009; Takahashi et al., 2000).

1.8.1.2 Nodal/ Activin signalling pathway

Extracellular homodimeric Nodal/ Activin ligands bind to Type II TGF-beta transmembrane receptors. Subsequently, Type II receptors form heterotetrameric complexes with Type I TGF-beta transmembrane receptors, also termed ALKs, with Nodal/ Activin signalling via ALK4/5/7 (Shen, 2007). Type II and Type I receptors have single pass transmembrane domains and are the only known family of serine-threonine kinases transmembrane receptors in mammals (Schmierer and Hill, 2007). For Nodal signalling, an extracellular membrane bound cofactor EGF-CFC, called cripto or cryptic in mammals and Tdgf1.3 in *Xenopus*, is also required in the membrane signalling complex (Gritsman et al., 1999; Schier, 2003; Yeo and Whitman, 2001).

When an extracellular TGF-beta ligand binds the membrane signalling complex, the Type II receptor phosphorylates serine and threonine residues in the cytoplasmic domain of the Type I receptor, resulting in receptor activation. This in turn phosphorylates the receptor regulated Smads (R-Smads), Smad2 and Smad3 (Shen, 2007). In the blastula staged *Xenopus laevis* embryo, Smad2 is the predominant Smad (van Boxtel et al., 2015). Smad proteins are phosphorylated by the Type I receptors on two serine residues at their extreme C terminus end, allowing release from the receptor (Schmierer and Hill, 2007). Phosphorylated Smad2/3 forms a trimeric complex with the common mediator Smad, Smad4, in the ratio of two R-Smads with one Smad4 (Shen, 2007). The Smad2/3-Smad4 complex then translocates into the nucleus where it regulates the expression of Nodal/ Activin dependent genes (Figure 1:3) (Nicolás et al., 2004). Smad proteins interact with DNA and other proteins through conserved MH1 and MH2 domains which are responsible for DNA binding and protein-protein interactions respectively. Smads also bind cofactors such as transcription factors (TFs) and chromatin remodelling proteins to influence the transcription of target genes (Kimelman, 2006; Schmierer and Hill, 2007). The linker region of Smads can be phosphorylated by other kinases, for example extracellular signal-regulated kinases (ERK), thereby integrating different signalling pathways (Schmierer and Hill, 2007). *nodal 5* and *6* transcripts are first expressed zygotically in

the dorsal-vegetal region of the early blastula embryo prior to midblastula transition and can induce mesoderm, endoderm other *nodal* transcripts (Takahashi et al., 2000). The expression of *nodal 1* and *2* is first detected in the vegetal region of the blastula stage embryo, with transcripts becoming localised to the dorsal marginal zone prior to decreasing during gastrulation (Jones et al., 1995). The expression of *nodal 1* reappears during tailbud stages in two regions either side of the posterior notochord (Lustig et al., 1996). *nodal 3* is expressed in the Spemann Organiser, however it lacks the mesoderm inducing capacity of other Nodal proteins (Smith et al., 1995). *nodal 4* is first expressed at the gastrula stages in the Spemann Organiser with expression prevailing in the notochord and neural tube throughout neurula stages (Joseph and Melton, 1997). *activin* is first detected homogeneously after midblastula transition, with expression restricted to the dorso-anterior region during the neurula stages (Dohrmann et al., 1993; Thomsen et al., 1990). *ALK4* is detected in the animal pole and marginal zone of the blastula staged *Xenopus* embryo, throughout the ectoderm, mesoderm and to a lesser extent endoderm during gastrulation with continued expression in multiple domains throughout neurula stages (Chen et al., 2005). *ALK5* has been found to be expressed throughout development in a microarray study spanning 14 stages of development from the blastula to tail bud stages, although gene localisation information is not available using this method (Yanai et al., 2011). *ALK7* has been found to be localised to the ectodermal and organiser regions in gastrula staged *Xenopus* (Reissmann et al., 2001); however there is little data on other stages of development. *Xenopus* EGF-CFC (Cripto) family members *XCR1* and *XCR3* transcripts are expressed ubiquitously both maternally and zygotically until early neurula stages (Dorey and Hill, 2006).

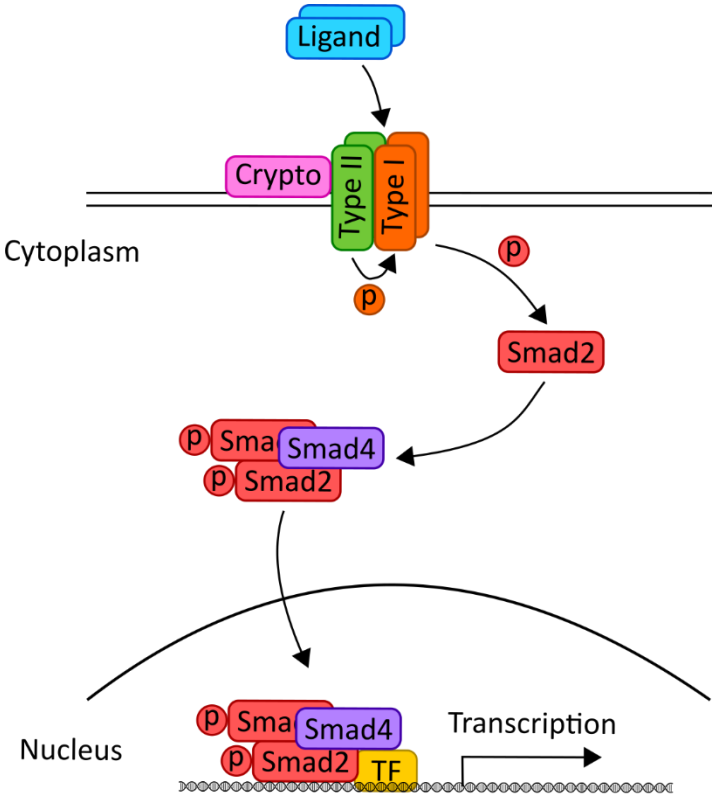

Figure 1:3 Schematic diagram illustrating Nodal/ Activin signalling

Arrows indicate the direction of signal transduction from extracellular TGF-beta ligand binding resulting in altered gene transcription. TF =transcription factor. P =phosphorylation event. Nodal requires the co-receptor Crypto to signal through the transmembrane receptors, whereas alternate TGF-beta ligands, such as Activin, do not.

1.8.1.3 Nodal/ Activin signalling regulation

Nodal/ Activin signalling is highly regulated at multiple levels, including ligand processing, receptor availability, and in positive and negative feedback loops (Shen, 2007). Nodal is secreted as a propeptide and is captured by co-receptor EGF-CFC to be processed by EGF-CFC bound subtilisin-like proprotein convertases (SPCs) (Blanchet et al., 2008; Schmierer and Hill, 2007). Nodal/ Activin signalling activates both positive and negative feedback loops within the cell, by inducing its own expression and the expression of repressors such as Lefty and Cerberus, whose expression can be detected originating from the dorsal side of the embryo from around midblastula transition (Shen, 2007; Yanai et al., 2011). Lefty proteins, divergent members of the TGF-beta superfamily, antagonise the EGF-CFC co-receptor, preventing TGF-beta receptor complex formation. They have also been shown to interact with Nodal ligands, preventing receptor binding (Chen and Shen, 2004). Cerberus, a member of the DAN family, is a multifunctional antagonist of Nodal, BMP and Wnts and works in the extracellular space by physically binding to the ligands to prevent ligand-receptor interactions (Piccolo et al., 1999). Receptor availability also affects signalling. Nodal/ Activin signalling activates expression of Dapper2, which binds the Type I receptor; enhancing the internalisation and degradation through the late endosome, thus decreasing cell surface receptor availability for transmitting signalling (Schier, 2009). Signal transmission is also controlled downstream of receptor activation; transcriptional co-repressors Tgif1 and Tgif2 competitively bind active Smad2, reducing the relative amount of available Smad2 in the nucleus (Powers et al., 2010). In addition, active nuclear Smad2/3 is dephosphorylated, promoting nuclear export (Lin et al., 2006; Nicolás et al., 2004), in conjunction with ubiquitination and degradation by the proteasome (Lo and Massague, 1999; Shi and Massague, 2003). Conversely, nuclear transcription factors, such as Forkhead Activin Signal Transducer (Foxh1), aid signalling by targeting Smads to the developmentally relevant promoters (Chen et al., 1997; Yeo et al., 1999). The combination of Nodal/Activin signalling propagation and inhibition balance, thus achieving the precise location, concentration and duration of Nodal/ Activin signalling necessary for patterning the early embryo.

1.8.1.4 Nodal/ Activin signalling in embryogenesis

Nodal/ Activin signalling has numerous roles throughout development. Initially, Nodal/ Activin signalling is required for establishing, and then subsequently patterning, the mesoderm and endoderm (Harland and Gerhart, 1997; Hill, 2001; Zorn and Wells, 2007). Furthermore, Nodal/ Activin is required for promoting gastrulation movements and for establishing the left-right axis (Hill, 2001; Schier, 2003; Smith and Howard, 1992). Midblastula transition (MBT) is the time point where maternal mRNA is degraded and zygotic gene transcription activated. A small number of genes in many organisms including fly, frog, zebrafish, and mouse do become active, however, before large scale zygotic transcription (Tadros and Lipshitz, 2009). In *Xenopus laevis,* the transcription of *nodal 5* and *6* is activated by maternal VegT before midblastula transition (Takahashi et al., 2000). *Nodal 5* and *6* activate their own expression and Nodal/ Activin signalling is apparent by midblastula transition, evident by the accumulation of phosphorylated-Smad2 (p-Smad2) (Skirkanich et al., 2011). This pre-midblastula transition *nodal 5* and *6* transcription is essential for induction of mesendodermal genes, germ layer specification and induction of *nodal 1, 2* and *4,* which are required for later processes such as gastrulation (Luxardi et al., 2010; Skirkanich et al., 2011). Nodal/ Activin signalling is initially enriched dorsally, due to VegT and Beta-catenin cooperation, and extends in a gradient across the *Xenopus laevis* embryo (Lee et al., 2001). By the onset of gastrulation (stage 10), Nodal/ Activin signalling is more evenly distributed across the dorsal-ventral axis (Figure 1:4) (Faure et al., 2000; Lee et al., 2001; Schohl and Fagotto, 2002). Following mesoderm induction, Nodal/ Activin activity patterns the mesoderm in a dose-dependent manner. In pluripotent *Xenopus laevis* explants, it has been demonstrated that low Activin concentrations are capable of inducing ventral mesoderm derivatives, and high Activin concentrations are capable of inducing dorsal mesoderm derivatives (Ariizumi et al., 1991; Kimelman, 2006; Okabayashi and Asashima, 2003). A dominant negative Activin receptor has been shown to block the ability of animal caps to respond to Activin treatments and *in vivo* for embryos to express the mesodermal marker *brachyury* (Hemmati-Brivanlou and Melton, 1992).

There is ongoing work to determine the relative contributions of Nodal/ Activin signalling timing, dose and length of exposure in patterning the early embryo.

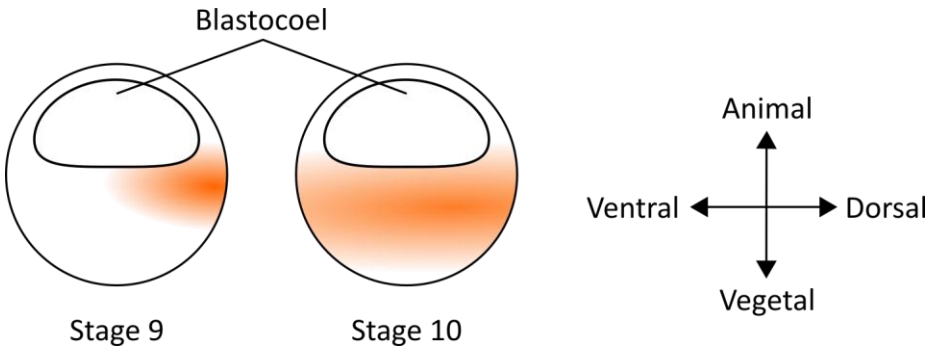

Figure 1:4 Active Nodal/ Activin signalling gradient in the early *Xenopus laevis* embryo

Diagrammatic depiction of Nodal/ Activin signalling activated phosphorylated-Smad2 localisation in the early *Xenopus laevis* embryo.

1.8.1.5 Nodal/ Activin signalling in cardiac specification

Research conducted in several model systems has implicated Nodal/ Activin signalling in cardiac specification. In *Xenopus laevis*, overexpression of Nodal family members, or constitutively active (CA) ALKs, has been shown to induce ectopic cardiac tissue, both *in vivo* and in animal pole explants (Foley et al., 2007; Logan and Mohun, 1993; Reissmann et al., 2001; Takahashi et al., 2000). A dose-response can be demonstrated in *Xenopus laevis* animal pole explants, with high concentrations of Activin A, Nodal ligands or CA-ALKs inducing cardiac tissue, in contrast to lower concentrations which result in alternative mesoderm derivatives including skeletal muscle, notochord and lateral plate mesoderm (Logan and Mohun, 1993; Reissmann et al., 2001; Takahashi et al., 2000). Likewise, Activin A has been shown to induce cardiac myogenesis in a dose-dependent manner in quail posterior epiblast explants, with Activin inhibition resulting in reduced cardiac cell number in chick posterior explants (Yatskievych et al., 1997). Conversely, disruption of Nodal/ Activin signalling by dominant negative ALKs can reportedly reduce cardiac marker expression in *Xenopus laevis* (Reissmann et al., 2001). It has been demonstrated that mice lacking the *cripto* gene fail to elicit cardiac marker expression and subsequently die prenatally. In addition, *nodal* hypomorphic mutants display abnormal heart tissue (Lowe et al., 2001; Xu et al., 1999). Dominant negative ALK receptors, or loss of *cripto*, has been shown to block cardiomyogenesis in mouse embryonic stem cells (Cai et al., 2012; Parisi et al., 2003; Xu et al., 1999). zebrafish *one-eyed pinhead* (*oep*; an EGF-CFC family member) mutants exhibit severe defects in myocardial development (Griffin and Kimelman, 2002; Reiter et al., 2001). In a *Xenopus laevis* explant conjugate model, the Nodal/ Activin signalling pathway has been demonstrated to have an early transient requirement for cardiogenesis (Samuel and Latinkić, 2009). These results suggest a role for Nodal/ Activin signalling in cardiac induction. However, many of the aforementioned experiments were not designed to isolate the role of Nodal/ Activin signalling in cardiac specification from alternative Nodal/ Activin signalling roles in mesoderm formation and embryonic patterning, as experiments largely used continuous Nodal/ Activin signalling inhibition or overexpression. As mesoderm formation is a prerequisite for cardiac mesoderm

induction, it is debatable whether the observed cardiac affects are a direct or indirect consequence of altered Nodal/ Activin signalling. In addition, the temporal requirement for Nodal/ Activin signalling in cardiac specification *in vivo* remains unknown. Careful manipulation of Nodal/ Activin signalling during precise time windows of development would begin to address more specifically the requirement for Nodal/ Activing signalling in cardiac specification. Whether Nodal/ Activin signalling interacts with other signalling pathways to confer cardiac specificity or is independently sufficient for initiating cardiogenesis by activating downstream signalling pathways remains to be resolved.

1.8.2 Fibroblast growth factors

1.8.2.1 Fibroblast growth factor family

The FGF family is a family of growth factors, conserved throughout metazoan evolution (Itoh and Ornitz, 2004). There are 22 identified FGF family members in mammals, with fewer in lower vertebrates, for example there are 17 known FGF family members in *Xenopus tropicalis* (Lea et al., 2009). The many *Xenopus* FGF ligands and receptors have dynamic expression patterns during development. The expression of *fgf 1, 2, 4, 8, 13, 20* and *22* and *fgfrs 1, 2* and *4* can be detected prior to mid-gastrula stages in a developmentally relevant time frame for cardiac specification. Whole mount *in situ* hybridisation analysis shows that *fgfrs* appear to be ubiquitously expressed with the aforementioned *fgfs* often expressed in the mesoderm or expressed ubiquitously with stronger expression in the mesoderm at gastrula stages (Lea et al., 2009). FGF signalling controls many biological processes including proliferation, survival, migration, differentiation and embryogenesis (Dorey and Amaya, 2010; Ornitz and Itoh, 2015; Thisse and Thisse, 2005).

1.8.2.2 Fibroblast growth factor signalling pathway

Two molecules of extracellular FGF ligands, connected by a heparan sulphate proteoglycan, signal through binding highly conserved FGF transmembrane receptors (FGFR), causing receptor dimerisation (Schlessinger et al., 2000; Turner and

Grose, 2010). Ligand dependent dimerization results in FGF receptors undergoing a conformational shift, leading to the transphosphorylation of the cytoplasmic tyrosine kinase domains. This allows the docking of adaptor proteins for multiple downstream signal transduction pathways. The two main FGF signalling transduction pathways involve Ras-mitogen-activated protein kinase (MAPK)/ ERK and phospholipase-C gamma (PLC-gamma), but signal propagation can also occur via phosphoinositide 3-kinase (Pi3K) and signal transducer and activator of transcription (STAT) branches (Kimelman, 2006; Thisse and Thisse, 2005). FGF predominantly signals through Ras-MAPK/ ERK during embryonic development (Corson et al., 2003; Thisse and Thisse, 2005). The Ras-MAPK/ ERK branch of signalling is transmitted by activated (phosphorylated) FGF receptors inducing the activation of the G-protein Ras, via small adaptor proteins. Ras activates Raf, which phosphorylates to activate mitogen-or-extracellular signal regulated protein kinase (MEK). MEK subsequently activates MAPK/ ERK by dual phosphorylation of the regulatory tyrosine or threonine residues, which are located only one residue apart at positions 202 and 204 respectively (Payne et al., 1991; Shaul and Seger, 2007). MAPK/ ERK enters the nucleus where it phosphorylates and activates transcription factors to regulate transcription of target genes (Figure 1:5) (Kimelman, 2006; Thisse and Thisse, 2005).

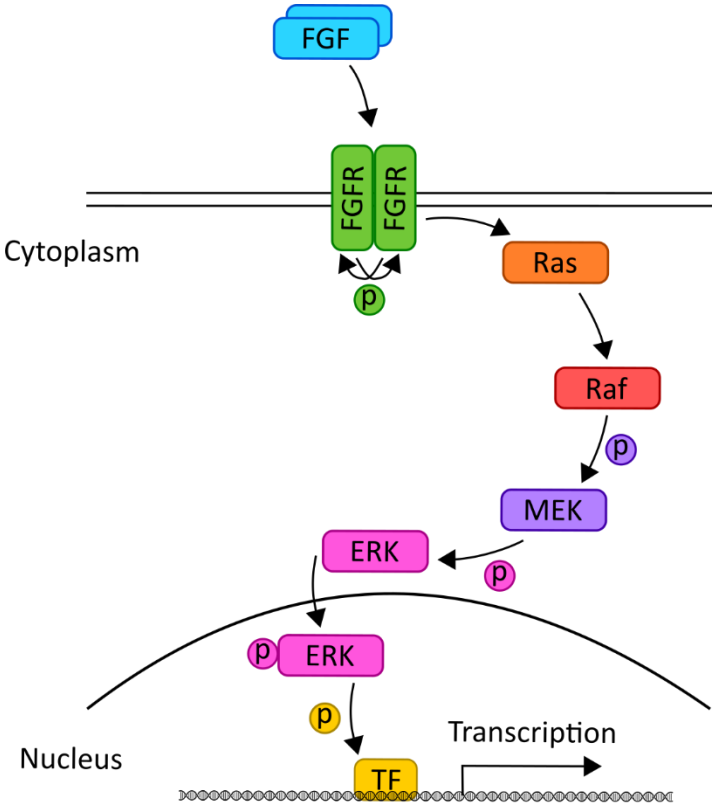

Figure 1:5 Schematic diagram illustrating FGF signalling

Arrows indicate the direction of signal transduction from extracellular FGF ligand binding to influencing gene transcription. TF =transcription factor. P =phosphorylation event.

1.8.2.3 Fibroblast growth factor signalling regulation

FGF signalling specificity is conferred by different ligand-receptor binding capabilities, and is tightly regulated at multiple levels by both positive and negative feedback loops (Thisse and Thisse, 2005). Secreted FGF proteins are sequestered in the extracellular matrix by Heparan Sulphate Proteoglycans and must be released by Heparanases. Conversely, cell surface Heparan Sulphate Proteoglycans stabilise the FGF ligand-receptor interaction (Harmer et al., 2004). FGF receptor activity can be modulated by receptor internalisation and ubiquitination following receptor activation. In addition, the negative regulator FGFRL1 lacks the tyrosine kinase domain for signal propagation but is still capable of binding FGF ligands (Wiedemann and Trueb, 2000). Intracellular proteins such as MAPK Phosphatases (Zhao and Zhang, 2001), Sprouty (Casci et al., 1999), Similar-expression-to-fgf-genes (Sef) (Furthauer et al., 2002) and Fibronectin leucine rich transmembrane protein 3 (Flrt3) (Böttcher et al., 2004) modulate the signal transduction cascade. MAPK Phosphatase negatively regulates MAPK by dephosphorylation, to deactivate signal transduction (Zhao and Zhang, 2001). *Sprouty* expression is induced by FGF signalling and the Sprouty protein inhibits FGF signalling upstream of MAPK/ ERK (Tsang and Dawid, 2004). Sef binds and inhibits MEK-MAPK/ ERK dissociation and thus blocks the nuclear translocation of active MAPK/ ERK (Thisse and Thisse, 2005). In contrast, Flrt3 interacts with FGF receptors to promote FGF signalling (Böttcher et al., 2004). These examples, and numerous other pathway enhancers or inhibitors, allow fine tuning at various levels for FGF signalling regulation.

1.8.2.4 Fibroblast growth factor signalling in embryogenesis

FGFs have numerous roles throughout many stages of embryogenesis, including induction, patterning, morphogenesis, axis formation, and differentiation (Coumoul and Deng, 2003; Thisse and Thisse, 2005). There is a large body of evidence suggesting that mesoderm induction and patterning is one of the earliest events requiring FGF signalling (Amaya et al., 1993; Fletcher et al., 2006; Isaacs et al., 1992; Kimelman and Kirschner, 1987; Slack et al., 1990). However, select mesoderm markers, for example eomesodermin, are unaffected by FGF signalling inhibition in

Xenopus laevis (Fletcher and Harland, 2008; Kumano et al., 2001), suggesting that FGF signalling is not required for all aspects of mesoderm induction. It is, however, apparent that FGF signalling is necessary for axial (notochord) and paraxial (somites and dermis) mesoderm formation (Amaya et al., 1993, 1991; Dorey and Amaya, 2010). Concurrently, FGF signalling, originating and dispersing from the future dorsal side of the embryo, inhibits ventral BMP spreading to establish the dorsal-ventral axis in zebrafish (Fürthauer et al., 2004). FGF signalling has been associated with the specification and development of several mesodermal tissue derivatives including blood, skeletal muscle and cardiac tissue (Isaacs et al., 2007; Keren-Politansky et al., 2009; Marques et al., 2008; Simões et al., 2011). It has been shown in *Xenopus* and mouse that FGF signalling is required for convergent extension cell movements during gastrulation, as FGF signalling inhibition results in aberrant cell movements and abnormal or incomplete gastrulation (Amaya et al., 1991; Ciruna and Rossant, 2001; Harvey, 2002; Nutt et al., 2001). FGF has numerous roles throughout later development, for example in patterning the mid-hindbrain in chick (Aragon and Pujades, 2009) and in limb induction, maintenance and development in chick (Martin, 1998).

1.8.2.5 Fibroblast growth factor signalling in cardiac specification

During the blastula to gastrula stages of development, FGF expression is prominent in the anterior endoderm tissue underlying the cardiac field, inferring FGF as a candidate cardiac inducing signal (Alsan and Schultheiss, 2002; Deimling and Drysdale, 2011; Lea et al., 2009). Research in several model systems has implicated FGF signalling in cardiac specification. The *Drosophila heartless* (FGFR) mutant lacks the dorsal vessel, reasoned to be due to the requirement of FGF signalling in both cell migration and fate assignment (Beiman et al., 1996; Michelson et al., 1998). However, it is questionable whether a common role for FGF signalling in tissue migration and organisation may account for pleiotropic defects in *heartless* mutants (Beiman et al., 1996). Studies in chick provide evidence that FGF signalling contributes to cardiac induction. Specifically, ectopic FGF signalling was shown to be capable of expanding the heart field laterally; however FGF signalling alone was

insufficient to initiate cardiogenesis in non-precardiac mesoderm (Alsan and Schultheiss, 2002; Lough et al., 1996). Likewise, in *Xenopus laevis* animal pole explants, FGF signalling was incapable of inducing differentiated cardiac marker expression (Logan and Mohun, 1993). Removal of the cardiac inducing endoderm in chick has been shown to result in the downregulation of a subset of cardiac markers, which can be rescued by exogenous FGF8 in cooperation with low levels of BMP signalling (Alsan and Schultheiss, 2002). In zebrafish, *fgf8* expression is thought to be necessary in heart precursors, and the *acerebellar* (*fgf8*) mutant has been shown to have reduced ventricular cardiomyocyte number (Marques et al., 2008; Reifers et al., 2000). Increased FGF signalling was demonstrated to result in increased cardiomyocyte number in zebrafish, thus it was reasoned that FGF signalling regulates heart size and chamber proportions during cardiac specification (Marques et al., 2008). Research in *Xenopus laevis* has shown that FGF pathway inhibition results in reduced cardiac marker expression (Deimling and Drysdale, 2011; Keren-Politansky et al., 2009) and that FGF signalling is required during the first hour of cardiac induction in an explant conjugate model for cardiogenesis (Samuel and Latinkić, 2009). Addressing the role of FGF in cardiac specification in mice has been problematic, as many FGF mutant mice die during gastrulation (Deng et al., 1994; Sun et al., 1999), although studies in mouse embryonic stem cells have implicated that FGFR1 is essential for cardiomyocyte development (Dell'Era et al., 2003).

The temporal and spatial expression of FGF ligands highlights the potential involvement of FGF signalling in cardiac specification, with emerging experimental evidence supporting the concept. However, a demonstration of a direct role for FGF signalling in cardiac specification remains elusive as many previous studies have not been designed to isolate the role of FGF signalling in cardiac specification from its broader functions in embryonic development. The timing and mechanism of action that FGF signalling may have in cardiac specification remains unanswered. An understanding of whether, and how, FGF signalling cooperates with other signalling pathways to induce cardiac mesoderm, or whether FGF signalling required after

initial cardiac specification to regulate heart development, is an important area of further research which will broaden our understanding of cardiogenesis.

1.8.3 Bone morphogenetic protein and Wnt

In addition to Nodal/ Activin and FGF signalling, BMP and Wnt signalling has been implicated in cardiac specification. However, there is conflicting evidence concerning the involvement of BMP and Wnt signalling in cardiac specification as opposed to later stages of heart development.

1.8.3.1 Bone morphogenetic protein

BMPs are members of the TGF-beta family. There are at least 15 BMPs which have been identified in vertebrates (Wang et al., 2014). BMP's have multiple roles throughout embryogenesis, for example in cell-type specification, dorsoventral axis determination, tissue patterning and organ development (Hogan, 1996; Wang et al., 2014). BMPs have been implicated in cardiogenesis; however, whether BMP signalling is involved in specification, or later development, is a subject of debate. In the chick, it has been shown that BMP signalling can act upon dorsal mesoderm to induce cardiac tissue, and that BMP antagonists can restrict the domain of cardiac tissue (Schultheiss et al., 1997). However, experiments in chick explant culture indicates that BMP signalling inhibits early cardiogenesis (Ladd et al., 1998). In mice, *bmp2* knockouts result in defects in cardiac development, however, cardiac tissue specification remains intact (Zhang and Bradley, 1996). In addition, in mouse, *bmp5* and *bmp6* knockouts have no gross cardiac abnormalities (J. Wang et al., 2011). In mouse cell culture, BMP signalling has been found to supress early cardiogenesis (Harada et al., 2008). In zebrafish, *Swirl* (*bmp2*) mutants show early myocardial marker, *gata5*, expression, but expression is not maintained, suggesting that BMP signalling regulates cardiogenic factors but is not involved in cardiac tissue induction (Reiter et al., 2001). Work in a *Xenopus laevis* explant model for cardiogenesis shows that early cardiac marker expression was observed unaffected after BMP inhibition. However, later heart development was abnormal after BMP inhibition, suggesting

that BMP is not required for cardiac specification *per se*, but for later stages of heart development, including heart field migration and/or fusion and differentiation (Samuel and Latinkić, 2009; Walters et al., 2001). These investigations show that there is conflicting evidence regarding the involvement of BMPs in cardiac specification and later heart development. However, in a number of model systems, including *Xenopus laevis*, the evidence suggests that BMP is not required for cardiac specification, hence BMP shall not be a focus for studies within this thesis.

1.8.3.2 Wnt

Wnts comprise a family of secreted glycoproteins which are conserved throughout metazoans (Komiya and Habas, 2008; MacDonald et al., 2009). In vertebrates, 19 Wnt proteins have been identified (Komiya and Habas, 2008). Wnts primarily signal via canonical (Wnt/ beta-catenin) or non-canonical (beta-catenin independent) branches of the Wnt signalling pathways (Komiya and Habas, 2008). Wnts control a variety of processes, including embryonic cell fate determination, cell polarity and migration, proliferation, differentiation and tissue homeostasis (Kikuchi et al., 2009; Logan and Nusse, 2004). There is conflicting data concerning the involvement of Wnt/ beta-catenin signalling in cardiac specification. In chick and *Xenopus laevis,* active canonical Wnt signalling in anterior mesoderm has been shown to supresses cardiac development, whereas Wnt antagonists Dickkopf and Frizzled stimulate cardiogenesis by establishing a zone of low Wnt activity (Marvin et al., 2001; Schneider and Mercola, 2001). In addition, endoderm specific knockout of beta-catenin in mice has been demonstrated to lead to multiple ectopic heart formation (Lickert et al., 2002). Wnt signalling in mice is potentiated by *nkx2.5*, implicating Wnt in supporting continued cardiac development (Cambier et al., 2014). However, in mouse embryonic stem cells (ESC) and in zebrafish, there is evidence for a biphasic role for Wnt in cardiac specification, with canonical Wnt promoting cardiac specification in early developmental stages but inhibiting cardiomyogenesis in later development (Naito et al., 2006; Nakamura et al., 2003; Ueno et al., 2007). Conversely, more recent work in human and mouse stem cells has demonstrated a high yield of functional cardiomyocytes after Wnt inhibition (Lian et al., 2013; H.

Wang et al., 2011). This suggests that although Wnt signalling has been shown to have a biphasic role in cardiac development, *in vivo* Wnt is not required for the induction of cardiac cells but it is likely to be required for continued further cardiac development. Therefore, Wnt signalling shall not be the focus of research conducted for this thesis.

1.8.4 p53

p53 was discovered in 1979 as a protein which interacts with the oncogenic Simian Vacuilating virus 40 (SV40) T antigen in SV40 infected cells (Lane and Crawford, 1979; Murray-Zmijewski et al., 2006). p53 is well known as a tumour suppressor protein due to its ability to induce cell-cycle arrest, DNA repair and apoptosis (Molchadsky et al., 2010). Mutations in the p53 gene often lead to cancer, with p53 being one of the most commonly mutated genes in human cancers (Kandoth et al., 2013). New roles for p53 are continuously being discovered, including in the regulation and differentiation of developmental pathways during embryogenesis (Danilova et al., 2008; Molchadsky et al., 2010).

1.8.4.1 The p53 family of transcription factors

The p53 family contains three known members: p53, p63 and p73. The transcripts are processed by alternative splicing, generating 12 isoforms (Khoury and Bourdon, 2011; Murray-Zmijewski et al., 2006). p53 family members have similar structures, consisting of an N-terminal transactivation domain, a DNA binding domain, an oligomerisation domain and a C-terminal basic domain, which also has DNA-binding capabilities (Murray-Zmijewski et al., 2006).

1.8.4.2 p53 signalling and regulation

p53 is a transcription factor, whose activity can be modulated by post-translational modifications, including acetylation, methylation, ubiquitination and phosphorylation at one or more of its approximately 24 phosphorylation sites (Dai and Gu, 2010; Danilova et al., 2008; Lavin and Gueven, 2006). Different post-

translational modifications influence p53 preferences for binding proteins and downstream targets, influencing diverse cellular events (Hill et al., 2008; Knights et al., 2006). During cellular homeostasis, Mdm2 and Mdm4 modulator proteins are required to moderate the levels of available p53, by targeting p53 for degradation or inhibiting transcription respectively (Ringshausen et al., 2006; Toledo and Wahl, 2006). In the absence of the Mdm2 modulator protein, the post-translation p53 protein is active (Ringshausen et al., 2006). Phosphorylation, by a range of kinases, including MAPK and checkpoint kinases, is an important method of modulating p53 activity (Danilova et al., 2008). For example, phosphorylation at Ser33, Thr81 and Ser315 by cell-cycle dependent kinases leads to new p53 interactions with binding partners and conformational changes, which enhance DNA binding to regulatory regions of target genes, promoting apoptosis (Zacchi et al., 2002; Zheng et al., 2002). The C-terminal domain of p53 is thought to weakly interact with DNA, allow sliding of the p53 protein along the DNA backbone in a one-dimensional manner (Tafvizi et al., 2008). It is thought that the C-terminal domain has an inhibitory function, as an alternatively spliced p53 variant, lacking the 26 C-terminus most amino acids, was found to have elevated capabilities for inducing mesoderm and endoderm marker gene expression in *Xenopus laevis* (Cordenonsi et al., 2003; Takebayashi-Suzuki et al., 2003). p53 can be regulated via its C-terminal domain, for example by the binding of the ectodermal protein zinc finger protein 585B (Znf585b), which prevents p53 induced activation of mesodermal genes in the ectoderm during *Xenopus laevis* development (Sasai et al., 2008). p53 interacts with proteins from different signalling pathways to integrate signalling branches and modulate cellular processes. For instance, during *Xenopus laevis* development, MAPK has been shown to phosphorylate the N-terminal region of p53, enabling p53 to interact with Smad2 to modulate Nodal/ Activin target genes for mesoderm induction (Cordenonsi et al., 2007, 2003; Piccolo, 2008). These signals and mechanisms highlight some of the strategies, which finely balance to tightly modulate p53 activity.

1.8.4.3 p53 in embryogenesis, homeostasis and cancer

New roles for p53 in embryogenesis are continuously being discovered. p53 is expressed during early development in organisms including mouse and *Xenopus laevis* (Schmid et al., 1991; Tchang et al., 1993). p53 downregulation in the early *Xenopus laevis* embryo has been shown to affect mesoderm induction, which impinges upon later development (Cordenonsi et al., 2003). However, p53 null mutant mouse embryos have been reported to develop normally until birth, albeit with a high portion presenting abnormalities including craniofacial malformations, neural tube closure defects and spontaneous tumour formation (Armstrong et al., 1995; Donehower et al., 1992; Sah et al., 1995). This difference is likely due to functional redundancy between the p53 family members in mouse. Indeed, in mouse p53, p63 and p73 expression is detected in the early embryo, and the family members have been shown to have overlapping functions in multiple processes (Hernández-Acosta et al., 2011; Levrero et al., 2000). *Xenopus laevis* expresses only p53 during early development, with p63 activated much later during organogenesis, and p73 not found in lower vertebrates (Cordenonsi et al., 2003; Lu et al., 2001). This lack of redundancy makes *Xenopus laevis* a good model to study the developmental requirements for p53.

p53 is believed to be required for normal cellular homeostasis, by regulating metabolic processes to reflect the proliferation and energy status of a cell (Olovnikov et al., 2009). In addition, p53 has a well-established role responding to cellular stress to activate appropriate repair mechanisms or initiate apoptosis (Lane, 1992; Olovnikov et al., 2009). The regulation, repair and apoptotic functions of p53 are crucial for cancer prevention and p53 misregulation or genetic mutations often result in cancer formation (Kandoth et al., 2013). A diverse range of mutations affect p53. Most mutations are single-base substitutions, which can occur across numerous positions throughout the coding region (Olivier et al., 2010). Genetic mutations often lead to p53 inactivation; however, mutated p53 proteins can also gain additional oncogenic functions, conferring proliferation and survival traits to cancerous cells (Rivlin et al., 2011). Although cancerous mutations can be found throughout the p53

gene, they are often located in conserved regions, with particular nucleotide changes prevailing in a high number of human cancers. For example, a single G to C point mutation at codon 280 results in an arginine to threonine change in human p53 (Sun et al., 1992). Arginine 280 is a fundamental component of the DNA binding domain, thus this mutation renders p53 inactive by disrupting interactions with the phosphate and base groups of DNA (Wright and Lim, 2007). An understanding of specific p53 tumorigenic mutations, and how they function, not only allows the mechanisms of cancers to be unravelled for the development of therapeutic treatments, but also allows specific p53 mutants to be utilised in embryological research. The importance of p53 in normal *Xenopus laevis* development has been investigated using inactivated p53 mutated at codon 280, from arginine to threonine, as a tool to downregulate p53 activity (Wallingford et al., 1997).

1.8.4.4 p53 as a signalling pathway integrator

How a comparatively small number of signalling pathways regulate a vast number of developmental processes is still the focus of ongoing research. Many genes are known to be regulated by the influence of multiple signalling pathways. It has been shown that p53 can integrate signalling pathways and influence a subset of target genes, conferring particular developmental decisions (Danilova et al., 2008). There are many examples of p53 being both positively and negatively regulated to integrate signalling pathways (Danilova et al., 2008). During mesoderm formation in *Xenopus laevis*, it has been suggested that p53 is required to integrate the FGF and Nodal/ Activin signalling pathways (Cordenonsi et al., 2007, 2003). It was demonstrated that FGF signalling results in the phosphorylation of p53, on serine 6 and 9 by Casein Kinase 1, allowing p53 to interact with Nodal/ Activin activated Smad2/3 and influence a subset of Nodal/ Activin target genes (Cordenonsi et al., 2007, 2003; Dupont et al., 2004). In human cells, MAPK has been demonstrated to be required for p53 phosphorylation, at serine 6 and 9, for Smad2 interactions integrating the MAPK and Nodal/ Activin pathways (Danilova et al., 2008; Wang et al., 2007). As both FGF and Nodal/ Activin signalling have been strongly implicated in cardiac specification, it is plausible that pathway crosstalk may be mediated by p53, initiating

successful cardiogenesis. Establishing whether p53 is required for cardiogenesis, and whether that potential requirement is to facilitate signalling pathway specificity or mediate pathway crosstalk is yet to be addressed.

1.9 The genetic control of cardiogenesis

Once specified, cardiac cells begin to express specific cardiac genes which modulate further cardiac development. These cardiac specific transcripts can act as markers for experimental analysis, allowing cells of a particular lineage to be identified. However, there is a lack of known cardiac markers that would allow presumptive cardiac cells to be traced from their time of specification throughout development (Scott, 2012). Several regulatory transcription factors have been investigated which act after initial specification for cardiac development, although none is exclusive to the cardiac lineage (Zaffran and Frasch, 2002). *In Xenopus*, cardiac cells initially comprise a small subset of *mespa*-positive cells (Kriegmair et al., 2013). *mespa*-positive cells are heterogeneous and are also fated to form anterior skeletal muscle and paraxial mesoderm derivatives (Saga et al., 1999). During late gastrula to early neurula stages, *mespa* expression is switched off and the expression of cardiogenic transcription factors *nkx2.5* and *gata* factors are up-regulated. In addition, *tbx5* and *isl1* expression is initiated, marking the primary and secondary heart fields respectively (Pandur et al., 2013). Many cardiomyocyte specific genes are expressed only in differentiated cardiac tissue, for example *myosin heavy chain 6* (*myh6*), *myosin light chain 7* (*myl7*) and *cardiac troponin* (*tnni3*) (Sell, 2013). These serve as useful markers in investigating the size, location and morphology of differentiated tissue.

In mouse, the domains and expression patterns of *mesp1* and *mesp2* were found to be overlapping in posterior mesoderm at the onset of gastrulation (Saga et al., 1997, 1996). *mesp1* and *mesp2* double knockouts in mouse proved lethal; mesoderm migration during gastrulation was found to be unsuccessful and structures such as the heart, somites and gut were not observed, suggesting that *mesp1* and *mesp2* are important for the development of mesoderm derivatives (Kitajima et al., 2000). However, only *mesp1* null-mice displayed abnormal heart development (Saga et al.,

1999), with *mesp2*-null mice displaying normal heart development but defective somitogenesis (Saga et al., 1997). In *Xenopus,* the *mesp1* homologue *mespa* occupies an expression domain during gastrulation which precedes the prospective heart field and is non-overlapping with *mesp1* homologues *mespb* or *mespo*. Knockdown of Mespa protein has been shown to result in the loss of cardiac markers, which can be rescued by *mespa* or human *mesp1*, but not *mespb* or *mespo* (Kriegmair et al., 2013). In addition, *mespa* has been show capable of inducing cardiac markers *in vivo* and *in vitro* (Kriegmair et al., 2013).

nkx2.5 is a member of the NK homeodomain family of transcription factors and is considered to be one of the earliest markers identifying cardiac precursor cells (Benson et al., 1999; Brand, 2003). *nkx2.5* is expressed from late gastrula stages in both the primary and secondary heart fields, and continues to be expressed in the mature heart throughout the left ventricle and atrial chambers (Kasahara et al., 1998; Komuro and Izumo, 1993; Lints et al., 1993; Tonissen et al., 1994). *nkx2.5* overexpression in *Xenopus laevis* and zebrafish can increase the size of the heart, and high concentrations can induce ectopic cardiac tissue (Chen and Fishman, 1996; Cleaver et al., 1996). *nkx2.5* promotes and maintains the expression of cardiac-specific genes, including the transcription factors *hand*, *mef2*, *myl7* and *gatas*, which are required for further development, differentiation and morphogenesis (Akazawa and Komuro, 2005; Brand, 2003; Evans, 1999; Mohun and Sparrow, 1997). *nkx2.5* functions to regulate the maturation of ventricular cardiomyocytes and the development of the conductive system (Thomas et al., 2001; Yamagishi et al., 2001).

Gata factors have multiple roles in embryonic development. *Gata 4, 5* and *6* are expressed throughout cardiac mesoderm, in a similar time and spatial manner to the expression of *nkx2.5* (Laverriere et al., 1994; Patient and McGhee, 2002; Zaffran and Frasch, 2002). *Gata 4* has been shown to induce cardiac tissue and beating foci in pluripotent *Xenopus laevis* cells (Latinkić et al., 2003). In *Drosophila,* co-expression of *gata* and *nkx2.5* homologues can induce ectopic cardiac cells (Gajewski et al., 1999). Cardiogenic *gata* factors have been found important for the regulation of cardiac specific genes, such as *nkx2.5*, and the promotion of genes for differentiated cardiac

tissue, for example *myh6* (Lien et al., 1999; Mohun and Sparrow, 1997; Reiter et al., 1999). In addition, cardiogenic *gata* factors are required for the migration and fusion of bilateral heart primordia and for ventral morphogenesis (Kuo et al., 1997; Molkentin et al., 1997).

T-box transcription factors encoded by *tbx5* and *20* are expressed in the primary heart fields of bilateral cardiac primordia from early neurula stages in *Xenopus laevis,* mouse, chick and fish embryos. At later stages in development, expression is restricted to the posterior of the atria and sinus venosus, and within the left ventricle (Brown et al., 2003; Bruneau et al., 1999; Chapman et al., 1996; Horb and Thomsen, 1999). *Tbx5* has a suggested role in promoting ventricular versus atrial fates and conferring identity along the anterior-posterior extent of the heart (Zaffran and Frasch, 2002). The proteins encoded by *tbx5* and *nkx2.5* have been shown to physically interact, suggesting functional cooperation (Hiroi et al., 2001). *Tbx5* downregulation in mouse or *Xenopus laevis* disrupts cardiac development and decreases in cardiac gene expression, including *nkx2.5*, *myl7* and *gata4*, are observed, suggesting a regulatory role (Bruneau et al., 2001).

isl1 is a LIM homeodomain protein which is first detected at the end of gastrulation in many organisms including *Xenopus laevis* (Brade et al., 2007; Gessert and Kühl, 2009). *isl1* is predominantly expressed in the secondary heart field, overlapping the more anterior domain of *nkx2.5* expression, with positive cells contributing to the outflow tract, portions of the atria and, where applicable, the right ventricle (Cai et al., 2003; Gessert and Kühl, 2009). *isl1* has roles in regulating early cardiac genes, morphogenesis and vasculogenesis (Brade et al., 2007).

1.10 Timing of cardiac specification

The time at which cells are specified into the cardiac lineage has not been precisely defined. At the neurula stages, presumptive cardiac cells excised from the *Xenopus laevis* embryo continue to develop and differentiate (Sater and Jacobson, 1989) and anterior endoderm explants are limited to mid-gastrulation for their ability to induce

cardiogenesis in responding tissue (Samuel and Latinkić, 2009). Cardiac gene transcripts, for example *mespa* and *nkx2.5*, are first detected during the late gastrula stages (Evans et al., 1995; Kriegmair et al., 2013; Tonissen et al., 1994). Transplantation of pre-gastrula presumptive cardiogenic mouse tissues into chick embryos at different locations results in the persistence of cardiac markers *nkx2.5* and *gata4* (Auda-Boucher et al., 2000). Evidence suggests that cardiac tissue has been specified by the end of gastrulation, but further research needs to be conducted to better understand the precise timing in which cells acquire a cardiac fate.

1.11 Cardiac disease and regenerative medicine

The heart is a vital organ, therefore any condition that negatively affects normal cardiovascular function can be life changing or fatal. Congenital heart disease (CHD) describes a range of birth defects which affect normal heart function, for example septal defects, aorta and pulmonary valve restrictions and artery transposition (Bruneau, 2008). Congenital heart diseases affect nearly 1% of new-borns and are the leading non-infectious cause of infant mortality in the western world (Bruneau, 2008; Roos-Hesselink et al., 2005). In addition, congenital heart diseases have an increased occurrence when assisted reproductive technologies have been employed (Tararbit et al., 2013), rendering congenital heart diseases an area which warrants further research. Defects in early cell signalling and fate decisions often cause congenital heart diseases, therefore an understanding of the complex mechanisms regulating cardiogenesis will aid in the development of therapies to reduce and treat congenital heart diseases cases (Harvey, 2002; Mohun et al., 2003).

The mature heart can be affected by diseases, such as coronary heart disease, where the coronary arteries become blocked by a build-up of fatty materials (Libby and Theroux, 2005). This can lead to cardiac infarction, where a lack of oxygen results in the death of cardiac-specific cells and replacement with non-cardiac scar tissue (Batalov and Feinberg, 2015). The vertebrate heart has limited potential to functionally repair itself and continued loss of contractile cardiomyocytes will result in cardiac failure, causing major mortality worldwide (Laflamme and Murry, 2005;

Roger, 2013; Xin et al., 2013). Therefore, the human heart is a target for developing regenerative medicine therapies. There are several approaches to therapeutic cardiac regenerative medicine, including transplanting cardiomyocytes derived from the directed differentiation of embryonic stem cells (ESC) or induced pluripotent stem cells (iPSC); converting heart fibroblasts into cardiomyocytes; or ideally by inducing self-repair *in situ* by stimulating a latent pool of cardiac progenitor cells.

ESCs and iPSCs can be directed to form cardiomyocytes, although reports describe them as resembling immature embryonic/ fetal cardiomyocytes (Batalov and Feinberg, 2015; Vidarsson et al., 2010). Therapeutic strategies aim to transplant these cardiomyocytes into damaged hearts to remuscularise and improve contractile function (Pawani and Bhartiya, 2013). Initial experiments have demonstrated that repair was apparent, but not sustainable, and problems such as arrhythmias arise (Pawani and Bhartiya, 2013; Wu et al., 2000). Human ESC and iPSC-derived cardiomyocytes are additionally utilised as platforms by the pharmaceutical industry to evaluate the efficacy and safety of new drugs (Vidarsson et al., 2010).

The activation of select cardiac-specific transcription factors in cardiac-residing fibroblasts can lead to the direct induction of cardiomyocyte-like cells, without the requirement for fibroblast to first be reprogrammed into the pluripotent state. With current techniques, the derived and native cardiomyocytes present some differences, including structural differences which can lead to arrhythmia (Efe et al., 2011; Fu et al., 2015; Ieda et al., 2010; Qian et al., 2012; Xin et al., 2013). However, with further research, the direct reprogramming of cardiac fibroblasts may provide a useful approach to cardiac regenerative medicine.

Until recently, the heart was considered to be a terminally differentiated organ. However, there is evidence that a latent myocardial progenitor cell population exists, which gradually renews cardiomyocytes at a turnover of less than 1% per year (Beltrami et al., 2003; Bergmann et al., 2009; Hierlihy et al., 2002). It is still debated whether new cardiomyocytes are formed from a latent pool of stem cells, or from the proliferation of existing cardiomyocytes (Bulatovic et al., 2015). A cardiac

progenitor population, which can be therapeutically stimulated to produce cardiomyocytes for repair, is an attractive target for further research. Furthermore, it abrogates the potential downfalls of alternative approaches, such as delivery strategy, integration or rejection success and the tumorigenicity of ESC and iPSC therapies (Mercola et al., 2011).

These studies provide strategies for improving treatments for cardiac damage using regenerative medicine. A comprehensive understanding of the mechanisms that govern the specification and development of cardiac cells throughout embryogenesis is imperative for developing superior protocols for the directed differentiation of cardiomyocytes for regenerative medicine.

1.12 Thesis aims

The aim of this thesis was to investigate the requirement and timing of Nodal/ Activin and FGF signalling in cardiac specification, and to identify whether p53 has a novel role in heart development, *in vivo* using *Xenopus laevis* embryos. Previous investigations have strongly implicated the Nodal/ Activin and FGF signalling pathways in cardiac specification (Sections 1.8.1.5 and 1.8.2.5). However, previous research has not clearly separated the role of Nodal/ Activin and FGF signalling from their preceding requirement in mesoderm induction and broader functions in embryonic development. Furthermore, the timing during which cardiac specification occurs is largely unknown (Section 1.10). Utilising a variety of techniques, including small soluble molecular inhibitors, morpholino oligonucleotide and dominant negative constructs, the Nodal/ Activin, FGF and p53 signalling pathways were manipulated, and the effects on cardiac tissue specification and later heart development examined.

2 Materials and Methods

2.1 *Xenopus Laevis* embryo manipulations

2.1.1 Obtaining embryos

Wild type adult *Xenopus laevis* were obtained from Nasco, US and grown in-house at Cardiff University. Transgenic cardiac actin –green fluorescent protein (CA-GFP) adult *Xenopus laevis* were grown in-house at Cardiff University. Adult *Xenopus laevis* were housed at 18^{O}C. Adults were injected into the dorsal lymph sac with an appropriate amount of human chorionic gonadotropin (HCG, Sigma), typically 600 units for females and 200 units for males depending on an individual's size. Natural mating was preferential so a male frog and female frog were left in water in a mating tank overnight at 18^{O}C to mate and embryos were collected the following day. For *in vitro* fertilisation (IVF), females were induced as described above and left overnight at 18^{O}C. Eggs were collected onto a petri dish by gently squeezing the female. Male frogs were sacrificed using procedures in home office Schedule 1 and testes were surgically removed and stored in Lebovitz's L15 medium (Sigma). Segments of testes were macerated and spread over the eggs, then left for 5 minutes to allow fertilisation. The dish of fertilised embryos was flooded with 10% Normal Amphibian Medium (1X NAM: 110 mM sodium chloride (NaCl, Fisher), 2 mM potassium chloride (KCl, Fisher), 1 mM calcium nitrate ($Ca(NO_3)_2$, Fisher), 1 mM magnesium sulphate ($MgSO_4$, Fisher), 0.1 mM ethylenediaminetetraacetic acid (EDTA, Fisher), 1 mM sodium bicarbonate ($NaHCO_3$, Sigma), 2 mM sodium phosphate (Na_3PO_4, Sigma) pH 7.4) (Sive et al., 2000; Slack and Forman, 1980) and left for 20 minutes to allow egg rotation. All embryos, fertilised naturally or using IVF, were de-jellied in 2% cysteine-hydrochloride (Sigma), pH 7.8, for 5-10 minutes as required and washed thoroughly in 10% NAM.

2.1.2 Maintaining embryos

Embryos were cultured in 10% NAM at 21^{O}C in plastic petri dishes (Fisher) during experiments, unless otherwise stated. Prior to microinjections, embryos were kept

at lower temperatures of 14-20^{O}C to reduce the speed of development, thus allowing more time for injecting.

2.1.3 Staging embryos

Xenopus laevis embryos undergo regular changes that are specific to particular developmental stages. Embryonic stage was assessed by comparison to Nieuwkoop and Faber normal table of *Xenopus laevis* development (Nieuwkoop and Faber, 1994).

2.1.4 Microinjection

Embryos were transferred into 3% Ficoll 400 (Sigma) in 75% NAM for injection and remained in this solution before being transferred to fresh 10% NAM prior to gastrulation. The 3% Ficoll in 75% NAM solution helps prevent the cytoplasm and injected material leaking from the embryo once the injection needle has been removed and helps cell healing. Fine glass needles were prepared from capillary tubing using a Kopf 720 Needle Puller (Kopf Instruments). Needles were connected to an IM 300 Micro-injector (Narishige Scientific) and injection samples were filled. Needles were calibrated to inject 10 nl in 4 bursts using a 10 mm graticule with 100 divisions of 0.1 mm (Graticule Limited). Embryos injected at the one, two or four cell stage received 10 nl, 5 nl or 2.5 nl per blastomere respectively (equivalent to 10 nl per embryo). Blastomeres of an 8 cell embryo received 2.5 nl each. Injections into the blastocoel of stage 8 or older embryos received 5 nl. Injections are often described either as uniform or targeted. Uniform injection refers to injections where an embryo has received the same injected material, equally, into all of its cells, regardless of which stage it was injected at. Targeted injections refer to an embryo which has been injected into a select portion of blastomeres, for example two cells of an eight cell embryo. Injection samples routinely incorporated a 10% mix of rhodamine-dextran (20 mg/ml, Invitrogen) and dextran-biotin (25 mg/ml, Invitrogen), allowing cells which received injected material to be traced by either fluorescence microscopy or colour stain development. Rhodamine-dextran emits red

fluorescence when excited at 570 nm, thus injected material was traced in live embryos using a Leica MZ16 Fluorescence microscope (Leica). Biotin lineage trace was detected following whole mount *in situ* hybridisation procedures, Section 2.7.

2.1.5 Soluble inhibitor media treatment

Stock solutions of inhibitors were made by dissolving in dimethyl sulfoxide (DMSO, Fisher) to the concentrations displayed in Table 2:1. Stock solutions were aliquoted into single-use volumes and stored at -80^{O}C. When new batches of inhibitor were purchased, each was titrated and tested for effectiveness to ensure that the new batch of inhibitor was used at a concentration that resulted in the same phenotype as the original batch. It was found that there was variation in efficacy of inhibitors between batches. In addition, there were variations in the response of batches of embryos to inhibitor treatment under identical treatment conditions. Therefore each experiment included a positive control consisting of embryos that were treated from the 2 cell stage.

Inhibitor treatments were carried out in plastic 12 well plates (Fisher) with a total volume of 1 ml, maximum 50 embryos per well. The inhibitor stock solution was diluted to a working concentration (Table 2:1) in 800 µl of 10% NAM immediately prior to *Xenopus laevis* embryos being transferred to treatment wells, allowing 200 µl of 10% NAM to be transferred with the embryos. Embryos were lightly rocked on a mechanical rocker for 5 minutes to allow inhibitor penetration. All treatments were kept at 21^{O}C in the dark, due to inhibitor light sensitivity. The embryos were treated with the inhibitors for different lengths of time. For 'continuous' incubation, embryos were incubated until at least stage 25. For inhibitor incubations not classified as continuous, the embryos were washed by two 5 minute washes, gently rocking in 30 ml of fresh 10% NAM and then the embryos were incubated in 10% NAM for further development. Control samples were treated with DMSO matching the largest volume of inhibitor solution used. Optimum inhibitor working concentrations were determined by selecting the concentration which consistently resulted in embryos lacking discernible axis and embryonic features upon treatment at the 2 cell stage,

without causing embryonic death. In each subsequent experiment involving inhibitors, inhibitor action was validated by confirming the expected phenotype, at tadpole stage, of embryos treated with inhibitor at the 2 cell stage, in addition to molecular analysis.

Name	Inhibits	Stock	Formula	IC_{50}	Mr	Source	Reference
SB505124	ALK 4/5/7	100 mM	$C_{20}H_{21}N_3O_2$	4/5: 129/47 nM	335.4	Tocris	(DaCosta Byfield et al., 2004; Luxardi et al., 2010; Vogt et al., 2011)
A-83-01	ALK 4/5/7	50 mM	$C_{25}H_{19}N_5S$	4/5/7: 45/12/7.5 nM	421.52	Tocris	(Samuel and Latinkić, 2009; Tojo et al., 2005; Vogt et al., 2011)
SB431542	ALK 4/5/7	75 mM	$C_{22}H_{16}N_4O_3$	5: 94 nM	384.39	Sigma	(Ho et al., 2006; Inman et al., 2002)
SU5402	FGFR1	50 mM	$C_{17}H_{16}N_2O_3$	30 µM	296.3	Calbiochem/ Sigma	(Deimling and Drysdale, 2011; Delaune et al., 2005; Samuel and Latinkić, 2009; Shifley et al., 2012)
PD0325901	MEK	10 mM	$C_{16}H_{14}F_3IN_2O_4$	5- 1500 nM	482.19	Selleckchem	(Anastasaki et al., 2012; Sebolt-Leopold and Herrera, 2004)
U0126	MEK 1/2	35 mM	$C_{18}H_{16}N_6S_2$	1/2: 72/28 nM	426.56	Sigma	(Favata et al., 1998; Samuel and Latinkić, 2009)
AZD4547	FGFR1-3	100 mM	$C_{26}H_{33}N_5O_3$	1/2/3: 0.2/2.5/1.8 nM	463.57	Selleckchem	(Gavine et al., 2012)
PD173074	FGFR1-3	100 mM	$C_{28}H_{41}N_7O_3$	1/3: 21.5/5 nM	523.67	Selleckchem	(Rankin et al., 2012)
SB203580	MAPK	2.65 mM	$C_{21}H_{16}FN_3OS$	3-5 µM	377.43	Calbiochem	(Hasegawa and Cahill, 2004)

Table 2:1. Molecular inhibitors

2.1.6 Dexamethasone treatment

To induce hormone-activated protein function of proteins fused to the glucocorticoid receptor (GR), dexamethasone (DEX), stored at –20^{O}C as a 2 mM stock in ethanol, was mixed directly with embryonic media to a final concentration of 2 µM. For removal of DEX, two 5 minute washes, gently rocking the embryos in 30 ml of fresh 10% NAM was carried out, allowing further development in 10% NAM.

2.1.7 Removing the vitelline membrane

The vitelline membrane is a thin transparent membrane close to the embryo's surface that is not removed during de-jellying by 2% cysteine-hydrochloride. Developing embryos naturally shed the vitelline membrane during the early tadpole stages of development. The vitelline membrane must be removed to allow embryonic manipulations, such as animal cap cutting, or before fixing embryos for whole mount *in situ* hybridisation to allow probe penetration. Vitelline membranes are removed manually using two pairs of sharp forceps; one pair holds the vitelline membrane whilst the other pair tears the vitelline membrane open to release the embryo.

2.1.8 Animal cap isolation and dissociation

Animal cap (AC) isolation and dissociation was as described in Sive *et al.* (Sive et al., 2000). Briefly, embryos were placed in 75% NAM and the vitelline membrane was removed. A pair of sharp forceps were used to remove the centre-most 50% of the AC, ensuring homogeneity and that no marginal zone cells are collected. For dissociation, ACs were gently pipetted until separation into single cells occurred, in a calcium magnesium free medium (CMFM: 88 mM NaCl, 1 mM KCl, 2.4 mM $NaHCO_3$, 5.7 mM Tris pH 7.6) to slow the process of cell aggregation. ACs and dissociated AC cells were cultured on 1% agarose (Bioline).

2.1.9 Activin treatment

Soluble Activin (Smith et al., 1990) was used to activate ALK4/5/7 signalling in dissociated animal cap cells. A solution of 75% NAM 0.1% bovine serum albumin (BSA, Sigma) was prepared, then Activin was added to a final working concentration of 16 U/ml from an 8 U/µl stock. Dissociated animal cap cells were transferred directly into this solution.

2.1.10 Imaging

Live embryos were anesthetised in 10% NAM containing 500 mg/L Ethyl 3-aminobenzoate methanesulfonate (MS222, Sigma). All samples, both live and those that had been processed for whole mount *in situ* hybridisation and immunohistochemistry, were imaged on 1% agarose in a plastic dish. Embryos which were made to appear transparent (clearing, Section 2.10.2) were imaged in a glass dish (Sigma). Images were obtained on a Leica MZ16 Fluorescence microscope using a Leica DFC300 FX camera (Leica).

2.1.11 Bimolecular fluorescence complementation

Bimolecular fluorescence complementation (BiFC) was used to visualise the Smad2-Smad4 complex using an enhanced yellow fluorescent protein called Venus. The N terminal of Venus is coupled to Smad4 (VNS4), whereas the C terminal portion is associated with Smad2 (VCS2) (Nagai et al., 2002; Saka et al., 2008, 2007). VCS2, VNS4 and mCherry (Shaner et al., 2004) mRNAs were injected uniformly into the animal hemisphere, and various inhibitor and Activin treatments were carried out. Dissociated animal cap cells were imaged for green Smad2-Smad4-Venus positive nuclei, bright-field and red mCherry, to positively identify cells containing injected material. The number of positive nuclei (green) to positively identified injected cells (red) was calculated, omitting cells that did not express mCherry. An unpaired 2-tailed t-test of equal variances was used to test whether the samples were significantly different at the 0.05 significance level.

2.2 *Xenopus tropicalis* embryo manipulations

2.2.1 Obtaining embryos

Adult *Xenopus tropicalis* were sourced from the European Xenopus Resource Centre (EXRC), Portsmouth and maintained at 24^{O}C. Adults were primed by injecting 20 units of HCG into the dorsal lymph sac. The following morning, adults received a booster with a further injection of approximately 100 units for males, or 200 units for females, depending on an individual's size. Individuals were left at 24^{O}C for 4-6 hours, then IVF was performed. Eggs were collected onto a petri dish by gently squeezing females. Male frogs were sacrificed using home office Schedule 1 and testes surgically removed and stored in Lebovitz's L15 medium. Segments of testes were macerated and spread over the eggs then left for 5 minutes to allow fertilisation. The dish of fertilised embryos was flooded with 0.1 X Marc's Modified Ringers (1X MMR; 100 mM NaCl, 2 mM KCl, 1 mM $MgSO_4$, 2 mM calcium chloride ($CaCl_2$, Fisher), 5 mM HEPES (Sigma), pH 7.5) for 10 minutes. Embryos were de-jellied in 2% cysteine-hydrochloride in MMR, pH 7.8, for 5-10 minutes as required and washed thoroughly in MMR.

2.2.2 Maintaining embryos

Embryos were cultured in 0.1X MMR, or 3% Ficoll in 0.1X MMR prior to gastrulation if injected, and incubated at 21-24^{O}C in plastic petri dishes.

2.2.3 Staging embryos

Embryonic stage was assessed by comparison to Nieuwkoop and Faber normal table of *Xenopus laevis* development (Nieuwkoop and Faber, 1994).

2.2.4 Microinjection

Embryos were transferred into a 3% Ficoll in 0.1X MMR solution for injection, and remained in this solution before being transferred to fresh 0.1X MMR prior to gastrulation. Fine glass needles were prepared from capillary tubing using a Kopf 720 Needle Puller. Needles were connected to an IM 300 Micro-injector and injection samples back-loaded. Needles were calibrated to inject 4 nl in 2 bursts using an eyepiece graticule. Injections were carried out at the one cell stage, with each embryo receiving a total injection volume of 4 nl.

2.3 Preparation of reagents for microinjection

2.3.1 RNA

2.3.1.1 Template preparation and purification

Circular plasmids were linearised using an appropriate restriction enzyme (Table 2:2). 1 µg circular plasmid, 1X enzyme specific buffer (NEB), 1X BSA (Promega) if required by enzyme, 10 units restriction enzyme (NEB) and ddH_2O to a final volume of 30 µl were mixed and incubated at the optimum temperature, specified by the restriction enzyme, for 1 hour. Linearised plasmids were purified using QIAquick PCR purification kit (Section 2.4.1).

2.3.1.2 RNA synthesis

SP6 polymerase synthesis was carried out using mMessage mMachine Kit (Ambion) according to the manufacturer's instructions - 1 µg linear template, 10 µl 2X NTP/CAP, 2 µl 10X Reaction Buffer, 2 µl enzyme mix and ddH_2O to 20 µl were mixed and incubated at 37^{O}C for 2 hour. This was followed by the addition of 2 units TURBO DNase for 15 minutes at 37^{O}C to degrade the DNA template.

2.3.1.3 RNA purification

mRNA was purified using a Zymo RNA Clean and Concentrator kit (Zymo Research) according to the manufacturer's instructions. The Zymo RNA Clean and Concentrator kit protocol is based on nucleic acid purification by silica adsorption (Boom et al., 1990). RNA was bound to the Zymo-Spin column silica membrane under high salt conditions with ethanol to aid RNA binding. The RNA-bound column was washed with a high salt and ethanol solution to remove enzymes, nucleotides and other impurities. mRNA was eluted under low salt conditions. The mRNA concentrations were determined by measuring the absorption at 260 nm on a SmartSpecPlus spectrophotometer (Bio-Rad). Quality control was carried out by visually assessing the presence of RNA by agarose gel electrophoresis (Section 2.4.2). RNA was stored at –20^{O}C. Information regarding injections and doses are listed throughout the results chapters.

Construct	Description	Species	Accession number	Vector	Restriction enzyme for linearisation	Polymerase for mRNA synthesis	Source	Reference
DN-FGFR1	Dominant negative FGF receptor 1	*Xenopus laevis*	BC170136	pSP64T	EcoRI	SP6	Amaya Lab	(Amaya et al., 1991)
GR-Smad2	Glucocorticoid receptor inducible Smad2	*Homo sapiens*	AF027964	pCS107	Asc1	SP6	Chang Lab	(Chang and Harland, 2007; M. Howell and Hill, 1997)
GR-tSmad2	Glucocorticoid receptor inducible truncated Smad2	*Homo sapiens*	AF027964	pCS107	Asc1	SP6	Chang Lab	(Chang and Harland, 2007; M. Howell and Hill, 1997)
Hp53	Human p53	*Homo sapiens*	AF307851	pSP64TS	Sac1	SP6	Vize lab	(Wallingford et al., 1997)
Hp53thr280	Human p53 containing Arginine 280 to Threonine mutation	*Homo sapiens*	Based on AF307851	pSP64TS	Sac1	SP6	Created by site directed mutagenesis	(Wallingford et al., 1997)

mCherry	His6-NLL-EcMetRS-mCherry fusion	Synthetic construct	KC608723	pCS2+	Not1	SP6	Mayor lab	(Shaner et al., 2004)
p53-ATG-HA	*Xenopus laevis* p53 starting from ATG, containing HA tag	*Xenopus laevis*	BC084064	pCS2+	Not1	SP6	Modified from Source Bioscience	(Cordenonsi et al., 2007)
p53-5'U92-HA	*Xenopus laevis* p53 including 92 bases of 5'UTR, containing HA tag	*Xenopus laevis*	BC084064	pCS2+	Not1	SP6	Modified from Source Bioscience	(Cordenonsi et al., 2007)
VCS2	C-terminal half of Venus conjugated to Smad2	Venus originates from *Aequorea victoria*, Smad2 is *Xenopus laevis*	Smad4 AB385155 Venus AB512479	pCS2+	Not1	SP6	Smith Lab	(Nagai et al., 2002; Saka et al., 2008, 2007)
VNS4	C-terminal half of Venus conjugated to Smad4	Venus originates from *Aequorea victoria*, Smad4 is *Homo sapiens*	Smad4 AB385155 Venus AB512479	pCS2+	Not1	SP6	Smith Lab	(Nagai et al., 2002; Saka et al., 2008, 2007)

Table 2:2. Templates for mRNA synthesis

2.3.2 Morpholino Oligonucleotides

Antisense Morpholino Oligonucleotides (MOs), see Table 2:3, were obtained from Gene Tools and were used to downregulate gene expression (Dash et al., 1987; Heasman, 2002). MOs were reconstituted in 5 mM HEPES, pH 7.6 (Sigma) to 12.5 µg/µl, except for the control MO to 40 µg/µl. Working stocks were prepared incorporating a 10% mix of rhodamine-dextran and dextran-biotin. Information regarding injections and doses are listed throughout the results chapters. All MO stocks were stored at -20^{O}C.

Name	Action	Sequence	Reference
Control MO	Control	GTAACGATTTGAGTTTGGTGTTCAT	(Haworth et al., 2008)
p53 MO1	Translation blocking. Binds at ATG site.	GAACCTTCCTCTGAGACCGGCATGG	(Cordenonsi et al., 2003)
p53 MO2	Translation blocking. Binds at ATG site.	GCCGGTCTCAGAGGAAGGTTCCATT	(Takebayashi-Suzuki et al., 2003)
p53 MO3	Translation blocking. Binds 65-40bp upstream of ATG	TTCTATCCTCTCTGCTTCCTCGTGC	New design
p53 MO E2I	Splice blocking	AAAGCACAAGAGGGACTCACCGTGC	New design
p53 MO E3I	Splice blocking	ATAAGAATGAAAGCACTCACCCTCC	New design

Table 2:3. Morpholino Oligonucleotides

2.3.3 Lefty Protein

Recombinant human Lefty A protein (R&D Systems) was reconstituted at 500 µg/ml in 0.2 µM cellulose filter sterilised (Anachem) phosphate buffered saline (PBS; 137 mM NaCl, 2.7 mM KCl, 10 mM sodium phosphate (Na_2HPO_4, Fisher)), 1.8 mM potassium phosphate (KH_2PO_4 pH 7, Fisher), pH 7.4, containing 0.1% BSA as a carrier protein and immediately aliquoted and stored at -20^{O}C. Working stocks were prepared incorporating a 10% mix of rhodamine-dextran and dextran-biotin.

2.4 Molecular biology techniques

2.4.1 DNA and RNA purification

DNA and RNA was purified using a QIAquick PCR purification kit (Qiagen) according to the manufacturer's instructions. The QIAquick PCR purification kit protocol is based on nucleic acid purification by silica adsorption (Boom et al., 1990; Cady et al., 2003). DNA samples were bound to the silica QIAquick membrane under high salt conditions. The silica membrane was washed with a high salt and ethanol solution to remove enzymes, primers, nucleotides, salts, and other impurities. DNA was eluted in a small volume of low salt solution.

2.4.2 Agarose gel electrophoresis

A 1% agarose in tris-borate-EDTA (TBE: 89 mM tris, 89 mM Boric acid (Fisher), 2 mM EDTA, pH 8.3) gel containing 0.5 µg/ml ethidium bromide (Fluka) was cast in a horizontal EM100 Mini Submarine Gel Unit (Electrophoresis). Once set, the cast was flooded with TBE. Samples were mixed with 5X DNA loading dye (Fermentas) and loaded one sample per well alongside a GeneRuler 1kb plus DNA ladder (Fermentas). 70V was applied across the gel for 30 minutes using a PowerPac (Bio-Rad) to separate the DNA or RNA fragments by size.

2.4.3 Bacteria transformation, selection and growth

Competent cells (silver efficiency ≥10^8 cfu/ µg, Bioline) were thawed on ice and 0.5 µg of circular plasmid DNA (see Table 2:2 and Table 2:4 for specific plasmids) was added at a volume of ≤10% plasmid. The competent cell-plasmid mix was incubated on ice for 30 minutes then subjected to heat shock at 42^{O}C for 30 seconds before being replaced on ice for a further 5 minutes. The solution was made up to 10X the volume using room temperature (RT) super optimal broth with catabolite repression (SOC) medium (2% bacto-tryptone (BD Bioscience), 0.5% yeast extract (Formedium), 10 mM NaCl, 2.5 mM KCL, 10 mM $MgSO_4$, 20 mM glucose (Sigma)) then shaken vigorously for 60 minutes at 37^{O}C. 100 µl of the transformation mix was spread onto a pre-warmed Luria broth agar plate (1% bacto-tryptone, 0.5% yeast extract, 171 mM NaCl, 1.5% bacto-agar (BD Bioscience)) supplemented with 1 µg/ml ampicillin (Sigma) and incubated at 37^{O}C until visible colonies formed. Colonies were picked using a sterile pipette tip and transferred into Luria broth (1% tryptone, 0.5% yeast extract, 171 mM NaCl) supplemented with 1 µg/ml ampicillin and vigorously shaken overnight at 37^{O}C. Luria broth and Luria broth agar were autoclaved at 121^{O}C for 20 minutes prior to the addition of the ampicillin.

2.4.4 Plasmid extraction

Plasmids were extracted using a QIAprep miniprep kit (Qiagen), according to the manufacturer's instructions. The QIAprep miniprep kit procedure was based on alkaline lysis of bacterial culture and selective alkaline denaturation of chromosomal DNA (Birnboim and Doly, 1979). Upon lysate neutralisation, chromosomal DNA forms insoluble aggregates (Birnboim and Doly, 1979). Soluble DNA was bound to the silica QIAprep membrane under high salt conditions. The DNA-bound QIAprep membrane was washed to remove proteins, salts and other impruities, then plasmid DNA was eluted in a low salt buffer. Plasmid concentrations were determined by UV spectrophotometry on a SmartSpecPlus (Bio-Rad) by measuring the absorption at 260 nm. Plasmids were sequenced (Eurofins) to verify the presence and identity of the gene of interest.

2.5 Site-directed mutagenesis of human p53

To create a dominant negative (DN) p53 construct (hp53thr280), previously reported by Wallingford *et al.* (Wallingford et al., 1997), a polymerase chain reaction (PCR)-based technique was utilised to create a single nucleotide modification. Codon 280 was altered from AGA to ACA, resulting in amino acid 280 Arginine (Arg, R) to Threonine (Thr, T) change. Arg280 forms the most important major grove contact with DNA, thus hp53thr280 has compromised DNA binding (Wright et al., 2002). p53 forms a tetramer (Friedman et al., 1993; Stenger et al., 1992) so theoretically one hp53thr280 protein can associate with up to three wild type p53 protein molecules, compromising the function of the tetramer, thus acting in a dominant negative manner.

Human p53 (hp53) (GenBank: AF307851) in pSP64TS was a gift from the Vize Lab. The following reagents were mixed: 1 µg hp53-pSP64TS, 1X Phusion high fidelity Buffer (Thermo Scientific), 1 mM deoxynucleotides (dNTP's, Invitrogen), 0.5 µM forward primer 5'-GTGTTTGTGCCTGTCCTGGGACAGACCGGCGCACAGAGGAAGAGAATCTCCGC -3' (Invitrogen), 0.5 µM reverse primer 5'-GCGGAGATTCTCTTCCTCTGTGCGCCGGTCTGTCCCAGGACAGGCACAAACAC -3' (Invitrogen), 1 unit Phusion High Fidelity DNA Polymerase (Thermo Scientific) and double distilled water (ddH_2O) to 25 µl. Using a MJ Mini Thermal Cycler PCR machine (Bio-Rad) the reaction was subject to the following cycling conditions:

$98^{O}C$ for 1 minute

$98^{O}C$ for 1 minute	30 cycles
$62^{O}C$ for 1 minute	
$72^{O}c$ for 5½ minutes	

$72^{O}c$ for 10 minutes

Following PCR, 20 units of the restriction enzyme Dpn1 (NEB) was added to digest the original template DNA, as Dpn1 only cleaves at methylated sites. The reaction

was incubated at 37^{O}C for 2 hours, followed by incubation at 80^{O}C for 15 minutes to inactivate Dpn1. The product of the PCR reaction was transformed and expanded (Section 2.4.3). Plasmid clones were sequenced to ensure that the plasmid selected for further use was correct. A verified purified plasmid was then used as a template to produce hp53thr280 mRNA for embryonic microinjection (Section 2.4.4 and 2.3.1).

2.6 Preparing *Xenopus laevis* p53 constructs

Xenopus laevis p53 (p53) was PCR amplified in two separate reactions to produce two different constructs (p53-ATG-HA and p53-92UTR-HA) from pCMVSport6-xp53 (Source Bioscience, accession number BC084064). A common 3' primer GCGGAATTCTCAAGCGTAATCTGGCACATCGTATGGGTATTCCGAGTCGGGCTGTT was used to introduce a human influenza hemagglutinin (HA) tag sequence at the carboxy-terminus. One 5' primer, sequence CGCGGATCCATGGAACCTTCCTCTGAGACC, began at the p53 ATG start site, whereas the other, sequence CGCGGATCCACACGAGGAAGCAGAGAGGA, incorporated 92 bases from the 5' untranslated region (5' UTR). Primers were purchased from Invitrogen. The following reagents were mixed: 1X Q5 high fidelity master mix (NEB), 0.5 µM 3' primer, 0.5 µM 5' primer, 1 µg pCMVSport6-xp53 and ddH_20 to 50 µl and subjected to the following cycling conditions using a PeqStar Thermocycler (Peqlab):

98^{O}C for 30 minutes

- 98^{O}C for 30 seconds
- 40^{O}C for 30 seconds
- 72^{O}c for 80 seconds

(2 cycles)

- 98^{O}C for 30 seconds
- 58^{O}C for 30 seconds
- 72^{O}c for 80 seconds

(33 cycles)

72^{O}c for 10 minutes

PCR products were purified using a QIAquick PCR purification kit (Section 2.4.1). Purified p53 amplicons were cleaved with BamHI (NEB) and EcoRI (NEB) restriction enzymes, whose restriction sites were incorporated into the amplification primers. 1 µg DNA, 1X buffer 4 (NEB), 40 units BamHI, 40 units EcoRI and ddH_2O to 30 µl were mixed and incubated for 3 hours at 37^OC. pCS2+ vector was also subject to the same restriction enzyme digestion, followed by the addition of 1X Antarctic Phosphatase reaction buffer (NEB) and 5 units of Antarctic Phosphatase (NEB) to remove the 5' phosphate from the DNA to facilitate the subsequent ligation reaction. DNA fragments were separated by size using agarose gel electrophoresis (Section 2.4.2). DNA fragments were visualised using an UVIpure transilluminator (UVItech) and the desired fragment (~1.2kb for p53 products, ~4kb for pCS2+), measured by size against the DNA ladder, was excised and purified using QIAquick gel extraction kit according to the manufacturer's instructions. The QIAquick gel extraction kit protocol is based on silica membrane bound nucleic acid purification (Boom et al., 1990; Cady et al., 2003). Excised gel slices were dissolved in high salt solution by incubating at 50^OC, aided by vortexing. DNA was adsorbed onto the silica QIAquick membrane under high salt conditions. The membrane was washed using an ethanol containing buffer to remove enzymes, salts, ethidium bromide, agarose, dyes and other impurities. DNA was eluted in a small volume of low salt solution.

p53 DNA fragments were ligated into pCS2+ using the Quick Ligation kit (NEB) according to manufacturer's instructions - 50 ng pCS2+, 45 ng p53 products, 1X Quick Ligation Buffer, 200 units Quick T4 DNA Ligase and ddH_2O to 10 µl were mixed and incubated at RT for 5 minutes, then chilled on ice. Circular plasmid numbers were amplified using bacterial culture then used as templates for the production of mRNA for embryonic microinjections (Section 2.4.3, 2.4.4 and 2.3.1).

2.7 Whole mount *in situ* hybridisation

Whole mount *in situ* hybridisation (WMISH) was used to detect the expression and localisation of specific mRNAs within an embryo. WMISH was adapted from procedures outlined in Sive *et al.* (Sive et al., 2000).

2.7.1 Riboprobe template preparation

The following reagents were mixed and incubated at 37^{O}C for one hour to linearise DNA: 1 µg circular plasmid DNA, 10 units restriction enzyme (various manufacturers), 1X restriction enzyme specific buffer (NEB), and ddH_2O to 20µl. An appropriate restriction enzyme (Table 2:4) was used to cut each plasmid approximately 500-1000bp from the reverse promoter in the plasmid. Purification of linearised DNA was carried out using QIAquick PCR purification kit (Section 2.4.1).

2.7.2 Riboprobe synthesis and purification

Riboprobes were labelled with either digoxigenin labelling mix (Roche) or fluorescein labelling mix (Roche) and transcribed using an appropriate polymerase (Table 2:4), either T7 (Roche) or SP6 (NEB). 200ng linearised DNA, 1X digoxigenin or fluorescein labelling mix (Roche), 1x transcription buffer containing DTT (Invitrogen), 2 U/µl RNA polymerase, 1 U/µl Ribolock RNase inhibitor (Thermo Scientific) and ddH_2O to 20µl were mixed and incubated at 37^{O}C for 2 hours. Riboprobes were purified using ProbeQuantTM G-50 micro columns (GE healthcare) according to the manufacturer's instructions. ProbeQuantTM G-50 micro columns contain Sephadex, which is a trademarked cross-linked dextran gel, and works by filtration chromatography (Porath and Flodin, 1959). Riboprobe samples were loaded into the centre of a G-50 spin column and centrifugation was used to purify the riboprobes. Quality control of riboprobe production and an estimation of the quantity riboprobe was carried out by visually assessing the riboprobe by agarose gel electrophoresis (Section2.4.2). Riboprobes were stored at –20^{O}C.

Gene symbol	Gene name	Used to visualise	Species	Vector	Restriction enzyme	Polymerase	Reference
hba3	*hemoglobin alpha 3 subunit*	Blood island	*Xenopus tropicalis*	pCS107	Pst1	T7	(Gilchrist et al., 2004)
isl1	*ISL LIM homeobox 1*	Cardiac progenitors	*Xenopus laevis*	pCS2	EcoRI	T7	(Brade et al., 2007)
myl7	*myosin light chain kinase 7*	Differentiated cardiac tissue	*Xenopus laevis*	pGemTeasy	Sal1	T7	(Chambers et al., 1994)
atp1a1	*ATPase, Na+/K+ transporting, alpha 1 polypeptide*	Pronephros (kidney)	*Xenopus laevis*	pCMV-Sport6	EcoRI	T7	(Uochi et al., 1997)
nkx2.5	*NK2 homeobox 5*	Cardiac progenitors	*Xenopus laevis*	GEM3Z	PvuII	T7	(Tonissen et al., 1994)
mpo	*myeloperoxidase*	Myeloid cells, anterior blood island	*Xenopus laevis*	pSport1	PvuII	SP6	(Smith et al., 2002)
tal1	*T-cell acute lymphocytic leukemia 1*	Blood island, hemangioblast	*Xenopus laevis*	pGEM7	Xmn1	SP6	(Ciau-Uitz et al., 2000)

Table 2:4. Templates for riboprobe synthesis

2.7.3 Collecting and fixing embryos

Embryos at the desired stage of development were fixed in MEMFA (0.1M Mops (Fisher) pH 7.4, 2 mM EDTA, 1 mM $MgSO_4$, 3.7% formaldehyde (Sigma)) by rolling for 1 hour at RT in 5 ml Wheaton glass vials (Sigma). The embryos were gradually dehydrated by a dilution series into 100% ethanol (Sigma) and stored at -20^{o}C. For sample collected prior to hatching, vitelline membrane were manually peeled prior to fixation.

2.7.4 Riboprobe hybridisation and washing

Embryos were rehydrated using 5 minute washes in an ethanol dilution series to 1X Tris buffered saline with Tween 20 (TBSTw: 5 mM Tris-Base (Fisher) pH 7.4, 20 mM NaCl, 0.1% Tween 20 (Sigma P1379)). Embryos were permeabilised using 10 µg/ml Proteinase K (Roche) in TBSTw for 15 minutes, rocking, followed by several TBSTw washes. Samples were refixed in MEMFA for 20 minutes then washed several times in TBSTw. Embryos were incubated in hybridisation buffer (50% formamide, redistilled (Sigma), 5X SSC (saline-sodium citrate buffer 1X: 15 mM NaCl, 150 mM sodium citrate (Fisher), pH 7), 1 mg/ml Torula RNA (Type IX, Sigma), 100 µg/ml heparin (Sigma), 1X Denharts solution (0.02% BSA, 0.02% Polyvinylpyrrolidone (Sigma), 0.02% Ficoll 400), 0.1% Tween 20 (Sigma), 0.1% CHAPS (Sigma)) for 10 minutes at 60^{O}C, moving, for prehybridisation. Hybridisation buffer was replaced and embryos incubated at 60^{O}C for 4-6 hours subsequent to replacing with fresh hybridisation buffer containing 0.5 µg/ml of labelled riboprobe and hybridised overnight at 60^{O}C. For fluorescein-labelled riboprobes, embryos were kept in the dark until the completion of the staining stage of the WMISH protocol.

Following overnight riboprobe hybridisation, the hybridisation mix containing the riboprobe was removed and kept for future use, and embryos were incubated in pre-warmed 75% formamide, 25% 2X SSC 0.1% CHAPS (Fisher) for 10 minutes at 60^{O}C. Embryos were washed three times in warm 2X SSC 0.1% CHAPS for 20 minutes, moving at 60^{O}C followed by two washes in pre-warmed 0.2X SSC with 0.1% CHAPS

for 30 minutes per wash moving at 60^{O}C. 0.2X SSC 0.1% CHAPS was gradually diluted to MABT (100 mM maleic acid (Sigma), 150 mM NaCl, 0.1% Triton (Fisher), pH 7.5) and embryos were rinsed in MABT for 10 minutes at RT.

2.7.5 Antibody incubation and washing

MABT was replaced with blocking reagent (MABT containing 1% blocking reagent (Roche), 10% heat-inactivated new-born calf serum (Sigma)) and rocked for one hour at RT before being replaced with blocking reagent containing a 1:2500 dilution of anti-digoxigenin (Roche) or 1:10000 anti-fluorescein antibody conjugated to Alkaline Phosphatase (Roche). Samples were left moving overnight at 4^{O}C. Following antibody incubation, embryos were rinsed in MABT prior to five 1 hour washes in MABT, with constant movement, at RT.

2.7.6 Stain development

Embryos were rinsed in Alkaline Phosphatase Buffer (APB: 100 mM Tris pH 9.5, 50 mM magnesium chloride ($MgCl_2$, Sigma), 100 mM NaCl, 0.1% Tween 20 (Sigma), 2 mM lavamisol (Sigma)) then washed in APB for two times 5 minutes, rocking. APB was replaced with an appropriate alkaline phosphatase substrate, either neat BMPurple (Roche), BCIP (5-bromo-4-chloro-3-indolyl phosphate, Promega) at 1:300 in APB or Magenta phosphate (Sigma) at 1:150 in APB and left at RT. Staining was monitored and when complete stopped by a dilution series to 100% ethanol.

2.7.7 Double whole mount in situ hybridisation

Multiple mRNAs can be detected in the same embryo using WMISH. When mRNA expression domains were non-overlapping, numerous riboprobes were hybridised and developed using one colour reaction. When mRNA expression domains were overlapping or adjacent then two differently labelled riboprobes, fluorescein and digoxigenin, were co-hybridised (Section 2.7.4). Subsequently, an anti-fluorescence or an anti-digoxigenin antibody was incubated (Section 2.7.5) and the WMISH

protocol followed until conclusion of stain development (Section 2.7.6). Embryos were then treated for 10 minutes at 65^{O}C in MAB containing 10 mM EDTA to inactivate Alkaline Phosphatase, dehydrated to 100% ethanol and then rehydrated to MABT, re-fixed in MEMFA for 20 minutes, then washed with MABT. The alternative antibody was then incubated (Section 2.7.5) and the WMISH protocol followed until the conclusion of stain development with a different Alkaline Phosphatase substrate (Section 2.7.6). The order of antibody incubation and Alkaline Phosphatase substrate was determined depending upon individual riboprobe strength.

2.8 Immunohistochemistry

Immunohistochemistry (IHC) utilises conjugated antibodies specifically binding to a biological antigen and in the work presented in this thesis, it was used to provide spatial information about gene expression in embryos. The antibodies used are peroxidase conjugated, therefore were visualised by a colour-producing reaction.

2.8.1 Collecting and fixing embryos

Embryos at the desired stage were fixed in MEMFA by rolling for 1 hour at RT in 5 ml Wheaton glass vials, and then dehydrated in an ethanol dilution series to 100% ethanol for storage at -20^{o}C.

2.8.2 Primary antibody incubation

Embryos were gradually re-hydrated to MABT then blocked for 1 hour in 10% NCS in MABT, moving at RT. Subsequently, embryos were incubated overnight at 4^{O}C with the appropriate primary antibody diluted to 1:100 in MABT: skeletal muscle marker 12/101 or notochord marker MZ15. Skeletal muscle marker was deposited to the DSHB by Jeremy Brockes (DSHB product 12/101, (Kintner and Brockes, 1984)). Anti-Keratin sulphate antibody was deposited to the DSHB by F.M. Watt (DSHB product MZ15 (Smith and Watt, 1985)).

2.8.3 Secondary antibody incubation

Embryos were washed five times for 1 hour in MABT and then incubated overnight at 4^{O}C with 1:500 Goat anti-Mouse IgG HRP (Merck-Millipore) in MABT, followed by five 1 hour MABT washes.

2.8.4 Stain development

1 mg/ml of 3β-Diaminobenzidine tetrahydrachloride (DAB, Sigma) in MABT solution was prepared by filtering through a 0.2 µM cellulose syringe filter (Anachem) and added to embryos for 10 minutes at 4^{O}C before addition of a small volume of 1:1 30% hydrogen peroxide (Sigma):MABT and moved at 4^{O}C until stained. Embryos were washed with MABT and dehydrated to 100% ethanol.

2.9 Whole mount *in situ* hybridisation combined with immunohistochemistry

Following on from the complete WMISH protocol (Section 2.7), embryos can be further stained by IHC, starting from primary antibody incubation to completion of stain development (Section 2.8.2-2.8.4).

2.10 Preparing whole mount *in situ* hybridisation and immunohistochemistry processed embryos for analysis and imaging

2.10.1 Bleaching embryos

Embryos were rehydrated by a dilution series to MABT. MABT was replaced with bleaching solution (1% hydrogen peroxide 5% Formamide (Fisher), 0.5X SSC) and vials were placed on aluminium foil close to a light source until sufficiently bleached (1-2 hours). Bleached embryos were washed with MABT for 30 minutes and kept at 4^{O}C prior to analysis and imaging.

2.10.2 Clearing embryos

After bleaching, where necessary, embryos were made to appear transparent (cleared) by gradually diluting to 100% ethanol, then to Murrays Clear (2 volumes benzyl benzoate (Sigma): 1 volume benzyl alcohol (Sigma)) for analysis and imaging (Sive et al., 2000).

2.10.3 Visualising lineage trace

Samples were incubated overnight at 4^{O}C with MABT containing a 1:7000 dilution of extraviden AP (Sigma), then rinsed in MABT prior to five 1 hour washes in MABT at RT. Fast Red table(s) (Roche) were dissolved in 0.1 M Tris-HCL, pH 8.2, passed through a 0.4 µM cellulose syringe filter, and added to embryos to allow colour development. Embryos were washed, stored, analysed and imaged in MABT.

2.11 Reverse transcription polymerase chain reaction (RT-PCR)

2.11.1 Sample collection

Embryos at the desired stage were collected into an RNase-free 1.5ml eppendorf (Fisher) and excess liquid was removed. For each sample, between 5 and 15 embryos were collected by lysing in Solution D ((Chomczynski and Sacchi, 1987); 4M Guanidinium thiocyanate (Sigma), 25 mM sodium citrate, 0.1% sarcosyl (Sigma), 0.1M β-Mercaptoethanol (Sigma), pH 7) and storing at -20^{O}C.

2.11.2 RNA extraction

Total cellular RNA extraction was done according to Chomczynski and Sacchi, 1987 (Chomczynski and Sacchi, 1987). Solution D, 0.1M β-Mercaptoethanol (Sigma), pH 7), 2 M sodium acetate pH 4 (Sigma), water saturated phenol (Fluka) and chloroform (Fisher) were added sequentially and mixed in the ratio 1:0.1:1:0.2. Samples were incubated on ice for 20 minutes then centrifuged at *10000xg* for 20 minutes. The

aqueous phase containing RNA was transferred to a fresh eppendorf and an equal volume of chilled isopropanol was added. Samples were incubated at -20^{O}C for one hour then centrifuged at *10000xg* for 20 minutes to pellet the RNA. The supernatant was removed and the RNA pellet washed with 70% ethanol then air-dried before being re-suspended in 25 µl ddH_2O. The RNA concentration was determined by spectrophotometry by measuring the absorption at 260nm. RNA was stored at -20^{O}C.

2.11.3 cDNA synthesis

1 µg RNA, 0.1 µg/µl random primers (Invitrogen), 0.5 mM dNTP and ddH_2O to 12 µl were mixed and heated to 65^{O}C for 5 minutes then immediately chilled on ice. 1X first strand buffer (Invitrogen), 100 mM dithiothreitol (DTT, Invitrogen) and 20 units Ribolock were subsequently added and incubated at 37^{O}C for 2 minutes. Following this, 200 units of RevertAid RT (Thermo scientific) were added to all samples except for the negative control and incubated at RT for 10 minutes, 37^{O}C for 1 hour, then 70^{O}C for 15 minutes.

2.11.4 Polymerase chain reaction

Primers were designed using Primer3Plus software (www.primer3plus.com) and span intron-exon boundaries, thus ensuring no false positive signal arises due to genomic DNA contamination. Primers were sourced from Invitrogen and re-suspended in ddH_2O to 0.1 mM. Primer sequence and cycling conditions are described in Table 2:5 and were optimised allowing for each product amplification to fall within the linear range. To each PCR reaction, complementary DNA, 0.4 µM forward primer, 0.4 µM reverse primer, 1X MyTaq red reaction buffer (containing 5 mM dNTPs, 15 mM $MgCL_2$, (Bioline)), 0.5 units KAPA polymerase (KAPA biosystems) and ddH_2O to 25 µl were mixed. PCR was carried out on PeqStar Thermocycler (Peqlab) using the following cycling conditions (see Table 2:5 for specific 'n' and 'x' values):

95^{O}C for 3 minutes

95^{O}C for 30 seconds
n^{O}C for 30 seconds } x cycles
72^{O}c for 30 seconds

72^{O}c for 10 minutes

PCR products were analysed by agarose gel electrophoresis (Section 2.4.2)

Gene symbol	Gene name	PCR primer sequence	Product length, bp	Annealing temperature, °C (n)	Cycle number (x)	Extension Time (s)
gsc	*goosecoid*	GGATTTTATAACCGGACTGTGG TGTAAGGGAGCATCTGGTGAG	240	28	34	30
odc1	*ornithine decarboxylase 1*	GCCATTGTGAAGACTCTCTCCATT TTCGGGTGATTCCTTGCCAC	220	58	26	30
t	*brachyury*	CTGGGATGTTGCCAATGAGT GATGAAAGCCTGGAATGTGC	283	58	32	30

Table 2:5 PCR primers

2.12 Western Blot

2.12.1 Sample collection

Five whole embryos per experimental condition were collected into pre-labelled 1.5 ml eppendorf tubes. Excess media was removed and embryos were snap frozen on dry ice and stored at -20^{O}C.

2.12.2 Sample preparation

Embryos were thawed on ice then homogenised by pipetting in 10 µl per embryo of 1X RIPA buffer (5X stock kept at 4^{O}C: 150 mM NaCl, 1% NP40 (Sigma), 0.5% sodium deoxycholate (Sigma), 0.1% sodium dodecyl sulfate (SDS, Sigma), 50 mM Tris-HCL pH 8) containing 1% protease inhibitor cocktail (P8340 Sigma; 104 mM AEBSF, 80 µM Aprotinin, 4 mM Bestatin, 1.4 mM E-64, 2 mM Leupeptin and 1.5 mM Pepstatin A) and 1% phosphatase inhibitor cocktail 3 (P0044 Sigma; Cantharidin, p-Bromolevamisole oxalate and Calyculin A). The protease inhibitor cocktail inhibits serine, cysteine and acid proteases as well as aminopeptidases and was used to prevent protein degradation by endogenous proteolytic enzymes released from subcellular compartments after cell lysis. The phosphatase inhibitor cocktail has been optimised to prevent alkaline and serine-threonine phosphatases from modifying proteins, thus was important for the detection of phosphorylated proteins. Samples were centrifuged at *18000xg* for 20 minutes then the supernatant was collected. An equal volume of 2X blue gel loading buffer (National Diagnostics) was added to the supernatant and mixed before incubating at 100^{O}C for 10 minutes to denature the proteins. Samples were centrifuged at *18000xg* for 5 minutes before loading 10 µl per sample per well onto a SDS-polyacrylamide gel.

2.12.3 SDS-polyacrylamide gel electrophoresis (SDS-PAGE)

SDS-polyacrylamide gels were prepared fresh and were 0.75 mm thick consisting of 5 cm of resolving gel (375 mM Tris pH 8.8, 10% Acrylamide (National diagnostics), 0.1% sodium dodecyl sulphate (SDS, 0.05% ammonium persulfate (APS, Fisher), 0.5% Tetramethylethylenediamine (TEMED, Bio-Rad) with 2 cm of stacking gel (125 mM Tris pH 6.8, 5% Acrylamide, 0.1% SDS, 0.1% TEMED) indented with loading wells created by Teflon combs (Bio-Rad). 10 µl of each sample, or 15 µl of Spectra Multicolor Broad Range Protein Ladder (Ladder, Fermentas), were loaded per lane and 5 µl of 2X blue gel loading buffer was loaded into any unused lanes. Gel electrophoresis was carried out at 100V for 10 minutes followed by 200V for 60-120 minutes in tris-glycine running buffer (25 mM Tris base, 192 mM Glycine, 0.1% SDS, pH 8.3) using a PowerPac.

2.12.4 Protein transfer

Following SDS-PAGE, gels were soaked in tris-glycine transfer buffer (48 mM Tris-base, 39 mM Glycine, pH 8.8) for 15 minutes to equilibrate them. Polyvinylidene fluoride (PVDF) membranes (Immobilon-P, Merck-Millipore) were prepared by soaking in pure methanol (Sigma) for 15 seconds then equilibrating in tris-glycine transfer buffer. Gel and membrane were held in close contact between filter paper (Fisher) and sponge pads (Bio-Rad) by a cassette (Bio-Rad) in a Mini Trans-Blot cell (Bio-Rad) containing tris-glycine transfer buffer and a cooling source. Transfer of proteins from gel to membrane was carried out at 350 mA for 80 minutes using a Bio-Rad PowerPac.

2.12.5 Antibody incubation

Membranes were washed three times in TBSTw and blocked for 1 hour in TBSTw containing 5% milk powder (Sigma) or 5% BSA (Sigma), rolling at RT. The desired primary antibody was incubated in TBSTw containing 5% milk powder or BSA overnight at 4^{O}C, rolling (Table 2:6). Following several washes in TBSTw, consisting of

3x5 minutes and 3x15 minutes, rolling at RT, membranes were incubated with the appropriate secondary antibody (Table 2:6) in TBSTw containing 5% milk or BSA, rolling at RT for 2 hours. Membranes were then washed for 3x5 minutes and 3x15 minutes in TBSTw, rolling at RT.

Antibody name	Type	Dilution	Block	Host	Size (kDa)	Storage	Supplier	Product
ERK	Primary	1:10000	Milk	Rabbit	41, 42	4^{O}C	Santa Cruz	SC-154
p-ERK (Thr202/Tyr204)	Primary	1:5000	BSA	Rabbit	44, 42	-20^{O}C	Cell Signalling	4370S
Smad2/3	Primary	1:3000	Milk	Mouse	58	-20^{O}C	BD Bioscience	610843
p-Smad2 (ser465/467)	Primary	1:750	Milk	Rabbit	60	-20^{O}C	Cell Signalling	3101
p53	Primary	1:500	Milk	Mouse	53	-20^{O}C	Abcam	Ab16465 [X77]
HA	Primary	1:2000	Milk	Rat	-	-20^{O}C	Roche	11867423001 (clone 3F10)
Rabbit	Secondary	1:50000	As primary	Goat	-	4^{O}C	Santa Cruz	SC-2004
Mouse	Secondary	1:10000	As primary	Goat	-	4^{O}C	Merck-Millipore	AP124P
Rat	Secondary	1:100000	As primary	Goat	-	4^{O}C	Merck-Millipore	AP136P

Table 2:6. Antibodies for Western Blotting

2.12.6 Signal detection

Membranes were coated in SuperSignal West Pico Chemiluminescent Substrate (Thermo Scientific) and left for 5 minutes in the light at RT before excess solution was removed and membranes were placed between plastic slips. In darkness, membranes were exposed to Amersham Hyperfilm ECL (GE Healthcare) for varying lengths of time required for visualisation of proteins, often between 1 second to 30 minutes, and films were developed using a Compact X4 Xograph (Xograph). Protein size was determined by reference to the ladder.

2.12.7 Stripping and re-probing membranes

Membranes were routinely stripped and re-probed with an antibody to a control protein, as a loading control. Membranes were briefly washed in TBSTw then incubated in Restore Western Blot Stripping Buffer (Thermo Scientific) for 15 minutes at RT, rolling, before further thorough washing in TBSTw. Antibody incubation and protein detection steps (Sections 2.12.5 and 2.12.6) were then repeated for the alternative antibody of choice.

2.13 CRISPR/ Cas9 mediated gene editing

Clustered regularly interspaced short palindromic repeat (CRISPR) technology is a recently discovered, powerful tool for genome editing. CRISPR technology adapts and exploits a bacterial immune system, aimed against invading viruses and plasmids, resulting in site specific DNA cleavage for genome editing (Jinek et al., 2012). Short guide RNAs (sgRNA), designed to complement a sequence within a target gene, guide Cas9 nuclease to DNA to induce site-specific cleavage. This DNA damage is repaired by error-prone non-homologous end joining, often resulting in insertions and deletions, disrupting gene function.

2.13.1 sgRNA template preparation

Two techniques were utilised for sgRNA template preparation. For p53 sgRNAs, a PCR-based method was used. A 5' oligonucleotide, containing the p53 target sequence, was used in a thermo cycling reaction with a common 3' oligonucleotide creating a double stranded template. Alternatively, for a Tyrosinase control, the pDR274 plasmid containing tyrosinase sgRNA was used.

p53 short guide RNAs were kindly designed by Dr Richard White (The Welcome Trust - Sanger Institute). 8 sgRNAs (Table 2:7) were selected for production based on their proximity to the start site of the p53 coding region, and their low off-target predicted score. The 5' sgRNA T7-fill-in-oligonucleotides listed in Table 2:7, along with a common 3' oligonucleotide, sequence AAAAGCACCGACTCGGTGCCACTTTTTCAAGTTGATAACGGACTAGCCTTATTTTAACTTGC TATTTCTAGCTCTAAAAC (Eurofins), were reconstituted to 100 µM in ddH_2O.

The following reagents were mixed to a final volume of 100 µl with ddH_20 (Nakayama et al., 2014): 1X High Fidelity Buffer (Thermo Scientific), 0.3 mM dNTP, 1 mM Mg_2SO_4 (Thermo Scientific), 2 µM 5' primer, 2 µM 3' primer, 2 U Phusion High-Fidelity DNA Polymerase (Thermo Scientific). The reaction was mixed and subjected to the following thermo-cycling conditions using a PeqStar Thermocycler (Peqlab):

98^{O}C for 5 minutes

98^{O}C for 20 seconds	20 cycles
58^{O}C for 20 seconds	
72^{O}c for 15 seconds	

72^{O}c for 5 minutes

Tyrosinase in plasmid pDR274 (pDR274tyr) was from Ira Blitz (Blitz et al 2013). pDR274tyr was linearised using Dra1 in the following reaction; 1 µg pDR274tyr, 1X Buffer 4 (NEB), 40 units Dra1 (NEB) and ddH_2O to 30 µl, incubated at 37^{O}C for 1 hour.

sgRNA templates were purified using QIAquick PCR purification kit (Section 2.4.1).

sgRNA	Target sequence	Target strand	Exon	T7-fill-in-oligonucleotide sequence
Xt tp53 sgRNA 1	AGGAGACCTTCGAGGATTTGTGG	+	1	TAATACGACTCACTATAGGGAGACCTTCGAGGATTTGGTTTTAGAGCTAGAAATAGCAAG
Xt tp53 sgRNA 2	GACCCCCTACAGACCGGGACAGG	+	2	TAATACGACTCACTATAGGCCCCCTACAGACCGGGACGTTTTAGAGCTAGAAATAGCAAG
Xt tp53 sgRNA 3	GACCTGTCCCGGTCTGTAGGGGG	-	2	TAATACGACTCACTATAGGCCTGTCCCGGTCTGTAGGGTTTTAGAGCTAGAAATAGCAAG
Xt tp53 sgRNA 4	AGGTCAGATGGAAAACTTTGCGG	+	2	TAATACGACTCACTATAGGGTCAGATGGAAAACTTTGGTTTTAGAGCTAGAAATAGCAAG
Xt tp53 sgRNA 5	GGAGTTTTCAGAGTACCCCCTGG	+	3	TAATACGACTCACTATAGGAGTTTTCAGAGTACCCCCGTTTTAGAGCTAGAAATAGCAAG
Xt tp53 sgRNA 6	GAACCGTCATGTCTGGCGCCAGG	-	3	TAATACGACTCACTATAGGACCGTCATGTCTGGCGCCGTTTTAGAGCTAATAGCAAG
Xt tp53 sgRNA 7	GACATGACGGTTCTGCAGGAAGG	+	3	TAATACGACTCACTATAGGCATGACGGTTCTGCAGGAGTTTTAGAGCTAGAAATAGCAAG
Xt tp53 sgRNA 8	AGACGAAGTCACGGTGGGCACGG	-	3	TAATACGACTCACTATAGGACGAAGTCACGGTGGGCAGTTTTAGAGCTAGAAATAGCAAG

Table 2:7. CRISPR sgRNAs targeted to *Xenopus tropicalis* p53

2.13.2 In vitro transcription of sgRNA

sgRNA synthesis was performed using MAXIscript T7 kit (Ambion) according to the manufacturer's instructions. 0.5 µg/µl of PCR based template or 1 µg/µl of plasmid based template, 1X transcription buffer, 0.5 mM ATP, 0.5 mM CTP, 0.5 mM GTP, 0.5 mM UTP, 30 units T7 RNA polymerase and ddH_2O to 20 µl were mixed and incubated at 37^OC for 1 hour, followed by the addition of 2 units TURBO DNase for a further 15 minutes.

sgRNA was purified by phenol-chloroform extraction and isopropanol precipitation. ddH_20 was added to increase the total volume to 180 µl, followed by the sequential addition and mixing of 3 M sodium acetate pH 5.2, phenol and chloroform in the ratio 0.2:0.5:0.5. Samples were incubated on ice for 15 minutes then centrifuged at *10000xg* for 20 minutes. The aqueous phase, containing RNA, was transferred to a fresh eppendorf and an equal volume of chilled isopropanol added. Samples were incubated at -20^OC for one hour, then centrifuged at *10000xg* for 20 minutes to pellet the RNA. The supernatant was removed and the RNA pellet was washed with 70% ethanol, then air-dried before being re-suspended in 20 µl ddH_2O. The concentration was determined using spectrophotometry by measuring the absorption at 260 nm. sgRNAs were stored at -20^OC.

2.13.3 Cas9 protein preparation

Cas9 protein (PNA Bio) was reconstituted in 50 µl ddH_2O containing 20% glycerol (PNA bio), to a concentration of 1 mg/ml. Cas9 solution was aliquoted into 5 µl measures, for storage at -20^OC.

2.13.4 Genomic DNA PCR amplification

Genomic DNA was prepared from a single embryo, by homogenising in 50 µl of 50 mM Tris-HC: pH 8.8, 1 mM EDTA, 0.5% Tween-20, 200 µg/ml proteinase K (Blitz et al., 2013). The homogenisation reaction was incubated overnight at 56^OC, followed by

10 minutes at 95^{O}C to inactivate proteinase K. 1 µl was added directly to the following PCR amplification: 1X Phusion high fidelity buffer, 0.2 mM dNTP's, 0.4 µM forward primer (as appropriate, see below), 0.4 µM reverse primer (as appropriate, see below), 1 unit Phusion High Fidelity DNA Polymerase and ddH_2O to 25 µl. The reaction was subject to the following multistep thermo-cycling conditions using a PeqStar Thermocycler:

98^{O}C for 5 minutes

- 98^{O}C for 20 seconds
- 65^{O}C for 20 seconds
- 72^{O}c for 30 seconds

} 13 cycles

- 98^{O}C for 20 seconds
- X^{O}C for 20 seconds
- 72^{O}c for 30 seconds

} X = 64^{O}C, 63^{O}C, 62^{O}C, 61^{O}C, 60^{O}C, 59^{O}C, for one cycle per temperature

- 98^{O}C for 20 seconds
- 65^{O}C for 20 seconds
- 72^{O}c for 30 seconds

} 25 cycles

72^{O}c for 5 minutes

PCR products were purified using QIAquick PCR purification kit (Section 2.4.1).

2.13.5 In vitro screen for sgRNA

An *in vitro* assay was used to assess the efficiency with which Cas9 is guided to, and cuts, a template DNA target. This screening allowed selection of working and efficient sgRNAs for *in vivo* experiments. Genomic DNA was amplified using PCR (Section 2.13.4) using the forward primer F1; GGGCACAAGCAGTAGCCTAA and reverse primer R5; CCAAACACACACAGGTGAGG. The following reagents were mixed and incubated at 37^{O}C for 1 hour; 300 ng Cas9, 150 ng sgRNA, 80 ng target DNA, 1X buffer 3 (NEB),

1X BSA (NEB), ddH_2O to 10 µl. 2 units of RNase H (Invitrogen) were added and the reaction was incubated at 37^{O}C for a further 15 minutes. 1 µl of stop solution (30% glycerol, 1.2% SDS, 250 mM EDTA pH8) was added and incubated at 37^{O}C for 15 minutes. Cleavage products were separated by agarose gel electrophoreses (Section 2.4.2).

2.13.6 In vivo CRISPR application and analysis

Stocks were mixed to a final concentration of 200-300 pg sgRNA and 1 ng Cas9 and were injected into a 1 cell staged, newly fertilised, embryo. After at least 5 hours of development, individual embryos were collected and genomic p53 DNA was amplified (Section 2.13.4) using the primers F3; GTCTCCCTGTTGGGTGTTGT, and R5; CCAAACACACACAGGTGAGG. PCR products were sent for sequencing (Eurofins) to check for successful CRISPR-Cas9 mediated gene disruption.

3 Nodal/ Activin signalling is required for cardiac specification

3.1 Introduction

The Nodal/ Activin subclass of TGF-beta ligands signal via ALK4/5/7 transmembrane receptors and intracellular signalling mediators Smad2/3 (Shen, 2007; Shi and Massague, 2003). Nodal/Activin –ALK4/5/7 signalling is required for multiple aspects of embryogenesis, including mesendoderm induction and patterning, gastrulation movements and left-right axis asymmetry (Hill, 2001). Furthermore, Nodal/ Activin signalling has been implicated in cardiac specification through numerous whole embryo, explant and stem cell models (Cai et al., 2012; Lowe et al., 2001; Parisi et al., 2003; Reissmann et al., 2001; Reiter et al., 2001; Samuel and Latinkić, 2009; Takahashi et al., 2000; Xu et al., 1999, 1998; Yatskievych et al., 1997). See Section 1.8.1.5 for more detail. Previous experiments have not been designed to distinguish the role of Nodal/Activin –ALK4/5/7 signalling in cardiac specification form its broader functions in embryonic development, questioning the specificity of the Nodal/ Activin signalling requirement in the induction of cardiac cells. In addition, the time at which Nodal/Activin –ALK4/5/7 signalling may be required for cardiac specification *in vivo* is largely unknown. Work presented in this chapter investigates the requirement and timing for Nodal/Activin –ALK4/5/7 signalling in cardiac specification *in vivo* in *Xenopus laevis*.

3.2 Experimental approach

The desired approach for investigating the role of Nodal/ Activin -ALK4/5/7 signalling in cardiac specification was to inhibit the ALK4/5/7 pathway and assess the effects on cardiac tissue. Commonly used techniques for investigating the role of signalling pathways in *Xenopus laevis* include antisense morpholino oligonucleotides (MO) and injecting the mRNA of signalling components, sometimes genetically manipulated, which can be used to alter protein levels and activity. However, these techniques are not the most appropriate for this investigation. MOs and mRNAs have to be injected into an early cleavage stage embryo, with the effects on protein activity and abundance most often acting directly and continuously throughout development.

Nodal/ Activin signalling has multiple functions throughout embryogenesis, including in mesoderm induction, which precedes and is required for cardiac cell induction (Smith et al., 1990; Vliet et al., 2012; Wu and Hill, 2009). Reagents which are injected into the early embryo to inhibit ALK4/5/7 signalling have been shown to result in aberrant mesoderm development, thus can indirectly affect cardiac specification (Luxardi et al., 2010). Therefore, a technique which allowed the time and duration of Nodal/ Activin -ALK4/5/7 signalling inhibition to be controlled was required. Pharmacological small soluble molecular inhibitors can be added directly to the media used for culturing *Xenopus laevis* embryos at any time point of development, to inhibit a particular pathway. Subsequently, the embryos can be removed from the inhibitor media, washed, and allowed to continue developing in fresh media, free from the inhibitor (Myers et al., 2014). These features allow time-dependent inhibition control of Nodal/ Activin -ALK4/5/7 signalling in *Xenopus laevis* to be carried out. Molecular inhibitors of the ALK4/5/7 pathway were therefore selected to be used in the work presented here.

3.3 Small molecular drugs SB505124 and A-83-01 as suitable ALK4/5/7 inhibitors

A selection of ALK4/5/7 inhibitors, added to *Xenopus laevis* embryos shortly after fertilisation and incubated continuously throughout development, were tested for their ability to reproduce phenotypes consistent with previously reported ALK4/5/7 signalling pathway inhibition (Table 3:1). Previous reports describe embryos presenting a truncated anterior-posterior axis accompanied by loss of identifiable landmark features, such as the cement gland (an anterior-dorsal mucus-secreting structure which attaches newly hatched embryos to a support before proficient swimming and feeding is achieved) and eyes, upon ALK4/5/7 signalling inhibition using soluble inhibitors or a dominant negative Activin receptor (Hemmati-Brivanlou and Melton, 1992; Luxardi et al., 2010; Skirkanich et al., 2011). This is consistent with what is expected of ALK4/5/7-Smad2 pathway inhibition, due to its documented role in mesoderm induction (reviewed in Kimelman, 2006). The selection of ALK4/5/7

inhibitors were tested at a range of concentrations from 20 to 300 µM. The range of concentrations was in part guided by previous studies utilising ALK4/5/7 inhibitors in *Xenopus laevis* (Luxardi et al., 2010; Samuel and Latinkić, 2009; Skirkanich et al., 2011) and zebrafish (Hagos et al., 2007; Hagos and Dougan, 2007; Lenhart et al., 2013). Concentrations of 75 – 200 µM of SB505124, A-83-01 and SB431542 have been used previously in *Xenopus laevis* work (Ho et al., 2006; Luxardi et al., 2010; Samuel and Latinkić, 2009; Skirkanich et al., 2011), with concentrations of 0.1 – 100 µM reportedly used in mouse and human cell culture (DaCosta Byfield et al., 2004; Inman et al., 2002; Tojo et al., 2005). For comparison, 30-75 µM of SB505124 has reportedly been used for ALK4/5/7 inhibition in zebrafish (Hagos et al., 2007; Hagos and Dougan, 2007; Lenhart et al., 2013).

Two structurally distinct inhibitors, SB505124 (SB) and A-83-01 (A83) (Figure 3:1), were selected for further testing and use from the range of ALK4/5/7 inhibitors tested. This was due to their ability to consistently reproduce phenotypes comparable with previously documented cases of ALK4/5/7 signalling inhibition. When optimum concentrations of SB505124 and A-83-01 were added to *Xenopus laevis* embryos shortly after fertilisation, no axis elongation or identifiable landmark embryonic features were observed by the tadpole stage. SB505124 and A-83-01 bind to, and inhibit, the intracellular serine-threonine kinase domain of the TGF-beta type 1 receptors ALK4/5/7. SB505124 and A-83-01 therefore prevent the phosphorylation of Smad2, thus inhibiting further signal transduction. SB505124 and A-83-01 have been reported to only weakly affect ALK1/2/3/6 and Mitogen-activated protein kinases pathways (DaCosta Byfield et al., 2004; Tojo et al., 2005; Vogt et al., 2011).

The IC_{50} for SB505124 has been previously determined as 129 nM for ALK4, and 47 nM for ALK5, in an *in vitro* cell culture system (DaCosta Byfield et al., 2004). The IC_{50} for A-83-01 has been reported as 45 nM, 12 nM and 7.5 nM for ALK4, 5 and 7 respectively (Tojo et al., 2005). Although these IC_{50} values are up to 3 orders of magnitude lower than the chosen inhibitor concentrations used throughout the work presented here, they were determined *in vitro* in cell culture and therefore they may

not be directly applicable to *in vivo* settings and in particular to the *Xenopus laevis* embryo, which contains fatty yolk potentially capable of sequestering the inhibitors.

Inhibitor	Concentrations tested (μM)	Phenotype observations at stage 32-36
SB505124	20-300	Truncated anterior-posterior axis in a dose-dependent manner accompanied by loss of identifiable landmark features, such as the cement gland and eyes, at higher concentrations.
A-83-01	20-400	Truncated anterior-posterior axis in a dose-dependent manner accompanied by loss of identifiable landmark features, such as the cement gland and eyes, at higher concentrations.
SB431542	150-300	Truncated anterior-posterior axis in a dose-dependent manner but only at the highest concentrations tested.

Table 3:1. ALK4/5/7 inhibitors tested

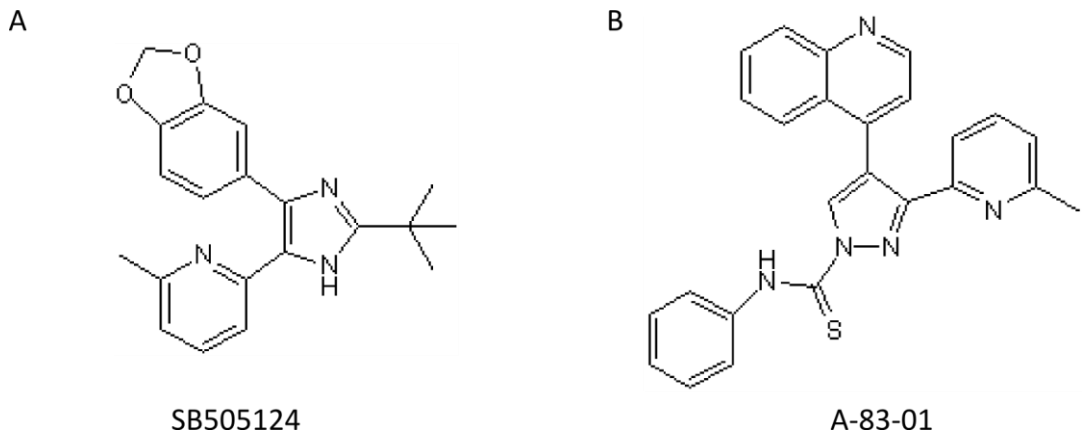

Figure 3:1. Chemical structures ALK4/5/7 inhibitors SB505124 and A-83-01

(A) Chemical structure of SB505124. (B) Chemical structure of A-83-01. (www.tocris.com).

3.4 SB505124 and A-83-01 adversely affect normal embryonic development in a dose-dependent manner

The optimum working concentration of the ALK4/5/7 inhibitors SB505124 and A-83-01 was determined by testing the effectiveness of the inhibitors at a range of concentrations from 20 µM to 300 µM. The ALK4/5/7 inhibitors were added to the *Xenopus laevis* embryos at the 2 cell stage and incubated continuously until the tadpole stage. Embryos were staged by untreated sibling controls, which presented a normal phenotype (Figure 3:2 A, B, M, N). The results show that 20 µM of ALK4/5/7 inhibitor treatment had a mild or no effect on the overall embryonic phenotype (Figure 3:2 C, D, O, P). When treated with inhibitor concentrations of 50 µM and 100 µM, a change in embryonic phenotype was observed, compared to the controls. A truncated anterior-posterior axis and a dose-dependent loss in distinguishable embryonic features, such as the cement gland and eyes, was evident at the tadpole stage (Figure 3:2 E-H, Q-T). These results show that A-83-01 appears to be more potent than SB505124 at lower concentrations, but there is little difference in the effects of these inhibitors on the whole embryo phenotype at concentrations above 100 µM. At higher concentrations of 200 µM and 300 µM, tadpoles lacked axial and landmark embryonic features, with little difference observed between the two concentrations (Figure 3:2 I-L, U-X). Throughout all experiments at all concentrations tested, scarce embryonic death was observed, suggesting that toxic levels of the ALK4/5/7 inhibitors were not reached. An optimum concentration of 200 µM of ALK4/5/7 inhibitors SB505124 and A-83-01 was selected for use in further investigations. This was due to the ability of a concentration of 200 µM to consistently result in tadpoles displaying a truncated anterior-posterior axis lacking identifiable tail, cement gland and eyes, thus indicating robust inhibition of the ALK4/5/7 signalling pathway. The concentration of 200 µM of ALK4/5/7 inhibitors is similar to concentrations of SB505124 and A-83-01 previously used in published *Xenopus laevis* research (Ho et al., 2006; Luxardi et al., 2010; Samuel and Latinkić, 2009; Skirkanich et al., 2011), but slightly higher than concentrations of 30-75 µM used in zebrafish work (Hagos et al., 2007; Hagos and Dougan, 2007; Lenhart et al.,

2013), presumably due to differences in *Xenopus laevis* and zebrafish embryos. The concentration of 200 µM of ALK4/5/7 inhibitors selected is higher than concentrations of 0.1 – 100 µM used in mouse and human cell culture (DaCosta Byfield et al., 2004; Inman et al., 2002; Tojo et al., 2005), but as previously discussed, an *in vitro* situation does not necessarily accurately reflect the *in vivo* scenario in *Xenopus laevis,* due to factors such as potential sequestering of inhibitors.

Comparison between repeated experiments throughout all investigations for this work allowed the observation that there was a difference in the potency of the ALK4/5/7 inhibitors on different batches of embryos, and even between embryos within the same batch. Additionally, differences were observed between different batches of inhibitors. Treated embryos presented the same phenotypic features, but the efficacy of a given drug treatment varied. For example, within a treatment regime causing a truncated anterior-posterior axis, some embryos presented a shorter axis compared with others subjected to the same treatment. The range of different phenotypes observed was narrow, and was within an acceptable limit for these investigations. In order to control for the variation in the efficacy of the drugs, each experiment included a positive control consisting of embryos that were treated from the 2 cell stage continuously with the ALK4/5/7 inhibitors. In addition, experiments were typically performed using both inhibitors independently to ensure consistent results. Throughout this results chapter the most representative images of ALK4/5/7 inhibition treatments are shown, although more and less severely affected embryonic phenotypes can be observed in the group images, permitting the range of phenotypes to be appreciated.

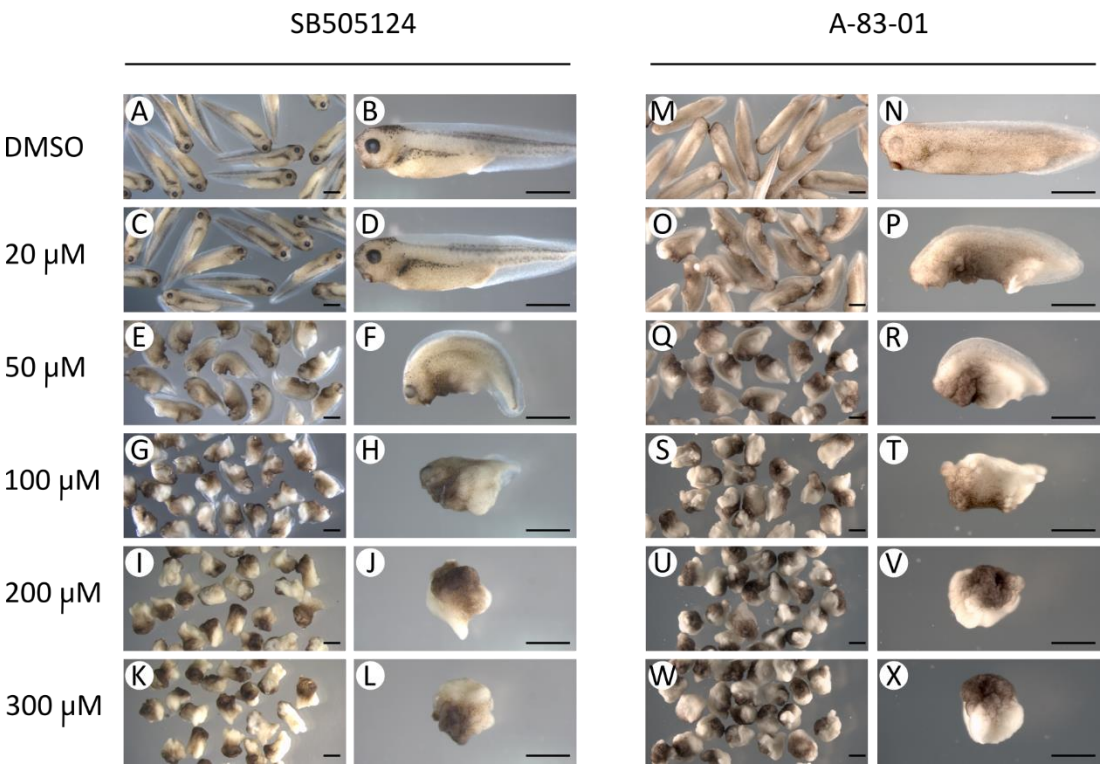

Figure 3:2. ALK4/5/7 inhibitors adversely affect normal embryonic development in a dose-dependent manner

Embryos were treated continuously from the 2 cell stage until the tadpole stage with (A, B, M, N) DMSO or increasing concentrations of the ALK4/5/7 inhibitors (C-L) SB505124 or (O-X) A-83-01, as displayed on the left. Representative images from at least 4 biological replicas per inhibitor. All individual embryo images are a lateral view orientated anterior left, dorsal up. Scale bar represents 1 mm. SB505124 column – DMSO n=81, 20 µM n=62, 50 µM n=52, 100 µM n=112, 200 µM n=116, 300 µM n=63. A-83-01 column – DMSO n=84, 20 µM n=59, 50 µM n=80, 100 µM n=113, 200 µM n=107, 300 µM n=58.

3.5 Activation and nuclear localisation of the ALK4/5/7 downstream signal transducer Smad2 is inhibited by SB505124 and A-83-01

To confirm that the ALK4/5/7 inhibitors SB505124 and A-83-01 were inhibiting Smad2 activation and thus preventing Nodal/ Activin signal transduction, the phosphorylation state of Smad2 was examined. Smad2 is phosphorylated by ALK4/5/7 in response to external ligand stimulation and is required for Nodal/ Activin signal propagation (Shi and Massague, 2003). Previously, it has been shown by immunoprecipitation of protein samples from approximately 100 embryos followed by western blot analysis, that phosphorylated-Smad2 (p-Smad2) can been detected as early as the 2000 and 4000 cell stages (stages 7.5 and 8 respectively) in untreated *Xenopus laevis* embryos (Skirkanich et al., 2011). Figure 3:3 A shows a western blot analysis of protein samples from five whole, pooled, *Xenopus laevis* embryos. Using this analysis, p-Smad2 was be detected by stage 9.5, levels increase to peak at the onset of gastrulation at stage 10 and then decrease. This is consistent with previously published work (Lee et al., 2001). When embryos were treated with SB505124 or A-83-01 at stage 8, the levels of p-Smad2 were strongly reduced by stage 10, in comparison to DMSO treated controls (Figure 3:3 B). This suggests that the inhibition of the Nodal/ Activin -ALK4/5/7 signalling pathway has been successfully achieved using both of the inhibitors tested here.

Once activated by ALK4/5/7, p-Smad2 forms a trimeric complex with Smad4 and another p-Smad2 molecule, leading to the nuclear accumulation of the trimeric complex to influence the expression of Nodal/ Activin dependent genes (Shen, 2007). The effects of Nodal/ Activin -ALK4/5/7 signalling inhibition on the nuclear localisation of the p-Smad2-Smad4 complex was examined using bimolecular fluorescence complementation (BiFC) in Activin treated dissociated *Xenopus laevis* animal cap cells (Heldin et al., 1997; Kerppola, 2008a, 2008b; Massagué, 1998). This method was employed as detection of endogenous p-Smad2 by immunohistochemistry in dissected *Xenopus laevis* embryos proved difficult, due to low sensitivity and high background. BiFC was used as an additional, complementary,

method to western blotting and allowed not only the presence of p-Smad2 to be interrogated, but also the visualisation of whether complex formation and nuclear translocation was inhibited after addition of soluble ALK4/5/7 inhibitors.

Embryos were co-injected uniformly into the animal hemisphere at the 2 cell stage with mRNA encoding N- and C- terminal portions of the enhanced yellow fluorescent protein Venus, fused to Smad4 (VNS4) and Smad2 (VNS2) respectively (Nagai et al., 2002; Saka et al., 2008, 2007). In addition, mRNA encoding the red fluorescent protein mCherry was co-injected, allowing all injected cells to be traced (Shaner et al., 2004). In response to Activin treatment in blastula stage dissociated animal cap cells, Smad2 is phosphorylated, associates with Smad4, and translocates into the nucleus. This brings together the two halves of Venus to complete the functional green fluorescence protein and nuclear fluorescence is observed (Figure 3:3 C-E). Addition of SB505124 significantly reduced the amount of nuclear Smad2-Venus-Smad4, suggesting that SB505124 is preventing the nuclear accumulation of p-Smad2 (Figure 3:3 F-H). The relative number of Smad2-venus-Smad4 (green) positive nuclei was calculated by working out the ratio of Smad2-venus-Smad4 nuclei to injected, mCherry positive (red), cells per sample, normalised to the control (DMSO) sample (Figure 3:3 I). Using an unpaired 2-tailed t-test of equal variances, a p-value of 0.026 was calculated. This is lower than the significance level of 0.05, indicating that there is a significant difference between DMSO and SB505124 treated samples. These findings suggest that the ALK4/5/7 inhibitor SB505124 prevents nuclear p-Smad2-Smad4 accumulation. This is in agreement with previous work in zebrafish, using p-Smad2 fluorescent immunostaining to demonstrates that nuclear p-Smad2 is absent after treatment with SB505124 (van Boxtel et al., 2015). Figure 3:3 J-M is a positive control in sibling embryos to those used in Figure 3:3 C-H, demonstrating that SB505124 and DMSO treatments acted as previously documented in Figure 3:2. SB505124 treatment resulted in truncated tadpoles, lacking a discernible axis and tail, head and cement gland features, whereas DMSO treated tadpoles were normal. Figure 3:3 N shows a western blot analysis of protein extracts from stage 10 embryos. This figure demonstrates that the treatment of *Xenopus laevis* embryos with

SB505124 and A-83-01 resulted in a reduction of p-Smad2 levels and that there was a small decrease in phosphorylated extracellular-signal-regulated kinase (ERK), which was used as a specificity control. In conclusion, the preceding work demonstrates that SB505124 and A-83-01 dose-dependently and specifically inhibit the ALK4/5/7 pathway and are suitable reagents for further use investigating the role of ALK4/5/7 signalling in cardiac specification.

Smad2-Venus-Smad4 BiFC has been a useful technique for this study in assessing the ability of SB505124 to inhibit nuclear p-Smad2 localisation and complex formation, and thus Nodal/ Activin signalling transduction. BiFC and western blot experiments presented here give a high level of confidence that the ALK4/5/7 inhibitors SB505124 and A-83-01 are successfully inhibiting the Nodal/ Activin –ALK4/5/7 signalling pathway. Further information concerning the reversibility of these inhibitors would also be beneficial. However, due to the unknown stability of the Venus complex, it is likely that endogenous Smad2-Smad4 complex dissociation and degradation dynamics may be changed, rendering BiFC an unsuitable tool for further investigations into inhibitor dynamics. A GFP-Smad2 fusion, which would be a suitable tool for investigating inhibitor dynamics, proved of insufficient sensitivity in repeated experiments (not shown).

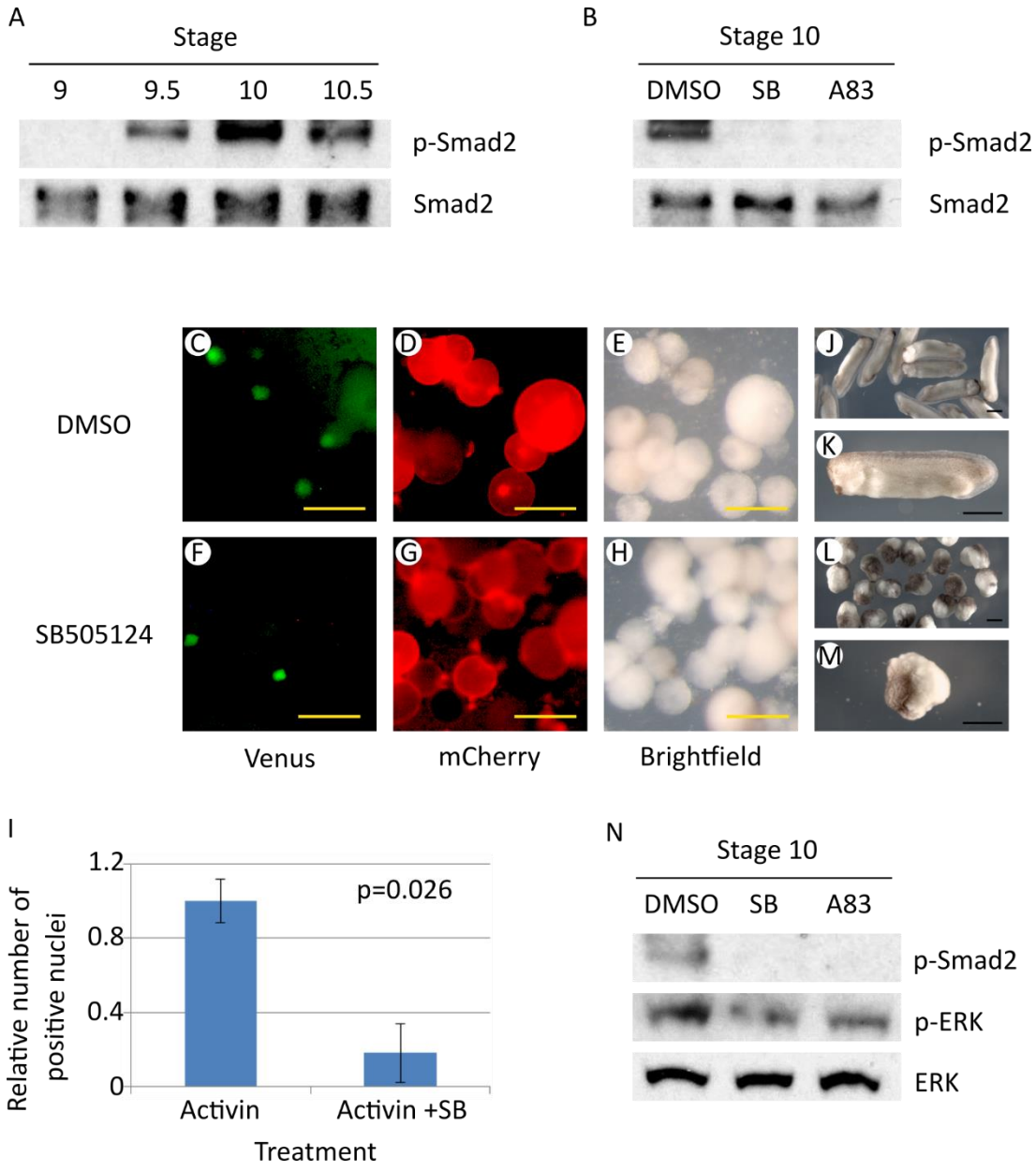

Figure 3:3. ALK4/5/7 signalling inhibition reduces Smad2 activation and nuclear accumulation

Embryos were treated with DMSO or 200 µM of SB505124 (SB) or A-83-01 (A83). (A) Embryos were treated with DMSO at stage 8 then analysed by western blot at the stage indicated. Smad2 is a loading control. (B) Embryos were treated at stage 8 and analysed by western blot analysis at stage 10. Smad2 is a loading control. Embryos were injected with 400 pg VCS2, 400 pg VNS4 and 400 pg mCherry mRNA uniformly into the animal hemisphere at the 2 cell stage and treated with (C-E) DMSO or (F-H) SB505124. Animal caps were harvested at stage 8, dissociated and additionally treated with 16 U/ ml Activin, continuously, for imaging

and analysis at between stage 8.5-9.5. C and F show Venus, D and G show mCherry and E and H are brightfield. C-E and F-H show the same field of view. Scale bar in C-H represents 100 µm. (I) The relative number of p-Smad2-Venus-Smad4 positive nuclei in all lineage traced injected cells of a sample, normalised to the control (DMSO) sample, from images analysed and represented in C-H. A p-value of 0.026 was calculated using an unpaired 2-tailed t-test of equal variances, indicating that there is a significant difference between DMSO and SB505124 treated samples. Activin n=167/430 (38%), Activin +SB n=39/499 (8%) of Venus/ mCherry positive cells. Sibling embryos, at tadpole stage, to those used in C-H were treated at the 2 cell stage and acted as a positive control for (J, K) DMSO and (L, M) SB505124 treatments. Individual images are a lateral view orientated anterior left, dorsal side up. Scale bar in J-M represents 1 mm. (N) Embryos were treated at stage 8 for western blot analysis at stage 10. ERK is a loading control.

3.6 ALK4/5/7 signalling is required for cardiogenesis

To address the requirement for ALK4/5/7 signalling in cardiac specification, molecular ALK4/5/7 inhibitors were utilised to impede signalling and the effect on cardiac tissue was examined. Initially, differentiated cardiac tissue was examined. There is a lack of known cardiac specific markers allowing cardiac cells to be traced from initial specification until terminal differentiated (Scott, 2012). Although there are known genes which are expressed by the cardiac progenitor cell population, such as *nkx2.5* and *isl1*, these genes are not unique to the cardiac lineage (Scott, 2012). Differentiated cardiac cells express genes, such as *myosin light chain 7* (*myl7*), which are specific to the cardiac lineage. Therefore, the staining of differentiated cardiac tissue was examined after ALK4/5/7 inhibition, with the intention of analysing cardiac progenitor cell populations should an effect on differentiated cardiac tissue be observed. The presence of cardiac tissue was initially analysed as a read-out of cardiac specification events, rather than the location and morphology of cardiac tissue which may reflect a requirement for ALK4/5/7 signalling in later cardiogenesis.

Embryos were treated with ALK4/5/7 inhibitors, starting from midblastula transition, proceeding to progressively later stages in development, continuously until the tadpole stage. Whole mount *in situ* hybridisation (WMISH) using the differentiated cardiac tissue *myl7* analysis was performed. Figure 3:4 A-F shows that inhibitor treatment commencing between stages 8-9 resulted in the loss or reduction of the heart field. However, additional phenotypes are observed including a truncated anterior-posterior axis, ventral pigmented folds in the epidermis, and at the earliest administered treatments, retarded anterior development. Inhibitor treatments commencing after stage 9 had a minimal overall phenotypic or specific cardiac effect (Figure 3:4 G-R), compared with the controls (Figure 3:4 S, T).

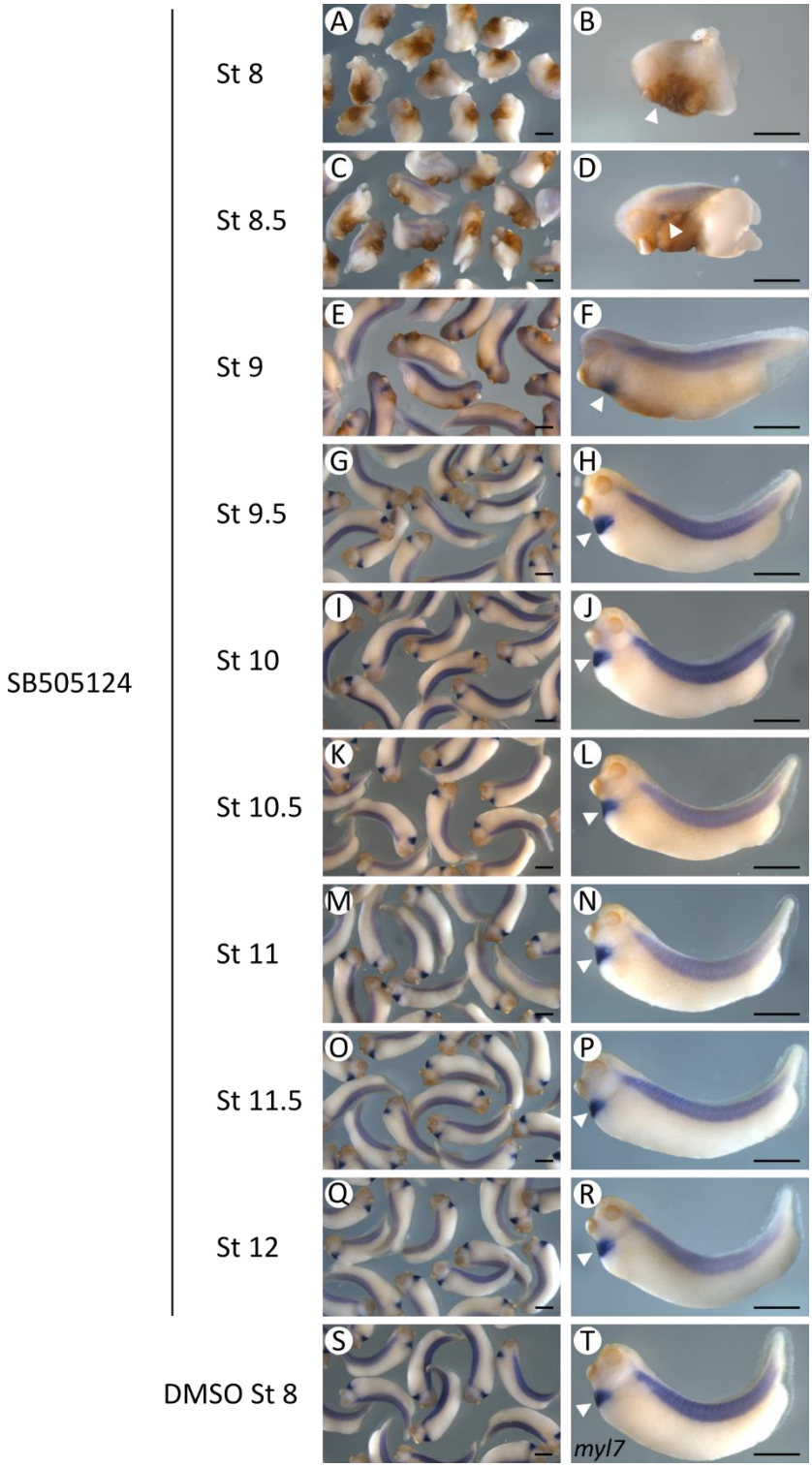

Figure 3:4. ALK4/5/7 signalling is required for cardiogenesis

(A- R) Embryos were treated with 100 µM of SB505124, starting at the stage (St) indicated. (S, T) Controls were treated with DMSO at stage 8. Tadpoles were analysed by whole mount *in situ* hybridisation using the cardiac marker *myl7* (white arrows). Due to overstaining,

colour stain developed in the somites, probably due to staining of the closely related skeletal muscle transcript *myosin light chain 1*. All individual images are a lateral view orientated anterior left, dorsal up. Scale bar represents 1 mm. DMSO n=151, Stage 8 n=144, 8.5 n=105, 9 n=123, 9.5 n=49, 10 n=65 10.5 n=50, 11 n=59, 11.5 n=22 12 n=20.

To further characterise the cardiac phenotypes, the extent of cardiac tissue, as assayed by *myl7* whole mount *in situ* hybridisation staining, was categorised relative to the control samples as either normal, reduced, severely reduced or absent and examples of the classifications are shown in Figure 3:5 B-E. These categories were used in subsequent experiments for a range of whole mount *in situ* hybridisation markers. As studies throughout this chapter are concerned with the first step in cardiogenesis, the induction of cardiac tissue, the extent of cardiac tissue staining present in an embryo was used as an indication of early specification events. The cardiac phenotypes of embryos treated with ALK4/5/7 inhibitors in Figure 3:4 were counted, categorised, and displayed in Figure 3:5 A. Inhibitor treatments commencing at stages 8 or 8.5 resulted in absent or reduced heart tissue in a time-dependent manner, with the earlier in development that the inhibitor was added, the more severe the reduction in cardiac tissue. Inhibitor treatment commencing after stage 9.5 had minimal effect on cardiac tissue.

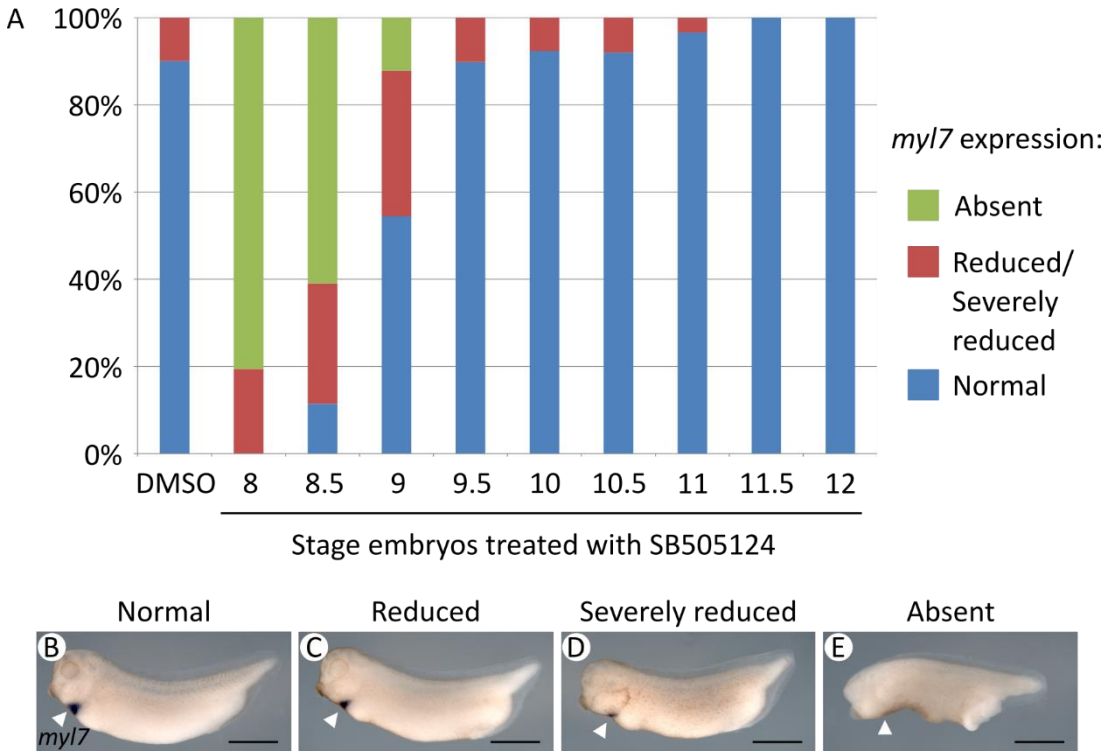

Figure 3:5. The extent of cardiac tissue staining observed in tadpoles subjected to ALK4/5/7 inhibition can be used as a measure of successful cardiac development

(A) Graph quantifying results from Figure 3:4. Embryos were treated continuously with DMSO or 100 µM of SB505124 from the stage indicated along the horizontal axis. Tadpoles were analysed by whole mount *in situ* hybridisation, and the extent of the marker staining indicating the extent of cardiac tissue was classified, illustrated here using *myl7* cardiac tissue staining. (B) Normal: the average staining pattern observed in a given control sample. (C) Reduced: between 50-90% of staining area and intensity observed in controls. (D) Severely reduced: between 1-50% of staining area and intensity observed in controls. (E) Absent: no staining observed. Images are a lateral view orientated anterior left, dorsal up. Scale bar represents 1mm. These categories of staining were subsequently utilised for alternate markers in tadpoles. DMSO n=151, Stage 8 n=144, 8.5 n=105, 9 n=123, 9.5 n=49, 10 n=65 10.5 n=50, 11 n=59, 11.5 n=22 12 n=20.

3.7 Phenotypic, but not p-Smad2, recovery occurs after ALK4/5/7 inhibitor removal

Nodal/ Activin –ALK4/5/7 signalling has multiple roles in the developing *Xenopus laevis* embryo (Hill, 2001). The addition of the soluble ALK4/5/7 inhibitors during the late blastula stages, in investigations reported above, likely allows the early Nodal/ Activin –ALK4/5/7 signalling requirement for mesoderm induction to be fulfilled, as an extended anterior-posterior axis and tail is observed. The presence of mesodermal markers and differentiated derivatives are examined in more detail below. Although the above experiments suggest a role for ALK4/5/7 signalling in heart development, they do not distinguish the requirement for ALK4/5/7 signalling in the specification of cardiac cells from further cardiac development, as the ALK4/5/7 inhibition employed was continuous. The above work has identified a time window of interest between stages 8 and 9.5 in which to conduct further studies into the precise timing and requirement for ALK4/5/7 signalling in cardiac specification. An experimental advantage of using the soluble inhibitors is their ability to be removed from the embryos, thus allowing reversible inhibition. Therefore, SB505124 and A-83-01 were tested for their ability to be removed from *Xenopus laevis* embryos to allow the restoration of Nodal/ Activin –ALK4/5/7 signalling and normal embryonic development. To this end, p-Smad2 levels and phenotypic analysis were conducted on siblings treated for one hour with ALK4/5/7 inhibitors, compared with continuous treatment.

Embryos were treated with ALK4/5/7 inhibitors SB505124 and A-83-01 starting from stage 8, from stage 8 +1 hour or stage 8 +2 hours (Figure 3:6 R). Inhibitor incubations were for either one hour, or continuous. Although shorter inhibitor incubation periods of 20 and 30 minutes were tested, it was found that, due to the variation between embryo batches and inhibitor effectiveness, the practical resolution afforded by this approach is approximately one hour. Figure 3:6 A shows that upon one hour, or continuous, ALK4/5/7 inhibition, the levels of p-Smad2 were decreased, in comparison to DMSO treated controls. Even when several hours had elapsed

before western blot analysis at stage 10 (5 hours after stage 8), there was no recovery in p-Smad2 levels observed. This suggests that the inhibitors might have acted irreversibly. However, Figure 3:6 B-Q shows that the phenotypes of embryos treated continuously with the ALK4/5/7 inhibitors were affected to a greater extent than the phenotypes of siblings treated for one hour, suggesting that some level of recovery did occur after inhibitor removal. Specifically, embryos treated with ALK4/5/7 inhibitor at stage 8, upon continuous inhibition, were severely truncated along the anterior-posterior axis and landmark embryonic features, such as the tail and head, were less defined (Figure 3:6 D, E). Conversely, embryos treated with ALK4/5/7 inhibitor for one hour had an elongated anterior-posterior axis with identifiable landmark features (Figure 3:6 F, G). A similar picture, albeit with a milder phenotype, was observed for treatments commencing at stage 8 +1 hour (Figure 3:6 F, G, N, O). Interestingly, in inhibitor treatments at stage 8 +2 hours (approximately stage 9), embryos presented a relatively normal phenotype upon one hour, or continuous, ALK4/5/7 inhibition (Figure 3:6 H, I, P, Q). However, inhibition resulted in the loss of detectable p-Smad2 by stage 10 (Figure 3:6 A). This suggests that ALK4/5/7 signalling has a minimal requirement beyond stage 9, as embryos developed normally, despite successful ALK4/5/7 inhibition. An alternative explanation is that, once the inhibitors were removed after one hour of incubation, a small amount of p-Smad2 may have been restored. This small quantity of p-Smad2 may have been sufficient to permit some level of normal embryonic development, resulting in the less severe phenotypes observed after one hour of treatment compared to continuous inhibition, but not enough to enter the detectable range of western blotting.

The whole embryonic phenotype, and in particular the presence of a tail and a fully elongated anterior-posterior axis, are good indications that mesoderm induction has been successful before the addition of the ALK4/5/7 inhibitors after midblastula transition. However, examination of known markers *brachyury* (*t*) and *goosecoid* (*gsc*) allows further confidence that ALK4/5/7 inhibition initiated from midblastula transition is having minimal effect on mesoderm induction. *brachyury* is expressed in presumptive mesodermal cells around the blastopore, and is required for mesoderm

formation (Cunliffe and Smith, 1992; Smith et al., 1991). *goosecoid* is expressed on the dorsal side of the late blastula staged embryo and cells are fated to contribute to endoderm and mesoderm, including the Spemann's Organiser (De Roberts et al., 1992). Embryos were treated with ALK4/5/7 inhibitors SB505124 and A-83-01 for one hour starting from stage 8, from stage 8 +1 hour or stage 8 +2 hours. Figure 3:7 shows a small reduction in the expression of *brachyury* and *goosecoid* upon ALK4/5/7 inhibition, compared with controls. These results are in general agreement with previously published work in *Xenopus laevis,* illustrating a slight reduction in *brachyury* and *goosecoid* expression upon SB505124 treatment from stage 8, but not upon treatment at stage 9 (Luxardi et al., 2010). This suggests that the requirement for Nodal/ Activin-ALK4/5/7 signalling activity in mesoderm induction has occurred before the addition of the ALK4/5/7 inhibitors. Therefore, the observed effects on cardiac tissue where ALK4/5/7 inhibition had been initiated after midblastula transition can be reasoned to be specific to the role of Nodal/ Activin –ALK4/5/7 signalling in cardiogenesis and not due to deficient mesodermal tissue. These finding are consistent with the known Nodal/ Activin –ALK4/5/7 signalling requirement, and p-Smad2 activity, for inducing mesendoderm before midblastula transition (Skirkanich et al., 2011).

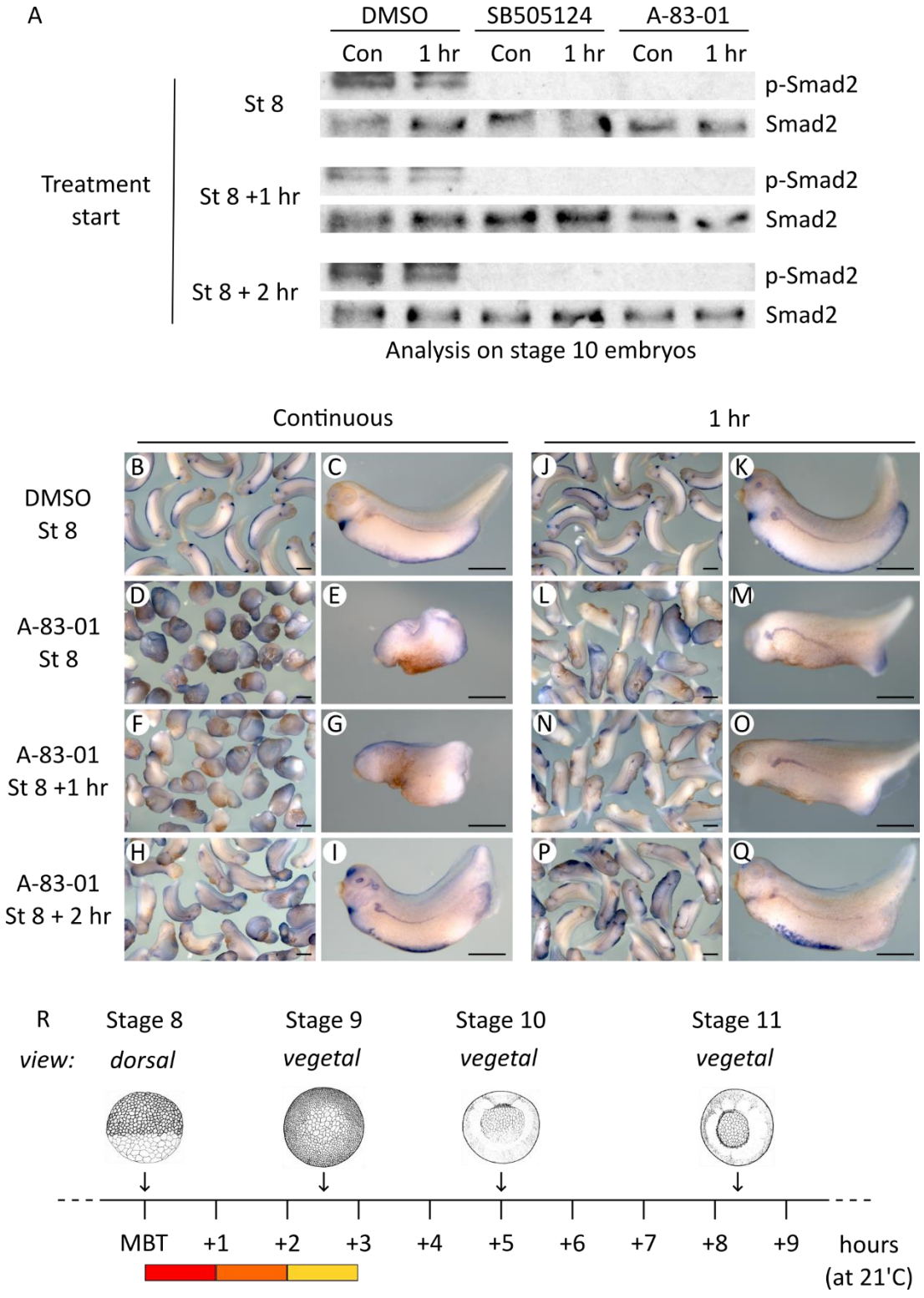

Figure 3:6. Phenotypic, but not p-Smad2, recovery occurs after ALK4/5/7 inhibitor removal

Embryos were treated with DMSO, or 200 µM of SB505124 or A-83-01 at stage 8, stage 8 +1 hour or stage 8 +2 hours. Treatments were either continuous, or for one hour, where inhibitor media was then removed by two 5 minute washes in 30 ml of fresh 10% NAM. (A)

Western blot analysis on stage 10 embryos. Smad2 is a loading control. Tadpole phenotypes after (B-I) continuous treatment, compared with (J-Q) one hour treatment. Individual images show a lateral view orientated anterior left, dorsal up. Scale bar represents 1 mm. Embryos have been stained by whole mount *in situ* hybridisation to better visualise mesoderm derivatives using riboprobes *myosin light chain 7*, *hemoglobin alpha 3 subunit* and *ATPase, Na+/K+ transporting, alpha 1 polypeptide* to detect cardiac, blood and pronephros tissue respectively; more information below in Section 3.11. Continuous treatment DMSO n=38, stage 8 n=53, stage 8+ 1 hour n=52, stage 8 +2 hours n=54. 1 hour treatments DMSO n=44, stage 8 n=56, stage 8+ 1 hour n=67, stage 8 +2 hours n=60. (R) Time line illustrating how stages of *Xenopus laevis* development correspond to time (in hours) after midblastula transition (MBT). Time windows for 1 hour treatments used in experiments are highlighted: stage 8 in red, stage 8 +1 hour in orange and stage 8 +2 hours in yellow.

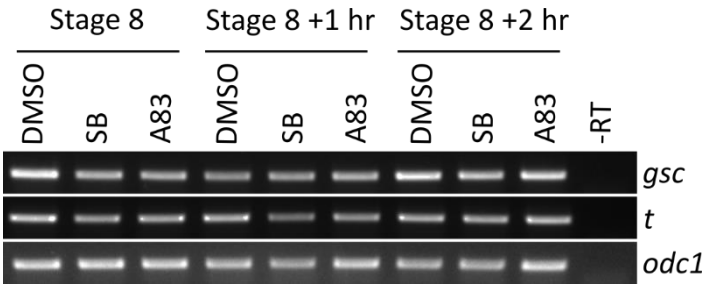

Figure 3:7 ALK4/5/7 inhibition initiated from midblastula transition has a minimal effect on mesodermal gene expression

Embryos were treated with DMSO or 200 µM of SB505124 (SB) or A-83-01 (A83), at stage 8, stage 8 +1 hour or stage 8 +2 hours. Treatments were for one hour, then embryos developed free of treatments until collection at stage 10.5 for RT-PCR analysis of mesodermal genes *brachyury* (*t*) and *goosecoid* (*gsc*). –RT is a negative control and *ornithine decarboxylase 1* (*odc1*) is a loading control.

3.8 Optimising inhibitor removal

Previous investigations reported here have utilised continuous ALK4/5/7 inhibition to surmise that Nodal/ Activin -ALK4/5/7 signalling is required for cardiogenesis. To further question the precise timing and requirement of Nodal/ Activin -ALK4/5/7 signalling in cardiac specification, an appropriate method for the optimum removal of the ALK4/5/7 inhibitors from the *Xenopus laevis* embryos was sought. An advantage of using small soluble molecular inhibitors in *Xenopus laevis* is the ability to change the embryonic media, removing the inhibitor solution, thus allowing time-dependent control of inhibition. It has been demonstrated in the work presented above that phenotypic recovery, but not molecular recovery of p-Smad2, can be detected and observed upon inhibitor removal. To ascertain the most appropriate method of inhibitor removal, several wash out regimes were tested after ALK4/5/7 inhibitor incubation. Inconsequential phenotypic differences were observed in embryos subjected to a range of wash-out techniques which are displayed in Figure 3:8, including 30 ml washes at 21^{O}C, 30 ml washes at 23^{O}C, 500 ml washes at 21^{O}C and chorion removal. Two five minute washes, gently agitated, each in 30 ml of 10% NAM at 21^{O}C was chosen as a standard technique to adopt in all future experiments where inhibitors were removed before the neurula stage. This technique was selected due to its ease to perform, as all techniques presented similar attributes. Interestingly, SB505124 appears to wash away from embryos more effectively than A-83-01, as the phenotypes at tadpole stage are less severe after SB505124 treatment for any given wash out technique (Figure 3:8).

Uncertainty remains regarding the effectiveness of inhibitor reversibility after media change. Upon three 30 ml media changes, the working concentration of SB505124 and A-83-01 would likely have been decreased from 200 µM to less than the lowest concentration of 20 µM tested in the dose response in Figure 3:2. As 20 µM of ALK4/5/7 inhibitors had minimal effect on the embryonic phenotype, it can be reasoned that any remaining inhibitor would be at such a low concentration as to have insignificant effect. However, the inhibitors may remain trapped in cells and

may not be released in a concentration-dependent manner. Consequentially, this may delay the end-point of inhibition until future release or receptor degradation and replacement. In an attempt to gain a better understanding of the dynamics of inhibitor removal and Nodal/ Activin –ALK4/5/7 signalling restoration, the phosphorylation and localisation of Smad2 following inhibitor removal was unsuccessfully examined by fluorescence in live cells and by nuclear fractionation (not shown). Alternatively, mass spectroscopy could have been utilised to examine the levels of inhibitors remaining within an embryo after removal of the inhibitor-containing media; however, mass spectroscopy was not practically feasible in this project. Comparison of siblings treated with the ALK4/5/7 inhibitors SB505124 and A-83-01, for one hour or continuously, in Figure 3:6 B-P, does reveal a difference in the whole embryonic phenotype between treatments. This gives confidence that the removal of the inhibitors has occurred and that some level of Nodal/ Activin –ALK4/5/7 signalling and normal embryonic development has been restored. Although these investigations have not provided direct evidence on a molecular level that the action of the inhibitors is reversible, phenotypic analysis suggests inhibitor reversibility. Therefore, SB505124 and A-83-01 inhibitors remain as appropriate reagents to use for time-dependent control of Nodal/ Activin-ALK4/5/7 signalling inhibition for further investigations in *Xenopus laevis*.

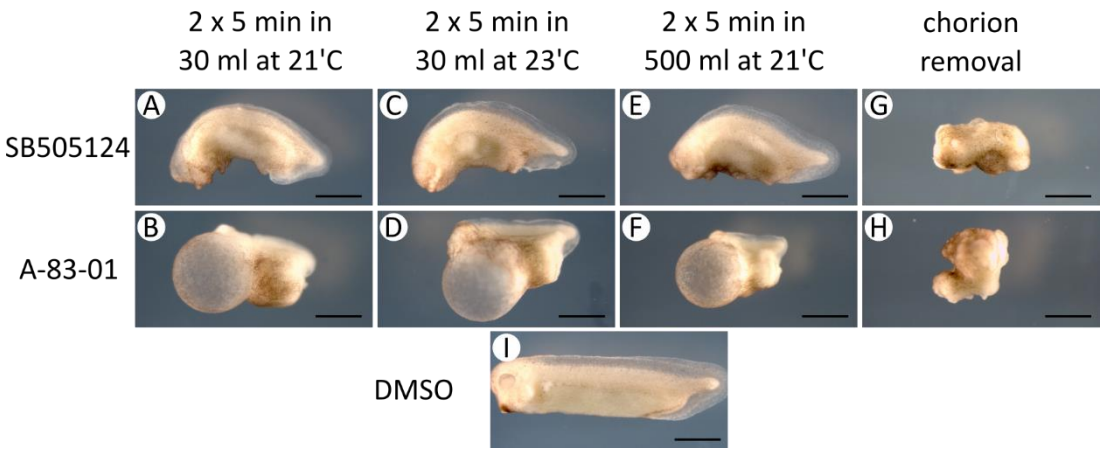

Figure 3:8. Optimising ALK4/5/7 inhibitor wash out

Embryos at the 4 cell stage were treated with DMSO or 200 µM of SB505124 or A-83-01, until stage 6.5, where inhibitor-containing media was washed away, testing a variety of methods. (A-B) Two 5 minute washes, gently agitated, in 30 ml 10% NAM at 21^{O}C. (C-D) Two 5 minute washes, gently agitated, in 30 ml 10% NAM at 23^{O}C. (E-F) Two 5 minute washes in 500 ml tap water at 21^{O}C. (G-H) chorion removal and (I) control. Images are of stage 32 embryos showing a lateral view orientated anterior left, dorsal up. Scale bar represents 1 mm.

3.9 A low level of ALK4/5/7 signalling is required from midblastula transition for cardiac specification

The time when pre-cardiac cells are given a specific fate to develop into the cardiac lineage has not been precisely defined. It is known from explant experiments that cardiac specification has occurred by the end of gastrulation, and that anterior endoderm tissue taken before mid-gastrulation can induce cardiac tissue in pluripotent responder cells (Samuel and Latinkić, 2009; Sater and Jacobson, 1989). Therefore, it is widely assumed that cardiac specification occurs during gastrulation. However, the data presented here demonstrates that ALK4/5/7 and p-Smad2 signalling can be inhibited during gastrulation and that embryos can develop normal cardiac tissue staining patterns. The work in this section focuses on a more precise investigation of the timing and requirement for ALK4/5/7 in cardiac specification, concentrating on the time window from midblastula transition (stage 8), but before the onset of gastrulation (stage 10).

Embryos were treated with ALK4/5/7 inhibitors SB505124 or A-83-01 for one hour, starting from stage 8, stage 8 +1 hour or stage 8 +2 hours. Once at the tadpole stage, whole mount *in situ* hybridisation analysis using the differentiated cardiac tissue marker *myl7* was performed. Embryos treated with ALK4/5/7 inhibitors for one hour from stage 8 developed no, or very little, cardiac tissue (Figure 3:9 A-D, O). Embryos treated from stage 8 +1 hour presented severely reduced cardiac tissue (Figure 3:9 E-H, O), whereas embryos treated from stage 8 +2 hours generally displayed a reduced level of cardiac tissue (Figure 3:9 I-J, O), bearing greater similarity to the levels observed in the controls (Figure 3:9 M, N, O). Embryos appeared to gastrulate, although the formation of the blastopore lip was delayed and often less pronounced in samples treated with the ALK4/5/7 inhibitors. The reduction in the size of the head could be partially due to compromised gastrulation, although the phenotype and elongation of the embryo does suggest that gastrulation has taken place.

Western blot analysis on protein extracts from stage 10 embryos revealed that p-Smad2 levels were reduced in ALK4/5/7 inhibitor-treated samples compared with

controls. Additionally, there did not appear to be a delay in p-Smad2 activation upon inhibitor removal after one hour of incubation (Figure 3:9 P). Using stage 8 +1 hour embryos subjected to one hour of ALK4/5/7 inhibition as an example, no recovery of p-Smad2 was observed. However, the natural decrease in p-Smad2 during gastrulation resulted in more comparable p-Smad2 levels between control and inhibited samples by +8 hours after midblastula transition (Figure 3:9 Q). See Figure 3:6 R for time comparison with developmental stage. Therefore, these results suggest that the peak of p-Smad2 observed at the onset of gastrulation (stage 10) is not required for cardiac tissue specification, as ALK4/5/7 signalling can be inhibited, p-Smad2 levels decrease, and embryos still developed cardiac tissue. In conclusion, these results suggest that a low level of ALK4/5/7 signalling which occurs around midblastula transition (stage 8) is required for cardiac specification, with the requirement being practically fulfilled by the end of stage 9, well before the onset of gastrulation. This is a novel time window identified for the involvement of Nodal/Activin –ALK4/5/7 signalling in cardiac specification, and is earlier than previously thought.

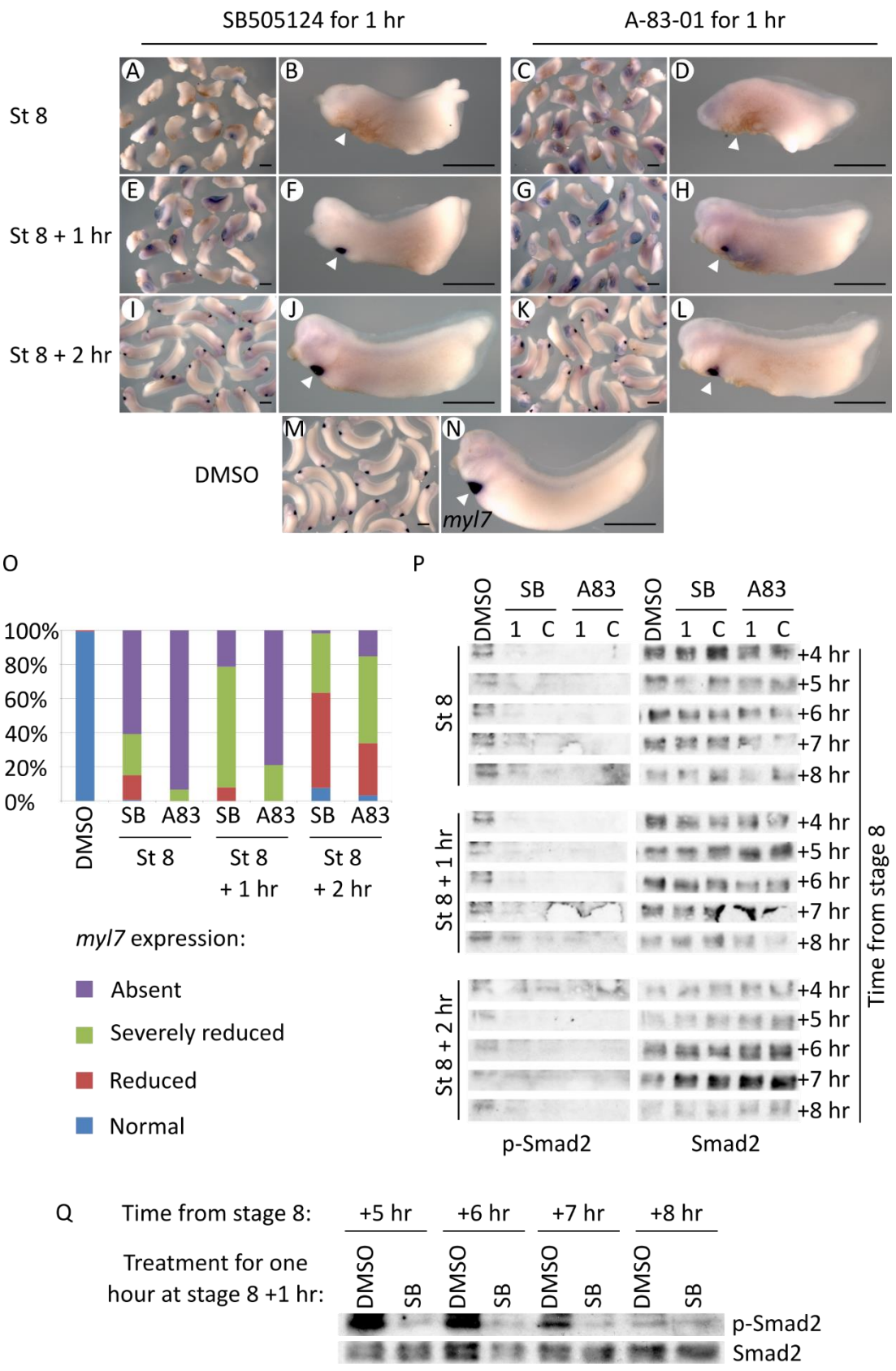

Figure 3:9. Active ALK4/5/7 signalling is required for 2-3 hours from midblastula transition for cardiac specification

Embryos were treated with DMSO or 200 µM of SB505124 (SB) or A-83-01 (A83), at stage 8, stage 8 +1 hour or stage 8 +2 hours. Treatments were either continuous (C), or for one hour (1). Tadpoles, treated for one hour, were analysed by whole mount *in situ* hybridisation using the cardiac marker *myl7* (white arrows). ALK4/5/7 inhibition for one hour from: (A-D) stage 8, (E-H) stage 8 +1 hour and (I-L) stage 8 +2 hours. (M, N) DMSO controls. All individual images are a lateral view orientated anterior left, dorsal up. Scale bar represents 1 mm. (O) Graph displaying results of A-N; DMSO n=153, St8 SB n=145, St8 A83 n=120, St8 +1 SB n=150, St8 +1 A83 n=90, St8 +2 SB n=52, St8 +2 A83 n=118. (P) Western blot analysis on a time series of continuous or one hour treated embryos prior to, and during, gastrulation. (Q) Western blot analysis on a time series during gastrulation of embryos treated for one hour at stage 8 +1 hour. Smad2 is a loading control.

3.10 The migration, fusion and remodelling of cardiac tissue is largely unaffected by ALK4/5/7 signalling inhibition

Additional information about cardiac development can be inferred from the morphology of the developing heart. Experimental samples that were scored for the relative staining of cardiac tissue in Figure 3:9 were examined for cardiac morphology. Briefly, embryos were treated with ALK4/5/7 inhibitors, or DMSO, continuously from stage 8, followed by analysis by whole mount *in situ* hybridisation using the differentiated cardiac tissue marker *myl7* and immunohistochemistry using the skeletal muscle marker 12/101. The morphology of the heart was observed at stage 36. DMSO treated control embryos displayed a heart of normal size, with the future atria, ventricle and outflow tract forming (Figure 3:10 A, B). By stage 35, the recently formed linear heart tube, which is originally orientated along the anterior-posterior axis, forms an anticlockwise spiral, bending towards the right hand side of the embryo. An s-shaped bulging cardiac tube is formed, aided by the anterior and dorsal movement of the future atrial region (Figure 3:10 K) (Kolker et al., 2000; Latinkić et al., 2004; Mohun et al., 2000). No cardiac tissue or cardiac morphology features were observed in embryos classified as having absent cardiac tissue (Figure 3:10 C, D). Tadpoles with severely reduced cardiac tissue frequently presented a small tube or cardiac cavity, often bulging slightly (Figure 3:10 E, F). Smaller areas of cardiac tissue staining than in controls, but with evidence of morphological movements and bulging, were observed in embryos with reduced cardiac tissue (Figure 3:10 G, H). Most often the cardiac fields fused on the ventral midline resulting in severely reduced or reduced cardiac tissue phenotypes. Occasionally cardia bifida was observed, where two independent chambers formed (Figure 3:10 I, J). Linear heart tubes were rarely observed. Landmark features, such as the presence of the eyes, head and cement gland were of the correct and comparable size between samples. Skeletal muscle development is complete and extends fully into the anterior region (Figure 3:10 A, C, E, G, I), suggesting normal anterior development with a specific cardiac effect in ALK4/5/7 inhibited embryos. These results indicate that ALK4/5/7 signalling is required for the specification of cardiac tissue, and once

specified the cardiac tissue is able to migrate, fuse and undergo morphological events.

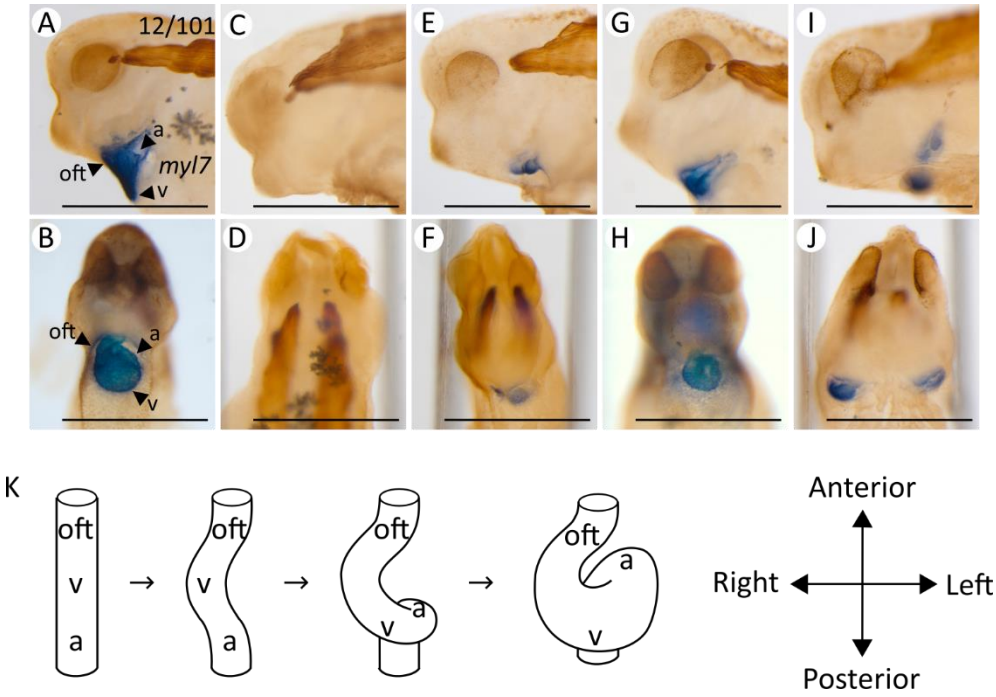

Figure 3:10. The migration, fusion and remodelling of cardiac tissue is largely unaffected by ALK4/5/7 signalling inhibition

Tadpoles subjected to treatments in Figure 3:9 were analysed by whole mount *in situ* hybridisation using the cardiac tissue marker *myl7* (blue stain), followed by immunohistochemistry using the skeletal muscle marker 12/101 (brown stain). (A, B) DMSO treated controls with future atrium (a), ventricle (v) and outflow tract (oft) highlighted (arrows). (C, D) Absent cardiac tissue. (E, F) Severely reduced cardiac tissue. (G, H) Reduced cardiac tissue. (I, J) Cardia bifida. C-J example embryos have been treated with 200 µM of A-83-01, and developed until the tadpole stage. Scale bar represents 1 mm. A, C, E, G and I show a lateral view, orientated anterior left. B, D, F, H and J show a ventral view, anterior upwards. These are example cardiac phenotypes from the experiments presented and quantified in Figure 3:9. (K) Schematic diagram of the linear heart tube bending rightwards, creating an anticlockwise spiral and bulging, aided by the anterior-dorsal movement of the posterior (atrial) region, to form the heart.

3.11 Skeletal muscle, notochord and pronephros are largely unaffected by ALK4/5/7 signalling inhibition from midblastula transition onwards

Mesoderm induction and cardiac specification occur sequentially and early in embryonic development, and both require Nodal/ Activin signalling. To test whether the addition of ALK4/5/7 inhibitors from midblastula transition stage onwards could be affecting mesoderm development, thus indirectly affecting cardiac specification, a range of differentiated mesoderm derivatives were examined.

Embryos were treated with ALK4/5/7 inhibitors SB505124 or A-83-01, for one hour, starting from stage 8, stage 8 +1 hour or stage 8 +2 hours. Once at the tadpole stage, triple whole mount *in situ* hybridisation to detect differentiated markers for cardiac tissue using *myl7* riboprobe, blood using *hemoglobin alpha 3 subunit* (*hba3*) riboprobe and pronephros using *ATPase, Na+/K+ transporting, alpha 1 polypeptide (atp1a1)* riboprobe was performed. Skeletal muscle, using 12/101 antibody, and notochord, using MZ15 antibody, were detected by immunohistochemistry.

No obvious difference in the extent of staining was observed in pronephros, skeletal muscle and notochord tissue in tadpoles in all ALK4/5/7 inhibitor-treated samples and in controls (Figure 3:11 A-P and R-T). Frequently, in ALK4/5/7 inhibitor treated samples, particularly where inhibition began earlier, the notochord was of a greater girth than in the control samples (compare Figure 3:11 D with H for example). This is most likely due to the reduced anterior-posterior axis length, as Nodal/ Activin has a known role in convergent extension movements for axis elongation (Luxardi et al., 2010). The full complement of notochord tissue appears to have formed, but elongation was compromised. This suggests that changes in notochord appearance between ALK4/5/7 inhibitor treated sample and controls was not due to deficient tissue specification. There were up to 10% fewer somites in ALK4/5/7 inhibitor-treated samples. Somites were fully sized and extended the full length along the anterior-posterior axis. Again, this reduction in somite number is likely due to the reduced length of the anterior-posterior axis, rather than the failure of mesoderm and skeletal muscle induction. Interestingly, the ventral blood island was affected in

a similar manner to cardiac tissue. ALK4/5/7 inhibition during the earliest time-window of treatment, starting from stage 8, resulted in tadpoles with no or very little blood. A severely reduced blood island is observed with ALK4/5/7 inhibition from stage 8 +1 hour, and a reduced area of staining for blood is seen when ALK4/5/7 inhibition commenced at stage 8 +2 hours (Figure 3:11 B, F, J, N, Q). The anterior, rather than posterior, blood island was most severely affected. This is not surprising as the anterior blood and heart primordia are adjacent in the early embryo, and have overlapping regulation (Sakata and Maeno, 2014).

In conclusion, the work presented here suggests that the Nodal/ Activin requirement in mesoderm induction has been fulfilled before the addition of ALK4/5/7 inhibitors from midblastula transition, as the staining pattern of mesoderm derivatives notochord, pronephros and skeletal muscle was largely unaffected. Effects observed on differentiated cardiac tissue upon ALK4/5/7 inhibition for 2-3 hours after midblastula transition were likely not caused by an effect on general mesoderm formation.

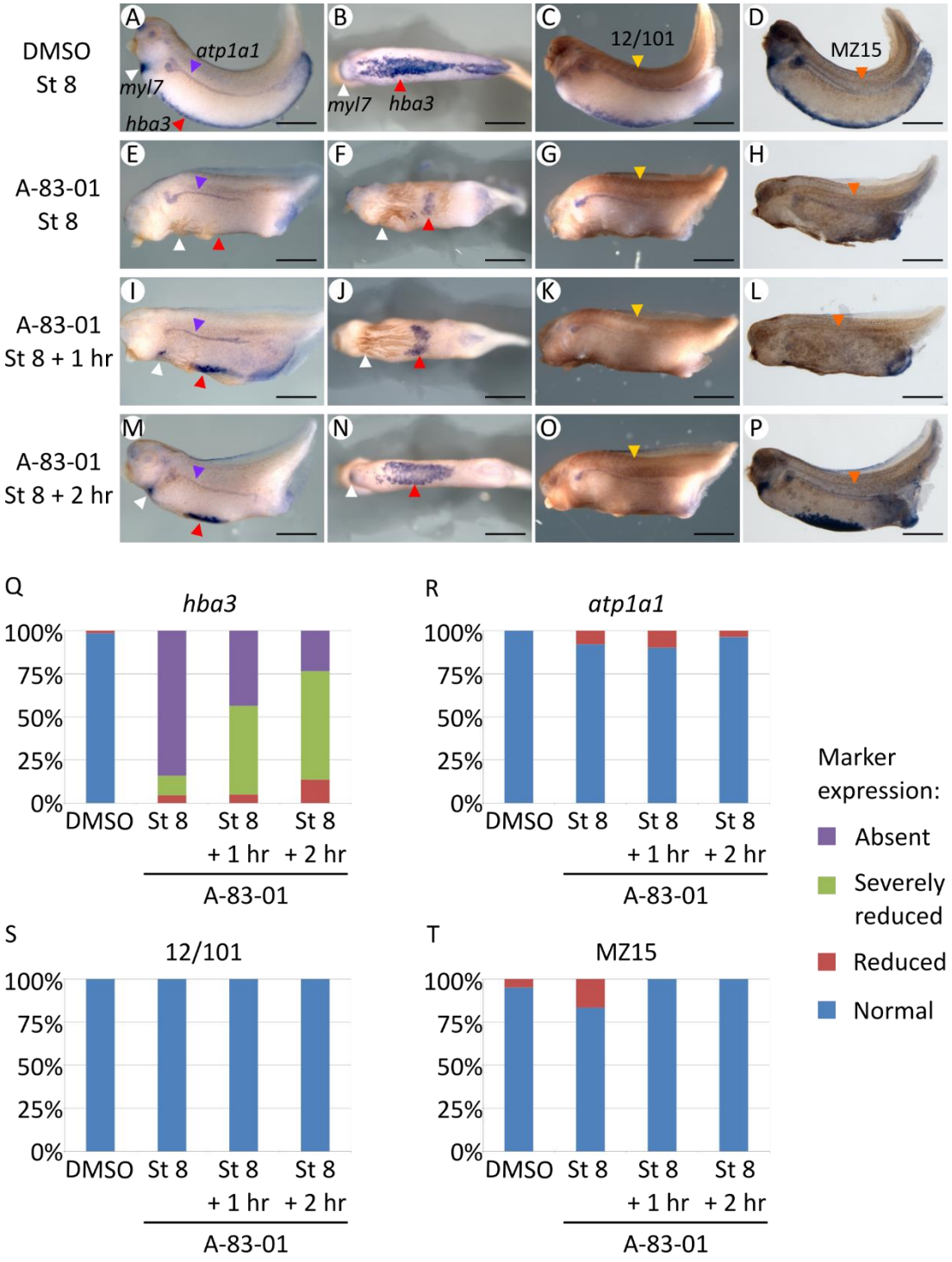

Figure 3:11. Skeletal muscle, pronephros and notochord are largely unaffected by ALK4/5/7 inhibition form midblastula transition onwards

Embryos were treated for one hour with DMSO or 200 µM of A-83-01, at stage 8, stage 8 +1 hour or stage 8 +2 hours. (A-P) Tadpoles were analysed by whole mount *in situ* hybridisation using the cardiac marker *myl7* (white arrows), the blood marker *hba3* (red arrows) and the

pronephros marker *atp1a1* (purple arrows). Tadpoles were subsequently processed by immunohistochemistry for (C, G, K, O) skeletal muscle marker 12/101 (yellow arrows) or (D, H, L, P) notochord marker MZ15 (orange arrows). Images show a lateral view orientated anterior left, dorsal up, except B, F, J and M which display a ventral view with anterior left. Scale bar represents 1 mm. Graphs displaying results of A-P; (Q) blood DMSO n=68, St8 n=88, St8 +1 n=101, St8 +2 n=81; (R) pronephros DMSO n=68, St8 n=88, St8 +1 n=101, St8 +2 n=81; (S) skeletal muscle DMSO n=69, St8 n=54, St8 +1 n=32, St8 +2 n=21; (T) notochord DMSO n=20, St8 n=30, St8 +1 n=39, St8 +2 n=28.

3.12 ALK4/5/7 signalling is required for cardiac progenitor cell specification

To gain a better understanding of the requirement for Nodal/ Activin in the initial stage of heart development, earlier cardiac lineage markers were analysed. The expression of transcription factors *nkx2.5* and *isl1* marks the earliest recognisable cardiac progenitor fields. *nkx2.5* is expressed in both the primary and secondary heart fields, and continues to be expressed in the mature heart throughout the left ventricle and atrial chambers (Kasahara et al., 1998; Komuro and Izumo, 1993; Lints et al., 1993; Tonissen et al., 1994). *isl1* is predominantly expressed in the secondary heart field, overlapping the more anterior domain of *nkx2.5* expression (Cai et al., 2003; Gessert and Kühl, 2009). The expression of *nkx2.5* and *isl1* is upregulated during the late gastrula stages (Brade et al., 2007; Tonissen et al., 1994). *Myeloperoxidase* (*mpo*) and *T-cell acute lymphocytic leukemia 1* (*tal1)* are early markers of the myeloid cells and ventral blood island respectively (Ciau-Uitz et al., 2000; Kallianpur et al., 1994; Tashiro et al., 2006). *Mpo* expression is upregulated from late gastrula stages and is expressed in myeloid cells of the anterior ventral mesoderm (Tashiro et al., 2006). *Tal1* is expressed from late gastrula stages in developing hematopoietic cells of the ventral blood island that give rise to all blood cell types (Kallianpur et al., 1994; Mead et al., 1998). Using ALK4/5/7 inhibitors in a time controlled manner, the timing and requirement for ALK4/5/7 signalling in specifying cardiac and hematopoietic progenitor cells was investigated.

Embryos were treated with ALK4/5/7 inhibitors SB505124 or A-83-01 for one hour, starting from stage 8, stage 8 +1 hour or stage 8 +2 hours. Once at stage 20 (neurula stage), double whole mount *in situ* hybridisation using *nkx2.5* and *mpo* or *isl1* and *tal1* was performed. The extent of staining was classified as either absent, severely reduced, reduced or normal and examples of each staining category are shown in Figure 3:12 Q-T. These results show that treating embryos with ALK4/5/7 inhibitors from midblastula transition resulted in the loss or reduction of the early cardiac (*nkx2.5*, *isl1*) and hematopoietic (*mpo*, *tal1*) fields in a time-dependent manner. This is in excellent agreement with results gained from differentiated tissue analysis

shown in Figure 3:11. Earlier ALK4/5/7 inhibitor treatments, starting at stage 8, resulted in embryos with absent or severely reduced cardiac and hematopoietic progenitor markers (Figure 3:12 C, D, K, L, U-X). Embryos treated with ALK4/5/7 inhibitors from stage 8 +1 hour displayed severely reduced or reduced cardiac and hematopoietic progenitor markers (Figure 3:12 E, F, M, N, U-X). Conversely, upon ALK4/5/7 inhibitor treatments commencing at stage 8 +2 hours, embryos displayed a reduced-to-normal levels of cardiac and hematopoietic progenitor markers (Figure 3:12 G, H, O, P, U-X), bearing more similarities to the controls (Figure 3:12 A, B, I, J, U-X) than earlier time points of inhibition. Therefore, these results suggest that there is a requirement for ALK4/5/7 signalling in the specification of the early cardiac and hematogenic progenitor pools.

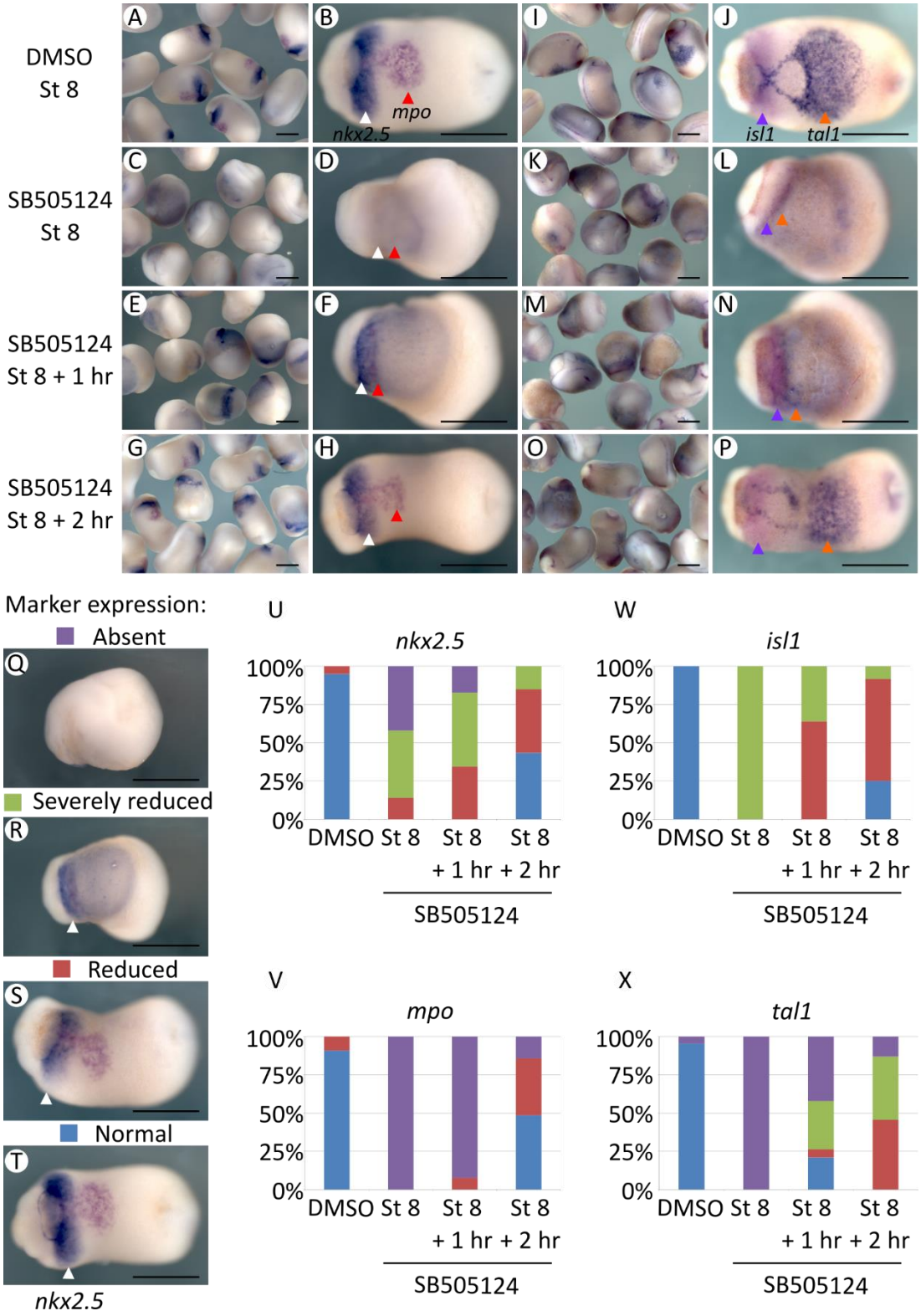

Figure 3:12. ALK4/5/7 signalling is required for cardiac progenitor cells

Embryos were treated for one hour with DMSO or 200 µM of SB505124, at stage 8, stage 8 +1 hour or stage 8 +2 hours. Stage 20 (neurula) embryos were analysed by whole mount *in*

situ hybridisation using (A-H) cardiac progenitor marker *nkx2.5* (blue stain, white arrows) and myeloid cell marker *mpo* (pink stain, red arrows), or (I-P) cardiac progenitor marker *isl1* (pink stain, purple arrows) and hematopoietic marker *tal1* (blue stain, orange arrows). The extent of marker staining was classified, illustrated here using *nkx2.5* cardiac tissue staining (blue stain, white arrows). (Q) Absent: no staining observed. (R) Severely reduced: between 1-50% of staining area and intensity observed in controls. (S) Reduced: between 50-90% of staining area and intensity observed in controls. (T) Normal: the average staining pattern observed in a given control sample. Graphs displaying results of A-P; (U) *nkx2.5* DMSO n=137, St8 n=50, St8 +1 n=87, St8 +2 n=53; (V) Pox2 DMSO n=22, St8 n=19, St8 +1 n=26, St8 +2 n=35; (W) *isl1* DMSO n=25, St8 n=22, St8 +1 n=25, St8 +2 n=24; (X) *tal1* DMSO n=25, St8 n=22, St8 +1 n=25, St8 +2 n=24. All individual images are a ventral view orientated anterior left. Scale bar represents 1 mm.

3.13 ALK4/5/7 signals via Smad2 for cardiac specification

To ascertain whether Smad2 is a key mediator of ALK4/5/7 signalling, to further confirm the specificity of ALK4/5/7 inhibition and in addition to address the nature of the requirement for ALK4/5/7 signalling in cardiac specification, a rescue experiment was be performed. ALK4/5/7 signalling was inhibited using SB505124 or A-83-01, then Smad2 was supplied and allowed to take effect to rescue the inhibition at the receptor level.

The mRNAs of two different Smad2 constructs, injected into the *Xenopus laevis* embryos, were tested for their suitability in the rescue experiment. The constructs included a glucocorticoid receptor (GR) binding domain, making them inducible by the addition of dexamethasone (DEX) (Sive et al., 2000). One construct contained the full length version of the Smad2 gene (GR-Smad2), and the other contained a truncated Smad2 gene (GR-tSmad2). The truncated Smad2 lacked the N-terminal 197 amino acids which comprise the DNA binding domain (Chang and Harland, 2007; M Howell and Hill, 1997; Shi et al., 1998). Nevertheless, it has previously been show that the truncated Smad2 protein can partially compensate for absent p-Smad2 (Das et al., 2009; M Howell and Hill, 1997; Skirkanich et al., 2011). The exact mechanism through which GR-Smad2 and GR-tSmad2 work is unknown, but presumably the overexpression of the inducible Smad2 protein overrides the phosphorylation requirement, enabling Smad2 to associate with Smad4 and activate gene transcription (Shimizu and Gurdon, 1999).

GR-Smad2 or GR-tSmad2 mRNA was injected uniformly into embryos at the 2 cell stage and DEX treatment implemented, until the tadpole stage. The results of these experiments show that qualitatively both mRNA species produced comparative results, with lower doses of mRNA inducing a partial secondary axis or outgrowths and higher doses resulting in a truncated anterior-posterior axis (Figure 3:13 A-L). Of note is that 200 pg of truncated Smad2 mRNA gave rise to the same phenotype as the full length Smad2 mRNA at the higher concentration of 500 pg (Figure 3:13 A, B, G, H). GR-tSmad2 appears to be more potent at lower doses thus was selected to be

used for further investigations. Nodal signalling induces the Spemann's Organiser, an embryonic signalling centre with a well-established ability to induce a secondary axis when transplanted to the ventral side of a host embryo (Gritsman et al., 2000; Spemann and Mangold, 1924). Smad2 mRNA has been shown to induce ectopic trunk-tail structures, commonly characterised as a posterior-type secondary axis, or an incomplete secondary axis lacking a head structure (Baker and Harland, 1996). Therefore, by introducing ectopic Smad2 expression, axial mesoderm and hence a secondary axis is induced. This can be used as a marker for the inducible activity of the Smad2 protein.

After treating GR-tSmad2 mRNA injected embryos with DEX for varying time periods, it became apparent that the DEX incubation time impacted upon the level of construct activity. In tadpoles, no external phenotypic effect was observed after 5 minutes of DEX incubation (Figure 3:13 Q, R). Small outgrowths occurred after one hour of DEX treatment (Figure 3:13 S, T). Tadpoles were truncated and develop abnormally when treated with DEX continuously (Figure 3:13 U, V). GR-tSmad2 mRNA injected embryos not treated with DEX had no external phenotypic effects (Figure 3:13 O, P) and were comparable to controls (Figure 3:13 M, N), demonstrating that the construct is not leaky at the phenotypic level of analysis. The activity of the GR-tSmad2 protein can be modulated by varying the length of the DEX incubation periods to give time-dependent control over induced Smad2 signalling.

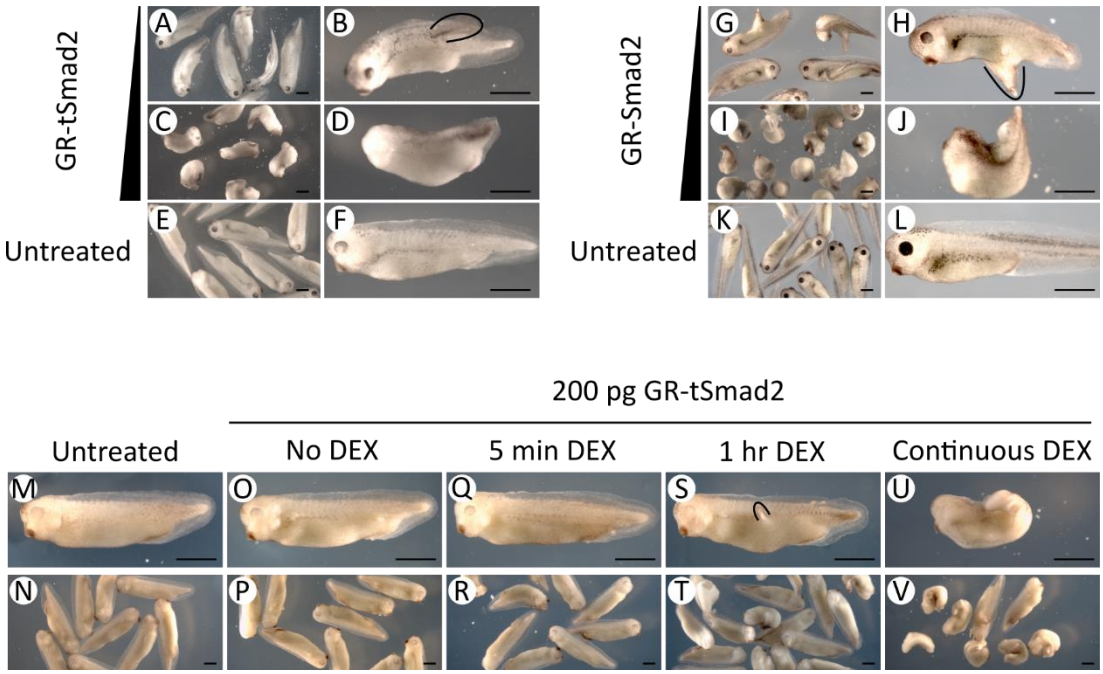

Figure 3:13. Assessing the activity of GR-Smad2 and GR-tSmad2 by phenotypic analysis

Embryos were injected uniformly with (A, B) 200 pg GR-tSmad2 mRNA (n=11), (C, D) 400 pg GR-tSmad2 mRNA (n=7) or (E, F) uninjected (n=12), and treated with 2 µM DEX at stage 7 until the tadpole stage. Embryos were injected uniformly with (G, H) 500 pg GR-Smad2 mRNA (n=9), (I, J) 1 ng GR-Smad2 mRNA (n=19) or (K, L) uninjected (n=22), and treated with 2 µM DEX at stage 3 until the tadpole stage. Embryos were either (M, N) uninjected (n=9) or injected uniformly with 200 pg GR-tSmad2 mRNA and were (O, P) untreated (n=9) or were treated with DEX from stage 8 (Q, R) for 5 minutes (n=9), (S, T) for one hour (n=18) or (U, V) continuously (n=8). All individual images are a lateral view orientated anterior left, dorsal up. Scale bars represent 1 mm. Secondary axis and outgrowths have been outlined.

To investigate whether cardiac specification is mediated by Smad2 downstream of Nodal/ Activin –ALK4/5/7, molecular ALK4/5/7 inhibitors were used to inhibit the ALK4/5/7 pathway, then Smad2 protein from the injected GR-tSmad2 mRNA was tested for its ability to rescue the embryonic phenotype from the effect of the inhibitors, in a time controlled manner. Embryos were injected with 50 pg per blastomere of GR-tSmad2 mRNA at the 8 cell stage, into two dorsal vegetal (DV) or two ventral vegetal (VV) blastomeres. Targeted injections were used instead of uniform injections, as the whole embryo phenotypes by the tadpole stage were more subtle and specific and therefore produced more robust data. At stage 8 +1 hour, embryos were treated for one hour with ALK4/5/7 inhibitors or DMSO, either alone or with DEX. Neurula and tadpole-stage embryos were analysed by whole mount *in situ* hybridisation using the cardiac progenitor marker *nkx2.5* and differentiated cardiac tissue marker *myl7*. The results show that embryos treated with ALK4/5/7 inhibitors at stage 8 +1 hour displayed severely reduced cardiac tissue and a slightly truncated anterior-posterior axis (Figure 3:14 I-L, U, V) , as observed in previous experiments presented above. Embryos subjected to ALK4/5/7 inhibition with enhanced Smad2 in VV cells, which are distant from the heart-forming region, presented severely reduced cardiac tissue and a truncated anterior-posterior axis (Figure 3:14 M-O, U, V). In contrast, ALK4/5/7 inhibitor-treated embryos with enhanced Smad2 in DV cells, fated to contribute to the heart, exhibited an increased area of cardiac tissue staining and had a more extended anterior-posterior axis (Figure 3:14 Q-T, U, V). Embryos that were treated with DEX alone presented the same phenotype as uninjected controls, and outgrowths were observed, but rarely (Figure 3:14 A-H, U, V). This one-hour DEX treatment-window was later in development than during the window used in the DEX time-optimisation experiments. Therefore, it is possible that cells may have had a reduced ability to respond to enhanced Smad2 and form a secondary axis or outgrowths. Excellent agreement was seen in the extent of cardiac tissue staining observed between the earlier and the later-staged embryos analysed. These results suggest that it is possible to partially rescue the cardiac and whole embryo phenotypes induced by the inhibition of the ALK4/5/7 pathway, by providing active Smad2. Interestingly, the

partial rescue of the anterior-posterior axis phenotype in DV injected samples is indicative of a non-cell autonomous effect. This is in keeping with the idea that Nodal/ Activin signalling is required for establishing the Spemann's Organiser on the dorsal side of the embryo, which acts as an inducer, releasing signals which can act distally (Gritsman et al., 2000; Niehrs, 2004). Developing the colour stain for the injected lineage tracer dextran-biotin allows cells which received injected material to be traced. Figure 3:14 W-D1 confirms that the correct targeted injections were achieved, and supports the observation that the anterior-posterior axis in DV injected embryos is partially rescued by a non-cell autonomous effect. It would appear that the expression of cardiac markers was not rescued by a non-cell autonomous effect when Smad2 was activated in VV cells. This perhaps suggests that Smad2 is required in future cardiac cells, or that higher concentrations of Smad2 are required for cardiac specification than can be achieved by a distal signal from the VV region.

Similar rescue experiments to those accomplished at stage 8 +1 hour were attempted with treatments at stage 8, but no rescue in cardiac marker expression or whole embryonic phenotype, in comparison to controls, was observed. This suggests that there is a greater requirement for Smad2 signalling from stage 8, which GR-tSmad2 is not rescuing. By stage 8 +1 hour it is possible that partial specification of cardiac tissue has occurred during the elapsed time from midblastula transition, thus the level of Smad2 signalling required from stage 8 +1 can be partially rescued by GR-tSmad2. GR-tSmad2 dose and DEX incubation time were altered in an attempt to achieve a successful rescue at stage 8, but did not produce informative results. Rescue experiments are a fine balance between opposing activities of different reagents and are more likely to work if the induced phenotypes are moderate.

In summary, the cardiac tissue and whole embryo phenotype observed after ALK4/5/7 inhibition can be rescued, at least in part, by time-dependent activation of Smad2. Smad2 appears to be the primary mediator for the ALK4/5/7 signalling requirement in cardiogenesis. The Smad2 requirement is absolute from midblastula transition, with a decreasing dependency on Smad2 towards the end of stage 9, for cardiac tissue specification. In addition, this work confirms the specificity of action of

the ALK4/5/7 inhibitors. It would be interesting to investigate the effects of a longer DEX incubation period, in conjunction with 1 hour of ALK4/5/7 inhibition, in addition to testing an increased dose of GR-tSmad2 mRNA for the rescue experiment.

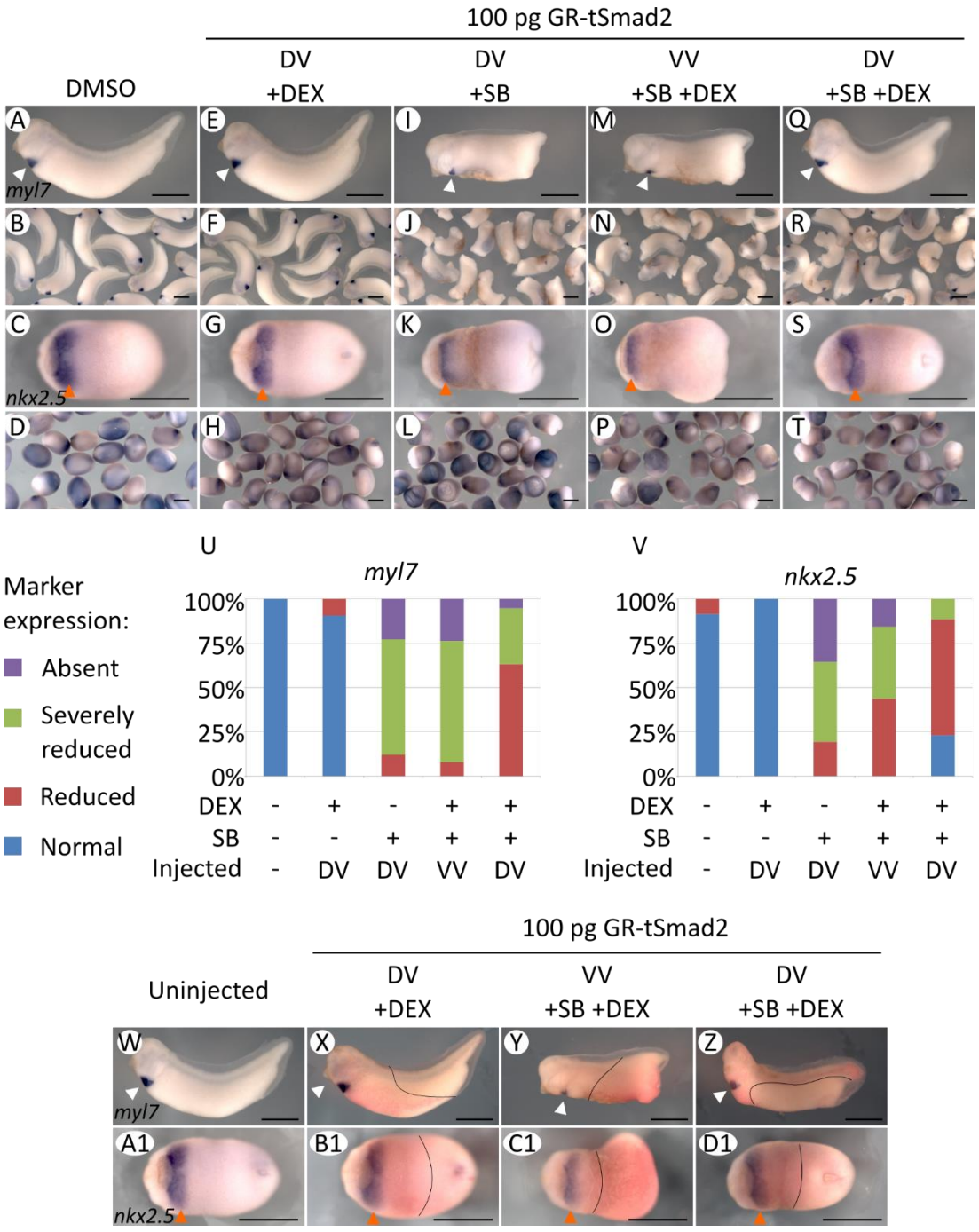

Figure 3:14. Timed activation of Smad2 rescues the effect of ALK4/5/7 inhibition on cardiac tissue

Embryos were injected at the 8 cell stage with 50 pg per blastomere of GR-tSmad2 mRNA, targeted to either two dorsal vegetal (DV) or two ventral vegetal (VV) cells. At stage 8 +1 hour embryos were treated for one hour with DMSO or 200 µM of SB505124 (SB), and/ or 2 µM dexamethasone (DEX). Embryos were analysed by whole mount *in situ* hybridisation using the cardiac marker *myl7* (white arrows) at tadpole stages, or cardiac progenitor marker

nkx2.5 (orange arrows) at neurula stages. (A-D) Uninjected controls. (E-H) DV injected treated with DMSO and DEX. (I-L) DV injected treated with SB. (M-P) VV injected treated with SB and DEX. (Q-T) DV injected treated with SB and DEX. Individual images A, B, E, F, I, J, M, N, Q and R are at the tadpole stage, displaying a lateral view orientated anterior left, dorsal up. C, D, G, H, K, L, O, S and T are at the neurula stage, displaying a ventral view with anterior left. Scale bar represents 1 mm. Graphs displaying results of A-T. (U) *Myl7* expression: control n=71, DV +DEX n=53, DV +SB n=66, VV +DEX +SB n=38, DV +DEX +SB n=57. (V) *nkx2.5* expression: control n=35, DV +DEX n=29, DV +SB n=31, VV +DEX +SB n=32, DV +DEX +SB n=26. (W-D1) Lineage tracing (outlined) highlights all cells containing injected material. Images are representative and show a lateral view orientated anterior left, dorsal up. Scale bars represent 1 mm.

3.14 Nodal is a likely TGF-beta ligand for cardiac specification

Nodal, Activin, TGF-betas and growth differentiation factors (GDFs) are TGF-beta ligands which all signal through ALK4/5/7 receptors (de Caestecker, 2004; Vilar et al., 2006). Nodal plays a fundamental role in patterning the early embryo (Shen 2007) and is present in the dorsal, future cardiac-forming region, of the blastula stage *Xenopus laevis* embryo (Faure et al., 2000; Gritsman et al., 2000; Lee et al., 2001). Therefore, Nodal is a key candidate for cardiac specification (Cai et al., 2012; Parisi et al., 2003; Reissmann et al., 2001; Samuel and Latinkić, 2009; Xu et al., 1999). Nodal requires the EGF-CFC co-receptor Cripto to propagate TGF-beta signalling, which can be specifically inhibited by the extracellular antagonist Lefty (Gritsman et al., 1999; Yeo and Whitman, 2001). Recombinant Lefty protein has previously been used in *Xenopus laevis* to explore the role of Nodal in mesoderm induction (Luxardi et al., 2010). The work presented here investigates whether Nodal is a likely TGF-beta ligand acting through ALK4/5/7 for cardiac specification in *Xenopus laevis*. Nodal signalling was inhibited and the effects on cardiac tissue were examined.

Initially, the suitability of Lefty protein for investigating the role of Nodal in cardiac specification was assessed and optimised. When Lefty protein was injected into the blastocoel of stage 8 embryos, normal embryonic development was affected in a dose-dependent manner. At low concentrations of 100 µg/ml, equivalent to 0.5 ng of Lefty protein per embryo, tadpole phenotypes were comparable to those of the controls (Figure 3:15 A-D, I, J). However, at higher concentrations of 250 µg/ml (1.25 ng of Lefty per embryo) and 450 µg/ml (2.25 ng of Lefty per embryo), tadpole phenotypes showed the presence of an increasingly truncated anterior-posterior axis (Figure 3:15 E-H) and presented similar phenotypes to those observed after small molecule-mediated ALK4/5/7 inhibition at stage 8 (Figure 3:9 and Figure 3:11). Western blot analysis of protein extracts from stage 10 embryos revealed that Lefty protein caused a reduction in the levels of p-Smad2 in a similar manner to that shown after treatment with the ALK4/5/7 inhibitors SB505124 and A-83-01, when all treatments began at stage 8 (Figure 3:15 K). Therefore, these results suggests that

Lefty protein injected into the blastocoel can diffuse within the embryo and can inhibit Nodal signalling, resulting in a reduction of activated Smad2. Additionally, by varying the stage of development in which embryos receive the Lefty protein injection, Lefty can be used to time-dependently control the commencement of Nodal inhibition for further investigations. 450 µg/ml was chosen as the optimum dose for further use. This is the highest dose achievable using the purchased reagents and additionally is the most appropriate dose which can produce the observed comparable phenotypic and molecular outcome as the soluble ALK4/5/7 inhibitors SB505124 and A-83-01.

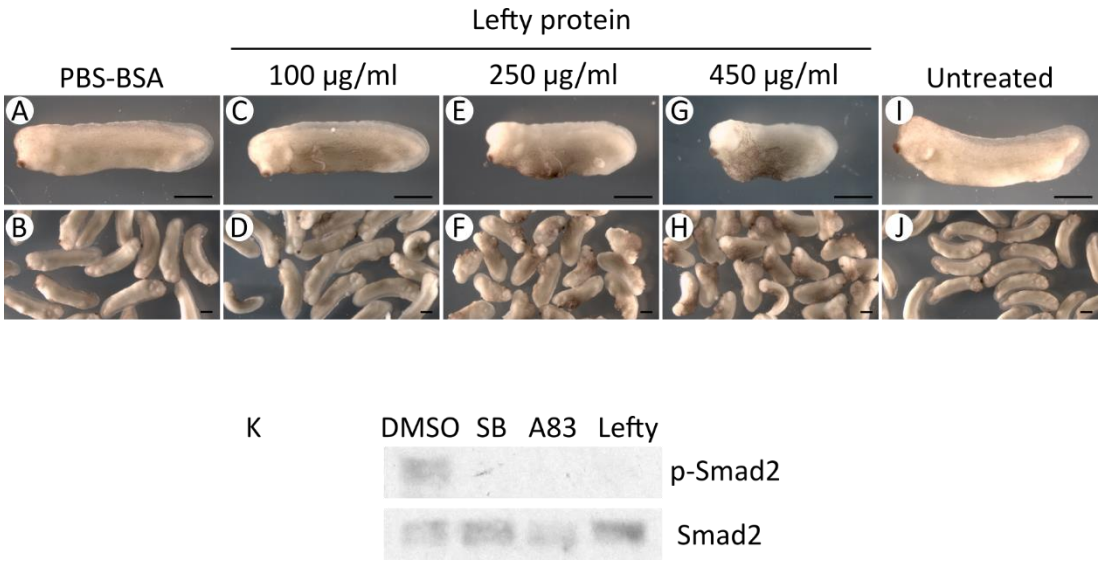

Figure 3:15. Lefty protein inhibits Smad2 activation and affects embryonic development in a dose-dependent manner

At stage 8 embryos were injected into the blastocoel with (A, B) PBS containing 0.1% BSA (PBS-BSA) (n=24) or (C, D) 100 µg/ml (n=30), (E, F) 250 µg/ml (n=27) or (G, H) 450 µg/ml (n=29) of Lefty protein, or (I, J) were untreated (n=31). All individual images are a lateral view orientated anterior left, dorsal up. Scale bar represents 1 mm. (K) Western blot analysis on stage 10 embryos after DMSO, 200 µM of SB505124 (SB) or A-83-01 (A83), or 450 µg/ml Lefty protein injection at stage 8. Smad2 is a loading control.

To investigate whether Nodal is a candidate TGF-beta ligand acting for cardiac specification, embryos were injected with 450 µg/ml of Lefty protein into the blastocoel at stage 8, stage 8 +1 hour or stage 8 +2 hours, and allowed to develop until the tadpole stage. Tadpoles were analysed by whole mount *in situ* hybridisation using the cardiac marker *myl7* and the blood marker *hba3*. Figure 3:16 E, F, K, L demonstrates that Nodal inhibition by Lefty protein at stage 8 resulted in tadpoles with absent or severely reduced cardiac and blood tissue, which also presented a truncated anterior-posterior axis. A similar, but milder, phenotype was observed upon Nodal inhibition by Lefty protein at stage 8 +1 hour (Figure 3:16 G, H, K, L). Nodal inhibition by Left protein at stage 8 +2 hours resulted in tadpoles with reduced cardiac and blood tissue (Figure 3:16 I, J, K, L), with the whole embryonic phenotype more comparable to that of the controls (Figure 3:16 A-D, K, L). Western blot analysis of protein extracts from stage 10 embryos illustrates that there was a reduction in p-Smad2 levels as a result of Lefty protein injections (Figure 3:16 M). These results bear remarkable similarity to those observed after ALK4/5/7 inhibition using molecular inhibitors in Figure 3:9. These results suggest that Nodal is a key ligand acting via ALK4/5/7 and Smad2 for cardiac specification.

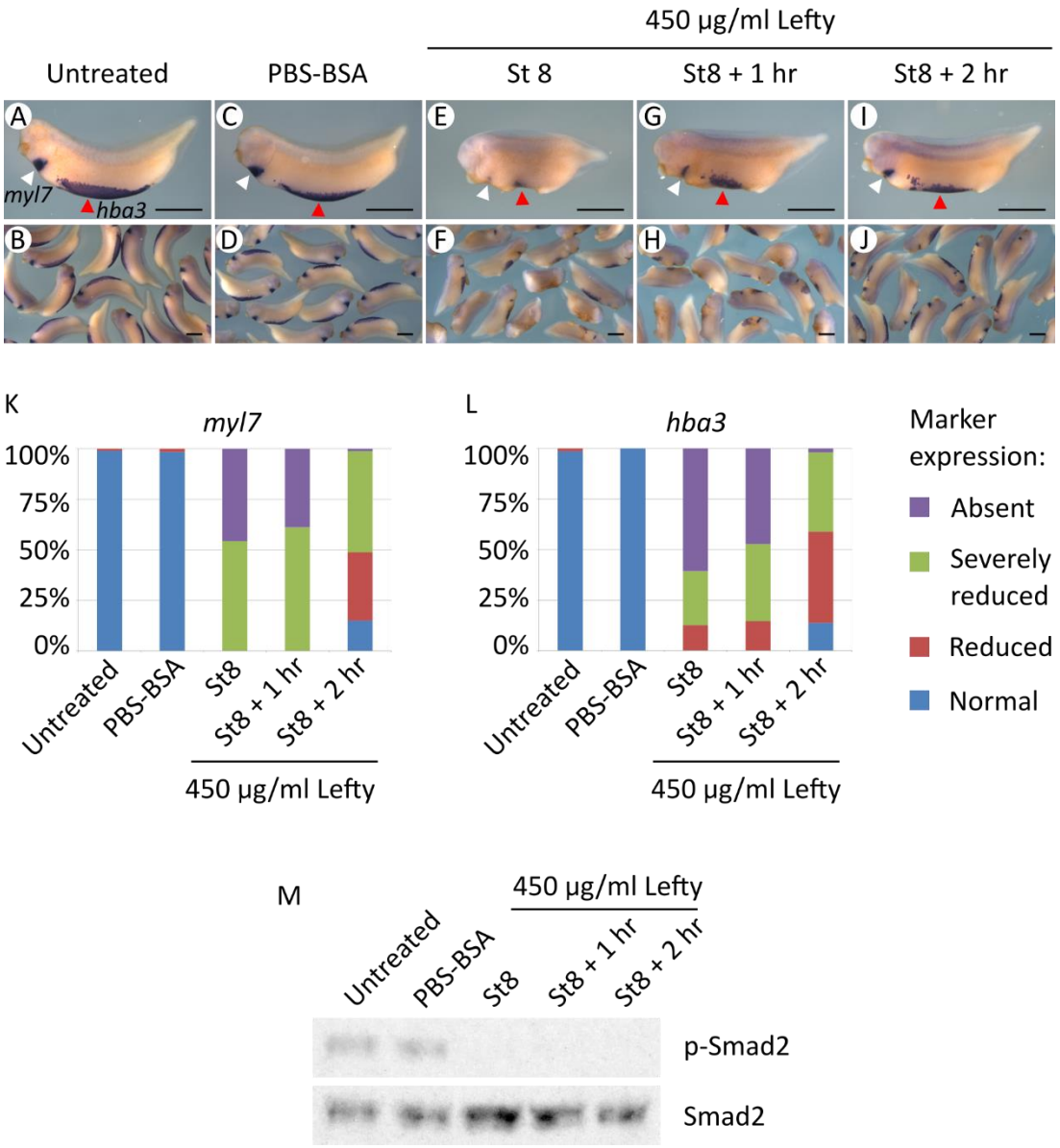

Figure 3:16. Nodal is a likely TGF-beta ligand for cardiac specification

Embryos were either (A, B) untreated controls or injected into the blastocoel with (C, D) PBS containing 0.1% BSA (PBS-BSA) at stage 8 or 450 µg/ml Lefty protein at (E, F) stage 8, (G, H) stage 8 +1 hour or (I, J) stage 8 +2 hours. Tadpoles were analysed by whole mount *in situ* hybridisation using the cardiac marker *myl7* (white arrows) and the blood marker *hba3* (red arrows). All individual images are a lateral view orientated anterior left, dorsal up. Scale bar represents 1 mm. Graphs display results of A-J showing (K) *myl7*: control n=96, PBS-BSA n=62, Lefty stage 8 n=81, Lefty stage 8 +1 n=85, Lefty stage 8 +2 n=80 and (L) *hba3*: control n=68, PBS-BSA n=43, Lefty stage 8 n=56, Lefty stage 8 +1 n=55, Lefty stage 8 +2 n=51. (M) Western blot analysis on stage 10 embryos. Smad2 is a loading control.

3.15 Discussion

3.15.1 There is an absolute requirement for ALK4/5/7 signalling in cardiac specification

Results presented here show that ALK4/5/7 signalling is required for the specification of cardiac progenitor cells, and thus for differentiated cardiac tissue *in vivo* in *Xenopus laevis*. This is in agreement with work in *Xenopus laevis* explants (Samuel and Latinkić, 2009), murine stem cell culture (Cai et al., 2012; Parisi et al., 2003; Sonntag et al., 2005; Xu et al., 1999, 1998), avian tissue interactions (Yatskievych et al., 1997) and *ex vivo* in zebrafish (Griffin and Kimelman, 2002; Reiter et al., 2001). Using various mutants, dominant negative (DN) constructs or molecular inhibitor techniques, the aforementioned investigations argue that there is a requirement for Nodal/ Activin signalling in cardiac specification. Additionally, the work in this chapter complements *in vivo* and *in vitro* work in *Xenopus laevis* that has shown that ectopic Nodal/ Activin signalling induces ectopic cardiac markers (Foley et al., 2007; Logan and Mohun, 1993; Reissmann et al., 2001) by illustrating the opposite - that time-dependent inhibition of ALK4/5/7 inhibits cardiogenesis. This is the first *in vivo* study in *Xenopus laevis* utilising soluble molecular inhibitors to directly examine the effects of ALK4/5/7 inhibition on cardiac specification. This has allowed the specific role of Nodal/ Activin signalling in cardiac induction to be examined, with minimal effect on alternative developmental processes which required Nodal/ Activin signalling during embryogenesis. Additionally, the molecular inhibitors have allowed the time at which Nodal/ Activin signalling is required for cardiac specification to be explored, increasing our knowledge as to the time frame of induction events in the early embryo.

3.15.2 ALK4/5/7 signalling is required for cardiac specification, separate to its role in general mesoderm induction

Cardiac primordia arise from within the mesoderm, with mesoderm induction and cardiac specification occurring temporally in rapid succession. The role of ALK4/5/7 signalling in these processes has not been fully uncoupled. Recent evidence illustrates the requirement for ALK4/5/7 signalling before midblastula transition for mesoderm formation (Skirkanich et al., 2011), and between midblastula transition and gastrulation for specifying various mesodermal cell types (Hagos and Dougan, 2007). A major concern during the early work of this chapter was that the inhibition of ALK4/5/7 was affecting mesoderm, thus indirectly affecting cardiac tissue. Data presented in this chapter demonstrated that the specification of mesoderm derivatives skeletal muscle, pronephros and notochord was largely unaffected by ALK4/5/7 inhibition after stage 8. This implied that ALK4/5/7 signalling had fulfilled its role in general mesoderm induction, and inhibition was specifically interfering with the initiation of cardiac tissue. Previous work demonstrates that Nodal/ Activin signalling is required in temporal succession for specifying somites, notochord and then heart tissue (Hagos and Dougan, 2007). Work within this thesis has identified a narrow time window that allows the specific interference of cardiac mesoderm, with minimal effect on alternate mesoderm derivatives, suggesting that the role of ALK4/5/7 in mesoderm induction and cardiac specification can be uncoupled.

Interestingly, blood was affected by ALK4/5/7 inhibition after midblastula transition. The heart and blood forming regions arise from adjacent mesoderm. The cardiac marker *nkx2.5* and myeloid marker *mpo* partially overlap at the neurula stage and the cardiac and blood lineage share common features in development (Tashiro et al., 2006). In zebrafish, *gata4, 5* and *6* are required for both myeloid and cardiac development (Peterkin et al., 2009). Knockdown of blood factors *spib* or *slurp1l* results in abnormal myeloid and heart development (Smith and Mohun, 2011) and cardiogenic *nkx2.5* has been shown necessary for heart and myeloid cell differentiation (Sakata and Maeno, 2014). However, these cardiogenic and hematopoietic factors, and additional influences, also compete to promote one

lineage whilst suppressing the alternative. FGF signalling is involved in the balance between cardiomyocytes and hemangioblasts, with FGF signalling inhibition resulting in enhanced hemangioblasts and diminished cardiomyocytes in *Xenopus laevis* and zebrafish (Simões et al., 2011; Walmsley et al., 2008). *nkx2.5* has been shown to repress hemangioblast development (Simões et al., 2011). The blood factor *tal1* binds to cardiogenic and hematopoietic enhancers, preventing cardiac factors from binding, thus preventing cardiogenesis (Org et al., 2015). *Tal1* utilises a pre-established epigenetic landscape (Org et al., 2015), perhaps established by earlier ALK4/5/7, or more precisely Nodal, signalling. Therefore, it would appear that both the heart and blood lineages require common early inputs, which is not surprising given their close spatial proximity. It is likely that Nodal/ Activin primes or specifies the cardiac and blood lineages, which diverge due to the action of opposing factors throughout further development.

3.15.3 ALK4/5/7 signalling is required for 2-3 hours from midblastula transition for cardiac specification

Work presented here demonstrates that ALK4/5/7 signalling is required for cardiac specification from midblastula transition for approximately 2-3 hours. The ALK4/5/7 requirement initially is absolute, gradually diminishing with the requirement fulfilled during stage 9. This is a more precise novel time window identified for cardiac specification that is earlier than previously thought (see below). Perhaps Nodal/ Activin signalling is required during this time window to activate cardiac specific genes. Alternatively, Nodal/ Activin signalling may be required to prime cells for receiving further cardiac inducing signals, distinguishing them from other mesoderm derivatives.

Previously, the timing of cardiac tissue specification was not precisely defined. Previous experimental evidence concluded that cardiac specification has occurred by the end of gastrulation, thus it was assumed that cardiac specification takes place during gastrulation (see Section 1.10) (Samuel and Latinkić, 2009; Sater and Jacobson, 1989). Nodal/ Activin signalling is additionally understood to be required

for gastrulation events, although whether that role is direct or indirect is unclear (Jones et al., 1995; Luxardi et al., 2010; Shen, 2007). The results of the initial experiments presented within this chapter, that showed that not only was the heart normal, but global embryonic development also appeared normal upon ALK4/5/7 inhibition from as early as stage 9, were surprising. The global embryonic phenotypes observed upon ALK4/5/7 inhibition treatments are in agreement with previous work demonstrating that tadpoles treated with SB505124 at stage 9 are largely normal (Skirkanich et al., 2011). However, results differ from other work which reports that SB505124 treatment at stage 9 disrupts gastrulation and the overall phenotype (Luxardi et al., 2010). It is likely that the latter result presents an extreme example, especially considering the conjunctive presentation of data demonstrating that early gastrula stage mesendodermal markers *Sox17-alpha*, *brachyury* and *goosecoid* were barely affected upon the same stage 9 SB505124 treatments (Luxardi et al., 2010). Taken together, the results presented here support the idea that pre-gastrulation ALK4/5/7 signalling is required for cardiac specification.

3.15.4 Phenotypic, but not detectable p-Smad2 recovery, occurs after ALK4/5/7 inhibitor removal

In experiments presented here involving timed ALK4/5/7 inhibitor incubation periods, it was observed that axial elongation phenotypes, but not p-Smad2 levels, recovered after ALK4/5/7 inhibitor removal. A possible explanation for this is that a small amount of p-Smad2 may be restored after inhibitor removal, sufficient to partially recover the phenotypes observed for stage 8 and stage 8 +1 inhibition, but not enough to enter the detectable range of western blotting. Nodal/ Activin signalling undergoes positive and negative auto-regulation. Conceivably, as a result of additional inhibition, the window of competency to fully activate the feedforward mechanism might be lost. For example, the TGF-beta ligand Nodal activates its own repressor Lefty, which diffuses at a faster rate than Nodal, thus limiting signalling (Sakuma et al., 2002). By adding the soluble ALK4/5/7 inhibitors for a brief time-period, the endogenous inhibitors may be prevailing, thus p-Smad2 signalling cannot

recover sufficiently after soluble inhibitor removal. Indeed, in a study demonstrating that the size of the Nodal signalling domain is determined by temporal Nodal signalling activation, it was predicted that once Lefty protein reaches a threshold level, Nodal signalling is no longer able to propagate (van Boxtel et al., 2015). Testing and confirming this hypothesis would include utilising mass spectroscopy to measure any remaining drugs, and analysing the levels and localisation of Lefty protein and active ALK4/5/7 signalling.

3.15.5 Active ALK4/5/7 signalling is required during a defined 2-3 hour time window after midblastula transition, for cardiac specification

Active ALK4/5/7 signalling appears to be required over 2-3 hours from midblastula transition, for cardiac specification. During this time window, very little p-Smad2 can be readily detected by conventional western blotting. One explanation for this is that although whole embryonic p-Smad2 levels are low, p-Smad2 may be present in only a small subset of cells at a high concentration. In agreement with this, p-Smad2 has been shown to be initiated from the dorsal side of the blastula embryo, with expression localised to the dorsal and ventral marginal zone and endoderm by gastrula stages (Faure et al., 2000; Lee et al., 2001). Alternatively, a low level of p-Smad2 may be sufficient for cardiac specification, with cells receiving Nodal/ Activin signals over an extended time window. It is debatable whether cell fate is determined by concentration or length of exposure to ALK4/5/7 ligands. In one model, known as the snapshot model, cells respond to the concentration of ALK4/5/7 ligands, regardless of the length of exposure, with the only role of time being to allow the ALK4/5/7 ligand gradient to expand (Harvey and Smith, 2009; Rogers and Schier, 2011). The ratchet model suggests that cells monitor ligand levels and respond to certain thresholds to stepwise induce different cell fates (Dyson and Gurdon, 1998; Gurdon et al., 1995). Alternatively, the cumulative dose model proposes that cells acquire certain fates depending on the length of time of ALK4/5/7 ligand exposure (Gritsman et al., 2000; Hagos and Dougan, 2007; Tian et al., 2003; van Boxtel et al., 2015). For cardiac specification, it appears that cells have a defined time window in

which they must be exposed to ALK4/5/7 signalling. However, within that time window it can be questioned whether the length of exposure, or total cumulative dose is important. Preliminary experiments demonstrate that tadpoles treated with 50 µM of SB505124 at stage 8 present comparable phenotypes to those subjected to 100 µM of SB505124 at stage 8+ 1 hour. This would argue against a strict duration of exposure model and in favour of exposure to a critical threshold, or cumulative dose, of Nodal/ Activin signalling. It would appear that duration and dose are inter-convertible, to an extent, with a greater ALK4/5/7 signalling exposure time required if signalling efficacy is compromised. Endogenous Nodal/ Activin inhibitors are likely regulating this temporal ALK4/5/7 signalling activity. Micro RNAs (miRNA) have been linked to early Nodal/ Activin signal regulation, and the regulation of Nodal/ Activin protein antagonists (Bassett et al., 2014; Choi et al., 2007; Rosa et al., 2009). Although Nodal/ Activin signalling activates its own repressors, signalling inhibition is delayed. miRNA-430 has been shown to temporarily inhibit Lefty translation (van Boxtel et al., 2015). This allows time for cells to be exposed to active Nodal/ Activin signalling before Lefty antagonism, allowing temporal exposure of cells to Nodal/ Activin signalling to be perceived.

3.15.6 Smad2 is capable of propagating the cardiac inducing signal

Rescue of the ALK4/5/7 inhibition phenotype by timed activation of Smad2 demonstrates the specificity of experimental inhibition treatments and affirms that ALK4/5/7 signalling can act via Smad2 for cardiac specification. Furthermore, cardiac tissue rescue was achieved in a cell-autonomous manner, suggesting that ALK4/5/7 signalling is required in presumptive cardiac cells for successful cardiac specification. This requirement is likely to be in regulating gene expression, activating cardiac genes and potentially repressing alternate lineages (Ross and Hill, 2008). Partial, but not complete, cardiac tissue rescue was achieved. This is potentially due to the requirement for another signalling mediator in addition to Smad2. An alternative explanation is that complete whole embryo phenotypic and specific tissue rescue is difficult to experimentally achieve. Embryos are exposed to high concentrations of

counteracting reagents, often not in a particularly cell-specific manner, thus balancing these influences to precisely achieve a 'normal' phenotype is unlikely. Therefore, although only partial rescue is achieved, it is a good indication of a successful rescue experiment. A successful rescue experiment was achieved at stage 8 +1 hour. Using the same experimental methods, rescue was not observed at stage 8. It is possible that with further work adjusting and optimising reagent concentrations and experimental procedures that this stage 8 rescue may work under altered conditions. However, the lack of rescue in itself is informative, revealing a greater requirement for active ALK4/5/7 signalling from midblastula transition. Presuming that cells become fated to the cardiac lineage upon being exposed to a threshold or cumulative dose of Nodal/ Activin signalling over time, these rescue experiments reveal further information about the specific time window of exposure required. Active ALK4/5/7 signalling from midblastula transition for the first hour appears vital, and even upon inhibitor removal after this time window, cells perhaps cannot be exposed to, or no longer have the competence to respond to, prolonged Nodal/ Activin signalling to acquire a cardiac fate. This may be due to the prevalence of endogenous Nodal/ Activin inhibitors, or that cells have received and are now responding to alternative fates, in the absence of early Nodal/ Activin signalling. Cells exposed to ALK4/5/7 inhibition at stage 8 +1 hour have previously received Nodal/ Activin signalling exposure, allowing partial, but not full, cardiac tissue specification. During the stage 8+ 1 hour rescue experiment, exogenous Smad2 inputs may be acting upon cells which have already received a certain level of Nodal/ Activin signalling from midblastula transition. Thus, the signalling requirement level or time of exposure for cells to become cardiac is being fulfilled. Altogether, this reasons that a low level of active ALK4/5/7 signalling, over a time period of 2-3 hours from midblastula transition, is fundamental to cardiac specification. Interestingly this is when Nodal5 and Nodal6 levels are raised (Luxardi et al., 2010; Takahashi et al., 2000), placing them as key Nodal ligands for cardiac specification.

3.15.7 Nodal is a key candidate TGF-beta ligand acting through ALK4/5/7 for cardiac specification

The work in this chapter demonstrated the similarity of effects between ALK4/5/7 inhibition, using soluble inhibitors, and Nodal inhibition, using Lefty protein, on the whole tadpole and cardiac phenotypes. This, with other work (Cai et al., 2012; Parisi et al., 2003; Reissmann et al., 2001; Samuel and Latinkić, 2009; Xu et al., 1999) suggests that Nodal is a key candidate ALK4/5/7 ligand for inducing cardiac tissue *in vivo* in *Xenopus laevis*. The specific Nodal inhibition phenotypes are slightly less severe than ALK4/5/7 inhibitor SB505124 and A-83-01 phenotypes. One explanation for this is the lower relative dose of Lefty protein used. The maximum concentration of Lefty protein which could be achieved was 450 µg/ml. Hence a higher level of inhibition could not be achieved without using an alternative more concentrated stock or injecting larger volumes, which could negatively impact upon embryonic development. There is no evidence that this was a suboptimal amount of Lefty protein for affecting Nodal signalling, as p-Smad2 levels are suitably decreased. Another interpretation is that there are additional ALK4/5/7 ligands also involved, for example Activin, which plays a role in mesoderm formation alongside other Nodal-related genes (Piepenburg et al., 2004). To test this, each ALK4/5/7 ligand would have to be inhibited independently. Alternatively, it has been shown that p-Smad2 levels decrease slowly upon Lefty treatment, compared to rapid signal termination with SB505124 (van Boxtel et al., 2015). This is presumably due to internalised receptor complexes in the early endosomes (Jullien and Gurdon, 2005; Vizán et al., 2013). Therefore, this temporarily sustained Nodal signalling may be resulting in the milder phenotypes observed. Current literature places Nodal spatially and temporarily as a suitable candidate, and work presented here demonstrates that Nodal is the most likely TGF-beta ligand acting via ALK4/5/7 and Smad2 for cardiac specification.

4 FGF/ MEK signalling is required for heart development after gastrulation

4.1 Introduction

Fibroblast growth factor (FGF) signalling plays multiple roles during early embryonic development, including in tissue induction, cell fate specification, axis determination, morphological movements and gene maintenance (Coumoul and Deng, 2003; Thisse and Thisse, 2005). Several FGF ligands are expressed in the anterior endoderm, which underlies the developing heart field, of the blastula and gastrula staged *Xenopus laevis* embryo, thus inferring a possible role for FGF signalling in cardiac cell induction or maintenance (Alsan and Schultheiss, 2002; Deimling and Drysdale, 2011; Lea et al., 2009). Studies in zebrafish, *Drosophila melanogaster, Xenopus laevis* and chick have highlighted that there is a requirement for FGF signalling in cardiac cell induction, regulation and development (see Section 1.8.2 for more information) (Beiman et al., 1996; Keren-Politansky et al., 2009; Lopez-Sanchez et al., 2015; Marques et al., 2008; Reifers et al., 2000; Samuel and Latinkić, 2009; Simões et al., 2011). However, there is little evidence that demonstrates a direct role for FGF signalling in cardiac specification. Previously, the role of FGF signalling in cardiac specification has not been separated from its broader functions in embryonic development. In addition, the time at which FGF signalling may be required for cardiac specification *in vivo* is largely unknown. An understanding of whether FGF signalling is required for cardiac cell specification and the time at which cardiac specification occurs will further our understanding of how signalling pathways orchestrate embryonic development. The work presented in this chapter investigates the requirement and timing for FGF/ MEK signalling in cardiac specification.

4.2 Optimisation of suitable reagents to inhibit the FGF/ MEK signalling pathway in *Xenopus laevis* embryos

4.2.1 Small molecular drugs SU5402 and PD0325901 are suitable FGF/ MEK signalling inhibitors

To investigate the requirement for the FGF signalling pathway in cardiac specification, FGF signalling was inhibited and the effects of the inhibition on cardiac tissue and whole embryonic development were observed. FGF signalling inhibition can be achieved using a variety of techniques, including dominant negative constructs, genetic mutants, morpholino oligonucleotides and small soluble molecular inhibitors (Amaya et al., 1991; Fletcher et al., 2006; Reifers et al., 1998; Samuel and Latinkić, 2009). There are a range of soluble molecular inhibitors available which inhibit various components of FGF signalling. These soluble FGF pathway inhibitors can be added to, or removed from, the embryonic media at any time point in development to permit time-controlled signalling inhibition, thus potentially allowing the diverse roles of FGF signalling in embryogenesis to be experimentally separated. FGF signalling can propagate via multiple transduction pathways downstream of the activated FGF receptors, including the ERK, PLC-gamma, Pi3K and STAT branches (Kimelman, 2006; Thisse and Thisse, 2005). However, FGF predominantly signals via the ERK branch during embryonic development (Corson et al., 2003; Thisse and Thisse, 2005).

Seven soluble inhibitors which act to inhibit components of the FGF signalling pathway were tested for their ability to effect embryonic development and result in phenotypes consistent with previous reports of FGF signalling inhibition. Previous research has shown that embryos subjected to suboptimal FGF inhibition presented a truncated anterior-posterior axis. Higher levels of FGF signalling inhibition resulted in embryos with incomplete gastrulation and neurulation, with the posterior region of the tadpole truncated and curling around towards the back of the head (Deimling and Drysdale, 2011; Delaune et al., 2005). This is as expected, as FGF signalling is

known to be involved in gastrulation movements and tail formation (Amaya et al., 1991; Fletcher and Harland, 2008). Several of the inhibitors selected for testing have previously been used in research at concentrations of 0.1-100 µM, in *Xenopus laevis* and zebrafish (Anastasaki et al., 2012; Deimling and Drysdale, 2011; Rankin et al., 2012; Samuel and Latinkić, 2009; Shifley et al., 2012). These concentrations were used to inform the choice of inhibitor concentrations tested here.

The FGF signalling inhibitors were added to *Xenopus laevis* embryos shortly after fertilisation and incubated continuously throughout development. Tadpole phenotypes were observed at stage 32-36. The inhibitors, signalling component inhibited, inhibitor concentrations and phenotypic observations of tadpoles after inhibitor treatments are shown in Table 4:1. Embryos treated with the FGFR inhibitors SU5402, AZD4547 and PD173074 resulted in tadpoles which presented similar phenotypes to each other and previous reports of FGF signalling inhibition. These phenotypes were also observed after embryonic treatment with the MEK inhibitors PD0325901, PD98059 and the MAPK inhibitor SB203580. The FGFR inhibitor AZD4547 was found to lose efficacy over several weeks in storage, so was not selected for further use. The FGFR inhibitor PD173074 required supplementation with 0.1 mM of adenosine triphosphate (ATP). However, it was observed here that 0.1 mM of ATP alone negatively affected whole embryonic development, resulting in tadpoles that were truncated with a curved anterior-posterior axis. Therefore, PD173074 was not selected for further use. The FGFR inhibitor SU5402 did not require ATP supplementation and retained efficacy after several months in storage, therefore it was selected for further testing. SU5402 (Figure 4:1 A) binds to and inhibits FGF receptor function (Mohammadi et al., 1997). SU5402 does not compete with the substrate peptide, but binds at the ATP site, acting as an ATP-competitive tyrosine kinase inhibitor. SU5402 has been found to have no, or very weak, inhibitory effects on related receptor tyrosine kinases such as insulin, epidermal growth factor (EGF) and platelet-derived growth factor (PDGF) (Mohammadi et al., 1997).

In addition to an inhibitor which acts at the FGFR level and hence can inhibit downstream signal propagation by multiple transduction branches, a soluble

inhibitor which inhibits the ERK branch of FGF signal transduction was selected. The MEK inhibitor U0126 tested here did not affect embryonic development at any concentration tested, so was not selected for further testing. The MAPK/ ERK inhibitor SB203580 did negatively affect normal embryonic development in a manner consistent with previous reports. However, as examining the phosphorylation (activation) state of ERK is a useful experimental method for determining whether the FGF/ ERK pathway is active, the use of an inhibitor which acts upstream of ERK was selected instead. The MEK inhibitors PD0325901 and PD98059 work upstream of ERK and were found to effect normal embryonic development to result in phenotypes comparable to those previously reported after FGF signalling inhibition. PD0325901 was found to work effectively at relatively low concentrations of 2-20 µM, compared with the higher concentrations of PD98059 which were required to achieve the same phenotypic effect, so was selected for further testing. PD0325901 (Figure 4:1 B) selectively binds to, and inhibits MEK (Sebolt-Leopold and Herrera, 2004). PD0325901 inhibits MEK in a non-ATP competitive manner, binding into a hydrophobic pocket and inducing conformational changes in MEK which renders the catalytic kinase function inactive. This binding occurs in a pocket with no known sequence homology to other kinases, hence MEK inhibition is highly selective (Sebolt-Leopold, 2008; Sebolt-Leopold and Herrera, 2004). Due to the choice of FGF signalling pathway inhibitors selected, inhibition shall commonly be referred to as FGF/ MEK signalling inhibition.

The concentrations of inhibitors tested here are similar to previously reported *in vivo* inhibitor use, although are higher than the IC_{50} values determined for cell culture. For example, previously SU5402 has been used at 50 µM, or at 10 µM when supplemented with 0.1 mM of ATP, in *Xenopus laevis* embryos or explants (Deimling and Drysdale, 2011; Samuel and Latinkić, 2009; Shifley et al., 2012). An IC_{50} of 10 -20 µM, in the presence of 1 mM of ATP, in cell culture, has previously been determined for SU5402 (Mohammadi et al., 1997). Previously, PD0325901 has been observed to have an IC_{50} of between 5 - 1500 nM, in a variety of cell cultures of different sensitivities (Henderson et al., 2010; Pratilas et al., 2008; Ricciardi et al., 2012).

PD0325901 has previously been used *in vivo* in zebrafish at concentrations of 0.1-1 µM (Anastasaki et al., 2012). It would appear that the concentration of inhibitor required between different *in vivo* and *in vitro* systems varies. This is most likely due to the sensitivity and traits of each system, in addition to the potency of the batch of inhibitor purchased. For example, the *Xenopus laevis* embryo contains a fatty yolk, which may be capable of sequestering the inhibitors. This might explain why higher inhibitor concentrations than those used in cell culture systems are necessary to achieve signalling inhibition *in vivo*.

Inhibitor	Inhibits	Concentrations tested (μM)	Phenotype observations at stage 32-36
SU5402	FGFR	1 - 100	Tadpoles were mildly truncated along the anterior-posterior axis at low concentrations. The severity of the phenotype became more prominent with increasing concentrations to result in tadpoles with a severely truncated anterior-posterior axis with the posterior region of the tadpole curling and signs of incomplete gastrulation and neurulation.
PD0325901	MEK	1 - 100	Tadpoles were mildly truncated along the anterior-posterior axis at low concentrations. The severity of the phenotype became more prominent with increasing concentrations to result in tadpoles with a severely truncated anterior-posterior axis with the posterior region of the tadpole curling and signs of incomplete gastrulation and neurulation.
U0126	MEK	35 - 70	No effect at concentrations tested
AZD4547	FGFR	50 - 100	Tadpoles were mildly truncated along the anterior-posterior axis at low concentrations. The severity of the phenotype became more prominent with increasing concentrations to result in tadpoles with a severely truncated anterior-posterior axis with the posterior region of the tadpole curling and signs of incomplete gastrulation and neurulation. Inconsistent working effect after minimal time in storage.
PD173074	FGFR	100 - 200	All inhibitor applications were supplemented with 0.1 mM of ATP. Tadpoles were mildly truncated along the anterior-posterior axis at low concentrations. The severity of the phenotype became more prominent with increasing concentrations to result in tadpoles with a severely truncated anterior-posterior axis with the posterior region of the tadpole curling and signs of incomplete gastrulation and neurulation.

SB203580	MAPK/ ERK	50 - 100	Tadpoles were mildly truncated along the anterior-posterior axis at low concentrations. The severity of the phenotype became more prominent with increasing concentrations to result in tadpoles with a severely truncated anterior-posterior axis with the posterior region of the tadpole curling and signs of incomplete gastrulation and neurulation.
PD98059	MEK	50 - 100	Tadpoles were mildly truncated along the anterior-posterior axis at low concentrations. The severity of the phenotype became more prominent with increasing concentrations to result in tadpoles with a severely truncated anterior-posterior axis with the posterior region of the tadpole curling and signs of incomplete gastrulation and neurulation.

Table 4:1. FGF signalling inhibitors

A

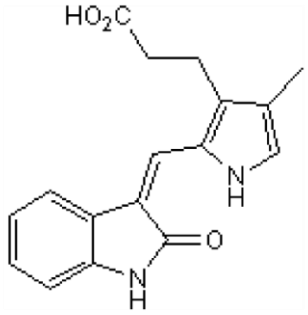

SU5402

B

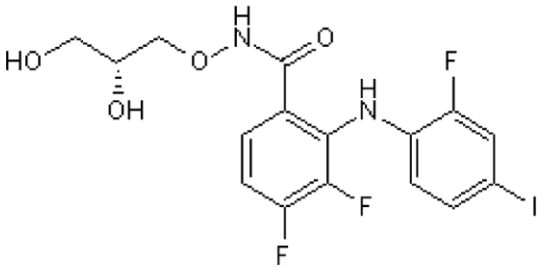

PD0325901

Figure 4:1 Chemical structure of FGF and MEK inhibitors

(A) Chemical structure of SU5402. (B) Chemical structure of PD0325901. (www.tocris.com)

4.2.2 FGF/ MEK inhibitors SU5402 and PD0325901 adversely affect normal embryonic development in a dose-dependent manner

FGF/ MEK inhibitors, SU5402 and PD0325901, were tested at a range of concentrations to establish the optimum concentration to use in further investigations in *Xenopus laevis* embryos. Embryos were treated at the 2 cell stage with increasing concentrations of the FGF/ MEK inhibitors and the tadpole phenotypes were examined. Both SU5402 and PD0325901 treatments produced a dose response. At the lowest dose of SU5402, 60 µM, a slightly truncated tadpole was observed (Figure 4:2 C, D), compared with the controls (Figure 4:2 A, B). The highest dose of 100 µM of SU5402 resulted in truncated tadpoles with deficient tail elongation and the posterior end curled towards the back of the head (Figure 4:2 I, J). Intermediate doses of 80 µM (Figure 4:2 E, F) and 90 µM of SU5402 (Figure 4:2 G, H) showed a dose response with a milder phenotype than after 100 µM, but more severe than with 60 µM, of SU5402 treatments. During the course of investigations contained within this chapter two different stocks of SU5402, from two different suppliers, were used: SU5402 from Calbiochem (SU5402-C) and SU5402 from Sigma (SU5402-S). SU5402-C at 20 µM resulted in the same phenotype as 100 µM of SU5402-S, with a similar dose response but at lower nominal concentrations. It shall be stated whether SU5402-C or SU5402-S was used for experiments in the corresponding figure legend.

Embryos treated with 2 µM of PD0325901 presented a truncated phenotype, bent along the anterior-posterior axis (Figure 4:2 M, N), with a similar but more severe effect observed at 5 µM (Figure 4:2 O, P), compared with the controls (Figure 4:2 K, L). Treatment with 10 µM of PD0325901 often resulted in embryos with a truncated anterior posterior axis and retarded tail development (Figure 4:2 Q, R). PD0325901 at 50 µM severely affected development, resulting in tadpoles with a barely distinguishable axis and landmark embryonic features including the eyes and cement gland (Figure 4:2 S, T).

The phenotypes observed here are in keeping with previously reported phenotypes of FGF/ MEK signalling downregulation, and the requirement for FGF/ MEK signalling in cellular movements during gastrulation and in maintaining the tailbud domain (Amaya et al., 1991; Deimling and Drysdale, 2011; Delaune et al., 2005; Fletcher and Harland, 2008; Pownall et al., 1996).

By comparing experimental replicas throughout all of the experiments presented here, it was apparent that the potency of the inhibitor treatment varied. This is consistent with previous reports (Fletcher and Harland, 2008). The same range of developmental features were observed, but the severity of phenotypes fluctuated between batches of embryos and between embryos within the same batch. Treated embryos presented the same phenotypic features, but the efficacy of a given drug treatment varied. For example, the tail was truncated to a greater extent in some embryos, but not others, which were subjected to the same FGF/ MEK inhibition treatment. Importantly, the range of different phenotypes observed was narrow and consistent. In order to control for the variation in the efficacy of the drugs, each experiment included a positive control consisting of embryos that were treated from the 2 cell stage, continuously, with the FGF/ MEK inhibitors. In addition, experiments were typically performed using both inhibitors independently to ensure consistent results. Throughout this results chapter the most representative images of FGF/MEK inhibition treatments are shown, although more and less severely affected embryonic phenotypes can be observed in the group images.

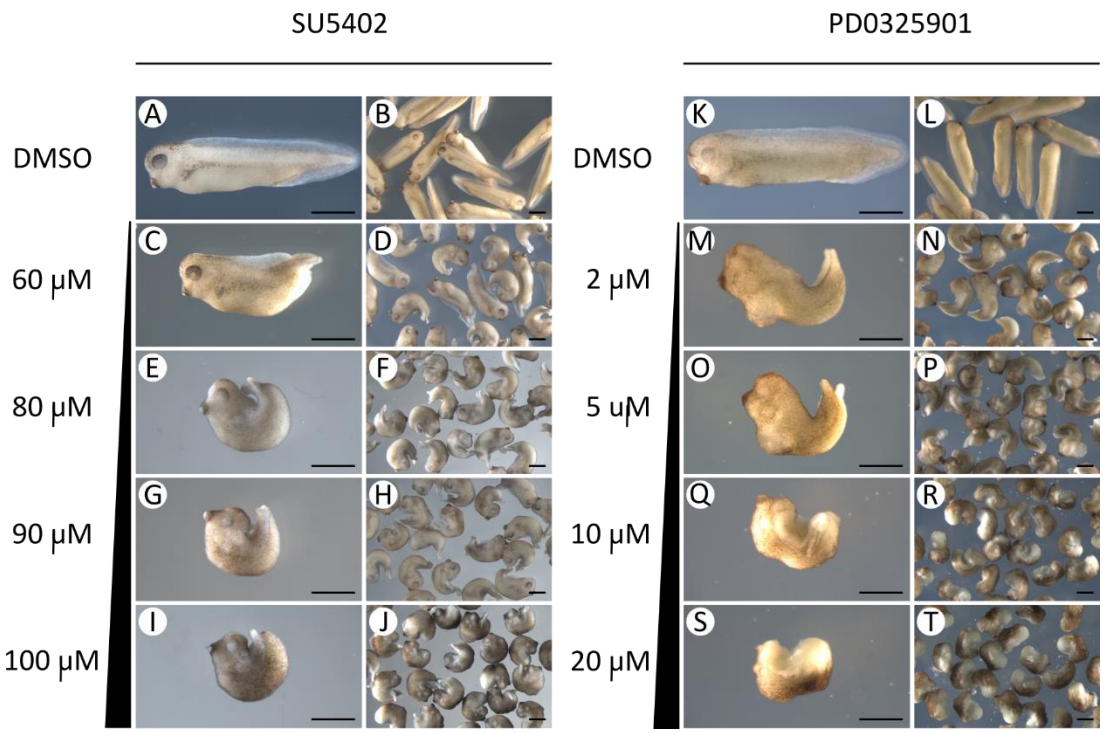

Figure 4:2. FGF/ MEK inhibitors SU5402 and PD0325901 adversely affect normal embryonic development in a dose-dependent manner

Embryos were treated continuously from the 2 cell stage with (A, B, K, L) DMSO or increasing concentrations of (C-J) SU5402-S or (M-T) PD0325901, displayed down the left of the images. All individual images are a lateral view orientated anterior left, dorsal up. Scale bar represents 1 mm. SU5402 column – DMSO n=25, SU5402 60 µM n=29, 80 µM n=27, 90 µM n=26, 100 µM n=27. PD0325901 column – DMSO n=77, SU5402 2 µM n=28, 5 µM n=89, 10 µM n=82, 20 µM n=91.

4.2.3 A dominant negative FGFR adversely affects normal embryonic development in a similar manner to SU5402 and PD0325901

In order to compare and validate the results observed using soluble inhibitors of the FGF/ MEK signalling pathway, a well-established dominant negative FGF receptor (DN-FGFR) (Amaya et al., 1991) was used to inhibit FGF signalling. The DN-FGFR is truncated at amino acid 398, directly downstream of the transmembrane domain, resulting in an absent intracellular tyrosine kinase domain (Amaya et al., 1991). In response to ligand binding under normal conditions, FGFR dimerisation and transphosphorylation of the intracellular tyrosine kinase domain is required for adaptor protein docking and downstream signal transduction (Turner and Grose, 2010). Hence, the mutated FGFR can form a dimer with endogenous FGFRs, however, the absence of the intracellular tyrosine kinase domain results in a non-functional receptor complex.

Xenopus laevis embryos were injected uniformly with mRNA encoding the DN-FGFR at the 2 cell stage. Tadpole phenotypes were observed at stage 32-36. Figure 4:3 G and H shows that embryos injected with DN-FGFR mRNA presented a truncated anterior-posterior axis and displayed a small trunk and tail, compared to the phenotypes of the controls (Figure 4:3 A, B). This tadpole phenotype is similar to tadpole phenotypes observed after embryos were treated with the FGF/ MEK inhibitors SU5402 and PD0325901 (Figure 4:3 C-F) and of previously reported FGF/ MEK signalling inhibition phenotypes (Deimling and Drysdale, 2011; Delaune et al., 2005).

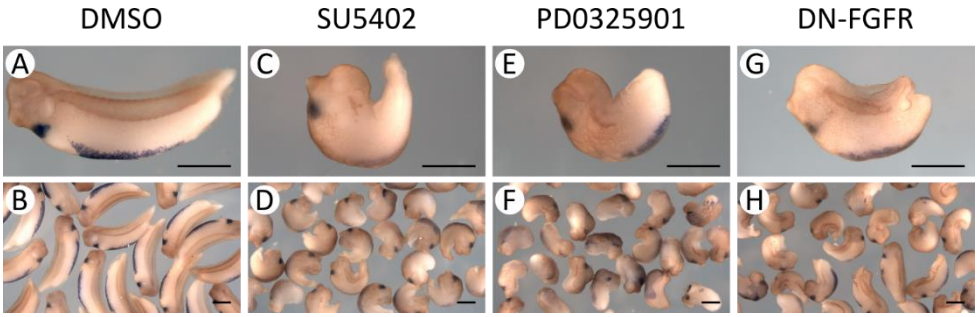

Figure 4:3 A DN-FGFR adversely affects normal embryonic development in a comparable manner to FGF/ MEK inhibitors SU5402 and PD0325901

Embryos were either treated with (A, B) DMSO (n=96), (C, D) 20 µM of SU5402-C (n=110), (G, H) 10 µM of PD0325901 (n=106) or (E, F) injected uniformly with 2 ng of DN-FGFR mRNA (n=101). Injections were at the 2 cell stage and all other treatments commenced at stage 8 and were continuous. Individual images are a lateral view orientated anterior left, dorsal up. Scale bar represents 1 mm. Embryos have been stained by whole mount *in situ* hybridisation for cardiac tissue (*myl7*) and blood (*hba3*) and by immunohistochemistry using the skeletal muscle marker 12/101; more information below in Section 4.4.

4.2.4 SU5402, PD0325901 and a DN-FGFR inhibit the activation of the FGF/ MEK downstream signalling transducer ERK

SU5402, PD0325901 and the DN-FGFR act to inhibit the FGF/ MEK signalling pathway upstream of the signalling mediator ERK. In response to FGF signal propagation, the FGF downstream signalling mediator ERK is activated by dual phosphorylation on its regulatory tyrosine and threonine residues, located at positions 202 and 204 respectively (Payne et al., 1991; Shaul and Seger, 2007). The phosphorylation state of ERK was examined after inhibition of the FGF/ MEK signalling pathway by using a phospho-specific ERK antibody to detect the phosphorylation of tyrosine 202 and threonine 204. Figure 4:4 shows a western blot analysis which demonstrates that the amount of phosphorylated-ERK (p-ERK) has decreased in embryos subjected to FGF/ MEK signalling inhibition by SU5402, PD0325901 or DN-FGFR, in comparison with control (DMSO) treated embryos. A small amount of remaining p-ERK was observed after FGF/MEK signalling inhibition, indicating that FGF/ MEK signalling inhibition resulted in substantial, but not complete, reduction of p-ERK levels. A minimal difference in the level of remaining p-ERK was observed between the FGF/ MEK inhibition reagents used. This suggests that all three methods of inhibition affect the phosphorylation of ERK.

In summary, SU5402, PD0325901 and the DN-FGFR inhibit the FGF/ MEK signalling pathway and they are all appropriate reagents for use in further investigations into the role of FGF/ MEK signalling in cardiac specification. This work has shown that there is agreement between phenotypic and molecular observations upon using three different FGF/ MEK signalling inhibition reagents.

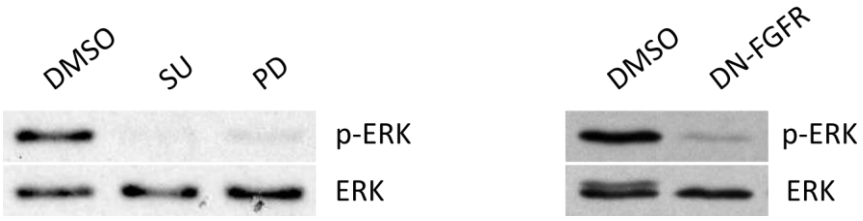

Figure 4:4. SU5402, PD0325901 and a DN-FGFR inhibit the activation of the FGF/ MEK downstream signalling transducer ERK

Embryos were either treated with DMSO, 20 µM of SU5402-C, 10 µM of PD0325901 or injected uniformly with 2 ng of DN-FGFR mRNA. Injections were at the 2 cell stage and all other treatments commenced at stage 8 and were continuous. Western blot analysis of protein extracts at stage 10-10.5. ERK is a loading control.

4.3 Cardiac tissue is marginally affected by FGF/ MEK signalling inhibition

To investigate the requirement for FGF/ MEK signalling in cardiac specification, the FGF/ MEK signalling pathway was inhibited and the effects on differentiated cardiac tissue were examined. ALK4/5/7 signalling was shown to be required from stage 8 for cardiac specification in Chapter 3, hence stage 8 was selected as an appropriate time point for commencing soluble FGF/ MEK inhibitor treatments. Embryos were treated with FGF/ MEK inhibitors, or DMSO, continuously from stage 8 or were injected with DN-FGFR mRNA at the 2 cell stage. Tadpoles were assayed by whole mount in situ hybridisation (WMISH) using the differentiated cardiac tissue marker *myosin light chain 7* (*myl7*). *Myl7* staining was classified as either absent, severely reduced, reduced or normal and examples of each classification are shown in Figure 4:5 I-L. Figure 4:5 A-H shows that FGF/ MEK signalling inhibition resulted in tadpoles which were truncated along the anterior-posterior axis, specifically affecting the tail and trunk structures. In addition, anterior features including the head and eyes were reduced in size. Cardiac tissue was observed, although staining was often modestly reduced, compared with DMSO treated controls. There is agreement in both the cardiac staining and whole embryo phenotypes between the three different FGF/ MEK signalling inhibition reagents.

Western blot analysis of protein extracts at stage 9 and 10.5 shows that there is a decrease in p-ERK levels in FGF/ MEK inhibitor treated samples compared with the controls (Figure 4:5 N). This suggests that FGF/ MEK signalling inhibition has been successful. Analysis at stage 9 reveals a minor difference in the p-ERK levels upon FGF/ MEK inhibitor treatments commencing at either stage 5 or stage 8 (Figure 4:5 N). This minor difference may be due to the natural variation between samples. Alternatively, it may reflect a slight delay in inhibition, potentially due to the diffusion rate for the inhibitors to reach their targets, or, if acting rapidly, the time it takes for pre-existing p-ERK to be dephosphorylated or recycled. However, as a substantial decrease in p-ERK levels is observed by stage 9, in FGF/ MEK inhibited samples

compared to controls. This suggests timely and effective FGF/ MEK signalling inhibition.

In summary, differentiated cardiac tissue was observed, although staining is reduced, after FGF/ MEK signalling inhibition. However, the whole embryonic phenotype is also reduced in size, with anterior features such as the head being noticeably smaller. This raises the question as to whether the modest reduction in cardiac tissue observed is the direct effect of a FGF/ MEK signalling requirement in cardiogenesis, or perhaps an indirect effect due to the adverse effects of FGF/ MEK inhibition on embryonic development. For example, FGF/ MEK signalling is known to be required for axis determination and convergent extension movements (Amaya et al., 1991; Ciruna and Rossant, 2001; Fürthauer et al., 2004; Nutt et al., 2001).

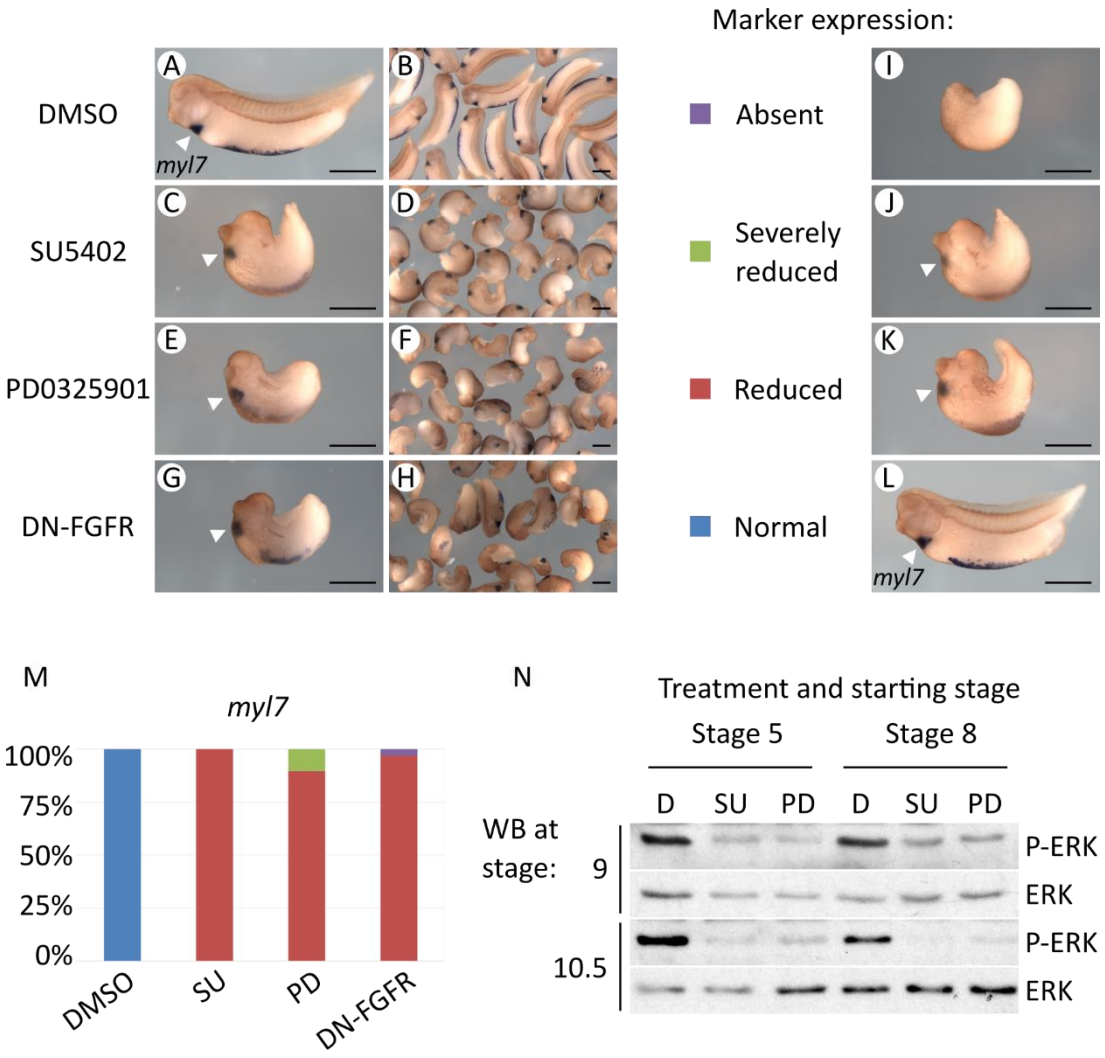

Figure 4:5. Cardiac tissue is observed, although is reduced, after FGF/ MEK signalling inhibition

Embryos were treated with DMSO (D), 20 µM of SU5402-C (SU) or 10 µM PD0325901 (PD) continuously from stage 8, or for western blot (WB) analysis from stage 5 or stage 8, or were injected uniformly with 1 ng of DN-FGFR mRNA at the 2 cell stage. Tadpoles were analysed by whole mount *in situ* hybridisation using the cardiac marker *myl7* (white arrows) and the blood marker *hba3* (blue stain at the ventral region of embryo, however, blood is not the focus of this current analysis) and by immunohistochemistry using the skeletal muscle marker 12/101 (brown stain). (A, B) DMSO, (C, D) SU5402, (E, F) PD0325901 or (G, H) DN-FGFR mRNA treatments. The extent of marker staining was classified. (I) Absent: no staining observed. (J) Severely reduced: between 1-50% of staining area and intensity observed in controls. (K) Reduced: between 50-90% of staining area and intensity observed in controls. (L) Normal: the average staining observed in a given control sample. All individual images are

a lateral view orientated anterior left, dorsal up. Scale bar represents 1 mm. (M) Graph quantifying *myl7* expression observed in A-H. DMSO n=134, SU n=66, PD n=58, DN-FGFR n=66. (N) Western blot analysis of protein extracts at stage 9 (top row) and stage 10.5 (bottom row). ERK is a loading control.

4.4 Cardiac morphogenesis is affected after continuous FGF/ MEK signalling inhibition from midblastula transition

In order to establish additional information about the role of FGF/ MEK signalling in cardiogenesis, the morphology of the developing heart was examined after embryos were treated with FGF/ MEK signalling inhibitors. Experimental samples from Figure 4:5 were examined for the morphology of the developing heart. Briefly, embryos were treated with FGF/ MEK inhibitors, or DMSO, continuously from stage 8, followed by analysis by whole mount *in situ* hybridisation using the differentiated cardiac tissue marker *myl7* and by immunohistochemistry using the skeletal muscle marker 12/101. The morphology of the heart was observed at stage 36. In DMSO treated embryo controls, normal hearts were observed (Figure 4:6 A, B). These samples show a normal heart phenotype resulting from having undergone the characteristic anticlockwise spiralling and anterior movements to create a rightward, s-shaped bend prior to chamber formation (Kolker et al., 2000; Latinkić et al., 2004; Mohun et al., 2000). In contrast, Figure 4:6 C and D shows that severely reduced hearts appeared as linear tubes, often bulging slightly, but with no indication of looping. In tadpoles classified as having reduced cardiac tissue, linear heart tubes were most frequently observed, where there were no signs of morphological movements and looping (Figure 4:6 E, F). A small proportion of tadpoles showed signs of cardiac morphological movements, for example, it is apparent in Figure 4:6 H that the most posterior end of the heart tube has moved in an anterior direction, but that the heart is not normal. In many cases, although the extent of cardiac tissue was classified as reduced compared with controls, there was still substantial cardiac tissue within the embryo, relative to the diminished size of the whole embryo (Figure 4:6 G, H). Cardiac bifida was infrequently evident, defined by the formation of two independent linear heart tubes or cavities (Figure 4:6 I, J). It is apparent from these results that skeletal muscle development is adversely affected by the inhibition of FGF/ MEK signalling, as the presence of skeletal muscle was rarely observed in treated tadpoles (Figure 4:6 A, C, E, G). This result is in agreement with previous work that has shown that there is a requirement for FGF/ MEK signalling in skeletal muscle

development (Isaacs et al., 2007) and that skeletal muscle is specified prior to cardiac tissue (Hagos and Dougan, 2007). Figure 4:6 A, C, E and G shows that the overall proportions of the head appeared to be moderately reduced in samples subjected to FGF/ MEK signalling inhibition. This could indicate abnormal anterior development, which raises the question as to whether the reduction in cardiac tissue is a direct or indirect effect of FGF/ MEK signalling inhibition. These results suggest that specified cardiac tissue has successfully migrated to the ventral midline but that morphological movements were often impeded. This could suggests a role for FGF/ MEK signalling in later heart develop.

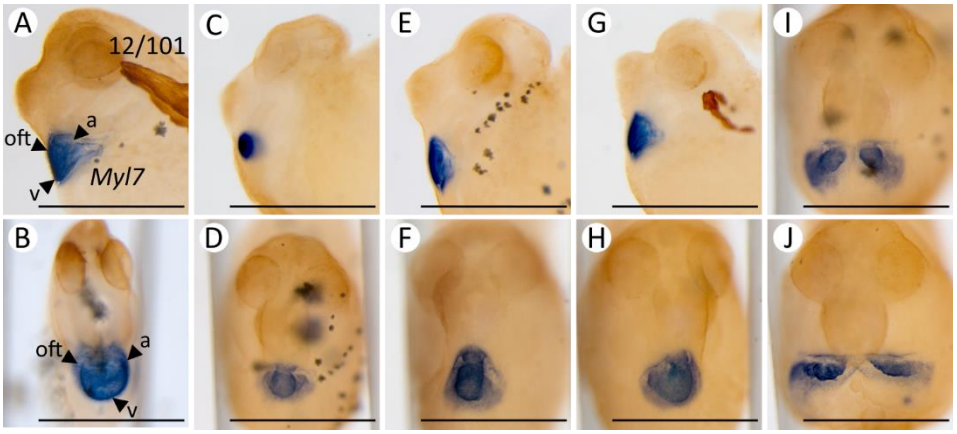

Figure 4:6. Cardiac morphogenesis is affected after continuous FGF/ MEK signalling inhibition from midblastula transition

Tadpoles subjected to treatments in Figure 4:5 were analysed by whole mount *in situ* hybridisation using the cardiac tissue marker *myl7* (blue stain), followed by immunohistochemistry using the skeletal muscle marker 12/101 (brown stain). (A, B) DMSO treated with future atrium (a), ventricle (v) and outflow tract (oft) highlighted (arrows). (C, D) Severely reduced cardiac tissue. (E, F) Tadpoles classified as having reduced cardiac tissue often presented a linear heart tube, orientated along the anterior-posterior axis but with no further signs of morphological movements or looping. (G, H) Tadpoles with reduced hearts displayed signs of morphological cardiac movements, with signs of cavities and looping. (I, J) Cardia bifida. C-J example embryos have been treated with 20 µM of SU5402-C, and developed until the tadpole stage. Scale bar represents 1 mm. A, C, E and G show a lateral view orientated anterior left. B, D, F, H, I and J show a ventral view, anterior upwards. These are example cardiac phenotypes from the experiments presented and quantified in Figure 4:5.

4.5 Maximal inhibition of FGF/ MEK signalling adversely affects normal embryonic development

Cardiac tissue has been shown to be present, albeit with a reduced staining pattern, after FGF/ MEK signalling inhibition. This reduction in cardiac tissue could be due to a requirement for FGF/ MEK signalling in cardiac specification. It is possible that complete FGF/ MEK pathway inhibition was not achieved using SU5402, PD0325901 or DN-FGFR treatments, as western blot analysis showed that the reduction in p-ERK levels was substantial but not complete (Figure 4:4). Therefore, it is possible that a low level of active FGF/ MEK may be necessary and sufficient for cardiac specification. To test this, a higher level of FGF/ MEK signalling inhibition was required. Higher concentrations of SU5402 and PD0325901 than in the aforementioned experiments were tested for use, but these concentrations frequently resulted in embryonic death by the tadpole stage. Therefore, the DN-FGFR was used in conjunction with SU5402 or PD0325901 to maximise FGF/ MEK pathway inhibition, whilst endeavouring to maintain embryonic viability.

Embryos were injected at the 2 cell stage with DN-FGFR mRNA. Injected and uninjected embryos were then further treated with either the FGF/ MEK inhibitors, or DMSO, continuously from stage 8. DN-FGFR, SU5402 or PD0325901 individual treatments resulted in truncated tadpoles with small anterior features and a truncated trunk and tail (Figure 4:7 C, D, E, F, I, J, M, N), compared with the controls (Figure 4:7 A, B, M, N). These treated tadpoles displayed only moderately reduced cardiac tissue, but minimal levels of skeletal muscle. Although there were no biological replicas for the skeletal muscle experiment, the results are consistent with previous work that shows a requirement for FGF/ MEK signalling for skeletal muscle development (Hagos and Dougan, 2007; Isaacs et al., 2007). DN-FGFR mRNA injections in conjunction with SU5402 or PD0325901 treatments resulted in a severely affected tadpole phenotype. These tadpoles were small, lacked landmark embryonic features including the tail, eyes and cement gland and had a barely identifiable embryonic axis. Figure 4:7 G, H, K, L, M, and N shows that tadpoles often

had absent or severely reduced cardiac tissue and absent skeletal muscle. In addition, Figure 4:7 O shows that p-ERK levels are reduced to a greater extent where DN-FGFR and molecular inhibitors are used together, as opposed to separate treatments. This suggests that a greater level of FGF/ MEK signalling inhibition was achieved in these experiments.

It can be reasoned that the increased phenotypic severity is specific to FGF/ MEK signalling downregulation, rather than general toxicity, as the two different drugs at two different concentrations, along with the DN-FGFR, still cause similar phenotypes. Determining whether the effect on cardiac tissue is directly or indirectly due to FGF/ MEK inhibition is, however, more problematic. The reduction in cardiac tissue could be due to a requirement for FGF/ MEK signalling in cardiogenesis, although given that cardiac tissue is observed it is likely that a low level of FGF/ MEK signalling would be required. However, developing embryos may have reached an FGF/ MEK depletion threshold where global embryonic development is unable to proceed normally and many embryonic features are compromised, regardless of a direct FGF/ MEK signalling requirement. If this is so, then cardiac tissue development could be indirectly affected by FGF/ MEK inhibition. Indeed, many embryonic features appear to be more widely affected after greater FGF/ MEK inhibition, but not all of them are affected proportionally. For example, skeletal muscle is more affected than cardiac tissue. Preliminary analysis reveals that blood is observed (Figure 4:7), suggesting that FGF/ MEK inhibition is having a greater effect on select mesoderm derivatives.

In summary, these results suggest that, should this increased level of FGF/ MEK inhibition be specific to cardiac development, then a low level of FGF/ MEK signalling is required for cardiac specification. A higher level of FGF/ MEK inhibition, as assessed by a further reduction in p-ERK levels, is associated with a severe phenotype affecting the entire embryo and its viability, characterised by the truncated anterior-posterior axis and loss or severe reduction of anterior and landmark features including the head, eyes and cement gland. These findings question the specificity of the effects on the heart.

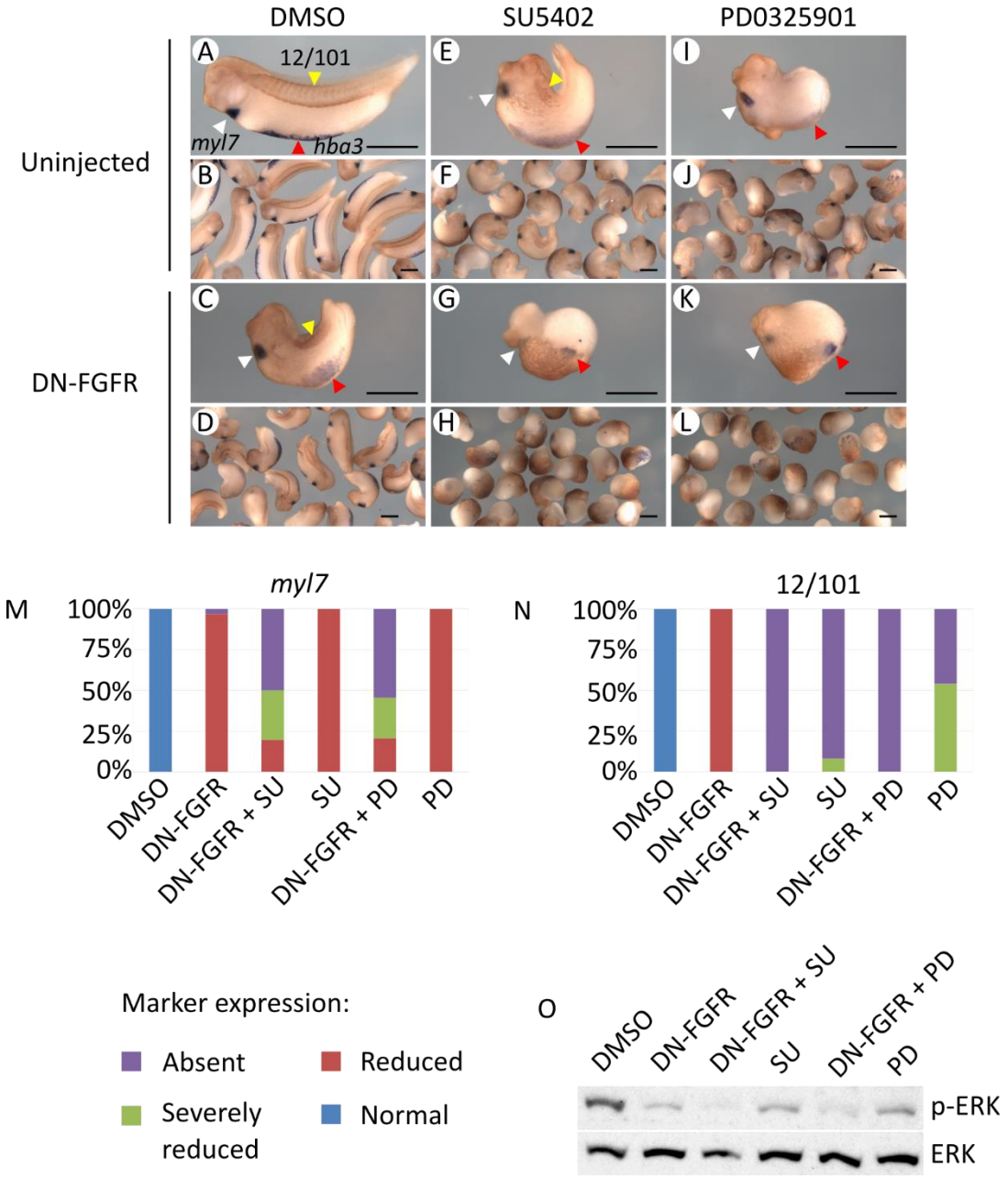

Figure 4:7. Maximal inhibition of FGF/ MEK signalling adversely affects normal embryonic development

Embryos were either uninjected or injected uniformly with 2 ng of DN-FGFR mRNA. Injected and uninjected embryos were treated with DMSO, 20 µM of SU5402-C (SU) or 10 µM of PD0325901 (PD) continuously. Injections were at the 2 cell stage and all other treatments commenced at stage 8. (A-L) Tadpoles were analysed by whole mount *in situ* hybridisation using the cardiac marker *myl7* (white arrows) and the blood marker *hba3* (red arrows) then subsequently stained by immunohistochemistry for skeletal muscle marker 12/101 (yellow arrows). All individual images show a lateral view orientated anterior left, dorsal up. Scale

bar represents 1 mm. Graphs quantifying data displayed in A-L. (M) *Myl7* DMSO n=71, DN-FGFR n=66, DN-FGFR +SU n=66, SU n=75, DN-FGFR +PD n=68, PD n=68. (N) 12/101 DMSO n=35, DN-FGFR n=32, DN-FGFR +SU n=36, SU n=37, DN-FGFR +PD n=36, PD n=37. (O) Western blot analysis of protein extracts at stage 9. ERK is a loading control.

4.6 FGF/ MEK signalling is not required before gastrulation for cardiogenesis

To investigate the requirement for FGF/ MEK signalling in cardiac specification further, time-controlled FGF/ MEK inhibition was utilised during the midblastula transition to gastrulation time window, where ALK4/5/7 signalling has been shown to be required (Chapter 3). Previously, SU5402 has been shown to act reversibly when removed from embryos (Delaune et al., 2005; Fletcher and Harland, 2008), with total recovery after SU5402 treatment taking 2 hours (Crump et al., 2004; Maroon et al., 2002; Marques et al., 2008). It was reasoned that using defined time windows of FGF/MEK inhibition should assist to alleviate some of the more general developmental abnormalities observed upon continuous FGF/ MEK inhibition, such as truncated anterior-posterior axis development.

Embryos were treated from stage 8 with FGF/ MEK inhibitors for three, five or twenty hours. Figure 4:8 A-F and I shows that embryos treated with FGF/ MEK inhibitors for three or five hours had normal phenotypes and normal cardiac tissue staining at the tadpole stage, compared with controls. These results are in agreement with previous work that has shown that FGF/ MEK signalling inhibition between midblastula transition and gastrulation, using SU5402, gave rise to tadpoles with tails, albeit also with expanded abdominal regions (Cha et al., 2008). Figure 4:8 G-I shows that only FGF/ MEK inhibition for an extended time period of 20 hours, which encompasses gastrulation and neurulation, resulted in tadpoles with a truncated anterior-posterior axis, a small head, eyes and cement gland and reduced cardiac tissue. This is consistent with work that demonstrates that FGF/ MEK inhibition from midblastula transition to stage 26, equivalent to the 20 hour treatment category, resulted in tadpoles with curved backs and shortened tails (Cha et al., 2008).

Western blot analysis of protein extracts from stage 10 embryos revealed that p-ERK levels in FGF/ MEK inhibited samples were lower than in the control. Samples that were treated with FGF/ MEK inhibitors for 3 hours showed higher levels of p-ERK compared with samples treated for 5 or 20 hours (Figure 4:8 J). Samples treated for

3 hours had 2 hours of recovery time after inhibitor removal prior to western blot analysis, whereas samples treated for 5 or 20 hours had not had the inhibitor removed at the time of protein extraction for western blot analysis. These results suggest that partial recovery of FGF/ MEK signalling had occurred after inhibitor removal. At stage 10, 5 hour and 20 hour samples subjected to FGF/ MEK signalling inhibition had thus far received the same treatments, hence they were replicas at that time point. This result shows that there was a slight variation in p-ERK protein levels between biological samples. This western blot analysis suggests that FGF/ MEK signalling inhibition has been achieved. Collectively, these results suggest that FGF/ MEK signalling is not required between midblastula transition and gastrulation for cardiac specification, but may be required later for normal heart development.

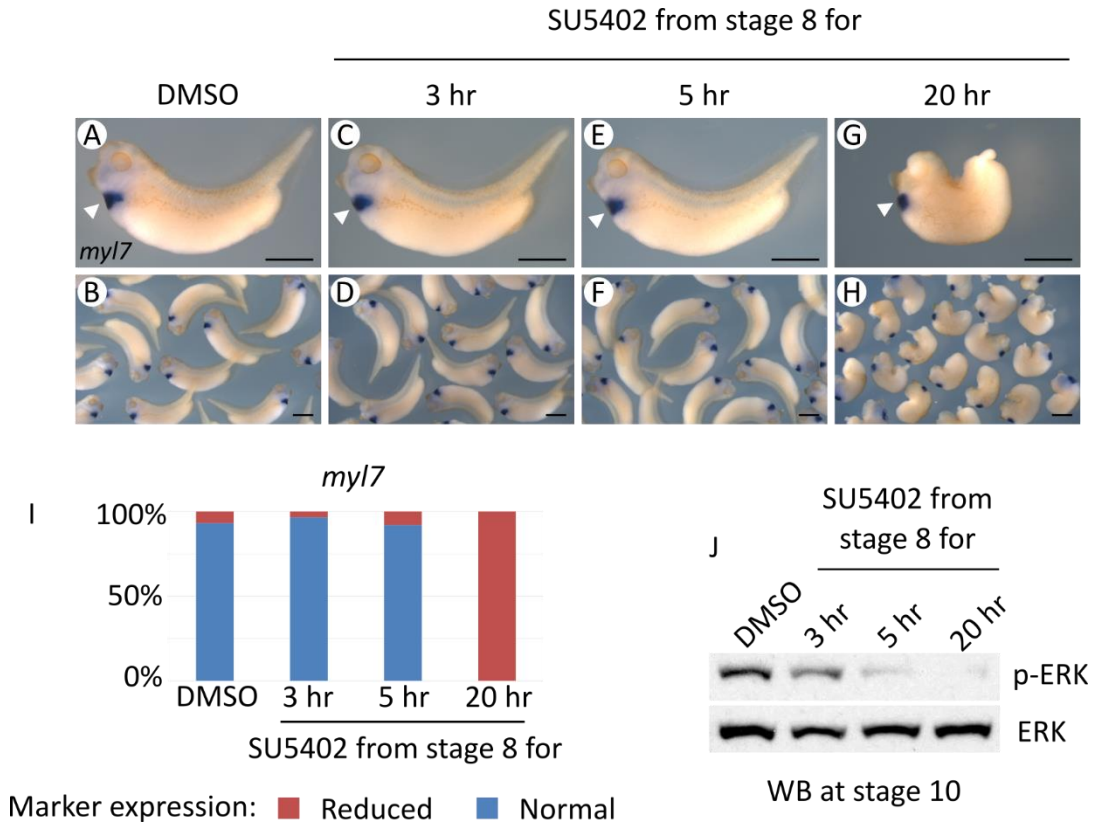

Figure 4:8. FGF/ MEK signalling is not required between midblastula transition and gastrulation for cardiogenesis

Embryos were treated with DMSO or with 100 µM of SU5402-S (SU). Treatments commenced at stage 8, for the time period indicated, then the treatment media was removed, and embryos were washed by two 5 minute washes in 30 ml of fresh 10% NAM. Tadpoles were analysed by whole mount *in situ* hybridisation using the cardiac marker *myl7* (white arrows). Treatments of (A, B) DMSO, or SU5402-C for (C, D) 3 hours, (E, F) 5 hours or (G, H) 20 hours. All individual images show a lateral view orientated anterior left, dorsal up. Scale bar represents 1 mm. (I) Graph quantifying the results displayed in A-H. DMSO n=44, SU 3hr n=59, SU 5hr n=63, SU 20hr n=35. (J) Western blot analysis at stage 10. ERK is a loading control.

To investigate the requirement for FGF/ MEK signalling before, during and proceeding gastrulation further, time-dependent FGF/ MEK signalling inhibition was carried out during select time windows and the morphology and extent of cardiac tissue was assessed in stage 36 tadpoles. Experimental protocol and analysis by Sarah Black, procedures and images were courtesy of Dr Branko Latinkic. FGF/ MEK signalling inhibition between midblastula transition and gastrulation (stages 8-10) resulted in tadpoles with normal cardiac size and morphology, comparable to the controls (Figure 4:9 A-F). This suggest that FGF/ MEK signalling is not required during the midblastula transition to gastrulation time window, where ALK4/5/7 signalling was shown to be necessary for cardiac specification (Chapter 3). FGF/ MEK signalling inhibition between stages 10-28 resulted in tadpoles that had linear heart tubes (Figure 4:9 G-I). These specimens appear to have only a slight reduction in cardiac tissue, but morphogenesis, including the anterior dorsal movement of the posterior, future atrial, cardiac region, and thus looping and chamber expansion have failed. A more striking phenotype was the prevalence of cardiac bifida and a reduced quantity of cardiac tissue upon FGF/ MEK signalling inhibition between stages 13-28 (Figure 4:9 J-L). This is surprising as this shorter time window of FGF/ MEK signalling inhibition resulted in a more severe cardiac phenotype than a longer inhibition period. These results support the aforementioned finding that suggested that FGF/ MEK signalling is not required between midblastula transition (stage 8) and the onset of gastrulation (stage 10) for cardiac specification. However, these results do provide evidence that suggests that FGF/ MEK signalling is required for continued normal heart development after cardiac specification.

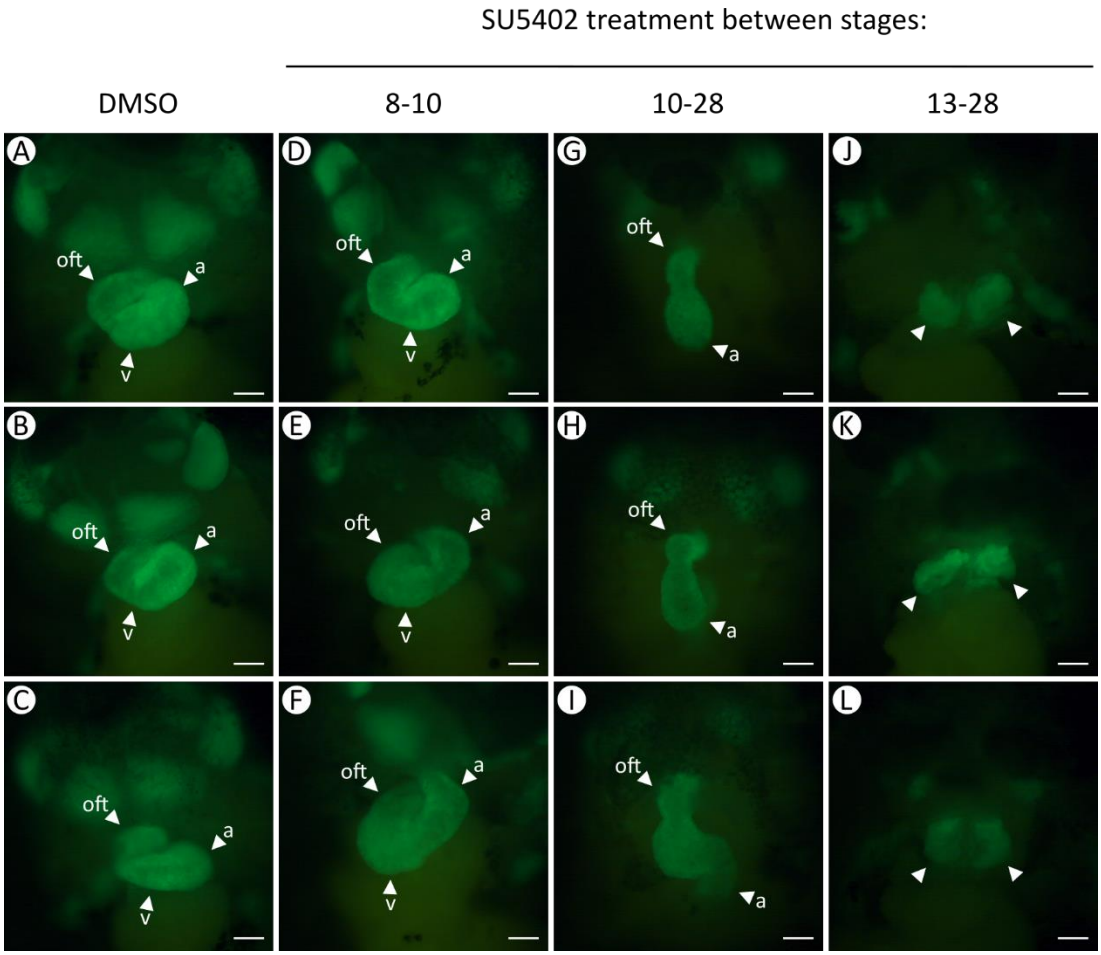

Figure 4:9. FGF/ MEK signalling is required after initial specification for correct heart formation

Embryos were treated with DMSO or with 100 µM of SU5402-S. Treatments commenced during the time period indicated, then treatment media was removed, by two 5 minute washes in 30 ml of fresh 10% NAM, and embryos developed until the tadpole stage. The *Xenopus laevis* used are transgenic for cardiac actin –green fluorescent protein (CA-GFP), thus the heart is visualised in live anesthetised tadpoles (green, white arrows) with three example per treatment shown in vertical columns. (A-C) DMSO n= 46/46. (D-F) SU5402-S treated between stages 8-10, n= 23/25. (G-I) SU5402-S treated between stages 10-28, n= 63/69. (J-L) SU5402-S treated between stage 13-28, n=32/47. The developing aorta (a), ventricle (v) and outflow tract (oft) can be identified (arrows). Images display a ventral view, with the anterior upwards. Scale bar represents 1 µm. Experimental protocol and analysis by Sarah Black, procedures and images were courtesy of Dr Branko Latinkic.

4.7 Discussion

4.7.1 FGF/ MEK signalling inhibition using three complementary reagents

FGF/ MEK signalling has been implicated in the specification of cardiac tissue in *Xenopus laevis* (Keren-Politansky et al., 2009; Samuel and Latinkić, 2009), zebrafish (Reifers et al., 2000) and chick (Alsan and Schultheiss, 2002). To investigate the requirement and timing of FGF/ MEK signalling in cardiac specification *in vivo* in *Xenopus laevis*, SU5402, PD0325901 and a DN-FGFR were used to inhibit the FGF/ MEK signalling pathway. Whole embryo phenotypes after treatment ranged from presenting a truncated posterior region at low effective concentrations of treatment, to embryos which were severely truncated along the anterior-posterior axis with underdeveloped anterior features at higher concentrations of inhibition, consistent with phenotypes shown in previous reports (Amaya et al., 1991; Deimling and Drysdale, 2011; Delaune et al., 2005; Fletcher and Harland, 2008; Isaacs et al., 2007). The use of three different FGF/ MEK signalling inhibition reagents throughout the work presented here demonstrated the specificity of FGF/ MEK signalling inhibition, as results gained using the different reagents were in agreement. Inhibition of FGF signalling at either the FGF receptor level, or at MEK, resulted in phenotypes that were similar between the different inhibition approaches. This suggests that FGF signalling is primarily acting via the MEK/ ERK pathway during early development.

4.7.2 Cardiac tissue and morphogenesis are affected by continuous FGF/ MEK signalling inhibition from midblastula transition

Cardiac tissue was observed in tadpoles despite early and continuous FGF/ MEK signalling inhibition. Cardiac tissue staining was reduced, but only modestly. The whole embryonic phenotype was affected with the anterior-posterior axis substantially truncated and anterior features including the head, eyes and cement gland were underdeveloped. These results suggested that either a low level of FGF/

MEK signalling is required for cardiac specification, or that FGF/ MEK signalling is not required and the observed reduction in cardiac tissue was a secondary effect of abnormal embryonic development. Previous research has shown that FGF/ MEK pathway inhibition results in the abolition (Rankin et al., 2012) or severe reduction (Deimling and Drysdale, 2011; Keren-Politansky et al., 2009; Reifers et al., 2000; Shifley et al., 2012) in the expression of the cardiac marker *nkx2.5*. This work is in conflict with data presented within this chapter demonstrating only a modest reduction in cardiac marker expression. However, analysis for alternate cardiogenic factors upon FGF/ MEK pathway inhibition show a reduction in cardiac progenitor marker *isl1* (Deimling and Drysdale, 2011), but that cardiogenic *gata4* is barely affected (Keren-Politansky et al., 2009). Analysis of differentiated cardiac markers *cardiac troponin* (Shifley et al., 2012) and *myocardin* (Keren-Politansky et al., 2009) show that there is a mild reduction in expression. However, this disagrees with other work illustrating the total loss of *cardiac troponin* (Deimling and Drysdale, 2011), presenting an inconsistent, conflicting result. In addition, it has been shown that, upon FGF/ MEK pathway inhibition, there is an early reduction in cardiac markers *nkx2.5* and *myocardin*, followed by recovery of those markers later in development (Keren-Politansky et al., 2009; Reifers et al., 2000). Therefore, although *nkx2.5* expression is commonly reported to be absent or severely reduced after FGF/ MEK signalling inhibition, it appears that differentiated cardiac tissue markers do not reliably reflect the severity of reduction seen in early cardiac field markers. Perhaps there is a compensatory mechanism allowing for alternate cardiogenic factors to ensure the development of differentiated cardiac tissue. Cardiac tissue has been specified and previous work, both in *Xenopus laevis* and zebrafish, suggests a role for FGF/ MEK in regulating heart size, survival and proliferation (Fletcher and Harland, 2008; Langdon et al., 2007; Marques et al., 2008; Simões et al., 2011). Therefore, it is plausible that FGF/ MEK signalling is required throughout development for the maintenance and promotion of cardiac cells.

4.7.3 FGF/ MEK signalling is not required before gastrulation for cardiac specification, but is required later for normal heart development

Nodal/ Activin signalling is required from midblastula transition, but before gastrulation, for cardiac specification (Chapter 3). To ascertain whether FGF/ MEK signalling is likewise required during this time window for cardiac specification, time-controlled inhibition of FGF/ MEK signalling was used. FGF/ MEK signalling inhibition between midblastula transition and gastrulation did not negatively affect cardiac specification or whole embryonic development. In addition, cardiac morphology in tadpoles was normal. This suggests that FGF/ MEK signalling is not required between midblastula transition and gastrulation for cardiac specification. However, experiments also demonstrated that sustained FGF/ MEK signalling inhibition, from midblastula transition, resulted in tadpoles displaying a reduced quantity of cardiac tissue. Therefore it is possible that FGF/ MEK signalling may have a role in later heart development after initial specification. Tadpoles displayed greater cardiac tissue staining when FGF/ MEK signalling inhibition commenced earlier, at midblastula transition (stage 8) or gastrulation onset (stage 10), compared with later, at the end of gastrulation (stage 13). This suggests that some exposure to FGF/ MEK signalling, followed by inhibition, is more severe than no exposure. There are several possible explanations. FGF/ MEK signalling is required post-gastrulation, but the loss of FGF/ MEK signalling from midblastula transition or gastrulation onset is sensed by the embryo, allowing for the activation of alternative compensation mechanisms, thus sufficient cardiac tissue was observed. Alternatively, FGF/ MEK signalling may first induce a cardiogenic inhibitor to regulate cardiac field dimensions, then later be required to positively regulate cardiogenesis, with this later step void in later experimental FGF/ MEK signalling inhibition. Finally, cardiac progenitors which are primed and committed during pre-gastrula and gastrula stages may be more susceptible to a lack of FGF/ MEK signalling later on than cardiac progenitors which are never exposed to FGF/ MEK signalling.

The differences in the amount of cardiac tissue between FGF/ MEK signalling inhibition treatments before and after the end of gastrulation suggests that the role

of FGF/ MEK signalling is not in cardiac specification, but in later heart development. Previously, it has been shown that cardiac tissue is specified by the end of gastrulation (Samuel and Latinkić, 2009; Sater and Jacobson, 1989), hence it is unlikely that this post-gastrula FGF/ MEK signalling requirement is in specifying cardiac tissue. Consistent with this, FGF/ MEK signalling may be required for maintaining and promoting cardiomyocyte development, and inhibiting alternative mesodermal fates, such as the blood lineage (Deimling and Drysdale, 2011; Isaacs et al., 2007; Shifley et al., 2012; Walmsley et al., 2008). Indeed, it has been proposed that FGF/ MEK signalling is required first for the induction of blood (Isaacs et al., 2007; Walmsley et al., 2008), and then for inhibiting blood progenitors to favour cardiac progenitor development (Deimling and Drysdale, 2011; Isaacs et al., 2007; Langdon et al., 2007; Simões et al., 2011; Walmsley et al., 2008). This contradicts work in *Xenopus laevis* animal cap and marginal zone explant experiments, which argue for the requirement of FGF/ MEK signalling in inducing cardiac markers (Keren-Politansky et al., 2009; Samuel and Latinkić, 2009). Although FGF/ MEK signalling has been shown to be required for cardiogenic induction in explant models, this may not reflect the true *in vivo* scenario. The results presented here are consistent with previous work that demonstrates that FGF/ MEK signalling inhibition, using molecular inhibitor PD173074, resulted in reduced cardiac tissue when acting between stages 18-23, with only a small effect seen after stage 23 (Shifley et al., 2012). Similarly, FGF/ MEK signalling inhibition, using SU5402, from the end of gastrulation until stage 28 resulted in absent cardiac tissue (Deimling and Drysdale, 2011). Therefore, the results presented here along with current literature suggest that FGF/ MEK signalling is not required for cardiac specification, but is required later in heart development, perhaps for the maintenance and promotion of cardiomyocytes.

In addition to reduced cardiac tissue, defective cardiac morphology upon post-gastrula FGF/ MEK signalling inhibition was shown here. Again, the most severe phenotypes were seen after FGF/ MEK signalling inhibition in the later and shorter time window (stage 13-28). FGF/ MEK signalling inhibition between midblastula transition (stage 8) and gastrulation onset (stage 10) had no obvious effect on the

heart size or morphology, reiterating that FGF/ MEK signalling is not required during this time window for cardiogenesis. During prolonged FGF/ MEK signalling inhibition from stage 10-28, linear heart tubes formed, with only modestly reduced cardiac tissue. Given the amount of cardiac tissue which has formed and migrated correctly to form a linear heart tube, it is likely that FGF/ MEK signalling may provide additional information necessary for correct morphological movements. This may occur directly, or by acting during neurula stages to activate genes which later control morphological events. Upon FGF/ MEK signalling inhibition from the end of gastrulation (stage 13), cardia bifida was observed, with reduced cardiac tissue. In agreement with these findings, previous work illustrates that cardia bifida prevails upon FGF/ MEK signalling inhibition, using SU5402, between stages 12.5-20 and 12.5-22 (Deimling and Drysdale, 2011). FGF/ MEK signalling inhibition from stages 18 (Shifley et al., 2012) or 24 (Deimling and Drysdale, 2011) resulted in reduced cardiac tissue. FGF/ MEK signalling inhibition from stages 23 or 28 had minimal effect on the amount of cardiac tissue (Shifley et al., 2012); however, no discernible heart tube was detected in another study (Deimling and Drysdale, 2011), suggesting that FGF/ MEK signalling is involved in the movements of cardiac cells, rather than their specification or quantity. The presentation of cardia bifida may be due to the reduction in cardiac tissue, and thus also migratory capacity, due to a FGF/ MEK signalling requirement in maintaining and promoting the expansion of cardiac progenitors. Additionally, FGF/ MEK signalling may be required for correct cardiac progenitor migration. FGF/ MEK signalling has been shown previously to be required for cell migration in the developing embryo (Beiman et al., 1996; Sun et al., 1999). Therefore, this could suggest that FGF/ MEK signalling may be required from late gastrulation into early neurulation for cardiac tissue maintenance and proliferation. FGF signalling may be further required during later neurula stages for correct cardiac morphology configuration.

In summary, the results suggest that FGF/ MEK signalling is not required before the end of gastrulation (stage 13) for cardiac specification. The evidence suggests that FGF/ MEK signalling is required for normal cardiac development, from the end of

gastrulation and throughout neurulation, perhaps for the maintenance, expansion, regulation of size and in conveying morphological cues to cardiac tissue. This is in keeping with a re-iterative role for FGF/ MEK signalling in cardiac development (Fletcher and Harland, 2008; Langdon et al., 2007; Marques et al., 2008; Simões et al., 2011).

5 A novel role for p53 in early heart development

5.1 Introduction

p53 is well known as a tumour suppresser protein but has also been shown to have a broad range of other functions including in DNA repair, cell survival, proliferation, adhesion, motility, differentiation, metabolism and development (Beckerman and Prives, 2010; Brady and Attardi, 2010). p53 can be modified by post-translational modifications in response to a variety of stimuli, which influence the function of p53 (Meek and Anderson, 2009; Vogelstein et al., 2000). New roles for p53 in embryonic development are constantly being uncovered, for example, during mesoderm induction in *Xenopus laevis* (Cordenonsi et al., 2007, 2003; Piccolo, 2008; Takebayashi-Suzuki et al., 2003). For mesoderm induction in *Xenopus laevis* it has been shown that FGF activated phosphorylated-ERK (p-ERK) phosphorylates p53, on Serine 6 and Serine 9, which then interacts with Nodal-activated phosphorylated-Smad2 (p-Smad2) (Cordenonsi et al., 2007, 2003). p-Smad2 and phosphorylated-p53 (p-p53) physically interact to regulate the transcription of some, but not all, TGF-beta target genes, therefore implicating p53 in mediating pathway crosstalk between the Nodal/ Activin and FGF signalling pathways for mesoderm induction (Cordenonsi et al., 2007, 2003; Dupont et al., 2004). Previous research implicates Nodal/ Activin and FGF signalling in cardiac specification, however, the relationship between the two pathways is unclear (Noseda et al., 2011). It is possible that p53 might be involved in mediating a putative interaction between Nodal/ Activin and FGF signalling for cardiac specification, or may be required to fine-tune the Nodal/ Activin signalling pathway for the induction of cardiac specific target genes. It has been shown that p53 knockout mice develop normal hearts, thus finding a developmental role for p53 in *Xenopus laevis* heart development may be surprising (Donehower et al., 1992). However, the expression of mouse p53, p63 and p73 are detected in the early mouse embryo and the family members have previously been shown to have overlapping functions (Hernández-Acosta et al., 2011; Levrero et al., 2000). In contrast, there is little evidence of redundancy within the p53 family members during early *Xenopus laevis* development, as p63 is not expressed until later in development and p73 is not found in lower vertebrates (Cordenonsi et al., 2003; Lu et al., 2001). This presents

Xenopus laevis as a good model to study the role of p53 in heart development. Work presented in this chapter uses antisense morpholino oligonucleotides and dominant negative p53 mRNA to downregulate endogenous p53 activity to investigate the role of p53 in heart development.

5.2 Experimental approach

To investigate the role of p53 in cardiac specification, p53 activity was downregulated *in vivo* in *Xenopus laevis* embryos and the effects on cardiac tissue were analysed. Antisense morpholino oligonucleotides (MOs) are short oligomers which bind to a specific RNA target sequence to inhibit cellular processes, such as RNA splicing or translation, and are used to downregulate the expression of a protein of interest. Previously reported MOs against *Xenopus laevis* p53 (p53) are targeted to two different sequences (Cordenonsi et al., 2003; Rana et al., 2011; Takebayashi-Suzuki et al., 2003). However, the sequences are nearly identical, overlapping in 21 out of 25 bases (Figure 5:1). One of these previously reported p53 MOs, here named p53 MO1, was used in this study (Figure 5:1 and Table 5:1). In addition, one new translation blocking MO which did not overlap the sequence of the previously published p53 MOs and two new splice blocking MOs were designed and tested for this study (Table 5:1). The available 5'UTR sequence of *Xenopus laevis* p53 is relatively short, which is perhaps why few successful translation blocking MOs have been previously reported.

Figure 5:1 and Table 5:1 show the sequences of the previously published p53 MOs and those designed for this study, in addition to the position in the p53 mRNA to which the translation blocking MOs are targeted. The translation blocking p53 MO designed for this study, named p53 MO3, is targeted to the 5'UTR upstream of the ATG site and does not overlap the sequences of the previously published p53 MOs, here named p53 MO1 and p53 MO2 (Figure 5:1). The translation blocking p53 MO1 and p53 MO3 were tested for their ability to downregulate the abundance of the p53 protein (see Section 5.3 below) and were selected as suitable reagents for further

use in investigating the requirement of p53 in heart development. p53 MO1, but not p53 MO3, was predicted to work in *Xenopus tropicalis* based on sequence homology.

Splice blocking MOs were targeted to block mRNA splicing events occurring at the exon 2 to intron (E2I) and exon 3 to intron (E3I) boundaries. Reverse transcription polymerase chain reaction (RT-PCR) analysis was performed to examine interrupted splicing events. However, no difference was observed in the quantity and size of the original amplicon spanning the E2I and E3I sites, indicating that splicing events have not been disrupted (not shown). The amplicon spanning the E2I and E3I sites was examined, rather than looking for a new predicted amplification fragment, as altered splicing events are difficult to predict. To rule out the possibility of a sequence mismatch between the *Xenopus laevis* sequence assembly and the animal stock used in this project as a potential reason for the lack of MO activity, genomic DNA, randomly selected from four individuals from the laboratory colony of *Xenopus laevis*, was sequenced and found to be homologous to the reference genome used for designing the MOs. With no indication that the p53 splice blocking MOs were altering splicing events, the splice blocking MOs were not utilised.

A control MO (cMO) was also utilised in all experiments to ensure that the observed effects were specific to p53 downregulation, and not a side-effect of MO treatments (Table 5:1). At the time that this study began, there was evidence of one orthologue of *Xenopus laevis* p53 within the genome. Despite recent improvements in the quality of the available sequence of the *Xenopus laevis* genome, no further *Xenopus laevis* p53 orthologues have been identified.

The soluble molecular p53 inhibitor, Pifithrin-α, was tested for its suitability to inhibit p53 for these studies (Komarov et al., 1999; Villiard et al., 2007). Soluble molecular inhibitors are experimentally advantageous, allowing the inhibitor to be added to, or removed from, the embryo containing media at any time point in development, allowing time-dependent inhibition control. Despite testing two batches of Pifithrin-α, at a range of concentrations up to 500 µM, no effect was observed on the phenotype of the whole embryo. This could have been be due to Pifithrin-α being

unable to penetrate through the vitelline or plasma membranes. To address this possibility, Pifithrin-α was injected to a final internal concentration of approximately 100 μM, in addition to 100 μM of external treatment, into the blastomeres of an embryo at the 2 cell stage, or into the blastocoel at stage 8. Embryos were examined at stages 32-36 (tadpole). Tadpoles which had been subjected to Pifithrin-α injections and treatment at the 2 cell stage either developed normally, or presented extremely retarded phenotypes lacking axis elongation and with underdeveloped landmark features including the tail, head, eyes and cement gland. Pifithrin-α injections and treatment at stage 8 did not affect the phenotypes of tadpoles. The disadvantages of having to inject Pifithrin-α includes the lack of penetrance knowledge and restricts the time of inhibitor administration to stages when injections can be performed. It was decided not to use Pifithrin-α for this study.

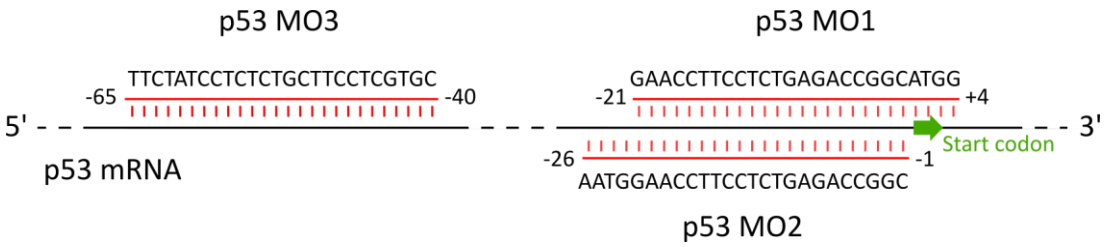

Figure 5:1. p53 translation blocking antisense morpholino oligonucleotides

Translation blocking p53 MO1, p53 MO2 and p53 MO3 bind p53 mRNA before and over the start site, inhibiting protein synthesis.

Name	Action	Sequence	Reference
cMO	Control	GTAACGATTTGAGTTTGGTGTTCAT	(Haworth et al., 2008)
p53 MO1	Translation blocking	GAACCTTCCTCTGAGACCGGCATGG	(Cordenonsi et al., 2003)
p53 MO2	Translation blocking	AATGGAACCTTCCTCTGAGACCGGC	(Takebayashi-Suzuki et al., 2003)
p53 MO3	Translation blocking	TTCTATCCTCTCTGCTTCCTCGTGC	New design
p53 MO E2I	Splice blocking	AAAGCACAAGAGGGACTCACCGTGC	New design
p53 MO E3I	Splice blocking	ATAAGAATGAAAGCACTCACCCTCC	New design

Table 5:1. p53 antisense morpholino oligonucleotides

5.3 p53 antisense morpholino oligonucleotides downregulate p53 protein

To confirm that p53 MO1 and MO3 efficiently downregulate p53 protein by blocking translation, the abundance of the p53 protein was examined using western blot (WB). Initially, detection of endogenous *Xenopus laevis* p53 protein using western blot was problematic, due to low sensitivity. Therefore, the overexpression of a tagged p53 protein was initially used to establish the effectiveness of the p53 MOs before confirmation and further analysis of endogenous p53.

A *Xenopus laevis* p53 construct was created, whose mRNA could be injected into embryos allowing p53 protein overexpression and detection. The construct incorporated 92 nucleotides of 5' untranslated region (UTR) and a human influenza hemagglutinin (HA) tag at the 3' terminus (p53-5'U92-HA). The inclusion of the 5'UTR was paramount, as this contains the target sequence of the p53 MOs. The HA tag aids detection by providing an epitope to an established antibody. Injecting 100 pg of p53-5'U92-HA mRNA into *Xenopus laevis* embryos resulted in the overexpression of p53 protein to such levels as can be readily detected by western blot, by both p53 and HA antibodies (Figure 5:2). The p53 MOs were co-injected into embryos at a range of doses, together with 100 pg of p53-5'U92-HA mRNA, to test and establish a MO dose which achieves p53 downregulation. Figure 5:2 A shows that p53 MO1 can effectively cause the downregulation of the p53 protein at all doses tested. Injection of 100 pg of p53-5'U92-HA mRNA and increasing doses of p53 MO3 likewise illustrated the robust downregulation of the p53 protein (Figure 5:2 B). Notably, 1 ng of p53 MO3 appeared to decrease p53 protein levels to a greater extent than 1 ng of p53 MO1, suggesting that p53 MO3 may be more potent. Although the p53 MOs appear to almost eradicate overexpressed p53 protein from detection at 1 ng, endogenous protein in untreated samples is barely observed, hence it is likely that a proportion of p53 protein may be remaining but has not entered the detectable range afforded by these western blots. Additionally, no obvious whole embryonic phenotype is observed at the lower doses tested. Therefore, a mid-range dose is likely to be the

most appropriate for reliable and consistent p53 protein downregulation, without affecting the viability of the embryo, in further investigations. A high level of agreement is perceived between p53 and HA antibodies, giving confidence in the observed results (Figure 5:2). 100 pg of p53-5'U92-HA mRNA caused toxicity and death in *Xenopus laevis* embryos by the neurula stage. This embryonic death can be prevented by injection of the higher doses of the p53 MOs.

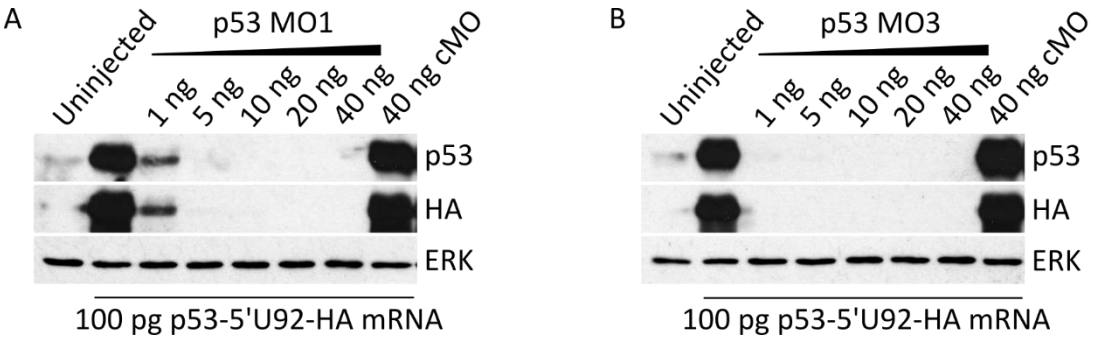

Figure 5:2. p53 antisense morpholino oligonucleotides efficiently downregulate overexpressed p53 protein

Embryos were either uninjected or injected uniformly at the 2 cell stage with 100 pg of p53-5'UTR-HA mRNA. Subsequently, at the 2-4 cell stage, embryos were injected uniformly with increasing amounts (as indicated in the figure) of p53 MO1, p53 MO3, 40 ng control MO (cMO) or did not receive further injection. At stage 9 protein extracts from embryos were analysed by western blot. ERK is a loading control.

Initially, the p53 protein appeared to have a narrow dynamic range of detectable expression, hence tagged-p53 mRNA injections were used to test whether the p53 MOs could effectively downregulate p53 protein expression. During initial experiments, the western blotting technique was optimised to increase the sensitivity and to enable the reliable detection of endogenous p53. Figure 5:3 A shows a western blot analysis of endogenous p53 protein levels throughout *Xenopus laevis* development. This western blot shows that endogenous p53 protein levels remain relatively constant throughout different developmental stages. Figure 5:3 B shows that treatment of *Xenopus laevis* embryos with doses of 10 ng, 20 ng and 40 ng of p53 MO1 resulted in the downregulation of endogenous p53 protein until at least stage 32. In embryos treated with 5 ng or 10 ng of p53 MO3, endogenous p53 protein was downregulated between stage 9 and 20 inclusive. However, unlike p53 MO1, p53 protein levels recovered to a level that was greater than the level of endogenous p53 in control samples by stage 32, despite robust inhibition at earlier stages (Figure 5:3 C). Interestingly the phenotypes of the tadpoles (Figure 5:4 and Figure 5:5) observed in embryos injected with p53 MO1 and p53 MO3 are highly similar.

It has been shown here that the translation blocking p53 MO1 and p53 MO3 resulted in the downregulation of both overexpressed and endogenous p53 protein in *Xenopus laevis*. These results suggest that p53 MO3 is slightly more potent than p53 MO1 at lower doses, but that the downregulation of p53 protein by p53 MO3 did not persist until the tadpole stages, whereas p53 MO1 downregulated p53 as far as stage 32. Both p53 MOs are suitable reagents for investigating the role of p53 in cardiogenesis.

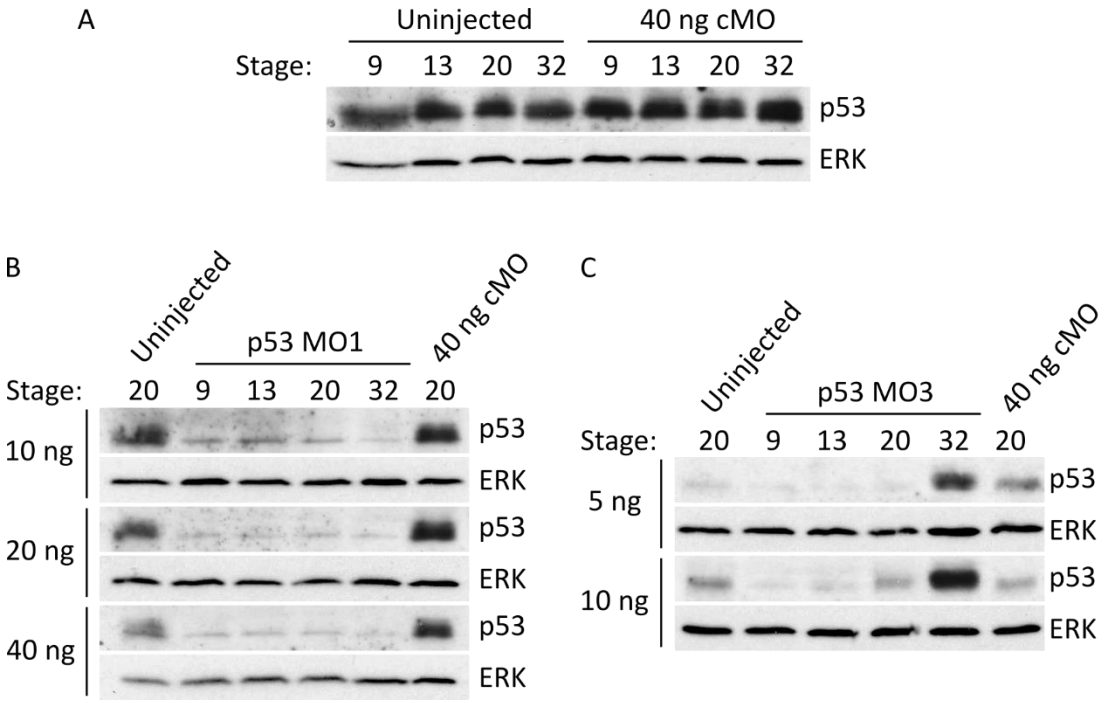

Figure 5:3. p53 antisense morpholino oligonucleotides efficiently downregulate endogenous p53 protein

Embryos were either uninjected or injected uniformly at the 2 cell stage with 40 ng of control MO (cMO), 10 ng, 20 ng, 40 ng of p53 MO1 or 10 ng, 20 ng of p53 MO3. At stage 9, 13, 20 or 32, as indicated, protein extracts from embryos were analysed by western blot. (A) Uninjected and cMO injected samples demonstrate that uniform levels of endogenous p53 protein are detected as embryonic development progresses. (B) p53 MO1 effectively downregulates endogenous p53 protein levels throughout development until at least stage 32. (C) p53 MO3 effectively downregulates endogenous p53 protein levels throughout development until the neurula stages, with p53 protein levels elevated above the level of endogenous protein by stage 32. ERK is a loading control.

5.4 p53 antisense morpholino oligonucleotides act in a dose dependent manner and affect cardiac tissue

To further establish the suitability and optimum dose of p53 MOs to utilise in investigating the role of p53 in cardiac specification, tadpoles were analysed after being injected with a range of doses of the p53 MOs. Embryos were injected with increasing doses of p53 MO1 or p53 MO3 at the 2 cell stage. At stage 32-36 (tadpole stage), embryos were analysed by whole mount *in situ* hybridisation (WMISH) using differentiated cardiac tissue marker *myosin light chain 7* (*myl7*) and whole embryonic phenotype. Control embryos presented a well-defined axis and a normal pattern of cardiac tissue staining (Figure 5:4 A-D). The normal appearance of embryos injected with cMO, which matched the highest dose of p53 MO used, suggests that, at this dose, the MO reagents are not having any obvious non-specific effects. Embryos injected with p53 MO1 demonstrated a dose-dependent response in the whole embryo phenotype, with the anterior-posterior axis becoming truncated and the tail less defined towards the higher doses tested (Figure 5:4 E-J). The phenotypes observed with the higher dose of 40 ng of p53 MO1 are in agreement with previously published work (Cordenonsi et al., 2007, 2003). Heart development, as assessed by the relative size of the cardiac-marker stained area, was reduced in p53 MO1 injected tadpoles, compared with the controls (Figure 5:4 A-J). Upon p53 MO3 injections a similar phenotypic dose-response was observed, with a truncated anterior-posterior axis and a less defined tail at the highest dose tested (Figure 5:4 K-P). Cardiac tissue staining appeared reduced in all p53 MO3 treated tadpoles in comparison to the controls (Figure 5:4 A-D, K-P). Both p53 MOs act in a dose-dependent manner, with p53 MO3 having similar effect as p53 MO1, but at slightly lower doses. From the data shown here and from published work, optimal doses of p53 MO were selected for use in further investigations. Although high doses of 40 ng and 50 ng of p53 MO1 (equivalent to 20 ng of p53 MO3) have been previously used (Cordenonsi et al., 2007; Sasai et al., 2008), lower doses, that exerted a cardiac phenotype with a less severely affected global embryonic phenotype, were selected as optimal for investigations

here. Doses of 20 ng of p53 MO1 and 10 ng of p53 MO3, when targeted uniformly into the embryo, were selected for use in further investigations.

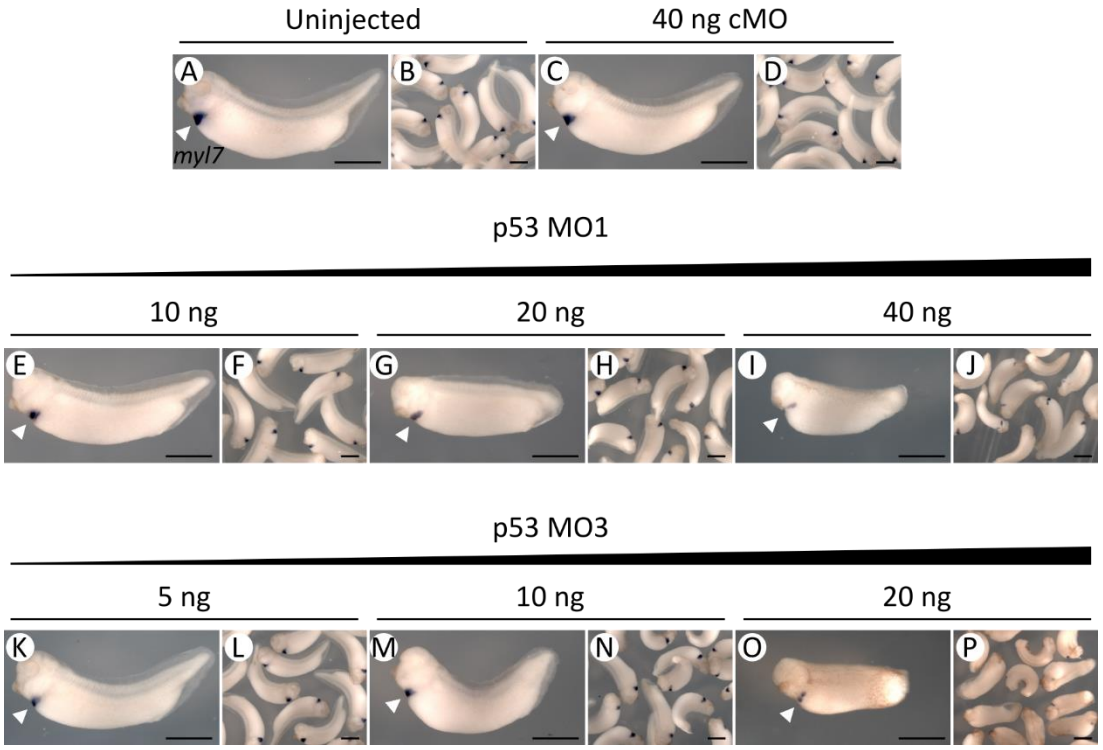

Figure 5:4. p53 antisense morpholino oligonucleotides act in a dose-dependent manner to affect cardiac tissue

Embryos were either (A, B) uninjected (n=127) or injected uniformly at the 2 cell stage with (C, D) 40 ng of control MO (cMO) (n=40), (E, F) 10 ng (n=19), (G, H) 20 ng (n=68), (I, J) 40 ng (n=52) of p53 MO1 or (K, L) 5 ng (n=23), (M, N) 10 ng (n=98), (O, P) 20 ng (n=15) of p53 MO3. Tadpoles were analysed by whole mount *in situ* hybridisation using the differentiated cardiac tissue marker *myl7* (white arrows).

5.5 p53 is required for normal heart development

Having established the effectiveness and selected optimum dose of p53 MO1 and MO3, these MOs were utilised to investigate the role of p53 in heart development. The focus of this study concerns the first step of heart development- the specification of cardiac tissue. There are currently no known cardiac specific markers allowing cardiac progenitor cells to be traced from initial specification, throughout development, until terminal differentiation (Scott, 2012). Although there are genes that are known to be expressed by the cardiac progenitor cell population, these are not unique to the cardiac lineage and are often expressed in progenitor cells of alternative lineages (Scott, 2012). Cardiac markers that are expressed in differentiated cardiac cells, for example *myl7*, are specific to the cardiac lineage and their relative expression can be used as an indirect readout of cardiac progenitor population specification. Therefore, the staining of differentiated cardiac tissue was analysed after p53 downregulation to examine the requirement for p53 in cardiac specification, with the intention to investigate whether heart field progenitor markers are altered should a reduction in differentiated cardiac tissue be observed.

Embryos were injected with the p53 MOs either uniformly or targeted to two dorsal vegetal (DV) or two ventral vegetal (VV) blastomeres of an 8 cell embryo. Work previously presented in this chapter demonstrated that 20 ng of p53 MO1 and 10 ng of p53 MO3 only caused subtle axial effects when injected uniformly, therefore it was reasoned that targeted injections at higher doses per blastomere might result in a more obvious specific cardiac effect, without a global phenotypic effect. At the tadpole stage (stage 32-36), embryos were analysed by whole mount *in situ* hybridisation using the differentiated cardiac tissue marker *myl7*. The staining pattern of *myl7* was categorised as either normal, reduced, severely reduced or absent and examples of each staining category are shown in Figure 5:5 L-O. The results displayed in Figure 5:5 A, D, G, J and K show that embryos injected uniformly with p53 MO1 or MO3 resulted in comparatively normal tadpoles, but with reduced cardiac tissue compared with the controls. p53 MOs targeted to the dorsal vegetal,

future cardiac, region presented a normal whole embryonic phenotype, including normal head and eyes, but with severely reduced cardiac tissue staining (Figure 5:5 B, E, H, K). p53 MOs targeted to the ventral vegetal blastomeres displayed normal cardiac tissue staining and a relatively normal anterior-posterior axis, although small posterior defects, for example reduced or bent tails, were commonly observed (Figure 5:5 C, F, I, K). These results suggest that p53 is required in dorsal vegetal, future cardiac, cells for heart development and that the p53 MOs had a specific effect in the injected region, as the anterior features of dorsal vegetal injected embryos appeared normal. The posterior region of ventral vegetal p53 MO injected embryos was relatively normal, providing evidence that a higher relative p53 MO dose per blastomere had minimal non-specific effects. Lineage tracing, which highlights all cells that received injected material, was used to first select embryos which had received the correctly targeted injection and then to examine the relative contribution of the injected region to the phenotype of the whole tadpole. Analysis of lineage traced embryos in Figure 5:5 P-S shows that the injected area appears to be of the correct size and proportion compared with the rest of the tadpole and with the controls. This would suggest that p53 MO is unlikely to be causing cell loss and that p53 is required cell-autonomously for heart development.

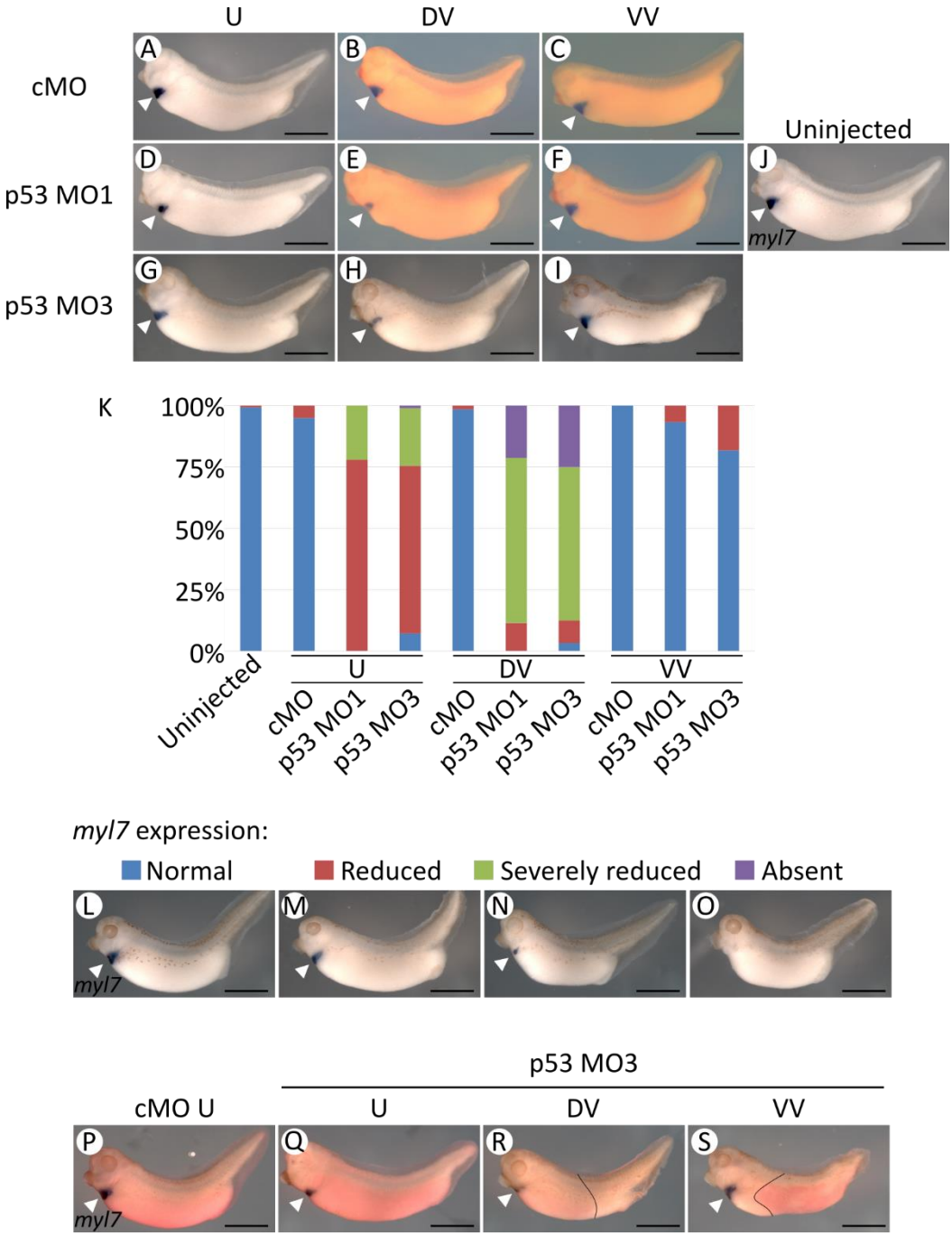

Figure 5:5. p53 MOs cause a reduction in differentiated cardiac tissue staining

Embryos were either (J) uninjected or injected uniformly (U) at the 2 cell stage with (A) 40 ng of control MO (cMO), (D) 20 ng of p53 MO1 or (G) 10 ng of p53 MO3. Alternatively embryos were injected at the 8 cell stage into two dorsal vegetal (DV) or ventral vegetal (VV) blastomeres with (B, C) 10 ng/ blastomere of cMO, (E, F) 10 ng/ blastomere of p53 MO1 or (H, I) 5 ng/ blastomere of p53 MO3. Tadpoles were analysed by whole mount *in situ* hybridisation using *myl7* (white arrows). (K) Graph displaying results of A-I. Uninjected

n=293, cMO U n=40, DV n=68, VV n=27, p53 MO1 U n=68, DV n=122, VV n=15, p53 MO3 U n=98, DV n=120, VV n=22. Following whole mount *in situ* hybridisation the extent of marker staining in tadpoles was classified. (L) Normal: the average staining observed in a given control sample. (M) Reduced: between 50-90% of staining area and intensity observed in controls. (N) Severely reduced: between 1-50% of staining area and intensity observed in controls. (O) Absent: no staining observed. (P-S) Lineage tracing (outlined) reveals the correct injection target. Images and show a lateral view orientated anterior left, dorsal up. Scale bars represent 1 mm.

5.6 The migration, fusion and remodelling of cardiac tissue is largely unaffected by p53 downregulation

The morphology of cardiac tissue in p53 morphants was analysed in more detail, to obtain additional information about heart development after p53 downregulation. Experimental samples that were scored for the relative staining of cardiac tissue in Figure 5:5 were examined for cardiac morphology. Uninjected controls presented a heart of normal size and morphology (Figure 5:6 A, B). At this stage of development (stage 34-36), the linear heart tube, which initially forms along the anterior-posterior axis, has begun to bend laterally towards the right side of the embryo as it forms an anticlockwise spiral (Kolker et al., 2000; Latinkić et al., 2004; Mohun et al., 2000). The posterior, future atrial region moves more anterior and dorsal, resulting in an s-shaped bulging cardiac tube. Distinct chamber cavities are formed later in development (Kolker et al., 2000; Latinkić et al., 2004; Mohun et al., 2000). Figure 5:6 E and F shows, in embryos displaying severely reduced cardiac tissue after p53 downregulation, that only a subtle area of cardiac cells was observed with no evidence of heart tube formation or cardiac looping. Tadpoles presenting reduced cardiac tissue most often had a small cavity, albeit lacking expansion, but with signs of looping (Figure 5:6 G, H). The vast majority of cardiac tissue was observed in the correct location on the ventral midline, indicating that cardiac primordia have maintained their migratory capability. Infrequently, cardia bifida was observed, where heart primordia failed to meet and fuse on the ventral midline. Where there was sufficient cardiac tissue, two cavities formed independently (Figure 5:6 I, J). Linear heart tubes were rarely observed suggesting that looping and morphogenesis could still occur. In some tadpoles, no cardiac tissue was observed, not even aberrantly localised (Figure 5:6 C, D). In all categories of staining it was apparent that normal anterior development proceeded. The size and location of landmark features, such as the eyes and cement gland, was normal. In addition, normal anterior skeletal muscle development was observed (Figure 5:6 A, C, E, G). In summary, the initial results suggest that the migratory, fusing, and looping capacities of cardiac tissue are largely unaffected after p53 downregulation. This suggests that p53 may have an

early role in heart development, perhaps in cardiac specification or early cardiac progenitor promotion.

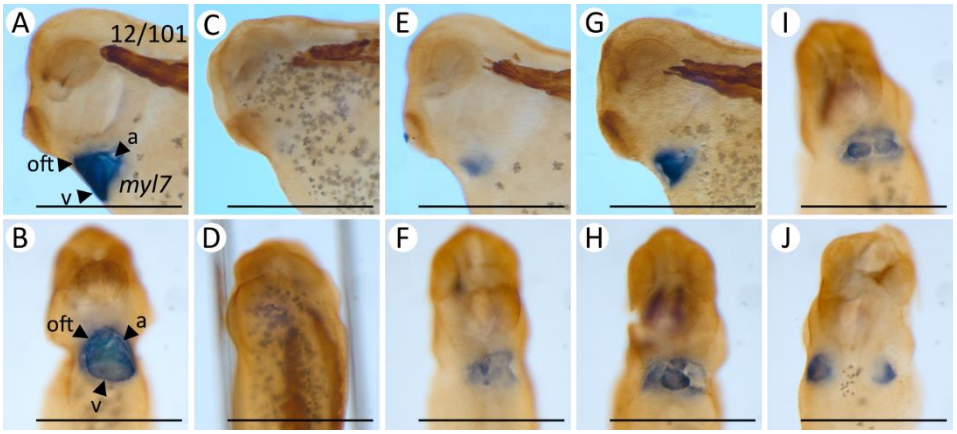

Figure 5:6. The migration, fusion and remodelling of cardiac tissue is largely unaffected by p53 downregulation

Following p53 inhibition treatment in Figure 5:5, tadpoles were analysed by whole mount *in situ* hybridisation using the cardiac tissue marker *myl7* (blue stain), followed by immunohistochemistry using the skeletal muscle marker 12/101 (brown stain). (A, B) Uninjected controls with the future atrium (a), ventricle (v) and outflow tract (oft) highlighted (arrows). (C, D) Absent cardiac tissue. (E, F) Severely reduced cardiac tissue. (G, H) Reduced cardiac tissue. (I, J) Cardia bifida. C-J examples have been injected at the 8 cell stage into two dorsal vegetal blastomeres with 20 ng/ blastomere of p53 MO1. Scale bar represents 1 mm. A, C, E, G show a lateral view orientated anterior left. B, D, F, H, I and J show a ventral view, anterior upwards. These are example cardiac phenotypes from the experiments presented and quantified in Figure 5:5.

5.7 A gain of function dominant negative p53 protein interferes with cardiogenesis

To validate the experiments carried out using p53 MOs, another independent method of downregulating p53 activity was utilised. mRNA encoding a dominant negative p53 protein, injected into the *Xenopus laevis* embryos, was utilised to downregulate active p53 signalling.

Human p53 (hp53) with a G to C point mutation at residue 974 results in an arginine to threonine (thr) substitution at codon 280 (hp53thr280) (Sun et al., 1992). Arginine 280 is a fundamental component of the DNA binding domain of p53, providing a positive charge to form ionic bonds with negative phosphate groups of the DNA major groove (Wright and Lim, 2007). Replacing arginine 280 with threonine interferes with the proteins ability to form a stable interaction with DNA (Wright and Lim, 2007). As p53 functions as a tetramer, one hp53thr280 protein can theoretically oligomerise with, and inhibit the function of, up to three wild type endogenous *Xenopus laevis* p53 proteins, thus acting in a dominant negative manner (Friedman et al., 1993; Sun et al., 1993; Wallingford et al., 1997). Hp53thr280 has been previously utilised for investigating the role of p53 in *Xenopus laevis* development, thus a similar approach was used in the work presented here (Wallingford et al., 1997).

Initially, wild type hp53 mRNA was tested by injecting into embryos and observing the tadpole phenotypes, to gauge an appropriate working dose for hp53thr280 and to compare the effect of the wild type hp53 mRNA phenotype to the hp53thr280 mRNA phenotype. When dorsal vegetal cells of an 8 cell embryo were injected with 0.5 ng of hp53 mRNA, the resulting tadpoles presented a slightly bent axis at early stages, but only subtle overall phenotypic abnormalities were observed by stage 40 (Figure 5:7 C, D), compared with the controls (Figure 5:7 A, B). A higher dose of 1 ng of hp53 mRNA, targeted to dorsal vegetal cells, had a more severe effect, resulting in a phenotype with a harshly bent axis at stage 28 and anterior developmental abnormalities presented by stage 40 (Figure 5:7 G, H). When ventral animal cells were

targeted with 0.5 ng of hp53 mRNA, tadpoles had small posterior outgrowths and abnormalities (Figure 5:7 E, F). The same injection target, but at 1 ng of hp53 mRNA, resulted in a more severe posterior disruption and a higher incident of outgrowths, notably with a high level of pigment localised to the extreme posterior end of the embryo at stage 28 (Figure 5:7 I, J). These results suggest that hp53 mRNA affects embryonic development in a dose dependent manner. Relatively high doses of hp53 mRNA were required to achieve the observed phenotypes. Concerns with doses greater than 1 ng globally being toxic were addressed by using targeted injections, which allowed a higher dose per blastomere without increasing the dose received by the whole embryo.

The hp53thr280 construct was created by site directed mutagenesis of the wild type p53 during this project (see Section 2.5). The difference in embryonic phenotypes observed between hp53 and hp53thr280 mRNA injected embryos were tested using similar doses and targets. Uniform injections of 1 ng of hp53thr280 mRNA did not affect the phenotype of the tadpoles, compared with uninjected controls (Figure 5:7 K, L). Injections of 1 ng of hp53thr280 mRNA, targeted to dorsal vegetal or ventral vegetal cells, had only a very subtle effect on the phenotype of the whole embryo, with normal axis formation, length and appearance and no observed outgrowths observed (Figure 5:7 M , N). This suggests that the site specific mutation between hp53 and hp53thr280 is effective to disrupt p53 signalling and circumvent the phenotypes caused by the same dose of wild type hp53 mRNA. Western blot analysis of protein extracts from stage 9 embryos shows that the hp53thr280 protein is produced in a dose dependent manner (Figure 5:7 O), but was less readily detected at lower doses than *Xenopus laevis* p53 (Figure 5:7 P). It would appear that hp53 is less effective than *Xenopus laevis* p53, hence higher doses of hp53 were necessary.

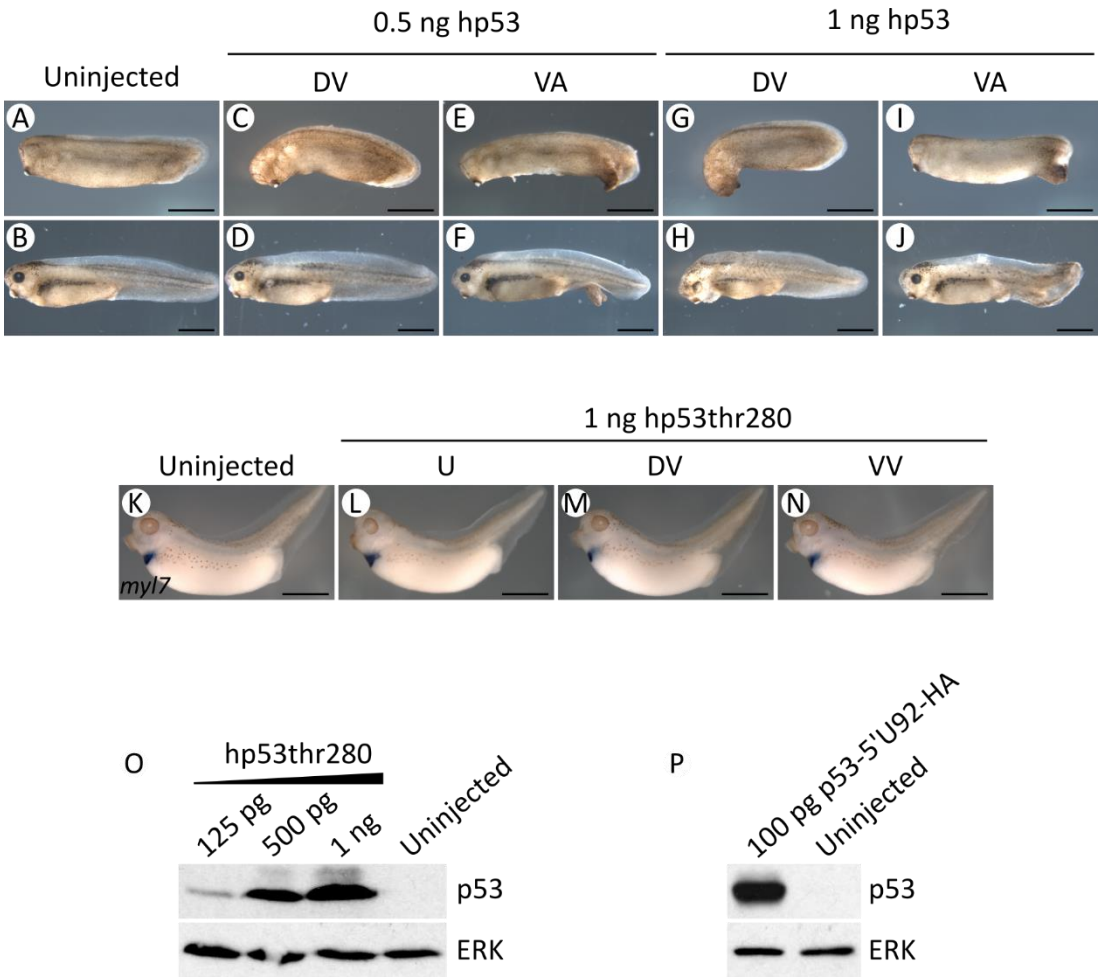

Figure 5:7. Dominant negative p53 gain of function optimisation

Embryos were either (A, B) uninjected, or injected at the 8 cell stage with 0.5 ng of hp53 mRNA into (C, D) two dorsal vegetal (DV) or (E, F) two ventral animal (VA) blastomeres (0.25 ng/ blastomere). 1 ng of hp53 mRNA was injected into (G, H) two DV or (I, J) two VA blastomeres (0.5 ng/ blastomere). Embryos developed until stage 28 (top row: A, C, E, G, I) or stage 40 (bottom row: B, D, F, H, J) for phenotypic analysis. Stage 28 – uninjected n=26, hp53 mRNA 0.5 ng DV n=22, 0.5 ng VV n=19, 1 ng DV n=20, 1 ng VV n=21. Stage 40 – uninjected n=25, hp53 mRNA 0.5 ng DV n=20, 0.5 ng VV n=18, 1 ng DV n=23, 1 ng VV n=21. Embryos were either (K) uninjected (n=124) or injected with 1 ng of hp53thr280 mRNA either (L) uniformly (U) (n=59), or into (M) two dorsal vegetal (n=110) or (N) two ventral vegetal (n=74) blastomeres of an 8 cell embryo (0.5 ng/ blastomere), and developed until the tadpole stage for phenotypic analysis. Embryos were analysed by whole mount *in situ* hybridisation using the cardiac tissue marker *myl7*. Images show a lateral view orientated anterior left, dorsal up. Scale bars represent 1 mm. (O) Embryos were injected uniformly with 125 pg, 500

pg or 1 ng of hp53thr280 mRNA, or left uninjected, and developed until stage 9 for western blot analysis for p53. (P) Embryos were injected uniformly with 100 pg of p53-5'U92-HA mRNA, or left uninjected, until western blot analysis at stage 9 for p53. ERK is a loading control.

To address whether p53 downregulation by hp53thr280 mRNA affects normal heart development, embryos were injected with hp53thr280 mRNA and cardiac phenotypes were examined at the tadpole stage. 1 ng of hp53thr280, injected uniformly, had no obvious effect on embryonic development or on cardiac tissue, with the phenotypes of the tadpoles similar to the uninjected controls (Figure 5:8 A-F, M). Hp53thr280 mRNA injections targeted to ventral vegetal, non-cardiac, regions presented a relatively normal embryonic phenotype, occasionally with a small posterior tail defect, but with normal cardiac tissue (Figure 5:8 J-L, M). Hp53thr280 mRNA injected into the dorsal vegetal, future cardiac regions resulted in a relatively normal whole embryo phenotype but notably with reduced cardiac tissue (Figure 5:8 G-I, M). This result suggests that p53 is required for normal heart development. Indeed, the effect of hp53thr280 appears to be specific to heart development, as other anterior features such as the eyes, cement gland and head appear to be normal, despite having also received hp53thr280 mRNA. Lineage tracing (Figure 5:8 C, F, I, L) was used to confirm the correct injection target. Analysis of lineage traced tadpoles shows that the domains of cells which received injected material appeared to be normally proportioned, suggesting that normal development had occurred with minimal cell loss or death. The relatively mild effects observed on the whole embryo phenotype after p53thr280 mRNA injection suggests that the cardiac effects observed here are likely to be specific and that p53 is required for heart development.

Previously, it has been shown that hp53thr280 forms a tetramer with endogenous p53 proteins, acting in a dominant negative manner to inhibit normal p53 function by disrupting DNA binding (Sun et al., 1993; Wallingford et al., 1997). p53 MO1 and MO3 bind p53 mRNA, inhibiting successful translation of the p53 protein. Hp53thr280 mRNA and p53 MOs are very different mechanisms for downregulating endogenous p53 activity. Nevertheless, both approaches yield similar results: a minimal effect on the global embryonic phenotype, but a specific effect resulting in the reduction of cardiac tissue in a cell-autonomous manner. The agreement of the

results of these two complementary approaches provides evidence that p53 is probably required for normal heart development.

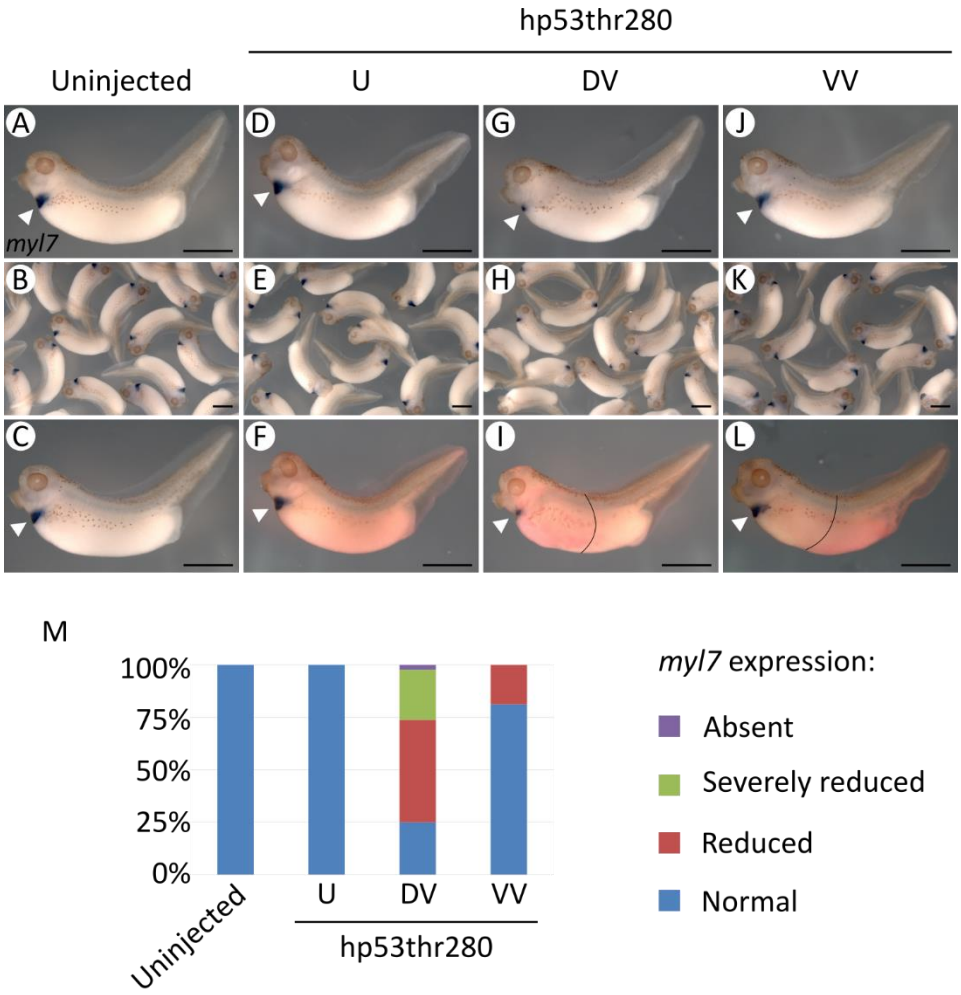

Figure 5:8. Dominant negative hp53 mRNA interferes with cardiogenesis

Embryo were either (A-C) uninjected or (D-F) injected uniformly (U) at the 2 cell stage with 1 ng of hp53thr280 mRNA. Alternatively, embryos were injected at the 8 cell stage into two (G-I) dorsal vegetal (DV) or (J-L) ventral vegetal (VV) blastomeres with 500 pg/ blastomere of hp53thr280 mRNA. Tadpoles were analysed by whole mount *in situ* hybridisation using *myl7* (white arrows). Lineage tracing (outlined) reveals the correct injection target. Images show a lateral view orientated anterior left, dorsal up. Scale bars represent 1 mm. (M) Graph displaying results of A-L. Uninjected n=70, hp53thr280 U n=42, DV n=88, VV n=69.

A rescue experiment was attempted using p53 MO3 and *Xenopus laevis* p53 mRNA beginning at the ATG site (p53-ATG-HA). p53-ATG-HA mRNA does not contain the 5'UTR sequence which p53 MO3 is targeted to, hence should not be affected by the p53 MO3. First, the p53-ATG-HA mRNA was tested at increasing doses to establish an appropriate dose to be combined with the p53 MO3 in an attempt to rescue the cardiac tissue and whole embryo phenotype. Doses of less than or equal to 20 pg of p53-ATG-HA mRNA did not negatively affect the embryonic phenotype throughout development (Figure 5:9 A, D). A dose of 50 pg p53-ATG-HA mRNA resulted in a truncated embryo with underdeveloped head and eyes, amongst other developmental abnormalities (Figure 5:9 B). 100 pg of p53-ATG-HA mRNA was toxic, resulting in embryonic death (Figure 5:9 C). Doses of 5 pg and 20 pg of p53-ATG-HA mRNA, along with 10 ng of p53 MO3, were utilised for rescue experiments. These amounts were reasoned to rescue p53 protein without causing toxicity, based on previously observed phenotypes and western blots. Rescue of the cardiac phenotype was not observed using these conditions, although it is noted that 10 ng, or greater, of p53 MO3 can prevent the toxic phenotype caused by 100 pg of p53 mRNA. Rescue experiments are particularly challenging to achieve especially when there is strong overexpression phenotype, such as embryonic death observed here (Eisen and Smith, 2008). In addition, the p53 MO phenotype is subtle, thus there is a narrow margin between no rescue to overloading and toxicity. Perhaps with further work and the use of the more active, alternatively spliced mouse p53 (mp53AS), which has been shown to induce secondary axis formation in *Xenopus laevis* (Cordenonsi et al., 2003), a rescue experiment might be achievable. Rescue experiments would additionally act as a control to address MO off-target effects. The results of experiments shown here using the two independent p53 MOs and the dominant negative hp53thr280 are in agreement, suggesting that these methods result in specific p53 downregulation, rather than non-specific effects of the reagents used. An interesting observation is the different gain of function activities which *Xenopus laevis*, human and mouse p53 have when expressed in *Xenopus laevis*. For example, the ability for hp53 and mp53AS, but not *Xenopus laevis* p53, to reliably induce a secondary axis or tail structure (Cordenonsi et al., 2003). This could possibly reflect

protein divergence, as Figure 5:10 shows that there is dissimilarity between the *Xenopus laevis* p53 amino acids and those of the human and mouse proteins. Although the sequences are highly similar, this protein alignment suggests that some degree of divergence has occurred between *Xenopus laevis*, human and mouse p53.

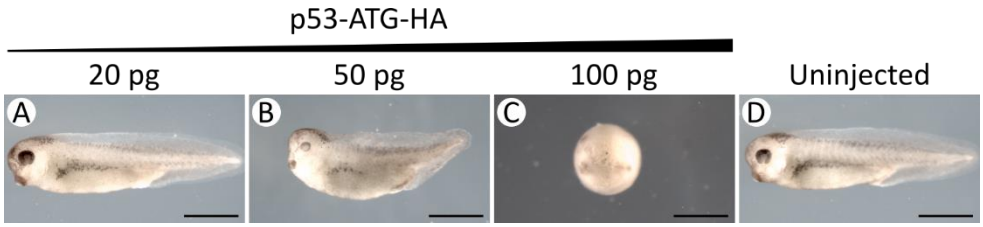

Figure 5:9. p53-ATG-HA mRNA dose response

Embryos were injected uniformly at the 2 cell stage with (A) 20 pg (n=64), (B) 50 pg (n=50) or (C) 100 pg (n=21) of p53-ATG-HA mRNA, or (D) left uninjected (n=81).

```
Human    1   ---MEEPQSDPSVEPPLSQETFSDLWKLLPENNVLsPLPsQAMDDLMLSPDDIEQWFTEDPGPDEAPRMPEAAPRVAPAP  77
Xenopus  1   M----EPSSETGMDPPLSQETFEDLWSLLPDP----------LQTVTCRLDNLSEFPDYPLAADMTVLQEGLMGNAVPTV  66
Mouse    1   MtaMEESQSDISLELPLSQETFSGLWKLLPPEDIL-PSP-HCMDDLLL-PQDVEEFFE---GPSEALRVSGAPAAQDPVT  74

Human   78   AAPTPAAPAPAPSWPLSSSVPSQKTYQGSYGFRLGFLHSGTAKSVTCTYSPALNKMFCQLAKTCPVQLWVDSTPPPGTRV  157
Xenopus 67   T---------------SCAVPSTDDYAGKYGLQLDFQQNGTAKSVTCTYSPELNKLFCQLAKTCPLLVRVESPPPRGSIL  131
Mouse   75   ETPGPVAPAPATPWPLSSFVPSQKTYQGNYGFHLGFLQSGTAKSVMCTYSPPLNKLFCQLAKTCPVQLWVSATPPAGSRV  154

Human  158   RAMAIYKQSQHMTEVVRRCPHHERCSD-SDGLAPPQHLIRVEGNLRVEYLDDRNTFRHSVVVPYEPPEVGSDCTTIHYNY  236
Xenopus 132  RATAVYKKSEHVAEVVKRCPHHERSVEpGEDAAPPSHLMRVEGNLQASYMEDVNSGRHSVCVPYEGPQVGTECTTVLYNY  211
Mouse  155   RAMAIYKKSQHMTEVVRRCPHHERCSD-GDGLAPPQHLIRVEGNLYPEYLEDRQTFRHSVVVPYEPPEAGSEYTTIHYKY  233

                                                    *
Human  237   MCNSSCMGGMNRRPILTIITLEDSSGNLLGRNSFEVRVCACPGRDRRTEEENLRKKGEPHHELPPGSTKRALPNNTSSSP  316
Xenopus 212  MCNSSCMGGMNRRPILTIITLETPQGLLLGRRCFEVRVCACPGRDRRTEEDNYTKKRGLK---PSGKRELAHPPSSEPPL  288
Mouse  234   MCNSSCMGGMNRRPILTIITLEDSSGNLLGRDSFEVRVCACPGRDRRTEEENFRKKEVLCPELPPGSAKRALPTCTSASP  313

Human  317   QPKKKPLD--GEYFTLQIRGRERFEMFRELNEALELKDAQAGKEPG-GSRAHSSHLKSKKGQSTSRHKKLMFKTEGPDSD  393
Xenopus 289  PKKRLVVDddEEIFTLRIKGRSRYEMIKKLNDALELQESLDQQKVTiKCRKCRDEIKPKKG------KKLLVKDEQPDSE  362
Mouse  314   PQKKKPLD--GEYFTLKIRGRKRFEMFRELNEALELKDAHATEESG-DSRAHSSYLKTKKGQSTSRHKKTMVKKVGPDSD  390
```

Figure 5:10. Human, *Xenopus laevis* and mouse p53 protein alignment showing conserved and diverging residues

The protein alignment was created by comparing *Homo sapiens* (human), *Xenopus laevis* and *Mus Musculus* (mouse) p53 protein sequences using the online Constraint-Based Multiple Alignment Tool (COBALT). Red highlights conserved amino acids, blue divergent amino acids. Asterisk and box shows the position of the mutated Arginine (R) in the p53thr280 protein.

5.8 p53 may be required for the specification of cardiac progenitors

Having surmised a role for p53 in heart development, investigations next addressed the timing of the p53 requirement. The effects of p53 downregulation on the cardiac progenitor pool was examined. *nkx2.5* and *isl1* are amongst the earliest known cardiac progenitor markers, with their expression commencing from the late gastrula stages (Brade et al., 2007; Tonissen et al., 1994). *nkx2.5* expression is detected in both the primary and secondary developing heart fields, and continues to be expressed in the left ventricle and atrial chambers in the mature heart (Kasahara et al., 1998; Komuro and Izumo, 1993; Lints et al., 1993; Tonissen et al., 1994). *isl1* expression is localised primarily in the secondary heart field and overlaps with the more anterior domain of *nkx2.5* expression (Cai et al., 2003; Gessert and Kühl, 2009). The expression of *nkx2.5* and *isl1* was examined after p53 downregulation.

Embryos were either injected uniformly, or injected at the 8 cell stage targeted to two dorsal vegetal or two ventral vegetal blastomeres, with p53 MO1, p53 MO3, cMO, hp53thr280 mRNA or left uninjected. Neurula stage embryos (stage 20) were analysed by whole mount *in situ* hybridisation for the expression of cardiac progenitor markers *nkx2.5* and *isl1*. The observed expression patterns were categorised as either normal, reduced or severely reduced and examples of these categories are shown in Figure 5:11 C1-E1. The cells which received injected material were traced and this observation was used to identify correct injection targets, and to ascertain whether observed phenotypic and staining effects were due to cell autonomous p53 downregulation. Control embryos demonstrated normal staining area and intensity of *nkx2.5* and *isl1* positive cardiac progenitor cells (Figure 5:11 A-I, B1, Figure 5:12 A-I, B1, Figure 5:13 A-D, M, N). Neurula stage embryos subjected to uniform p53 downregulation presented reduced cardiac progenitor tissue (Figure 5:11 J-L, S-U, B1, Figure 5:12 J-L, S-U, B1). Embryos with downregulated p53 in dorsal vegetal cells showed reduced to severely reduced *nkx2.5* and *isl1* positive cardiac progenitors (Figure 5:11 M-O, V-X, B1, Figure 5:12 M-O, V-X, B1, Figure 5:13 E-H, M, N). Upon p53 downregulation in ventral vegetal cells, the *nkx2.5* and *isl1* positive

cardiac progenitor pool was more comparable to that of the controls (Figure 5:11 P-R, Y-A1, B1, Figure 5:12 P-R, Y-A1, B1, Figure 5:13 I-L, M, N). This suggests that p53 is required for the specification of *nkx2.5* and *isl1* positive cardiac progenitor cells in a cell autonomous manner.

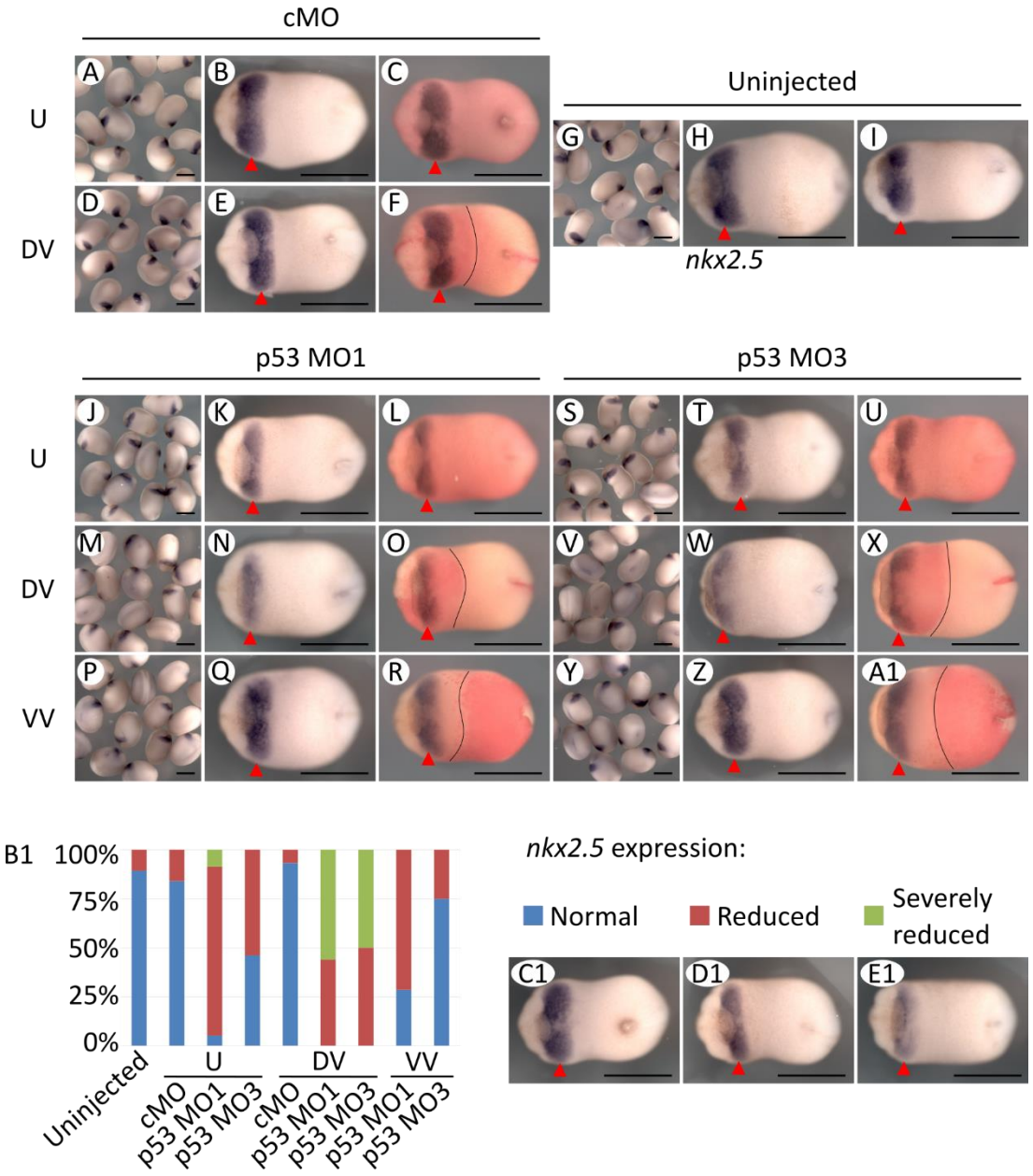

Figure 5:11. Cardiac progenitor cell marker *nkx2.5* expression is reduced by p53 antisense morpholino oligonucleotides

Embryos were either (A-C) injected uniformly (U) at the 2 cell stage with 20 ng of control MO (cMO), (D-F) injected into two dorsal vegetal (DV) blastomeres with 10 ng/ blastomere of cMO, or (G-I) uninjected, as controls. Embryos were either (J-L) injected U at the 2 cell stage with 20 ng of p53 MO1, or injected at the 8 cell stage into (M-O) two DV or (P-R) two ventral vegetal (VV) blastomeres with 10 ng/ blastomere of p53 MO1. Embryos were (S-U) injected uniformly at the 2 cell stage with 10 ng of p53 MO3, or injected at the 8 cell stage into (V-X) two DV or (Y-A1) two VV blastomeres with 5 ng/ blastomere of p53 MO3. Neurula staged

embryos were analysed by whole mount *in situ* hybridisation using the cardiac progenitor marker *nkx2.5* (red arrows). Lineage tracing (outlined) reveals the correct injection target. Images show a ventral view orientated anterior left. Scale bars represent 1 mm. (B1) Graph displaying results of A-A1. Uninjected n=25, cMO U n=50, DV n=15, p53 MO1 U n=58, DV n=50, VV n=14, p53 MO3 U n=65, DV n=40, VV n=12. Following whole mount *in situ* hybridisation, the extent of marker staining in neurula stage embryos was classified, illustrated here using *nkx2.5* cardiac tissue staining. (C1) Normal: the average staining observed in a given control sample. (D1) Reduced: between 50-90% of staining area and intensity observed in controls. (E1) Severely reduced: between 1-50% of staining area and intensity observed in controls. All example images shown are from the same experiment.

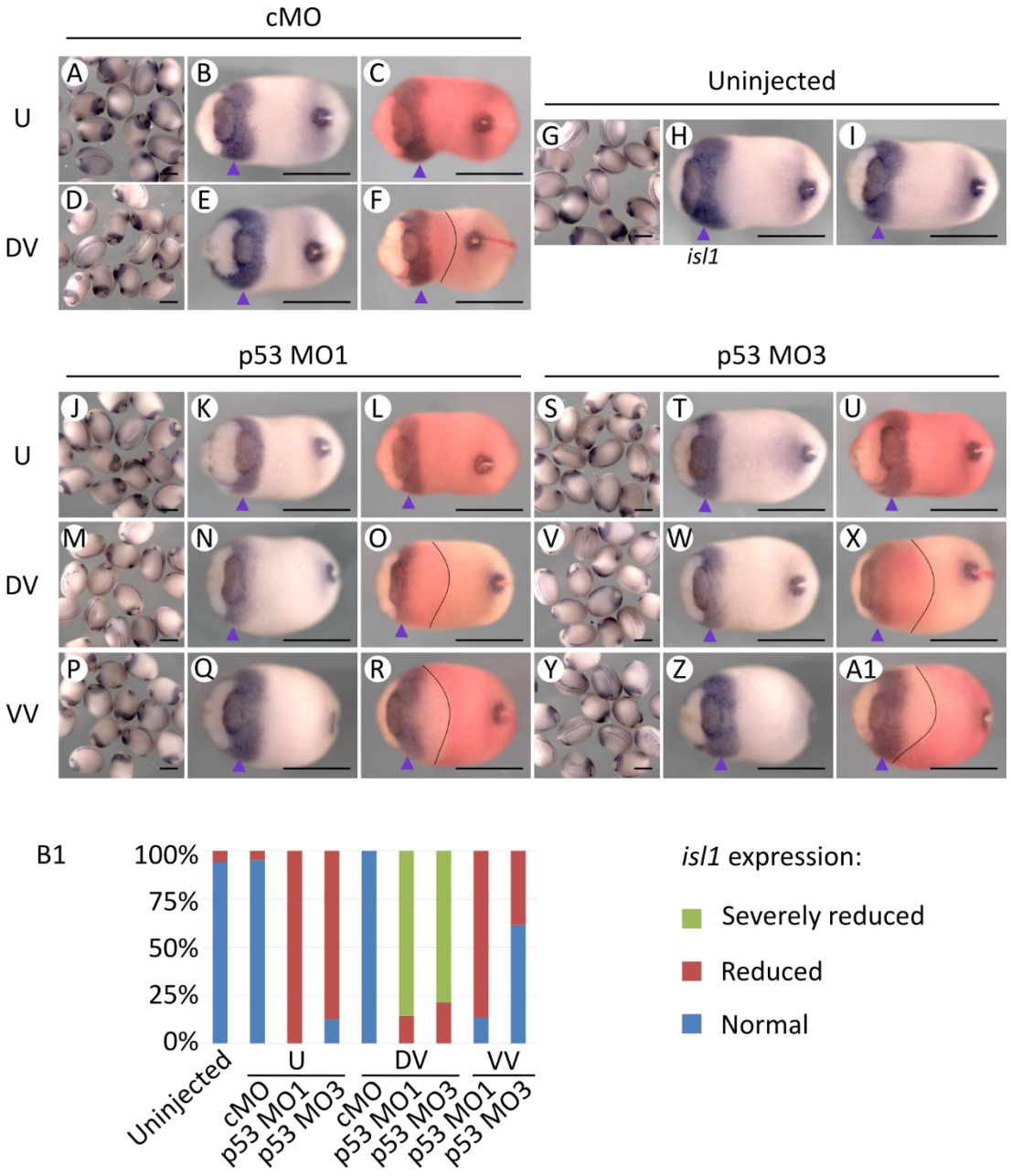

Figure 5:12. Cardiac progenitor cell marker *isl1* expression is reduced by p53 antisense morpholino oligonucleotides

Embryos were either (A-C) injected uniformly (U) at the 2 cell stage with 20 ng of control MO (cMO), (D-F) injected into two dorsal vegetal (DV) blastomeres with 10 ng/ blastomere of cMO, or (G-I) uninjected, as controls. Embryos were either (J-L) injected uniformly at the 2 cell stage with 20 ng of p53 MO1, or injected at the 8 cell stage into (M-O) two DV or (P-R) two ventral vegetal (VV) blastomeres with 10 ng/ blastomere of p53 MO1. Embryos were (S-U) injected U at the 2 cell stage with 10 ng of p53 MO3, or injected at the 8 cell stage into (V-X) two DV or (Y-A1) two VV blastomeres with 5 ng/ blastomere of p53 MO3. Neurula staged

embryos were analysed by whole mount *in situ* hybridisation using the cardiac progenitor marker *isl1* (purple arrows). Lineage tracing (outlined) reveals the correct injection target. Images show a ventral view orientated anterior left. Scale bars represent 1 mm. All example images shown are from the same experiment. (B1) Graph displaying results of A-A1. Uninjected n=17, cMO U n=21, DV n=14, p53 MO1 U n=15, DV n=14, VV n=15, p53 MO3 U n=16, DV n=14, VV n=13.

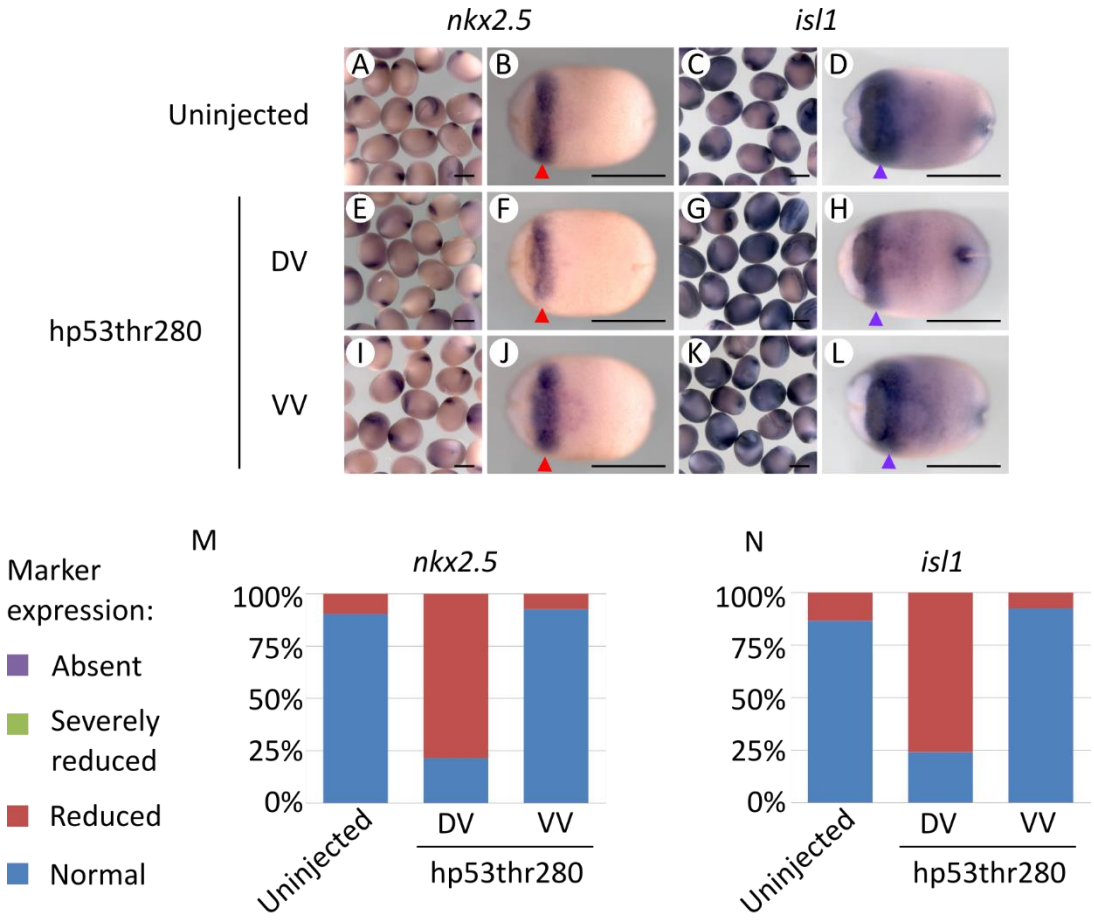

Figure 5:13. The expression of the cardiac progenitor cell markers *nkx2.5* and *isl1* is reduced after expression of a dominant negative hp53

Embryos were either (A-D) uninjected or injected at the 8 cell stage into (E-H) two dorsal vegetal (DV) or (I-L) two ventral vegetal (VV) blastomeres with 500 pg/ blastomere of hp53thr280 mRNA. Neurula staged embryos were analysed by whole mount *in situ* hybridisation using the cardiac progenitor markers *nkx2.5* (red arrows) or *isl1* (purple arrows). Images show a ventral view orientated anterior left. Scale bars represent 1 mm. Graph displaying results of A-L. (M) *nkx2.5*; uninjected n=31, hp53thr280 DV n=28, hp53thr280 VV n=27. (N) *isl1*; uninjected n=30, hp53thr280 DV n=29, hp53thr280 DV n=27.

Intriguingly, there appears to be a difference in cardiac tissue expression between the neurula and tadpole stages. For example, in targeted p53 downregulation in the dorsal vegetal region, at the neurula stage there is predominantly reduced to severely reduced cardiac tissue. However, by the tadpole stage, cardiac tissue is predominantly severely reduced to absent. The cardiac phenotype appears to become more severe as development progresses. Direct comparison of sibling embryos subjected to p53 downregulation and collected at stages 20 and 36 for whole mount *in situ* hybridisation analysis using *nkx2.5* and *Myl7*, respectively, confirms these results. As previously highlighted, the areas of injected, lineage traced cells appeared to be complete and in proportion and embryonic phenotypes were largely unaffected by p53 downregulation. Therefore, it is unlikely that this reduction in cardiac tissue was due to cell loss.

These results suggest that p53 plays an early role in specifying *nkx2.5* and *isl1* positive cardiac progenitors, due to the reduction in *nkx2.5* and *isl1* staining after p53 downregulation. The more severe reduction observed in differentiated cardiac tissue marker *myl7* at the tadpole stage suggests that p53 may have a continued role throughout development in cardiogenesis. If indeed p53 is required for progenitor specification and maintenance, then it would be expected that *nkx2.5* and *isl1* levels would become progressively further reduced prior to linear heart tube formation. p53 levels recover by stage 32 in p53 MO3 treated samples, but p53 MO1 and p53 MO3 injected embryos show comparable phenotypes (Figure 5:4). Therefore, these results suggest that p53 is required early, perhaps for cardiac specification, and also slightly later during the neurula stage, but before the tadpole stage, for normal heart development.

5.9 Mesoderm induction is largely unaffected by p53 downregulation

Previous publications have alluded to the importance of p53 in mesoderm induction, which precedes cardiac specification (Cordenonsi et al., 2007, 2003; Sasai et al., 2008). However, it was found here that the phenotypes of tadpoles after p53 downregulation appear to be normal with no, or minimal, axial defects (Figure 5:4

and Figure 5:7). Additionally, should mesoderm induction be disrupted, it would be expected that cardiac tissue development would be affected, as cardiac cells are derived from mesoderm. To investigate this further, the presence of the pan-mesodermal marker, *Xenopus laevis brachyury* (*t*), was examined by whole mount *in situ* hybridisation after p53 downregulation. *brachyury* staining was categorised as either normal or reduced and examples of the staining categories are shown in Figure 5:14 R and S. Figure 5:14 and Figure 5:15 show that embryos that were subjected to p53 downregulation have normal *brachyury* staining, suggesting that normal mesodermal tissue formation has occurred. No difference was observed upon uniform or target p53 MO or hp53thr280 injections, compared with the controls. This implies that p53 downregulation has not affected mesoderm induction, consistent with the observation that tadpoles with downregulated p53 activity show normal embryonic and axial development. This is in apparent contradiction to previously reported results that implicate p53 in mesoderm induction (Cordenonsi et al., 2007, 2003; Piccolo, 2008; Sasai et al., 2008). During the investigations presented here a lower p53 MO dose is utilised than in previously published work, which has demonstrated specific cardiac effects without more general embryonic phenotypes. However, data presented here agrees with other published work which shows no change in markers *brachyury* and *goosecoid* after p53 downregulation using hp53thr280 mRNA (Wallingford et al., 1997).

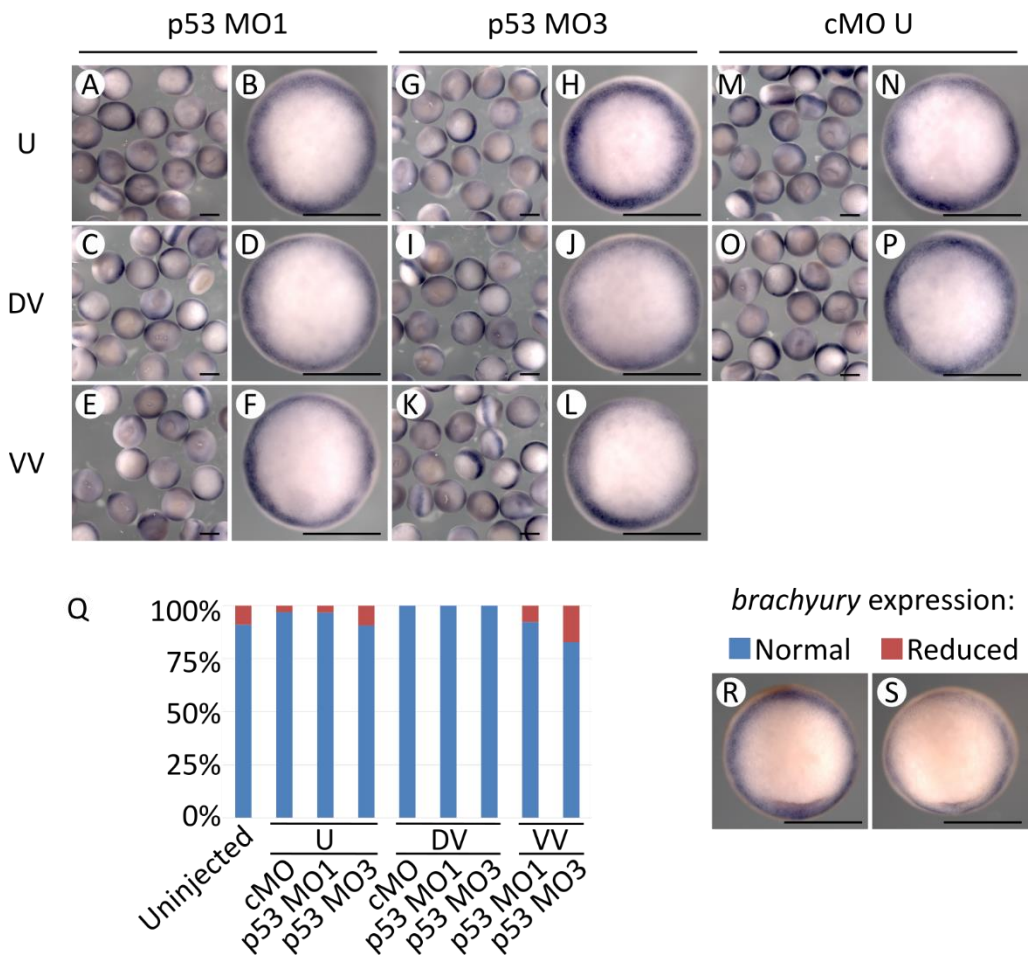

Figure 5:14. Mesodermal marker *brachyury* expression is largely unaffected by p53 antisense morpholino oligonucleotides

Embryos were either (A, B) injected uniformly (U) at the 2 cell stage with 20 ng of p53 MO1, or injected at the 8 cell stage into (C, D) two dorsal vegetal (DV) or (E, F) two ventral vegetal (VV) blastomeres with 10 ng/ blastomere of p53 MO1. Embryos were (G, H) injected U at the 2 cell stage with 10 ng of p53 MO3, or injected at the 8 cell stage into (I, J) two DV or (K, L) two VV blastomeres with 5 ng/ blastomere of p53 MO3. Embryo were either (M, N) injected U at the 2 cell stage with 20 ng of control MO (cMO) or (O, P) injected into two DV blastomeres with 10 ng/ blastomere of cMO. Stage 10 embryos were analysed by whole mount *in situ* hybridisation using the pan-mesodermal marker *brachyury*. (Q) Graph displaying results of A-P. Uninjected n=67, cMO U n=66, DV n=28, p53 MO1 U n=62, DV n=31, VV n=26, p53 MO3 U n=64, DV n=27, VV n=29. Following whole mount *in situ* hybridisation, the extent of marker staining was classified. (A) Normal: the average staining pattern observed in a given control sample. (B) Reduced: between 1-90% of staining intensity, thickness and completeness observed in controls encompassing intensity, thickness and

completeness of the characteristic *brachyury* circle. Changes in staining are subtle but apparent. All example images shown are from the same experiment. Images show a ventral view. Scale bars represent 1 mm.

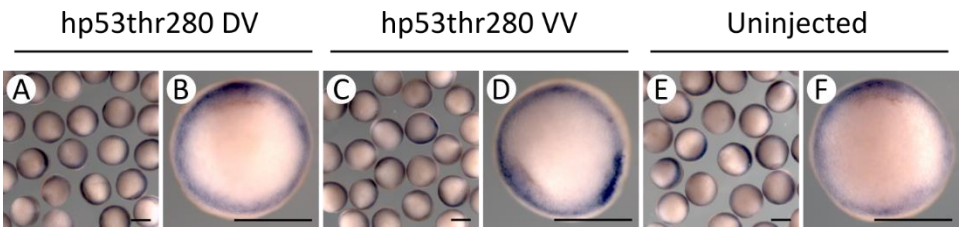

Figure 5:15. Mesodermal marker *brachyury* expression is largely unaffected the expression of a dominant negative hp53

Embryos were injected at the 8 cell stage into (A, B) two dorsal vegetal (DV) or (C, D) two ventral vegetal (VV) blastomeres with 500 pg/ blastomere of hp53thr280 mRNA, (E, F) or left uninjected. Stage 10 embryos were analysed by whole mount *in situ* hybridisation using the pan-mesodermal marker *brachyury*. Uninjected n=33, hp53thr280 DV=32, VV=26.

5.10 CRISPR technology attempted in *Xenopus* p53 gene

Clustered regularly interspaced short palindromic repeat (CRISPR) technology is a recently developed, powerful tool for genome editing (reviewed in Sander and Joung, 2014). The CRISPR/ Cas9 system takes advantage of the bacterial adaptive immune system for guiding targeted DNA cleavage. It was decided to use this technique to knowkdown the p53 gene in *Xenopus* as an alternative and complementary approach to those used previously to study p53 in the work presented in this thesis. A CRISPR approach for knocking down the p53 gene was attempted during the final months of investigations. Although the work reported here did not progress as far as achieving meaningful experiments to investigate the role of p53 in heart development, numerous protocols and reagents were developed and tested which will provide useful information for future investigations into the roles of p53 in *Xenopus* development.

Initial CRISPR attempts were made in *Xenopus laevis,* using Cas9 mRNA injections along with the designed guide RNAs. However, after multiple optimisation experiments, initial tests did not produce positive results. This could for a number of reasons, for example, a delay in the translation of the injected Cas9 mRNA. Injected Cas9 mRNA must first be translated before being guided to DNA to induce gene editing events. Recombinant Cas9 protein can induce target specific gene editing events immediately after injection, and in addition is degraded rapidly, reducing off-target effects (Kim et al., 2014). CRISPR technology has been used successfully in *Xenopus tropicalis* (Blitz et al., 2013; Guo et al., 2014; Nakayama et al., 2013). Therefore, it was decided to use *Xenopus tropicalis,* and adopting the strategy of injecting Cas9 protein.

Short guide RNAs (sgRNAs) targeting *Xenopus tropicalis* p53 were kindly designed by Dr Richard White (The Welcome Trust - Sanger Institute) using in-house developed tools. From multiple potential sgRNAs, 8 were selected for production and further screening (Table 5:2). As sgRNA have a range of efficiencies, which are not necessarily predictable, the 8 sgRNAs were tested *in vitro* for the ability to cleave an amplicon of

Xenopus tropicalis p53 DNA. sgRNA5 and sgRNA8 proved capable of guiding *in vitro* cleavage, thus were further tested *in vivo* (Figure 5:16). The sgRNAs target the initial 3 exons of p53, upstream of the DNA binding and oligomerisation domains. It was reasoned that a gene editing event at the N-terminus of p53 was most likely to cause global gene disruption, by homologous recombination creating a missense transcript. sgRNA5 and sgRNA8 both target sequences in exon 3, which contributes to the proline rich domain of the p53 protein. Gene editing events guided by sgRNA5 and sgRNA8 were predicted to occur around amino acids 40-47 and 62-69, respectively (Figure 5:17). After a number of attempts and optimisation strategies using sgRNA5, sgRNA8 and Cas9 protein *in vivo*, no indication of successful DNA cleavage was observed. A known working CRISPR control, editing the tyrosinase gene, also did not yield positive results, indicating unsuccessful CRISPR application. With further optimisation work this approach could be successful and a valuable tool for investigating the role of p53 in cardiac specification. Further work on p53 CRISPR/ Cas9 in *Xenopus tropicalis* was continued as a collaboration with Dr Harry Isaacs (York University).

sgRNA Name	Target sequence	Target strand	Exon
Xt tp53 sgRNA 1	AGGAGACCTTCGAGGATTTGTGG	+	1
Xt tp53 sgRNA 2	GACCCCCTACAGACCGGGACAGG	+	2
Xt tp53 sgRNA 3	GACCTGTCCCGGTCTGTAGGGGG	-	2
Xt tp53 sgRNA 4	AGGTCAGATGGAAAACTTTGCGG	+	2
Xt tp53 sgRNA 5	GGAGTTTTCAGAGTACCCCCTGG	+	3
Xt tp53 sgRNA 6	GAACCGTCATGTCTGGCGCCAGG	-	3
Xt tp53 sgRNA 7	GACATGACGGTTCTGCAGGAAGG	+	3
Xt tp53 sgRNA 8	AGACGAAGTCACGGTGGGCACGG	-	3

Table 5:2. CRISPR sgRNAs targeted to *Xenopus tropicalis* p53

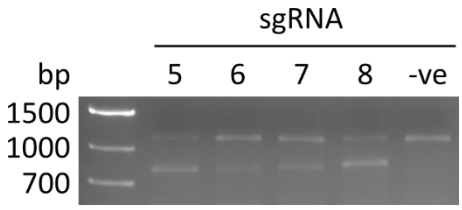

Figure 5:16. *In vitro* assay for successful sgRNA-Cas9-mediated DNA cleavage

sgRNAs guide Cas9 protein to successfully cleave a fragment of PCR-amplified genomic p53 DNA, *in vitro*.

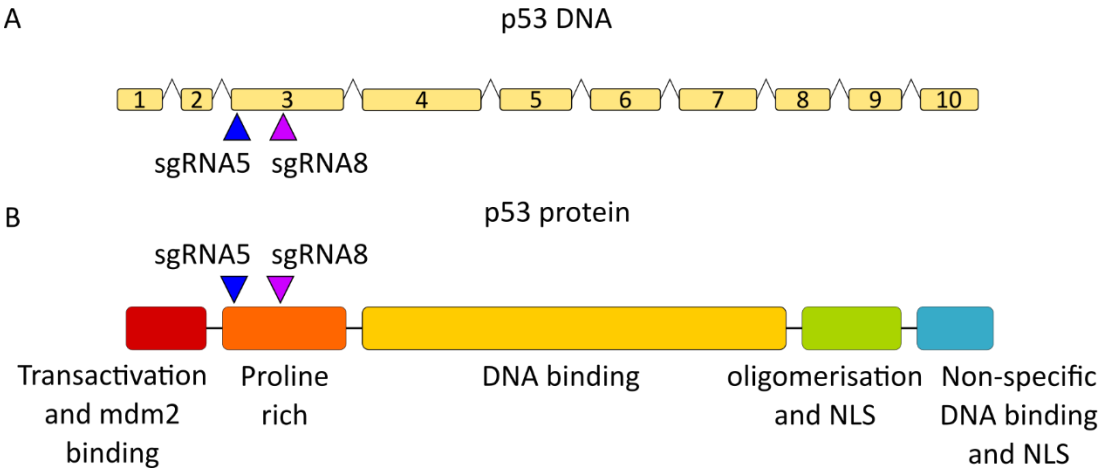

Figure 5:17. sgRNA target sites for p53 CRISPR

(A) sgRNA5 and sgRNA8 are targeted to exon 3 in p53 genomic DNA. (B) sgRNA5 and sgRNA8 target sequences are within the proline rich domain of the p53 protein. NLS = nuclear localisation signal.

5.11 Discussion

5.11.1 p53 is required for early heart development

The aim of this chapter was to investigate the requirement for p53 in heart development. Two different translation blocking p53 MOs and a dominant negative p53 protein were utilised to downregulate endogenous *Xenopus laevis* p53 activity. The p53 MOs were shown to effectively downregulate overexpressed and endogenous *Xenopus laevis* p53 protein. All three p53 downregulation techniques were shown to have minor effects on global phenotypic development, but gave rise to tadpoles with diminished cardiac tissue. At the neurula stages, the cardiac progenitor pool, which expresses *nkx2.5* and *isl1* markers, was reduced, in a cell-autonomous manner. By the tadpole stage, corresponding samples to neurula stages presented severely reduced differentiated cardiac tissue. Cardiac marker expression decreased between the neurula and tadpole stages, with *myl7* expression reduced to a greater extent than *nkx2.5* and *isl1* expression. This suggests that p53 is required early, perhaps for the specification of cardiac progenitor cells, in addition to having a role during the neurula to late neurula stage. Perhaps this later role is in maintaining the existing cardiac progenitor pool, or in promoting further proliferation and development. It is unlikely that p53 is required after the neurula stages for cardiac tissue development. In p53 MO3 injected samples, endogenous p53 protein levels recovered by stage 32. However, p53 MO1 and p53 MO3 injected tadpoles were indistinguishable in both the whole embryo and cardiac phenotypes. Therefore, as p53 protein recovery is having minimal noticeable effect on phenotypes, this suggests that p53 is required earlier, before protein levels recover. It is unlikely that cell death is contributing to the loss of cardiac progenitors and differentiated cardiac tissue. Any non-specific toxic effects due to p53 MOs which alter embryonic viability would be expected to be apparent by an early stage. Prior to staining, neurula stage embryos from different treatment regimes appear to be indistinguishable, suggesting that p53 downregulation is not negatively affecting general embryonic development. Indeed, morphological landmark features such as the cement gland

were of comparable sizes between all samples. Lineage traced targeted injection domains of neurula and tadpole staged embryos were comparable to that of controls, implying that p53 MO and hp53thr280 treatments are having specific, and non-toxic, effects. Another possibility is cell fate change, where targeted cells are correctly located but adopt an alternative, non-cardiac fate. This minimal phenotypic global effect, but defined cardiac effect, suggests that p53 is required specifically for heart development. This work suggests that p53 has an additional novel role in *Xenopus laevis* cardiac specification and development.

The power of the CRISPR-Cas9 system to specifically knock-out the *Xenopus* p53 gene would have been a useful and complementary method to the p53 MO and hp53thr280 methods utilised in these investigations. First utilised in 2012 for genome editing, the CRISPR-Cas9 system takes advantage of the bacterial adaptive immune system for guiding targeted DNA cleavage (Jinek et al., 2012). CRISPR technology has advanced rapidly in recent years, becoming a mainstream method in research for editing genomic DNA targets (Sander and Joung, 2014). With such a new technology, its flaws and limitations are largely unknown, and are slowly coming to light as further CRISPR applications are tested. CRISPR-mediated gene editing is believed to be highly specific, but recent studies are highlighting off-target and unknown effects (Rossi et al., 2015; Zhang et al., 2015). In a study comparing morphants (MO-induced) to mutants (CRISPR-induced), phenotypes were often not comparable (Kok et al., 2015). It was suggested that MOs frequently generate non-specific effects, and should only be utilised once validated against a corresponding mutant (Kok et al., 2015). However, in a subsequent study it was shown that embryos can compensate for genomic mutations, but not for alterations resulting from MOs treatment (Rossi et al., 2015). Indeed, mutants, additionally treated with MO, did not succumb to morphant phenotypes, whereas wild type MO treated samples were affected (Rossi et al., 2015). It is apparent that further studies are required to ascertain if, and how, such compensation works, and to understand the differences observed in morphant and mutant phenotypes, in addition to investigating CRISPR off-target effects. CRISPR/ Cas9 technology is revolutionary and is an important new technique for

investigating gene function. However, until the technology is fully understood, it is prudent to use a variety of complementary methods.

5.11.2 Mesoderm specification is unaffected by p53 downregulation

The role of p53 in cardiac specification was investigated here as previous work had shown that p53 was involved in mediating pathway crosstalk for mesoderm induction, so it was hypothesised that a similar mechanism could be functioning for cardiac specification (Cordenonsi et al., 2007, 2003; Sasai et al., 2008). However, the results presented here, observing the overall tadpole phenotype and analysis of the pan-mesodermal marker *brachyury*, suggests that mesoderm induction is unaffected by the level of p53 inhibition utilised throughout this investigation. Direct comparison of tadpoles between this work and previously published data is not possible, as there are no published examples of p53 MO injected *Xenopus laevis* embryos developed until the tadpole stages. The tadpole phenotype can be highly informative, as without normal mesoderm formation, embryonic processes including gastrulation, axial patterning and elongation are compromised (Keller et al., 2000). Hence, where embryonic development appears to be relatively normal, this is a good indication that mesoderm induction has occurred. Cordenonsi et al. (2003) report the attenuation of *brachyury*, cell-autonomously, upon p53 downregulation, using 10 ng of p53 MO1 injected into 1 blastomere of a 4 cell embryo (Cordenonsi et al., 2003). This dose and targeted injection is not dissimilar to experiments performed here, but with a conflicting result. In the work presented here, a phenotypic dose response to the p53 MOs was observed, however, p53 protein detected by western blotting appeared to be sufficiently decreased at lower p53 MO concentrations. As the detection of p53 protein by western blotting is subtle this could suggest that a residual amount of p53 protein remains but has not entered the detectable range, or that higher doses of p53 MOs are creating artefactual, non-specific phenotypic effects. For this reason intermediate doses of 20 ng p53 MO1 or 10 ng p53 MO3 were used for uniform injections throughout experiments presented in this chapter, rather than the higher dose of 40 ng p53 MO1 injected uniformly by Cordenonsi et al. (2007) and

Takebayashi-Suzuki et al., 2003. At the neurula stage, the expression of the dorsal mesoderm derivative *myod1*, which is required for skeletal muscle formation (Hopwood and Gurdon, 1991), was previously shown to be reduced (Cordenonsi et al., 2003). It would, however, be informative to observe how, and whether, these embryos developed into the tadpole stages, and developed differentiated skeletal muscle. Cordenonsi et al. (2003) employ unilateral p53 MO injections, using the uninjected half of the embryo as an internal control to demonstrate abnormal development. However, it is known that some MO injections can cause slight developmental delay, thus it would have been advantageous to observe these embryos at a later stage of development. Reportedly, significant proportions of the embryos failed to gastrulate properly (23%), and a number lacked tail structure and developed a shortened trunks (n=76, 54%) (Cordenonsi et al., 2003). Examples given for this analysis were at a relatively early stage (tailbud). Extended analysis at a later stage would perhaps better summarise the full extent of the reduced tail and trunk phenotypes, ensuring that effects seen are consistent throughout development and are not due to developmental delay. It was documented that 54% of embryos which survived beyond the neurula stage lacked tail structures and were truncated (Cordenonsi et al., 2003). Presumably, the remaining 46% retained these features, indicating successful mesoderm induction. It is apparent from neurula staged p53 MO injected sample images, displaying reduced *myod1*, that gastrulation has occurred and axis elongation is underway, albeit slightly hindered compared with the uninjected side of the embryo (Cordenonsi et al., 2003). Critical analysis reveals that the case is not as simple as p53 downregulation resulting in defective *brachyury* expression and thus defective mesoderm, as despite reports of *brachyury* reduction there are still indications that mesoderm formation has occurred. Examining published RT-PCR data, in an animal cap model for mesoderm induction, reveals that, upon p53 downregulation, using 40 ng of p53 MO1, *brachyury* expression was reduced but not abolished (Cordenonsi et al., 2007). Additionally, it was shown that p53 mRNA can induce mesodermal marker genes. However, the ability to induce an event in a model such as animal caps shows the capacity of a protein to induce an event, but this does not necessarily reflect an *in vivo* role. p53 downregulation by

overexpression of the p53 inhibitor Znf585b, or by p53 MO1, was shown to result in the severe reduction of *brachyury* expression (Sasai et al., 2008). Doses of 50 ng per blastomere of p53 MO1, injected at the 4 or 8 cell stage, are higher than those used throughout the work presented here. This may account for the discrepancy in results. However, there are no embryos or markers older than the gastrula stage from which to examine and extrapolate additional information about mesoderm development (Sasai et al., 2008). In agreement with the results in this chapter, Wallingford *et al.* demonstrate that interference with p53 activity, using hp53thr280, does not affect the expression of mesodermal markers *brachyury* and *goosecoid* (Wallingford et al., 1997). In addition, tadpole embryos appear to have gastrulated and have an extended anterior-posterior axis, indicating intact mesoderm development (Wallingford et al., 1997).

As documented above, there are discrepancies between different studies as to the effect of p53 inhibition on mesodermal gene expression and ultimately mesoderm development. It could be reasoned that, during experimental investigations in this chapter, complete p53 inhibition was not achieved, and this could explain the difference in *brachyury* expression between the work presented here and published data. However, the doses of p53 MOs selected for these investigations, and lower doses, resulted in the robust downregulation of p53 protein, therefore making this explanation less plausible. Ultimately, further studies may reveal the true role, if any, of p53 in mesoderm induction. Experimental results presented here do not find a correlation between p53 inhibition and aberrant mesoderm induction.

5.11.3 A potential mechanism of action for p53 in cardiac specification

The p53 protein undergoes a variety of posttranslational modifications, has multiple signalling partners, and primarily acts as a transcription factor (Beckerman and Prives, 2010; Meek and Anderson, 2009; Vogelstein et al., 2000). As a potential role for p53 in cardiac specification has been suggested in this work, the next challenge is to understand the mechanisms involved in its role in cardiac specification. The hp53 arginine 280 to threonine mutation disrupts DNA binding, thus suggesting that

binding DNA is an important function for p53 in cardiac specification. This could suggest that p53 is acting as a transcription factor for cardiac specification. p53 forms complexes with other transcription factors to regulate gene transcription. ALK4/5/7 activated Smad2 is a known p53 binding partner (Cordenonsi et al., 2007, 2003; Takebayashi-Suzuki et al., 2003) which is required for cardiac specification (Chapter 3). p53 N-terminal Serine 6 and Serine 9 have been shown to be important phosphorylation modifications required for the p53-Smad2 interaction (Cordenonsi et al., 2007). Further investigations could focus on whether these p53 N-terminus phosphorylation modifications are important for the role of p53 in cardiac specification, potentially by interacting with Smad2.

6 Discussion

The purpose of this study was to investigate the requirement and timing of Nodal/ Activin and FGF/ MEK signalling in cardiac specification, and whether p53 may have a role in cardiac specification, perhaps by mediating an interaction between the Nodal/ Activin and FGF/ MEK pathways. Work presented in this study demonstrates the requirement for Nodal/ Activin signalling for the specification of cardiac tissue, separate from its well-established role in mesoderm induction. Furthermore, Nodal/ Activin signalling was shown to be required over a 2-3 hour time-window after midblastula transition, for cardiac specification, which is well before gastrulation and at an earlier time point than previously suggested. FGF/ MEK signalling was shown to be required during gastrulation for normal cardiac development. Contrary to expectations, the results did not show a requirement for FGF/ MEK signalling prior to gastrulation, during the time-window in which Nodal/ Activin signalling specifies cardiac tissue. Work presented here also provides evidence for a novel role for p53 in early cardiac development, potentially with a role in the specification and then promotion and/ or maintenance, of cardiac progenitors.

6.1 Nodal/ Activin signalling is required for cardiac specification hours before gastrulation

Throughout development, a relatively small number of signalling pathways are used to orchestrate embryogenesis. The time of action, duration of signalling, spatial localisation and utilisation of different pathway combinations are all factors which influence cellular fates and behaviour. Deciphering the roles of the specific components of the signalling pathways and the crosstalk between these pathways required during early development remains an ongoing challenge. To define the role of Nodal/ Activin signalling in cardiac specification, soluble molecular inhibitors were used in the work presented here to study the effects of time-dependent pathway inhibition. This demonstrated that Nodal/ Activin signalling is required for cardiac specification and that the role of Nodal/ Activin signalling in mesoderm induction and cardiac specification can be uncoupled.

The time of cardiac specification was defined as a 2-3 hour time-window succeeding midblastula transition. This time-window is earlier than the previously predicted occurrence during gastrulation (Section 1.10). These results are in agreement with previous work where Skirkanich *et al.* (2011) have shown that Nodal transcripts can be detected as early as the 128 cell stage, with active signalling confirmed by midblastula transition, supporting the idea that active Nodal/ Activin signalling has a role inducing mesoderm before midblastula transition (Skirkanich et al., 2011). Previous work suggests that Nodal/ Activin signalling is required initially to induce mesodermal genes and FGF signalling, with FGF signalling maintaining mesoderm without requiring further Nodal/ Activin signalling inputs (Fletcher and Harland, 2008; Kimelman, 2006; van Boxtel et al., 2015). Taken together, the findings presented in this thesis provide evidence to show that Nodal/ Activin signalling has fulfilled its role in mesoderm and FGF induction prior to midblastula transition, and is subsequently involved in cardiac specification during a specific 2-3 hour time-window following midblastula transition.

During investigations into the role of Nodal/ Activin signalling in heart development, there was no indication that Nodal/ Activin signalling was required after cardiac induction for normal cardiac tissue development. Cardiac tissue persisted upon Nodal/ Activin signalling inhibition after specification (after stage 9), suggesting that Nodal/ Activin signalling is not required for cardiac cell maintenance or proliferation. This is consistent with a previously published explant experiment that demonstrated that Nodal is only required during the first hour of cardiogenesis (Samuel and Latinkić, 2009). In addition, a transient requirement for Nodal/ Activin signalling is consistent with the role of Nodal/ Activin signalling in the activation of tissue specific genes and signalling pathways which maintain that gene expression (Fletcher and Harland, 2008; Kimelman, 2006; van Boxtel et al., 2015). Previous research has established a role for Nodal/ Activin signalling in left-right axis asymmetry, which is important for the asymmetric formation of visceral organs including the heart (Brennan et al., 2002; Ramsdell, 2005). Asymmetric expression of *Nodal 1* in the left lateral plate mesoderm during neural tube closure was found to be important for

cardiac asymmetry (Lohr et al., 1998, 1997). Bilateral or absent *Nodal 1* expression resulted in cases of cardiac reversal, where the heart tube loops to the right instead of the left (Lohr et al., 1997). In work shown here, the morphology of the heart in tadpoles that were subjected to continuous Nodal/ Activin inhibition after cardiac tissue specification was not examined. However, analysis of cardiac morphology was carried out in tadpoles which had disrupted cardiac tissue specification due to ALK4/5/7 signalling inhibition during the 2-3 hour time window following midblastula transition. However, the ALK4/5/7 inhibitors had been removed before then time when asymmetric Nodal/ Activin expression is prevalent at approximately stage 20. Regardless, the reduction in the size of the heart was such that the direction of heart tube looping could not be accurately detected. In summary, this suggests that Nodal/ Activin is required for cardiac specification, but not for further cardiac tissue maintenance, proliferation, migration and morphogenesis, but is involved in conveying cardiac left-right asymmetry.

6.2 Cardiac specification by Nodal/ Activin signalling occurs at a time when p-Smad2 cannot be readily detected

P-Smad2 is readily detectable at the onset of gastrulation; however, prior to stage 9 detection is difficult to achieve using methods such as western blotting or immunohistochemistry (Faure et al., 2000; Lee et al., 2001 and this work). Skirkanich *et al.* (2011) have shown that p-Smad2 can be detected at midblastula transition by immunoprecipitation of over 100 embryos, followed by western blotting (Skirkanich et al., 2011). Despite difficulties in detecting p-Smad2 prior to stage 9 in this work, Nodal/ Activin signalling inhibition revealed the functional significance of active signalling around the time of midblastula transition. It was shown here that Nodal/ Activin signalling is required for cardiac specification during a time-window when very little p-Smad2 could be detected. This raises the question as to how seemingly globally low levels of active Nodal/ Activin signalling can convey a cardiac fate, when previously it has been shown that high levels of Nodal/ Activin signalling are required for the specification of cardiac tissue (Ariizumi et al., 1991; Kimelman, 2006;

Okabayashi and Asashima, 2003). The effects of timing, dose or length of exposure to active Activin/ Nodal signalling to specify cells within an early embryo is of great interest.

6.3 A cumulative dose of Nodal/ Activin signalling conveys cardiac specificity within a specific time-window

There are various models, and evidence to support each of them, to explain how Nodal/ Activin signalling may be received and interpreted by cells in the early embryo (Shen, 2007). The approach employed in this study was to observe, in an unbiased manner, the effects of Nodal/ Activin inhibition, in an attempt to understand how the timing, dose, and length of exposure apply.

6.3.1 The timing of Nodal/ Activin signalling

It was shown here that Nodal/ Activin signalling is required to specify cardiac cells within a 2-3 hour time-window after midblastula transition. Inhibiting Nodal/ Activin signalling for one hour starting from midblastula transition severely disrupted the formation of cardiac tissue, highlighting the importance of Nodal/ Activin signalling in this time-window. This contrasts with the results obtained in zebrafish, which suggest that cells are specified depending on the total level of Nodal/ Activin signalling which they receive, rather than specification being restrained to a discreet time-window (Hagos and Dougan, 2007). There are numerous examples across development where cells must respond to temporal signals within a specific time-window. For example, *Xenopus laevis* animal cells remain competent to respond to mesoderm inducing signals for approximately 7 hours during the blastula stage (Wolpert et al., 2015). In the absence of a sufficient levels of Nodal/ Activin signalling at the appropriate time, it is possible that cells will no longer be able to respond to Nodal/ Activin signalling, or that alternative signals from different pathways will specify a different fate onto presumptive cardiac mesoderm, which cannot be reassigned by later exposure to Nodal/ Activin signalling.

6.3.2 The Dose of Nodal/ Activin signalling

In *Xenopus laevis* it has been shown that pluripotent animal cap explants will respond to Activin treatments, in a concentration dependent manner, to form tissues that are derived from mesoderm, including blood, muscle, notochord, and heart. Heart tissue formation requires the highest concentration of Activin (Ariizumi et al., 1991; Kimelman, 2006; Logan and Mohun, 1993; Okabayashi and Asashima, 2003). In zebrafish, Nodal/ Activin signalling was found to specify cell fates in a time dependent manner, with tissues requiring high levels of Activin for specification, such as the heart, being specified after tissues requiring low Activin levels, such as skeletal muscle (Hagos and Dougan, 2007). It would appear that a high level of Nodal/ Activin signalling is required to specify cardiac cells, yet cardiac specification occurs at a time when only low levels of p-Smad2 can be detected.

6.3.3 The Length of exposure to Nodal/ Activin signalling

At midblastula transition, p-Smad2 is enriched dorsally (Lee et al., 2001; Schohl and Fagotto, 2002; Skirkanich et al., 2011). Cardiac tissue originates from dorsal mesoderm, therefore pre-cardiac mesoderm will be one of the first regions exposed to Nodal/ Activin signalling and will be exposed continuously as Nodal/ Activin signalling spreads across the marginal zone (Lee et al., 2001).

6.3.4 Cells are exposed to a cumulative dose of Nodal/ Activin signalling within a specific time window to become cardiac cells

Considering the influences of time, dose and length of exposure to Nodal/ Activin signalling, it can be speculated how each contributes to the final outcome of cardiac cell specification. It was found here that the Nodal/ Activin signalling requirement for cardiac specification is temporally limited to within a 2-3 hour time-window after midblastula transition. However, this window is relatively broad. As pre-cardiac mesoderm is one of the first mesodermal regions to be exposed to Nodal/ Activin signalling, and will be exposed over the longest time period, the total cumulative

dose of Nodal/ Activin which cells receive will be the highest. This supports the concept that cells respond to the cumulative dose of Nodal/ Activin signalling which they are exposed to and once a threshold dose is established, cells become fated to form cardiomyocytes.

Endogenous p-Smad2 levels continue to increase up to the onset of gastrulation, but no further cardiac tissue is specified elsewhere along the margin. This reinforces the idea that a competency window exists for time-dependent specification, but may also suggest that the activation of negative regulators might occur as a mechanism for controlling cardiac progenitor number and tissue dimensions. Conceivably, negative regulators may be activated by Nodal/ Activin signalling itself, which is known to cooperate in negative feedback loops (Chen and Meng, 2004; Shen, 2007; van Boxtel et al., 2015). Lefty could be such a negative regulator. Previously, it has been shown that microRNAs temporarily repress the translation of Lefty, allowing Nodal/ Activin signal propagation before Lefty translation and diffusion at a faster rate, thus negatively regulating Nodal/ Activin signalling (Sakuma et al., 2002; van Boxtel et al., 2015). Alternatively, or in addition, the induction of the multifunctional antagonist Cerberus, by Nodal, has been shown to be important for establishing the correct timing and/ or level of Nodal signalling for cardiac induction (Foley et al., 2007). Negative regulators may also originate from outside of the cardiac-forming region to negatively influence Nodal/ Activin signalling, or p-Smad2 binding partners, to define tissue boundaries.

6.4 Cardiac specification is primarily mediated by Nodal via Smad2

Drosophila melanogaster, mouse and mouse embryonic stem cells containing mutant Cripto provide evidence for the involvement of Nodal in cardiac specification, but these experiments do not separate the role Nodal plays in mesoderm induction from cardiac specification (Parisi et al., 2003; Reiter et al., 2001; Xu et al., 1999). In this work, the use of soluble recombinant Lefty protein allowed the time-dependent inhibition of Nodal signalling, without affecting the signalling of alternate family members, such as Activin or TGF-betas. This allowed the key role of Nodal in *Xenopus*

laevis cardiac specification to be demonstrated. In the work presented here, compensation for the loss of Nodal was not observed, suggesting that Nodal is an indispensable ligand for inducing a cardiac fate. However, a role for other Nodal/ Activin family members in cardiac specification cannot be ruled out. Further experimentation, inhibiting other Nodal/ Activin family members, whilst leaving Nodal signalling intact could be done. In mouse embryonic stem cells it has been shown that Nodal induces TGF-beta2, with both ligands further controlling cardiac fate (Cai et al., 2012). A similar system may be acting in *Xenopus laevis*, and such a mechanism could explain the severity of Nodal inhibition, if Nodal were acting upstream of further Nodal/ Activin family members which are required for normal heart development.

Nodal/ Activin signalling can propagate via Smad2 or Smad3 (Shi and Massague, 2003). Smad2 is predominant in the blastula stage *Xenopus laevis* embryo (van Boxtel et al., 2015), and Smad2 mutant mice display a range of early developmental defects in mesoderm formation, gastrulation and left-right patterning (Nomura and Li, 1998). Previously, Smad2 has been shown to be capable of mimicking Vg1, Activin and Nodal activity by inducing the formation of dorsal mesoderm (Baker and Harland, 1996; Graff et al., 1996). This suggests that Smad2 is a candidate for transmitting Nodal/ Activin signalling in the early embryo and for cardiac specification. The use of Smad2, induced in an appropriate timely manner to bypass ALK4/5/7 timed inhibition, was shown here to partially rescue the cardiac and whole embryo phenotype. This provides evidence that Smad2 is capable of propagating the cardiac inducing signal. The regulation of Smad2 may additionally contribute to defining the cardiac domain. For example, *Xenopus laevis* Pias4 has been shown to downregulate Smad2 transcriptional activity resulting in the negative regulation of mesoderm induction (Daniels et al., 2004). Smurf2 can decrease Smad2, but not Smad3, protein levels by targeting Smad2 for ubiquitination and proteasome-mediated degradation (Zhang et al., 2001). A complex containing Foxh1 and Smad2 constitutes an active DNA-binding factor (Chen et al., 1997). Therefore, a combination of positive and negative Smad2 regulators may be cooperating to influence cardiac progenitors.

6.5 The targets of Nodal/ Activin signalling for cardiac specification are largely unknown

Although the requirement for Nodal/ Activin signalling in cardiac specification has been demonstrated here, how cardiac specification is being mediated, and which cardiogenic transcripts are being activated by the Nodal/ Activin pathway is largely unknown. A deeper understanding of Nodal/ Activin signalling targets may aid in the identification of potential candidate genes which are required to modulate or assist Nodal/ Activin signalling for cardiac specification. Initial unpublished RNA-sequencing data has identified a selection of genes whose expression is altered after ALK4/5/7 signalling inhibition during the time when ALK4/5/7 signalling is required for cardiac specification. In addition, a range of different transcripts were found to be differentially expressed between two time-windows that were only 1 hour apart. Further analysis of these transcripts may confirm the identity of novel Nodal/ Activin targets and will help to further decipher the mechanism of Nodal/ Activin signalling in cardiac tissue induction.

6.6 FGF/ MEK signalling is not required for cardiac specification

Soluble molecular inhibitors and a dominant negative FGFR were used here to inhibit FGF/ MEK signalling in a time-controlled manner to investigate the role of FGF/ MEK signalling in early heart development. In this work, normal cardiac development was observed after FGF/ MEK signalling inhibition during the midblastula transition to gastrulation time-window, when ALK4/5/7 signalling is required for cardiac specification. This suggested that FGF/ MEK signalling is not required for cardiac specification, which contradicts previous research suggesting a role for FGF/ MEK signalling in cardiac specification. In addition, the finding that continuous FGF/ MEK signalling inhibition, commencing before gastrulation, resulted in a only a modest reduction in differentiated cardiac tissue was surprising given that previous reports have shown that there is severe reduction or loss of cardiac marker expression upon FGF/ MEK signalling downregulation in *Xenopus laevis* and zebrafish (Deimling and Drysdale, 2011; Keren-Politansky et al., 2009; Rankin et al., 2012; Reifers et al., 2000;

Shifley et al., 2012). However, previous studies have largely relied on the analysis of cardiac progenitor markers, such as *nkx2.5* and *isl1* (Deimling and Drysdale, 2011; Keren-Politansky et al., 2009; Rankin et al., 2012; Reifers et al., 2000; Shifley et al., 2012). It has been shown here and in previous studies that differentiated cardiac tissue marker expression is mildly reduced after FGF/ MEK signalling downregulation (Keren-Politansky et al., 2009; Shifley et al., 2012 and Chapter 4). However, these results are in conflict with other published work (Deimling and Drysdale, 2011). In addition, the cardiogenic factor *gata4* has been demonstrated to be barely affected upon FGF/ MEK signalling inhibition (Keren-Politansky et al., 2009). This supports a reiterative role for FGF/ MEK signalling in the regulation and/ or maintenance of *nkx2.5* and *isl1* positive cardiac progenitor cells, rather than in the specification of a cardiac progenitor pool. It is conceivable that, with a reduction in *nkx2.5* and *isl1* expression due to reduced FGF/ MEK signalling, alternative cardiogenic factors, for example *gata4*, may be able to regulate the cardiac program, resulting in differentiated cardiac tissue.

6.7 FGF/ MEK signalling is required after gastrulation for normal heart development

In addition to the post-blastula roles that FGF/ MEK signalling plays in cellular movements and trunk and tail development (Amaya et al., 1991; Griffin and Kimelman, 2003), FGF/ MEK signalling has been shown to have reiterative roles in cardiomyocyte regulation during development (Marques et al., 2008; Simões et al., 2011). From this work it is apparent that there is a post-gastrula role for FGF/ MEK signalling, but whether this role is in maintaining cell fate, migration, survival or proliferation of cardiomyocytes is not clear.

Throughout embryonic development, it has been demonstrated that FGF/ MEK signalling is required for the maintenance of select tissue types, for example in mesoderm maintenance in *Xenopus laevis* (Fletcher and Harland, 2008) and in neural progenitor maintenance in mouse (Mathis et al., 2001). FGF/ MEK signalling may likewise participate in cardiac progenitor maintenance. FGF/ MEK may be required

for the maintenance of genes such as *nkx2.5* and *isl1*, as previously discussed, and/ or the repression of alternative lineages, such as blood. The importance of FGF/ MEK signalling in promoting cardiac progenitor cells by inhibiting the formation of blood has previously been reported (Peterkin et al., 2009; Simões et al., 2011; Walmsley et al., 2008). Cardiac and blood progenitors are located adjacent to each other on the ventral midline of the developing embryo and it has been shown that their control is partially overlapping, for example by *gata4*, *5* and *6* in zebrafish (Peterkin et al., 2009; Simões et al., 2011). In zebrafish, FGF signalling inhibition results in the loss of cardiac tissue accompanied by the expansion of blood markers (Isaacs et al., 2007; Simões et al., 2011). There is conflicting data in *Xenopus laevis*, with reports that FGF inhibition does (Isaacs et al., 2007; Walmsley et al., 2008) or does not (Deimling and Drysdale, 2011) result in the expansion of blood progenitors in conjunction with cardiomyocyte loss. Therefore, FGF/ MEK signalling could be required to maintain normal cardiac proportions, plausibly at the expense of blood. Alternatively, FGF/ MEK signalling may be required to prevent terminal differentiation of cardiomyocytes, in a similar manner to in neural progenitors, allowing sufficient proliferation and expansion of cardiac progenitor cells (Diez del Corral et al., 2003). This is a less favourable hypothesis, as the level of differentiated cardiac tissue observed in tadpoles which had been subjected to FGF/ MEK inhibition was only minimally reduced in comparison to controls. Defective cardiomyocyte migration, due to deficient FGF/ MEK signalling, would incorrectly relocate cells, altering contacts with underlying tissues and resulting in cardiac progenitors perhaps not receiving the correct signals. Cardiac tissue is most frequently observed correctly located on the ventral midline upon FGF/ MEK signalling disruption, except in the more severe cases of cardiac bifida, but these were observed infrequently. This suggests that FGF/ MEK signalling may have a role in role in contributing to cardiac cell migration after initial cardiac specification.

The evidence suggests a reiterative role for FGF/ MEK signalling in the maintenance of cardiac progenitors. However, there may be alternative complementary pathways allowing the cardiogenic program to persist in the absence of FGF/ MEK signalling.

Gata4 has been found responsive to BMP signalling, with BMP implicated in regulating *gata4* and *fgf8* for normal cardiac development in chick (Alsan and Schultheiss, 2002; Andrée et al., 1998; Schultheiss et al., 1997). Both of the FGF/ MEK and BMP signalling pathways might have a role in maintaining, promoting and regulating the cardiac program after specification. This is in agreement with work highlighting the role of BMP in regulating cardiac progenitor cell development (Reiter et al., 2001; Walters et al., 2001; Zhang and Bradley, 1996). A successive FGF/ MEK signalling requirement in regulating heart size and chamber proportions, and then promoting ventricular development, has been shown previously (Marques et al., 2008; Reifers et al., 2000; Simões et al., 2011). This study is in agreement, promoting a reiterative role for FGF/ MEK signalling in cardiac progenitor maintenance. The presentation of linear heart tubes, or cardia bidifa, as a result of FGF/ MEK signalling downregulation may be due to an underdeveloped ventricular region, highlighting an interesting avenue for further investigations.

A surprising observation in this work was the more severe cardiac phenotype observed upon later and shorter FGF/ MEK signalling inhibition, in comparison to earlier and longer inhibition. Explanations such as compensation mechanisms upon early detection of FGF/ MEK signalling downregulation or susceptibility of cells which earlier received FGF/ MEK signalling can only be conjectured, and this could prove an interesting line of enquiry for future work. This work does, however, highlight a time-window from late gastrulation into neurulation in which FGF/ MEK signalling appears important for normal cardiac development. Focused analysis during this time-window may further pinpoint a more precise requirement.

6.8 p53 is required during early cardiac development

With the recent finding that p53 is required to modulate the TGF-beta response for mesoderm development (Cordenonsi et al., 2007, 2003), it was hypothesised that a similar mechanism could be working for cardiac specification. Work presented here identifies a novel role for p53 in heart development, but also highlights a potential biphasic role with an early and late function. This early action is likely to be in the

establishment of the early cardiac progenitor pool, possibly cooperating with Nodal/ Activin signalling for cardiac specification. It was reasoned that the later function occurs during the late neurula to early tailbud stages of development, due to the observed recovery of p53 protein by stage 32 upon the use of p53 MO3, and the consistency between phenotypes of either p53 MO treated sample. It is unlikely that the loss of cardiac cells upon p53 downregulation is due to apoptosis, as lineage traced areas of tadpoles were of the correct size and proportion, but this would have to be tested directly, for example by a Terminal deoxynucleotidyl transferase (TdT) dUTP Nick-End Labeling (TUNEL) assay, to provide confirmation. Therefore, this suggests that cells may not be maintaining their cardiac fate and deviate into an alternative lineage. It is not known how p53 is acting early to influence cardiogenesis but one possibility is that p53 might cooperate with Smad2. Previously published bioinformatics screens have revealed that a large proportion of TGF-beta target genes also contain putative p53 binding sites (Dupont et al., 2004). Transcriptome analysis for Nodal/ Activin signalling targets, combined with bioinformatics identifying genes which are potentially co-regulated, may aid in the identification of novel cardiogenic factors and a greater understanding of the mode of action of p53 and Nodal/ Activin signalling in early cardiogenesis. p53 may be required later in heart development for proliferation, maintenance, migration or inhibition of alternative lineages. Despite the previously established role of p53 in restraining proliferation, it has been shown that, in the correct environment, p53 can cooperate for the proliferation and maintenance of progenitor cells (Cicalese et al., 2009; Li et al., 2015; Schoppy et al., 2010). The maintenance of Nodal/ Activin activated genes, particularly genes co-regulated by Nodal/ Activin and p53, could require the presence of p53. p53 may be required to facilitate the migration of cardiomyocytes, with p53 downregulation resulting in aberrantly localised cardiac tissue, disrupting correct tissue interactions for cardiomyocyte maintenance and expansion (Alexandrova et al., 2000; Elyada et al., 2011; Guo et al., 2003). p53 has been shown to impede the self-renewal of haematopoietic stem cells, highlighting a potential role in inhibiting the expansion of blood progenitors (Pant et al., 2012).

It has been shown here that the hypothesis that FGF/ MEK signalling is required to activate p53 to mediate crosstalk with the Nodal/ Activin pathway in cardiac specification is unlikely to be true. It was shown that FGF/ MEK signalling is not required during the early pre-gastrula stages of cardiogenesis. However if p53 were required at an earlier stage than FGF/ MEK signalling, the task remains to identify the factor(s) which induce p53 to positively regulate heart development. Plausibly, p53 could be under the control of an unidentified signalling pathway during early, and then FGF/ MEK signalling during late, heart development. In addition, p53 antagonists may be involved in defining the cardiac boundaries. p53 antagonists residing in non-cardiac mesoderm may restrict the activation of cardiac targets requiring the cooperation of Nodal/ Activin signalling and p53 to within the intended pre-cardiac region. This could be in a similar manner to how the p53 ectodermal antagonist Znf585b limits mesoderm boundaries (Sasai et al., 2008). It has been shown here that the temporal requirements of Nodal/ Activin, p53 and FGF/ MEK signalling in mesoderm induction and cardiac specification are different. This may lead to identifying the mechanisms involved in the control of these two different processes which occur in rapid succession in the early embryo.

6.9 Concluding remarks

This work has expanded and improved upon previous research, highlighting an indispensable role for Nodal/ Activin signalling in cardiac specification and demonstrating that this can be uncoupled from its role in mesoderm induction. Furthermore, a novel early time-window for cardiac specification has been identified, where cells respond to a cumulative dose of Nodal/ Activin signalling within a 2-3 hour time-window succeeding midblastula transition. Cardiac specification signalling is most likely mediated by Nodal, and transduced via Smad2, although alternative Nodal/ Activin family ligands, and Smad3, may be involved. It was found that FGF/ MEK signalling is not required for cardiac specification, but is required after initial specification for normal heart development, perhaps for the continued maintenance of cardiac cells. A novel role for p53 in heart development was demonstrated. These

findings aid in the understanding of how signalling pathways orchestrate developmental processes. This knowledge can be utilised to better comprehend the causes of congenital heart defects and improve directed differentiation protocols for regenerative medicine in the treatment of cardiac disease or infarction.

7 Bibliography

Akazawa, H., Komuro, I., 2005. Cardiac transcription factor Csx/Nkx2-5: Its role in cardiac development and diseases. Pharmacology & Therapeutics 107, 252–268. doi:10.1016/j.pharmthera.2005.03.005

Al Naieb, S., Happel, C.M., Yelbuz, T.M., 2013. A detailed atlas of chick heart development in vivo. Annals of Anatomy - Anatomischer Anzeiger 195, 324–341. doi:10.1016/j.aanat.2012.10.011

Alexandrova, A., Ivanov, A., Chumakov, P., Kopnin, B., Vasiliev, J., 2000. Changes in p53 expression in mouse fibroblasts can modify motility and extracellular matrix organization. Oncogene 19, 5826–5830. doi:10.1038/sj.onc.1203944

Alsan, B.H., Schultheiss, T.M., 2002. Regulation of avian cardiogenesis by Fgf8 signaling. Development 129, 1935–1943.

Amaya, E., Musci, T.J., Kirschner, M.W., 1991. Expression of a dominant negative mutant of the FGF receptor disrupts mesoderm formation in Xenopus embryos. Cell 66, 257–70.

Amaya, E., Offield, M.F., Grainger, R.M., 1998. Frog genetics: Xenopus tropicalis jumps into the future. Trends in Genetics 14, 253–255. doi:10.1016/S0168-9525(98)01506-6

Amaya, E., Stein, P.A., Musci, T.J., Kirschner, M.W., 1993. FGF signalling in the early specification of mesoderm in Xenopus. Development 118, 477–487.

Anastasaki, C., Rauen, K.A., Patton, E.E., 2012. Continual low-level MEK inhibition ameliorates cardio-facio-cutaneous phenotypes in zebrafish. Disease Models & Mechanisms 5, 546–552. doi:10.1242/dmm.008672

Andrée, B., Duprez, D., Vorbusch, B., Arnold, H.H., Brand, T., 1998. BMP-2 induces ectopic expression of cardiac lineage markers and interferes with somite formation in chicken embryos. Mech. Dev. 70, 119–131.

Aragon, F., Pujades, C., 2009. FGF signaling controls caudal hindbrain specification through Ras-ERK1/2 pathway. BMC Developmental Biology 9, 61. doi:10.1186/1471-213X-9-61

Ariizumi, T., Sawamura, K., Uchiyama, H., Asashima, M., 1991. Dose and time-dependent mesoderm induction and outgrowth formation by activin A in Xenopus laevis. Int. J. Dev. Biol. 35, 407–414.

Armstrong, J.F., Kaufman, M.H., Harrison, D.J., Clarke, A.R., 1995. High-frequency developmental abnormalities in p53-deficient mice. Curr. Biol. 5, 931–936.

Artmann, G.M., Minger, S., Hescheler, J., 2010. Stem Cell Engineering: Principles and Applications. Springer Science & Business Media.

Auda-Boucher, G., Bernard, B., Fontaine-Pérus, J., Rouaud, T., Mericksay, M., Gardahaut, M.-F., 2000. Staging of the Commitment of Murine Cardiac Cell Progenitors. Developmental Biology 225, 214–225. doi:10.1006/dbio.2000.9817

Baker, J.C., Harland, R.M., 1996. A novel mesoderm inducer, Madr2, functions in the activin signal transduction pathway. Genes Dev. 10, 1880–1889. doi:10.1101/gad.10.15.1880

Bassett, A.R., Azzam, G., Wheatley, L., Tibbit, C., Rajakumar, T., McGowan, S., Stanger, N., Ewels, P.A., Taylor, S., Ponting, C.P., Liu, J.-L., Sauka-Spengler, T., Fulga, T.A., 2014. Understanding functional miRNA-target interactions in vivo

by site-specific genome engineering. Nat Commun 5, 4640. doi:10.1038/ncomms5640

Batalov, I., Feinberg, A.W., 2015. Differentiation of Cardiomyocytes from Human Pluripotent Stem Cells Using Monolayer Culture. Biomark Insights 10, 71–76. doi:10.4137/BMI.S20050

Beckerman, R., Prives, C., 2010. Transcriptional Regulation by P53. Cold Spring Harb Perspect Biol 2, a000935. doi:10.1101/cshperspect.a000935

Bedzhov, I., Graham, S.J.L., Leung, C.Y., Zernicka-Goetz, M., 2014. Developmental plasticity, cell fate specification and morphogenesis in the early mouse embryo. Phil. Trans. R. Soc. B 369, 20130538. doi:10.1098/rstb.2013.0538

Beiman, M., Shilo, B.Z., Volk, T., 1996. Heartless, a Drosophila FGF receptor homolog, is essential for cell migration and establishment of several mesodermal lineages. Genes & development 10, 2993–3002.

Beltrami, A.P., Barlucchi, L., Torella, D., Baker, M., Limana, F., Chimenti, S., Kasahara, H., Rota, M., Musso, E., Urbanek, K., Leri, A., Kajstura, J., Nadal-Ginard, B., Anversa, P., 2003. Adult cardiac stem cells are multipotent and support myocardial regeneration. Cell 114, 763–776.

Benson, D.W., Silberbach, G.M., Kavanaugh-McHugh, A., Cottrill, C., Zhang, Y., Riggs, S., Smalls, O., Johnson, M.C., Watson, M.S., Seidman, J.G., Seidman, C.E., Plowden, J., Kugler, J.D., 1999. Mutations in the cardiac transcription factor NKX2.5 affect diverse cardiac developmental pathways. The Journal of clinical investigation 104, 1567–73. doi:10.1172/jci8154

Bergmann, O., Bhardwaj, R.D., Bernard, S., Zdunek, S., Barnabé-Heider, F., Walsh, S., Zupicich, J., Alkass, K., Buchholz, B.A., Druid, H., Jovinge, S., Frisén, J., 2009. Evidence for cardiomyocyte renewal in humans. Science 324, 98–102. doi:10.1126/science.1164680

Birnboim, H.C., Doly, J., 1979. A rapid alkaline extraction procedure for screening recombinant plasmid DNA. Nucleic Acids Res. 7, 1513–1523.

Blanchet, M.H., Le Good, J.A., Mesnard, D., Oorschot, V., Baflast, S., Minchiotti, G., Klumperman, J., Constam, D.B., 2008. Cripto recruits Furin and PACE4 and controls Nodal trafficking during proteolytic maturation. The EMBO journal 27, 2580–91. doi:10.1038/emboj.2008.174

Blitz, I.L., Biesinger, J., Xie, X., Cho, K.W., 2013. Biallelic genome modification in F(0) Xenopus tropicalis embryos using the CRISPR/Cas system. Genesis (New York, N.Y. : 2000) 51, 827–34. doi:10.1002/dvg.22719

Boom, R., Sol, C.J., Salimans, M.M., Jansen, C.L., Wertheim-van Dillen, P.M., van der Noordaa, J., 1990. Rapid and simple method for purification of nucleic acids. J. Clin. Microbiol. 28, 495–503.

Böttcher, R.T., Pollet, N., Delius, H., Niehrs, C., 2004. The transmembrane protein XFLRT3 forms a complex with FGF receptors and promotes FGF signalling. Nat. Cell Biol. 6, 38–44. doi:10.1038/ncb1082

Brade, T., Gessert, S., Kühl, M., Pandur, P., 2007. The amphibian second heart field: Xenopus islet-1 is required for cardiovascular development. Developmental Biology 311, 297–310. doi:10.1016/j.ydbio.2007.08.004

Brady, C.A., Attardi, L.D., 2010. p53 at a glance. J Cell Sci 123, 2527–2532. doi:10.1242/jcs.064501

Brand, T., 2003. Heart development: molecular insights into cardiac specification and early morphogenesis. Developmental biology 258, 1–19.

Brennan, J., Norris, D.P., Robertson, E.J., 2002. Nodal activity in the node governs left-right asymmetry. Genes Dev 16, 2339–2344. doi:10.1101/gad.1016202

Brown, D.D., Binder, O., Pagratis, M., Parr, B.A., Conlon, F.L., 2003. Developmental expression of the Xenopus laevis Tbx20 orthologue. Development genes and evolution 212, 604–7. doi:10.1007/s00427-002-0276-6

Bruneau, B.G., 2008. The developmental genetics of congenital heart disease. Nature 451, 943–948. doi:10.1038/nature06801

Bruneau, B.G., Logan, M., Davis, N., Levi, T., Tabin, C.J., Seidman, J.G., Seidman, C.E., 1999. Chamber-specific cardiac expression of Tbx5 and heart defects in Holt-Oram syndrome. Dev. Biol. 211, 100–108. doi:10.1006/dbio.1999.9298

Bruneau, B.G., Nemer, G., Schmitt, J.P., Charron, F., Robitaille, L., Caron, S., Conner, D.A., Gessler, M., Nemer, M., Seidman, C.E., Seidman, J.G., 2001. A Murine Model of Holt-Oram Syndrome Defines Roles of the T-Box Transcription Factor Tbx5 in Cardiogenesis and Disease. Cell 106, 709–721. doi:10.1016/S0092-8674(01)00493-7

Buckingham, M., Meilhac, S., Zaffran, S., 2005. Building the mammalian heart from two sources of myocardial cells. Nature reviews. Genetics 6, 826–35. doi:10.1038/nrg1710

Bulatovic, I., Månsson-Broberg, A., Sylvén, C., Grinnemo, K.-H., 2015. Human fetal cardiac progenitors: The role of stem cells and progenitors in the fetal and adult heart. Best Pract Res Clin Obstet Gynaecol. doi:10.1016/j.bpobgyn.2015.08.008

Burridge, P.W., Keller, G., Gold, J.D., Wu, J.C., 2012. Production of De Novo Cardiomyocytes: Human Pluripotent Stem Cell Differentiation and Direct Reprogramming. Cell Stem Cell 10, 16–28. doi:10.1016/j.stem.2011.12.013

Burridge, P.W., Matsa, E., Shukla, P., Lin, Z.C., Churko, J.M., Ebert, A.D., Lan, F., Diecke, S., Huber, B., Mordwinkin, N.M., Plews, J.R., Abilez, O.J., Cui, B., Gold, J.D., Wu, J.C., 2014. Chemically Defined and Small Molecule-Based Generation of Human Cardiomyocytes. Nat Methods 11, 855–860. doi:10.1038/nmeth.2999

Cady, N.C., Stelick, S., Batt, C.A., 2003. Nucleic acid purification using microfabricated silicon structures. Biosens Bioelectron 19, 59–66.

Cai, C.-L., Liang, X., Shi, Y., Chu, P.-H., Pfaff, S.L., Chen, J., Evans, S., 2003. Isl1 identifies a cardiac progenitor population that proliferates prior to differentiation and contributes a majority of cells to the heart. Dev. Cell 5, 877–889.

Cai, W., Guzzo, R.M., Wei, K., Willems, E., Davidovics, H., Mercola, M., 2012. A Nodal-to-TGFβ Cascade Exerts Biphasic Control Over Cardiopoiesis. Circulation Research 111, 876–881. doi:10.1161/circresaha.112.270272

Cambier, L., Plate, M., Sucov, H.M., Pashmforoush, M., 2014. Nkx2-5 regulates cardiac growth through modulation of Wnt signaling by R-spondin3. Development (Cambridge, England) 141, 2959–71. doi:10.1242/dev.103416

Casci, T., Vinos, J., Freeman, M., 1999. Sprouty, an intracellular inhibitor of Ras signaling. Cell 96, 655–65.

Cha, S., Lee, J.-W., Hwang, Y., Chae, J.-P., Park, K.M., Cho, H.J., Kim, D.S., Bae, Y.C., Park, M.J., 2008. Spatiotemporal regulation of fibroblast growth factor signal blocking for endoderm formation in Xenopus laevis. Exp Mol Med 40, 550–557. doi:10.3858/emm.2008.40.5.550

Chambers, A.E., Logan, M., Kotecha, S., Towers, N., Sparrow, D., Mohun, T.J., 1994. The RSRF/MEF2 protein SL1 regulates cardiac muscle-specific transcription of a myosin light-chain gene in Xenopus embryos. Genes & Development 8, 1324–1334. doi:10.1101/gad.8.11.1324

Chang, C., Harland, R.M., 2007. Neural induction requires continued suppression of both Smad1 and Smad2 signals during gastrulation. Development (Cambridge, England) 134, 3861–72. doi:10.1242/dev.007179

Chapman, D.L., Garvey, N., Hancock, S., Alexiou, M., Agulnik, S.I., Gibson-Brown, J.J., Cebra-Thomas, J., Bollag, R.J., Silver, L.M., Papaioannou, V.E., 1996. Expression of the T-box family genes, Tbx1-Tbx5, during early mouse development. Dev. Dyn. 206, 379–390. doi:10.1002/(SICI)1097-0177(199608)206:4<379::AID-AJA4>3.0.CO;2-F

Chen, C., Shen, M.M., 2004. Two modes by which Lefty proteins inhibit nodal signaling. Current biology : CB 14, 618–24. doi:10.1016/j.cub.2004.02.042

Chen, J.N., Fishman, M.C., 1996. Zebrafish tinman homolog demarcates the heart field and initiates myocardial differentiation. Development 122, 3809–3816.

Chen, X., Weisberg, E., Fridmacher, V., Watanabe, M., Naco, G., Whitman, M., 1997. Smad4 and FAST-1 in the assembly of activin-responsive factor. Nature 389, 85–89. doi:10.1038/38008

Chen, Y., Whitaker, L.L., Ramsdell, A.F., 2005. Developmental analysis of activin-like kinase receptor-4 (ALK4) expression in Xenopus laevis. Dev. Dyn. 232, 393–398. doi:10.1002/dvdy.20232

Chen, Y.G., Meng, A.M., 2004. Negative regulation of TGF-β signaling in development. Cell Res 14, 441–449. doi:10.1038/sj.cr.7290246

Choi, W.-Y., Giraldez, A.J., Schier, A.F., 2007. Target protectors reveal dampening and balancing of Nodal agonist and antagonist by miR-430. Science 318, 271–274. doi:10.1126/science.1147535

Chomczynski, P., Sacchi, N., 1987. Single-step method of RNA isolation by acid guanidinium thiocyanate-phenol-chloroform extraction. Analytical Biochemistry 162, 156–159. doi:10.1016/0003-2697(87)90021-2

Ciau-Uitz, A., Walmsley, M., Patient, R., 2000. Distinct origins of adult and embryonic blood in Xenopus. Cell 102, 787–96.

Cicalese, A., Bonizzi, G., Pasi, C.E., Faretta, M., Ronzoni, S., Giulini, B., Brisken, C., Minucci, S., Di Fiore, P.P., Pelicci, P.G., 2009. The tumor suppressor p53 regulates polarity of self-renewing divisions in mammary stem cells. Cell 138, 1083–1095. doi:10.1016/j.cell.2009.06.048

Ciruna, B., Rossant, J., 2001. FGF Signaling Regulates Mesoderm Cell Fate Specification and Morphogenetic Movement at the Primitive Streak. Developmental Cell 1, 37–49. doi:10.1016/S1534-5807(01)00017-X

Cleaver, O.B., Patterson, K.D., Krieg, P.A., 1996. Overexpression of the tinman-related genes XNkx-2.5 and XNkx-2.3 in Xenopus embryos results in myocardial hyperplasia. Development 122, 3549–3556.

Cordenonsi, M., Dupont, S., Maretto, S., Insinga, A., Imbriano, C., Piccolo, S., 2003. Links between Tumor Suppressors: p53 Is Required for TGF-β Gene Responses by Cooperating with Smads. Cell 113, 301–314. doi:10.1016/S0092-8674(03)00308-8

Cordenonsi, M., Montagner, M., Adorno, M., Zacchigna, L., Martello, G., Mamidi, A., Soligo, S., Dupont, S., Piccolo, S., 2007. Integration of TGF-ß and Ras/MAPK Signaling Through p53 Phosphorylation. Science 315, 840–843. doi:10.1126/science.1135961

Corson, L.B., Yamanaka, Y., Lai, K.M., Rossant, J., 2003. Spatial and temporal patterns of ERK signaling during mouse embryogenesis. Development (Cambridge, England) 130, 4527–37. doi:10.1242/dev.00669

Coumoul, X., Deng, C.-X., 2003. Roles of FGF receptors in mammalian development and congenital diseases. Birth Defects Research Part C: Embryo Today: Reviews 69, 286–304. doi:10.1002/bdrc.10025

Crump, J.G., Maves, L., Lawson, N.D., Weinstein, B.M., Kimmel, C.B., 2004. An essential role for Fgfs in endodermal pouch formation influences later craniofacial skeletal patterning. Development 131, 5703–5716. doi:10.1242/dev.01444

Cunliffe, V., Smith, J.C., 1992. Ectopic mesoderm formation in Xenopus embryos caused by widespread expression of a Brachyury homologue. Nature 358, 427–430. doi:10.1038/358427a0

DaCosta Byfield, S., Major, C., Laping, N.J., Roberts, A.B., 2004. SB-505124 Is a Selective Inhibitor of Transforming Growth Factor-β Type I Receptors ALK4, ALK5, and ALK7. Molecular Pharmacology 65, 744–752. doi:10.1124/mol.65.3.744

Dai, C., Gu, W., 2010. p53 post-translational modification: deregulated in tumorigenesis. Trends Mol Med 16, 528–536. doi:10.1016/j.molmed.2010.09.002

Daniels, M., Shimizu, K., Zorn, A.M., Ohnuma, S., 2004. Negative regulation of Smad2 by PIASy is required for proper Xenopus mesoderm formation. Development 131, 5613–5626. doi:10.1242/dev.01449

Danilova, N., Sakamoto, K.M., Lin, S., 2008. p53 family in development. Mechanisms of Development 125, 919–931. doi:10.1016/j.mod.2008.09.003

Das, D., Randall, R.A., Hill, C.S., 2009. An N-terminally truncated Smad2 protein can partially compensate for loss of full-length Smad2. Biochem. J. 417, 205–212. doi:10.1042/BJ20080014

Dash, P., Lotan, I., Knapp, M., Kandel, E.R., Goelet, P., 1987. Selective elimination of mRNAs in vivo: complementary oligodeoxynucleotides promote RNA degradation by an RNase H-like activity. Proc Natl Acad Sci U S A 84, 7896–7900.

de Caestecker, M., 2004. The transforming growth factor-beta superfamily of receptors. Cytokine Growth Factor Rev. 15, 1–11.

De Robertis, E.M., Kuroda, H., 2004. Dorsal-ventral patterning and neural induction in Xenopus embryos. Annu. Rev. Cell Dev. Biol. 20, 285–308. doi:10.1146/annurev.cellbio.20.011403.154124

De Robertis, E.M., Larraín, J., Oelgeschläger, M., Wessely, O., 2000. The establishment of Spemann's organizer and patterning of the vertebrate embryo. Nat. Rev. Genet. 1, 171–181. doi:10.1038/35042039

De Roberts, E.M., Blum, M., Niehrs, C., Steinbeisser, H., 1992. Goosecoid and the organizer. Dev. Suppl. 167–171.

Deimling, S.J., Drysdale, T.A., 2011. Fgf is required to regulate anterior–posterior patterning in the Xenopus lateral plate mesoderm. Mechanisms of Development 128, 327–341. doi:10.1016/j.mod.2011.06.002

Delaune, E., Lemaire, P., Kodjabachian, L., 2005. Neural induction in Xenopus requires early FGF signalling in addition to BMP inhibition. Development 132, 299–310. doi:10.1242/dev.01582

Dell'Era, P., Ronca, R., Coco, L., Nicoli, S., Metra, M., Presta, M., 2003. Fibroblast Growth Factor Receptor-1 Is Essential for In Vitro Cardiomyocyte Development. Circulation Research 93, 414–420. doi:10.1161/01.RES.0000089460.12061.E1

Deng, C.X., Wynshaw-Boris, A., Shen, M.M., Daugherty, C., Ornitz, D.M., Leder, P., 1994. Murine FGFR-1 is required for early postimplantation growth and axial organization. Genes & development 8, 3045–57.

Diez del Corral, R., Olivera-Martinez, I., Goriely, A., Gale, E., Maden, M., Storey, K., 2003. Opposing FGF and retinoid pathways control ventral neural pattern, neuronal differentiation, and segmentation during body axis extension. Neuron 40, 65–79.

Dohrmann, C.E., Hemmati-Brivanlou, A., Thomsen, G.H., Fields, A., Woolf, T.M., Melton, D.A., 1993. Expression of activin mRNA during early development in Xenopus laevis. Dev. Biol. 157, 474–483. doi:10.1006/dbio.1993.1150

Donehower, L.A., Harvey, M., Slagle, B.L., McArthur, M.J., Montgomery, C.A., Butel, J.S., Allan, 1992. Mice deficient for p53 are developmentally normal but susceptible to spontaneous tumours. Nature 356, 215–221. doi:10.1038/356215a0

Dorey, K., Amaya, E., 2010. FGF signalling: diverse roles during early vertebrate embryogenesis. Development 137, 3731–3742. doi:10.1242/dev.037689

Dorey, K., Hill, C.S., 2006. A novel Cripto-related protein reveals an essential role for EGF-CFCs in Nodal signalling in Xenopus embryos. Developmental Biology 292, 303–316.

Dupont, S., Zacchigna, L., Adorno, M., Soligo, S., Volpin, D., Piccolo, S., Cordenonsi, M., 2004. Convergence of p53 and TGF-beta signaling networks. Cancer Letters 213, 129–138. doi:10.1016/j.canlet.2004.06.008

Dyer, L.A., Kirby, M.L., 2009. The Role of Secondary Heart Field in Cardiac Development. Dev Biol 336, 137–144. doi:10.1016/j.ydbio.2009.10.009

Dyson, S., Gurdon, J.B., 1998. The interpretation of position in a morphogen gradient as revealed by occupancy of activin receptors. Cell 93, 557–568.

Efe, J.A., Hilcove, S., Kim, J., Zhou, H., Ouyang, K., Wang, G., Chen, J., Ding, S., 2011. Conversion of mouse fibroblasts into cardiomyocytes using a direct reprogramming strategy. Nat Cell Biol 13, 215–222. doi:10.1038/ncb2164

Eisen, J.S., Smith, J.C., 2008. Controlling morpholino experiments: don't stop making antisense. Development (Cambridge, England) 135, 1735–43. doi:10.1242/dev.001115

Elyada, E., Pribluda, A., Goldstein, R.E., Morgenstern, Y., Brachya, G., Cojocaru, G., Snir-Alkalay, I., Burstain, I., Haffner-Krausz, R., Jung, S., Wiener, Z., Alitalo, K., Oren, M., Pikarsky, E., Ben-Neriah, Y., 2011. CKIα ablation highlights a critical role for p53 in invasiveness control. Nature 470, 409–413. doi:10.1038/nature09673

Evans, S.M., 1999. Vertebrate tinman homologues and cardiac differentiation. Seminars in cell & developmental biology 10, 73–83. doi:10.1006/scdb.1999.0282

Evans, S.M., Yan, W., Murillo, M.P., Ponce, J., Papalopulu, N., 1995. tinman, a Drosophila homeobox gene required for heart and visceral mesoderm specification, may be represented by a family of genes in vertebrates: XNkx-2.3, a second vertebrate homologue of tinman. Development (Cambridge, England) 121, 3889–99.

Faure, S., Lee, M.A., Keller, T., ten Dijke, P., Whitman, M., 2000. Endogenous patterns of TGFbeta superfamily signaling during early Xenopus development. Development 127, 2917–2931.

Favata, M.F., Horiuchi, K.Y., Manos, E.J., Daulerio, A.J., Stradley, D.A., Feeser, W.S., Dyk, D.E.V., Pitts, W.J., Earl, R.A., Hobbs, F., Copeland, R.A., Magolda, R.L., Scherle, P.A., Trzaskos, J.M., 1998. Identification of a Novel Inhibitor of Mitogen-activated Protein Kinase Kinase. J. Biol. Chem. 273, 18623–18632. doi:10.1074/jbc.273.29.18623

Fishman, M.C., Olson, E.N., 1997. Parsing the heart: genetic modules for organ assembly. Cell 91, 153–6.

Fletcher, R.B., Baker, J.C., Harland, R.M., 2006. FGF8 spliceforms mediate early mesoderm and posterior neural tissue formation in Xenopus. Development 133, 1703–1714. doi:10.1242/dev.02342

Fletcher, R.B., Harland, R.M., 2008. The role of FGF signaling in the establishment and maintenance of mesodermal gene expression in Xenopus. Developmental Dynamics 237, 1243–1254.

Foley, A.C., Gupta, R.W., Guzzo, R.M., Korol, O., Mercola, M., 2006. Embryonic heart induction. Annals of the New York Academy of Sciences 1080, 85–96. doi:10.1196/annals.1380.008

Foley, A.C., Korol, O., Timmer, A.M., Mercola, M., 2007. Multiple Functions of Cerberus Cooperate to induce Heart downstream of Nodal. Dev Biol 303, 57–65. doi:10.1016/j.ydbio.2006.10.033

Friedman, P.N., Chen, X., Bargonetti, J., Prives, C., 1993. The p53 protein is an unusually shaped tetramer that binds directly to DNA. Proc. Natl. Acad. Sci. U.S.A. 90, 3319–3323.

Fu, Y., Huang, C., Xu, X., Gu, H., Ye, Y., Jiang, C., Qiu, Z., Xie, X., 2015. Direct reprogramming of mouse fibroblasts into cardiomyocytes with chemical cocktails. Cell Res 25, 1013–1024. doi:10.1038/cr.2015.99

Furthauer, M., Lin, W., Ang, S.L., Thisse, B., Thisse, C., 2002. Sef is a feedback-induced antagonist of Ras/MAPK-mediated FGF signalling. Nature cell biology 4, 170–4. doi:10.1038/ncb750

Fürthauer, M., Van Celst, J., Thisse, C., Thisse, B., 2004. Fgf signalling controls the dorsoventral patterning of the zebrafish embryo. Development 131, 2853–2864. doi:10.1242/dev.01156

Gajewski, K., Fossett, N., Molkentin, J.D., Schulz, R.A., 1999. The zinc finger proteins Pannier and GATA4 function as cardiogenic factors in Drosophila. Development 126, 5679–5688.

Garcia-Martinez, V., Schoenwolf, G.C., 1993. Primitive-Streak Origin of the Cardiovascular System in Avian Embryos. Developmental Biology 159, 706–719. doi:10.1006/dbio.1993.1276

Gavine, P.R., Mooney, L., Kilgour, E., Thomas, A.P., Al-Kadhimi, K., Beck, S., Rooney, C., Coleman, T., Baker, D., Mellor, M.J., Brooks, A.N., Klinowska, T., 2012. AZD4547: An Orally Bioavailable, Potent, and Selective Inhibitor of the Fibroblast Growth Factor Receptor Tyrosine Kinase Family. Cancer Research 72, 2045–2056. doi:10.1158/0008-5472.can-11-3034

Gessert, S., Kühl, M., 2009. Comparative gene expression analysis and fate mapping studies suggest an early segregation of cardiogenic lineages in Xenopus laevis. Developmental Biology 334, 395–408. doi:10.1016/j.ydbio.2009.07.037

Gilbert, S.F., 2000. Developmental Biology. 6th edition. Sinauer Associates, Sunderland.

Gilchrist, M.J., Zorn, A.M., Voigt, J., Smith, J.C., Papalopulu, N., Amaya, E., 2004. Defining a large set of full-length clones from a Xenopus tropicalis EST project. Developmental biology 271, 498–516. doi:10.1016/j.ydbio.2004.04.023

Graf, T., Enver, T., 2009. Forcing cells to change lineages. Nature 462, 587–594. doi:10.1038/nature08533

Graff, J.M., Bansal, A., Melton, D.A., 1996. Xenopus Mad proteins transduce distinct subsets of signals for the TGF beta superfamily. Cell 85, 479–487.

Grainger, R.M., 2012. Xenopus tropicalis as a Model Organism for Genetics and Genomics: Past, Present and Future. Methods Mol Biol 917, 3–15. doi:10.1007/978-1-61779-992-1_1

Griffin, K.J.P., Kimelman, D., 2003. Interplay between FGF, one-eyed pinhead, and T-box transcription factors during zebrafish posterior development. Dev. Biol. 264, 456–466.

Griffin, K.J.P., Kimelman, D., 2002. One-Eyed Pinhead and Spadetail are essential for heart and somite formation. Nat Cell Biol 4, 821–825. doi:10.1038/ncb862

Gritsman, K., Talbot, W.S., Schier, A.F., 2000. Nodal signaling patterns the organizer. Development (Cambridge, England) 127, 921–32.

Gritsman, K., Zhang, J., Cheng, S., Heckscher, E., Talbot, W.S., Schier, A.F., 1999. The EGF-CFC protein one-eyed pinhead is essential for nodal signaling. Cell 97, 121–32.

Guo, F., Gao, Y., Wang, L., Zheng, Y., 2003. p19Arf-p53 tumor suppressor pathway regulates cell motility by suppression of phosphoinositide 3-kinase and Rac1 GTPase activities. J. Biol. Chem. 278, 14414–14419. doi:10.1074/jbc.M300341200

Guo, X., Zhang, T., Hu, Z., Zhang, Y., Shi, Z., Wang, Q., Cui, Y., Wang, F., Zhao, H., Chen, Y., 2014. Efficient RNA/Cas9-mediated genome editing in Xenopus tropicalis. Development 141, 707–714. doi:10.1242/dev.099853

Gurdon, J.B., Mitchell, A., Mahony, D., 1995. Direct and continuous assessment by cells of their position in a morphogen gradient. Nature 376, 520–521. doi:10.1038/376520a0

Hagos, E.G., Dougan, S.T., 2007. Time-dependent patterning of the mesoderm and endoderm by Nodal signals in zebrafish. BMC Dev Biol 7, 1–18. doi:10.1186/1471-213X-7-22

Hagos, E.G., Fan, X., Dougan, S.T., 2007. The role of maternal Activin-like signals in zebrafish embryos. Developmental Biology 309, 245–258. doi:10.1016/j.ydbio.2007.07.010

Harada, K., Ogai, A., Takahashi, T., Kitakaze, M., Matsubara, H., Oh, H., 2008. Crossveinless-2 Controls Bone Morphogenetic Protein Signaling during Early Cardiomyocyte Differentiation in P19 Cells. J Biol Chem 283, 26705–26713. doi:10.1074/jbc.M801485200

Harland, R., Gerhart, and J., 1997. Formation and Function of Spemann's Organizer. Annual Review of Cell and Developmental Biology 13, 611–667. doi:10.1146/annurev.cellbio.13.1.611

Harmer, N.J., Ilag, L.L., Mulloy, B., Pellegrini, L., Robinson, C.V., Blundell, T.L., 2004. Towards a resolution of the stoichiometry of the fibroblast growth factor (FGF)-FGF receptor-heparin complex. Journal of molecular biology 339, 821–34. doi:10.1016/j.jmb.2004.04.031

Harvey, R.P., 2002. Patterning the vertebrate heart. Nat Rev Genet 3, 544–556. doi:10.1038/nrg843

Harvey, S.A., Smith, J.C., 2009. Visualisation and Quantification of Morphogen Gradient Formation in the Zebrafish. PLoS Biol 7, e1000101. doi:10.1371/journal.pbio.1000101

Hasegawa, M., Cahill, G.M., 2004. Regulation of the circadian oscillator in Xenopus retinal photoreceptors by protein kinases sensitive to the stress-activated protein kinase inhibitor, SB 203580. J. Biol. Chem. 279, 22738–22746. doi:10.1074/jbc.M401389200

Haworth, K.E., Kotecha, S., Mohun, T.J., Latinkic, B.V., 2008. GATA4 and GATA5 are essential for heart and liver development in Xenopus embryos. BMC developmental biology 8, 74. doi:10.1186/1471-213x-8-74

Heasman, J., 2006. Patterning the early Xenopus embryo. Development 133, 1205–1217. doi:10.1242/dev.02304

Heasman, J., 2002. Morpholino Oligos: Making Sense of Antisense? Developmental Biology 243, 209–214. doi:10.1006/dbio.2001.0565

Heasman, J., Wylie, C.C., Hausen, P., Smith, J.C., 1984. Fates and states of determination of single vegetal pole blastomeres of X. laevis. Cell 37, 185–194.

Heldin, C.-H., Miyazono, K., ten Dijke, P., 1997. TGF-β signalling from cell membrane to nucleus through SMAD proteins. Nature 390, 465–471. doi:10.1038/37284

Hellsten, U., Harland, R.M., Gilchrist, M.J., Hendrix, D., Jurka, J., Kapitonov, V., Ovcharenko, I., Putnam, N.H., Shu, S., Taher, L., Blitz, I.L., Blumberg, B.,

Dichmann, D.S., Dubchak, I., Amaya, E., Detter, J.C., Fletcher, R., Gerhard, D.S., Goodstein, D., Graves, T., Grigoriev, I.V., Grimwood, J., Kawashima, T., Lindquist, E., Lucas, S.M., Mead, P.E., Mitros, T., Ogino, H., Ohta, Y., Poliakov, A.V., Pollet, N., Robert, J., Salamov, A., Sater, A.K., Schmutz, J., Terry, A., Vize, P.D., Warren, W.C., Wells, D., Wills, A., Wilson, R.K., Zimmerman, L.B., Zorn, A.M., Grainger, R., Grammer, T., Khokha, M.K., Richardson, P.M., Rokhsar, D.S., 2010. The genome of the Western clawed frog Xenopus tropicalis. Science (New York, N.Y.) 328, 633–6. doi:10.1126/science.1183670

Hemmati-Brivanlou, A., Melton, D.A., 1992. A truncated activin receptor inhibits mesoderm induction and formation of axial structures in Xenopus embryos. Nature 359, 609–614. doi:10.1038/359609a0

Henderson, Y.C., Chen, Y., Frederick, M.J., Lai, S.Y., Clayman, G.L., 2010. MEK Inhibitor PD0325901 Significantly Reduces the Growth of Papillary Thyroid Carcinoma Cells In vitro and In vivo. Mol Cancer Ther 9, 1968–1976. doi:10.1158/1535-7163.MCT-10-0062

Hernández-Acosta, N.C., Cabrera-Socorro, A., Morlans, M.P., Delgado, F.J.G., Suárez-Solá, M.L., Sottocornola, R., Lu, X., González-Gómez, M., Meyer, G., 2011. Dynamic expression of the p53 family members p63 and p73 in the mouse and human telencephalon during development and in adulthood. Brain Research 1372, 29–40. doi:10.1016/j.brainres.2010.11.041

Hierlihy, A.M., Seale, P., Lobe, C.G., Rudnicki, M.A., Megeney, L.A., 2002. The post-natal heart contains a myocardial stem cell population. FEBS Lett. 530, 239–243.

Hill, C.S., 2001. TGF-beta signalling pathways in early Xenopus development. Curr. Opin. Genet. Dev. 11, 533–540.

Hill, R., Bodzak, E., Blough, M.D., Lee, P.W.K., 2008. p53 Binding to the p21 promoter is dependent on the nature of DNA damage. Cell Cycle 7, 2535–2543.

Hiroi, Y., Kudoh, S., Monzen, K., Ikeda, Y., Yazaki, Y., Nagai, R., Komuro, I., 2001. Tbx5 associates with Nkx2-5 and synergistically promotes cardiomyocyte differentiation. Nat. Genet. 28, 276–280. doi:10.1038/90123

Ho, D.M., Chan, J., Bayliss, P., Whitman, M., 2006. Inhibitor-resistant type I receptors reveal specific requirements for TGF-beta signaling in vivo. Dev. Biol. 295, 730–742. doi:10.1016/j.ydbio.2006.03.050

Hogan, B.L., 1996. Bone morphogenetic proteins: multifunctional regulators of vertebrate development. Genes & development 10, 1580–94.

Hopwood, N.D., Gurdon, J.B., 1991. Gene activation in the amphibian mesoderm. Dev. Suppl. 1, 95–104.

Horb, M.E., Thomsen, G.H., 1999. Tbx5 is essential for heart development. Development (Cambridge, England) 126, 1739–51.

Howell, M., Hill, C.S., 1997. XSmad2 directly activates the activin-inducible, dorsal mesoderm gene XFKH1 in Xenopus embryos. The EMBO journal 16, 7411–21. doi:10.1093/emboj/16.24.7411

Howell, M., Hill, C.S., 1997. XSmad2 directly activates the activin-inducible, dorsal mesoderm gene XFKH1 in Xenopus embryos. EMBO J 16, 7411–7421. doi:10.1093/emboj/16.24.7411

Hutson, M.R., Kirby, M.L., 2007. Model systems for the study of heart development and disease. Cardiac neural crest and conotruncal malformations. Semin. Cell Dev. Biol. 18, 101–110. doi:10.1016/j.semcdb.2006.12.004

Ieda, M., Fu, J.-D., Delgado-Olguin, P., Vedantham, V., Hayashi, Y., Bruneau, B.G., Srivastava, D., 2010. Direct Reprogramming of Fibroblasts into Functional Cardiomyocytes by Defined Factors. Cell 142, 375–386. doi:10.1016/j.cell.2010.07.002

Inman, G.J., Nicolas, F.J., Callahan, J.F., Harling, J.D., Gaster, L.M., Reith, A.D., Laping, N.J., Hill, C.S., 2002. SB-431542 is a potent and specific inhibitor of transforming growth factor-beta superfamily type I activin receptor-like kinase (ALK) receptors ALK4, ALK5, and ALK7. Molecular pharmacology 62, 65–74.

Isaacs, H.V., Deconinck, A.E., Pownall, M.E., 2007. FGF4 regulates blood and muscle specification in Xenopus laevis. Biology of the Cell 99, 165–173. doi:10.1042/BC20060103

Isaacs, H.V., Tannahill, D., Slack, J.M., 1992. Expression of a novel FGF in the Xenopus embryo. A new candidate inducing factor for mesoderm formation and anteroposterior specification. Development 114, 711–720.

Itoh, N., Ornitz, D.M., 2004. Evolution of the Fgf and Fgfr gene families. Trends Genet. 20, 563–569. doi:10.1016/j.tig.2004.08.007

Jacobson, A.G., Sater, A.K., 1988. Features of embryonic induction. Development (Cambridge, England) 104, 341–59.

Jinek, M., Chylinski, K., Fonfara, I., Hauer, M., Doudna, J.A., Charpentier, E., 2012. A Programmable Dual-RNA–Guided DNA Endonuclease in Adaptive Bacterial Immunity. Science 337, 816–821. doi:10.1126/science.1225829

Jones, C.M., Kuehn, M.R., Hogan, B.L., Smith, J.C., Wright, C.V., 1995. Nodal-related signals induce axial mesoderm and dorsalize mesoderm during gastrulation. Development 121, 3651–3662.

Joseph, E.M., Melton, D.A., 1997. Xnr4:AXenopusNodal-Related Gene Expressed in the Spemann Organizer. Developmental Biology 184, 367–372. doi:10.1006/dbio.1997.8510

Joubin, K., Stern, C.D., 2001. Formation and maintenance of the organizer among the vertebrates. Int. J. Dev. Biol. 45, 165–175.

Jullien, J., Gurdon, J., 2005. Morphogen gradient interpretation by a regulated trafficking step during ligand-receptor transduction. Genes Dev. 19, 2682–2694. doi:10.1101/gad.341605

Kallianpur, A.R., Jordan, J.E., Brandt, S.J., 1994. The SCL/TAL-1 gene is expressed in progenitors of both the hematopoietic and vascular systems during embryogenesis. Blood 83, 1200–1208.

Kaltenbrun, E., Tandon, P., Amin, N.M., Waldron, L., Showell, C., Conlon, F.L., 2011. Xenopus: An emerging model for studying congenital heart disease. Birth defects research. Part A, Clinical and molecular teratology 91, 495–510. doi:10.1002/bdra.20793

Kandoth, C., McLellan, M.D., Vandin, F., Ye, K., Niu, B., Lu, C., Xie, M., Zhang, Q., McMichael, J.F., Wyczalkowski, M.A., Leiserson, M.D.M., Miller, C.A., Welch, J.S., Walter, M.J., Wendl, M.C., Ley, T.J., Wilson, R.K., Raphael, B.J., Ding, L.,

2013. Mutational landscape and significance across 12 major cancer types. Nature 502, 333–339. doi:10.1038/nature12634

Kasahara, H., Bartunkova, S., Schinke, M., Tanaka, M., Izumo, S., 1998. Cardiac and extracardiac expression of Csx/Nkx2.5 homeodomain protein. Circ. Res. 82, 936–946.

Keller, R., 2002. Shaping the Vertebrate Body Plan by Polarized Embryonic Cell Movements. Science 298, 1950–1954. doi:10.1126/science.1079478

Keller, R., Davidson, L., Edlund, A., Elul, T., Ezin, M., Shook, D., Skoglund, P., 2000. Mechanisms of convergence and extension by cell intercalation. Philos Trans R Soc Lond B Biol Sci 355, 897–922.

Keren-Politansky, A., Keren, A., Bengal, E., 2009. Neural ectoderm-secreted FGF initiates the expression of Nkx2.5 in cardiac progenitors via a p38 MAPK/CREB pathway. Developmental biology 335, 374–84. doi:10.1016/j.ydbio.2009.09.012

Kerppola, T.K., 2008a. Bimolecular Fluorescence Complementation: Visualization of Molecular Interactions in Living Cells, in: Kevin, F.S. (Ed.), Methods in Cell Biology. Academic Press, pp. 431–470.

Kerppola, T.K., 2008b. BIMOLECULAR FLUORESCENCE COMPLEMENTATION (BiFC) ANALYSIS AS A PROBE OF PROTEIN INTERACTIONS IN LIVING CELLS. Annu Rev Biophys 37, 465–487. doi:10.1146/annurev.biophys.37.032807.125842

Khoury, M.P., Bourdon, J.-C., 2011. p53 Isoforms An Intracellular Microprocessor? Genes & Cancer 2, 453–465. doi:10.1177/1947601911408893

Kiecker, C., Bates, T., Bell, E., 2015. Molecular specification of germ layers in vertebrate embryos. Cell. Mol. Life Sci. doi:10.1007/s00018-015-2092-y

Kikuchi, A., Yamamoto, H., Sato, A., 2009. Selective activation mechanisms of Wnt signaling pathways. Trends in cell biology 19, 119–29. doi:10.1016/j.tcb.2009.01.003

Kim, S., Kim, D., Cho, S.W., Kim, J., Kim, J.-S., 2014. Highly efficient RNA-guided genome editing in human cells via delivery of purified Cas9 ribonucleoproteins. Genome Res 24, 1012–1019. doi:10.1101/gr.171322.113

Kimelman, D., 2006. Mesoderm induction: from caps to chips. Nat Rev Genet 7, 360–372. doi:10.1038/nrg1837

Kimelman, D., Kirschner, M., 1987. Synergistic induction of mesoderm by FGF and TGF-β and the identification of an mRNA coding for FGF in the early xenopus embryo. Cell 51, 869–877. doi:10.1016/0092-8674(87)90110-3

Kintner, C.R., Brockes, J.P., 1984. Monoclonal antibodies identify blastemal cells derived from dedifferentiating limb regeneration. Nature 308, 67–69.

Kitajima, S., Takagi, A., Inoue, T., Saga, Y., 2000. MesP1 and MesP2 are essential for the development of cardiac mesoderm. Development 127, 3215–3226.

Knights, C.D., Catania, J., Di Giovanni, S., Muratoglu, S., Perez, R., Swartzbeck, A., Quong, A.A., Zhang, X., Beerman, T., Pestell, R.G., Avantaggiati, M.L., 2006. Distinct p53 acetylation cassettes differentially influence gene-expression patterns and cell fate. J. Cell Biol. 173, 533–544. doi:10.1083/jcb.200512059

Kok, F.O., Shin, M., Ni, C.-W., Gupta, A., Grosse, A.S., van Impel, A., Kirchmaier, B.C., Peterson-Maduro, J., Kourkoulis, G., Male, I., DeSantis, D.F., Sheppard-Tindell, S., Ebarasi, L., Betsholtz, C., Schulte-Merker, S., Wolfe, S.A., Lawson, N.D.,

2015. Reverse Genetic Screening Reveals Poor Correlation between Morpholino-Induced and Mutant Phenotypes in Zebrafish. Developmental Cell 32, 97–108. doi:10.1016/j.devcel.2014.11.018

Kolker, S.J., Tajchman, U., Weeks, D.L., 2000. Confocal Imaging of Early Heart Development in Xenopus laevis. Developmental Biology 218, 64–73. doi:10.1006/dbio.1999.9558

Komarov, P.G., Komarova, E.A., Kondratov, R.V., Christov-Tselkov, K., Coon, J.S., Chernov, M.V., Gudkov, A.V., 1999. A chemical inhibitor of p53 that protects mice from the side effects of cancer therapy. Science 285, 1733–1737.

Komiya, Y., Habas, R., 2008. Wnt signal transduction pathways. Organogenesis 4, 68–75.

Komuro, I., Izumo, S., 1993. Csx: a murine homeobox-containing gene specifically expressed in the developing heart. Proc Natl Acad Sci U S A 90, 8145–8149.

Kriegmair, M.C., Frenz, S., Dusl, M., Franz, W.M., David, R., Rupp, R.A., 2013. Cardiac differentiation in Xenopus is initiated by mespa. Cardiovascular research 97, 454–63. doi:10.1093/cvr/cvs354

Kumano, G., Ezal, C., Smith, W.C., 2001. Boundaries and functional domains in the animal/vegetal axis of Xenopus gastrula mesoderm. Dev. Biol. 236, 465–477. doi:10.1006/dbio.2001.0341

Kuo, C.T., Morrisey, E.E., Anandappa, R., Sigrist, K., Lu, M.M., Parmacek, M.S., Soudais, C., Leiden, J.M., 1997. GATA4 transcription factor is required for ventral morphogenesis and heart tube formation. Genes Dev. 11, 1048–1060.

Ladd, A.N., Yatskievych, T.A., Antin, P.B., 1998. Regulation of avian cardiac myogenesis by activin/TGFbeta and bone morphogenetic proteins. Dev. Biol. 204, 407–419. doi:10.1006/dbio.1998.9094

Laflamme, M.A., Murry, C.E., 2005. Regenerating the heart. Nat Biotech 23, 845–856. doi:10.1038/nbt1117

Lane, D.P., 1992. Cancer. p53, guardian of the genome. Nature 358, 15–16. doi:10.1038/358015a0

Lane, D.P., Crawford, L.V., 1979. T antigen is bound to a host protein in SV40-transformed cells. Nature 278, 261–263.

Langdon, Y.G., Goetz, S.C., Berg, A.E., Swanik, J.T., Conlon, F.L., 2007. SHP-2 is required for the maintenance of cardiac progenitors. Development 134, 4119–4130. doi:10.1242/dev.009290

Latinkić, B.V., Cooper, B., Smith, S., Kotecha, S., Towers, N., Sparrow, D., Mohun, T.J., 2004. Transcriptional regulation of the cardiac-specific MLC2 gene during Xenopus embryonic development. Development 131, 669–679. doi:10.1242/dev.00953

Latinkić, B.V., Kotecha, S., Mohun, T.J., 2003. Induction of cardiomyocytes by GATA4 in Xenopus ectodermal explants. Development 130, 3865–3876. doi:10.1242/dev.00599

Laverriere, A.C., MacNeill, C., Mueller, C., Poelmann, R.E., Burch, J.B., Evans, T., 1994. GATA-4/5/6, a subfamily of three transcription factors transcribed in developing heart and gut. J. Biol. Chem. 269, 23177–23184.

Lavin, M.F., Gueven, N., 2006. The complexity of p53 stabilization and activation. Cell Death Differ. 13, 941–950. doi:10.1038/sj.cdd.4401925

Lea, R., Papalopulu, N., Amaya, E., Dorey, K., 2009. Temporal and spatial expression of FGF ligands and receptors during Xenopus development. Dev Dyn 238, 1467–79. doi:10.1002/dvdy.21913

Lee, M.A., Heasman, J., Whitman, M., 2001. Timing of endogenous activin-like signals and regional specification of the Xenopus embryo. Development 128, 2939–2952.

Lei, Y., Guo, X., Liu, Y., Cao, Y., Deng, Y., Chen, X., Cheng, C.H.K., Dawid, I.B., Chen, Y., Zhao, H., 2012. Efficient targeted gene disruption in Xenopus embryos using engineered transcription activator-like effector nucleases (TALENs). Proc. Natl. Acad. Sci. U.S.A. 109, 17484–17489. doi:10.1073/pnas.1215421109

Lenhart, K.F., Holtzman, N.G., Williams, J.R., Burdine, R.D., 2013. Integration of Nodal and BMP Signals in the Heart Requires FoxH1 to Create Left–Right Differences in Cell Migration Rates That Direct Cardiac Asymmetry. PLoS Genet 9, e1003109. doi:10.1371/journal.pgen.1003109

Levrero, M., De Laurenzi, V., Costanzo, A., Gong, J., Wang, J.Y., Melino, G., 2000. The p53/p63/p73 family of transcription factors: overlapping and distinct functions. J. Cell. Sci. 113 (Pt 10), 1661–1670.

Li, Y., Liu, J., Li, W., Brown, A., Baddoo, M., Li, M., Carroll, T., Oxburgh, L., Feng, Y., Saifudeen, Z., 2015. p53 enables metabolic fitness and self-renewal of nephron progenitor cells. Development 142, 1228–1241. doi:10.1242/dev.111617

Lian, X., Zhang, J., Azarin, S.M., Zhu, K., Hazeltine, L.B., Bao, X., Hsiao, C., Kamp, T.J., Palecek, S.P., 2013. Directed cardiomyocyte differentiation from human pluripotent stem cells by modulating Wnt/β-catenin signaling under fully defined conditions. Nat. Protocols 8, 162–175. doi:10.1038/nprot.2012.150

Libby, P., Theroux, P., 2005. Pathophysiology of Coronary Artery Disease. Circulation 111, 3481–3488. doi:10.1161/CIRCULATIONAHA.105.537878

Lickert, H., Kutsch, S., Kanzler, B., Tamai, Y., Taketo, M.M., Kemler, R., 2002. Formation of multiple hearts in mice following deletion of beta-catenin in the embryonic endoderm. Developmental cell 3, 171–81.

Lien, C.L., Wu, C., Mercer, B., Webb, R., Richardson, J.A., Olson, E.N., 1999. Control of early cardiac-specific transcription of Nkx2-5 by a GATA-dependent enhancer. Development 126, 75–84.

Lin, X., Duan, X., Liang, Y.Y., Su, Y., Wrighton, K.H., Long, J., Hu, M., Davis, C.M., Wang, J., Brunicardi, F.C., Shi, Y., Chen, Y.G., Meng, A., Feng, X.H., 2006. PPM1A functions as a Smad phosphatase to terminate TGFbeta signaling. Cell 125, 915–28. doi:10.1016/j.cell.2006.03.044

Lints, T.J., Parsons, L.M., Hartley, L., Lyons, I., Harvey, R.P., 1993. Nkx-2.5: a novel murine homeobox gene expressed in early heart progenitor cells and their myogenic descendants. Development 119, 419–431.

Liu, J., Stainier, D.Y.R., 2012. Zebrafish in the study of early cardiac development. Circ. Res. 110, 870–874. doi:10.1161/CIRCRESAHA.111.246504

Lo, R.S., Massague, J., 1999. Ubiquitin-dependent degradation of TGF-beta-activated smad2. Nature cell biology 1, 472–8. doi:10.1038/70258

Logan, C.Y., Nusse, R., 2004. The Wnt Signaling Pathway in Development and Disease. Annual Review of Cell and Developmental Biology 20, 781–810. doi:10.1146/annurev.cellbio.20.010403.113126

Logan, M., Mohun, T., 1993. Induction of cardiac muscle differentiation in isolated animal pole explants of Xenopus laevis embryos. Development 118, 865–875.

Lohr, J.L., Danos, M.C., Groth, T.W., Yost, H.J., 1998. Maintenance of asymmetric nodal expression in Xenopus laevis. Dev. Genet. 23, 194–202. doi:10.1002/(SICI)1520-6408(1998)23:3<194::AID-DVG5>3.0.CO;2-0

Lohr, J.L., Danos, M.C., Yost, H.J., 1997. Left-right asymmetry of a nodal-related gene is regulated by dorsoanterior midline structures during Xenopus development. Development 124, 1465–1472.

Lohr, J.L., Yost, H.J., 2000. Vertebrate model systems in the study of early heart development: Xenopus and zebrafish. American journal of medical genetics 97, 248–57.

Lopez-Sanchez, C., Franco, D., Bonet, F., Garcia-Lopez, V., Aranega, A., Garcia-Martinez, V., 2015. Reciprocal repression between Fgf8 and miR-133 regulates cardiac induction through Bmp2 signaling. Data Brief 5, 59–64. doi:10.1016/j.dib.2015.08.009

Lough, J., Barron, M., Brogley, M., Sugi, Y., Bolender, D.L., Zhu, X., 1996. Combined BMP-2 and FGF-4, but neither factor alone, induces cardiogenesis in non-precardiac embryonic mesoderm. Developmental biology 178, 198–202. doi:10.1006/dbio.1996.0211

Lowe, L.A., Yamada, S., Kuehn, M.R., 2001. Genetic dissection of nodal function in patterning the mouse embryo. Development (Cambridge, England) 128, 1831–43.

Lu, P., Barad, M., Vize, P.D., 2001. Xenopus p63 expression in early ectoderm and neurectoderm. Mech. Dev. 102, 275–278.

Lustig, K.D., Kroll, K., Sun, E., Ramos, R., Elmendorf, H., Kirschner, M.W., 1996. A Xenopus nodal-related gene that acts in synergy with noggin to induce complete secondary axis and notochord formation. Development 122, 3275–3282.

Luxardi, G., Marchal, L., Thomé, V., Kodjabachian, L., 2010. Distinct Xenopus Nodal ligands sequentially induce mesendoderm and control gastrulation movements in parallel to the Wnt/PCP pathway. Development 137, 417–426. doi:10.1242/dev.039735

MacDonald, B.T., Tamai, K., He, X., 2009. Wnt/β-catenin signaling: components, mechanisms, and diseases. Dev Cell 17, 9–26. doi:10.1016/j.devcel.2009.06.016

Manner, J., Wessel, A., Yelbuz, T.M., 2010. How does the tubular embryonic heart work? Looking for the physical mechanism generating unidirectional blood flow in the valveless embryonic heart tube. Developmental dynamics : an official publication of the American Association of Anatomists 239, 1035–46. doi:10.1002/dvdy.22265

Maroon, H., Walshe, J., Mahmood, R., Kiefer, P., Dickson, C., Mason, I., 2002. Fgf3 and Fgf8 are required together for formation of the otic placode and vesicle. Development 129, 2099–2108.

Marques, S.R., Lee, Y., Poss, K.D., Yelon, D., 2008. Reiterative roles for FGF signaling in the establishment of size and proportion of the zebrafish heart. Developmental biology 321, 397–406. doi:10.1016/j.ydbio.2008.06.033

Martin, G.R., 1998. The roles of FGFs in the early development of vertebrate limbs. Genes Dev. 12, 1571–1586.

Martinsen, B.J., 2005. Reference guide to the stages of chick heart embryology. Dev. Dyn. 233, 1217–1237. doi:10.1002/dvdy.20468

Marvin, M.J., Di Rocco, G., Gardiner, A., Bush, S.M., Lassar, A.B., 2001. Inhibition of Wnt activity induces heart formation from posterior mesoderm. Genes & Development 15, 316–327. doi:10.1101/gad.855501

Massagué, J., 1998. TGF-beta signal transduction. Annu. Rev. Biochem. 67, 753–791. doi:10.1146/annurev.biochem.67.1.753

Mathis, L., Kulesa, P.M., Fraser, S.E., 2001. FGF receptor signalling is required to maintain neural progenitors during Hensen's node progression. Nat. Cell Biol. 3, 559–566. doi:10.1038/35078535

Mead, P.E., Kelley, C.M., Hahn, P.S., Piedad, O., Zon, L.I., 1998. SCL specifies hematopoietic mesoderm in Xenopus embryos. Development 125, 2611–2620.

Meek, D.W., Anderson, C.W., 2009. Posttranslational modification of p53: cooperative integrators of function. Cold Spring Harbor perspectives in biology 1, a000950. doi:10.1101/cshperspect.a000950

Mercola, M., Ruiz-Lozano, P., Schneider, M.D., 2011. Cardiac muscle regeneration: lessons from development. Genes & Development 25, 299–309. doi:10.1101/gad.2018411

Michelson, A.M., Gisselbrecht, S., Zhou, Y., Baek, K.H., Buff, E.M., 1998. Dual functions of the heartless fibroblast growth factor receptor in development of the Drosophila embryonic mesoderm. Developmental genetics 22, 212–29. doi:10.1002/(sici)1520-6408(1998)22:3<212::aid-dvg4>3.0.co;2-9

Mohammadi, M., McMahon, G., Sun, L., Tang, C., Hirth, P., Yeh, B.K., Hubbard, S.R., Schlessinger, J., 1997. Structures of the tyrosine kinase domain of fibroblast growth factor receptor in complex with inhibitors. Science 276, 955–960.

Mohun, T., Orford, R., Shang, C., 2003. The origins of cardiac tissue in the amphibian, Xenopus laevis. Trends in cardiovascular medicine 13, 244–8.

Mohun, T., Sparrow, D., 1997. Early steps in vertebrate cardiogenesis. Current opinion in genetics & development 7, 628–33.

Mohun, T.J., Leong, L.M., Weninger, W.J., Sparrow, D.B., 2000. The Morphology of Heart Development in Xenopus laevis. Developmental Biology 218, 74–88. doi:10.1006/dbio.1999.9559

Molchadsky, A., Rivlin, N., Brosh, R., Rotter, V., Sarig, R., 2010. p53 is balancing development, differentiation and de-differentiation to assure cancer prevention. Carcinogenesis 31, 1501–1508. doi:10.1093/carcin/bgq101

Molkentin, J.D., Lin, Q., Duncan, S.A., Olson, E.N., 1997. Requirement of the transcription factor GATA4 for heart tube formation and ventral morphogenesis. Genes Dev. 11, 1061–1072.

Moody, S.A., 1987. Fates of the blastomeres of the 32-cell-stage Xenopus embryo. Developmental Biology 122, 300–319. doi:10.1016/0012-1606(87)90296-X

Moon, R.T., Kimelman, D., 1998. From cortical rotation to organizer gene expression: toward a molecular explanation of axis specification in Xenopus. Bioessays 20, 536–545. doi:10.1002/(SICI)1521-1878(199807)20:7<536::AID-BIES4>3.0.CO;2-I

Moorman, A., Webb, S., Brown, N.A., Lamers, W., Anderson, R.H., 2003. Development of the heart: (1) formation of the cardiac chambers and arterial trunks. Heart (British Cardiac Society) 89, 806–14.

Murray-Zmijewski, F., Lane, D.P., Bourdon, J.-C., 2006. p53/p63/p73 isoforms: an orchestra of isoforms to harmonise cell differentiation and response to stress. Cell Death Differ. 13, 962–972. doi:10.1038/sj.cdd.4401914

Myers, C.T., Appleby, S.C., Krieg, P.A., 2014. Use of small molecule inhibitors of the Wnt and Notch signaling pathways during Xenopus development. Methods 66, 380–389. doi:10.1016/j.ymeth.2013.08.036

Nadal-Ginard, B., Kajstura, J., Leri, A., Anversa, P., 2003. Myocyte death, growth, and regeneration in cardiac hypertrophy and failure. Circulation research 92, 139–50.

Nagai, T., Ibata, K., Park, E.S., Kubota, M., Mikoshiba, K., Miyawaki, A., 2002. A variant of yellow fluorescent protein with fast and efficient maturation for cell-biological applications. Nat Biotech 20, 87–90. doi:10.1038/nbt0102-87

Naito, A.T., Shiojima, I., Akazawa, H., Hidaka, K., Morisaki, T., Kikuchi, A., Komuro, I., 2006. Developmental stage-specific biphasic roles of Wnt/beta-catenin signaling in cardiomyogenesis and hematopoiesis. Proceedings of the National Academy of Sciences of the United States of America 103, 19812–7. doi:10.1073/pnas.0605768103

Nakamura, T., Sano, M., Songyang, Z., Schneider, M.D., 2003. A Wnt- and beta -catenin-dependent pathway for mammalian cardiac myogenesis. Proceedings of the National Academy of Sciences of the United States of America 100, 5834–9. doi:10.1073/pnas.0935626100

Nakayama, T., Blitz, I.L., Fish, M.B., Odeleye, A.O., Manohar, S., Cho, K.W.Y., Grainger, R.M., 2014. Chapter Seventeen Cas9-Based Genome Editing in Xenopus tropicalis. Methods Enzymol 546, 355–375. doi:10.1016/B978-0-12-801185-0.00017-9

Nakayama, T., Fish, M.B., Fisher, M., Oomen-Hajagos, J., Thomsen, G.H., Grainger, R.M., 2013. Simple and efficient CRISPR/Cas9-mediated targeted mutagenesis in Xenopus tropicalis. Genesis (New York, N.Y. : 2000) 51, 835–43. doi:10.1002/dvg.22720

Nicolás, F.J., De Bosscher, K., Schmierer, B., Hill, C.S., 2004. Analysis of Smad nucleocytoplasmic shuttling in living cells. J. Cell. Sci. 117, 4113–4125. doi:10.1242/jcs.01289

Niehrs, C., 2004. Regionally specific induction by the Spemann–Mangold organizer. Nat Rev Genet 5, 425–434. doi:10.1038/nrg1347

Nieuwkoop, P., Faber, J., 1994. Normal Table of Xenopus laevis (Daudin). Garland Publishing Inc, New York ISBN 0-8153-1896-0.

Nomura, M., Li, E., 1998. Smad2 role in mesoderm formation, left–right patterning and craniofacial development. Nature 393, 786–790. doi:10.1038/31693

Noseda, M., Peterkin, T., Simões, F.C., Patient, R., Schneider, M.D., 2011. Cardiopoietic factors: extracellular signals for cardiac lineage commitment. Circ. Res. 108, 129–152. doi:10.1161/CIRCRESAHA.110.223792

Nutt, S.L., Dingwell, K.S., Holt, C.E., Amaya, E., 2001. Xenopus Sprouty2 inhibits FGF-mediated gastrulation movements but does not affect mesoderm induction and patterning. Genes Dev 15, 1152–1166. doi:10.1101/gad.191301

Okabayashi, K., Asashima, M., 2003. Tissue generation from amphibian animal caps. Current Opinion in Genetics & Development 13, 502–507. doi:10.1016/S0959-437X(03)00111-4

Olivier, M., Hollstein, M., Hainaut, P., 2010. TP53 Mutations in Human Cancers: Origins, Consequences, and Clinical Use. Cold Spring Harb Perspect Biol 2. doi:10.1101/cshperspect.a001008

Olovnikov, I.A., Kravchenko, J.E., Chumakov, P.M., 2009. Homeostatic functions of the p53 tumor suppressor: Regulation of energy metabolism and antioxidant defense. Seminars in Cancer Biology, The Warburg Effect: The Re-discovery of the Importance of Aerobic Glycolysis in Tumor Cells 19, 32–41. doi:10.1016/j.semcancer.2008.11.005

Olson, E.N., 2006. Gene regulatory networks in the evolution and development of the heart. Science (New York, N.Y.) 313, 1922–7. doi:10.1126/science.1132292

Olson, E.N., Srivastava, D., 1996. Molecular pathways controlling heart development. Science (New York, N.Y.) 272, 671–6.

Org, T., Duan, D., Ferrari, R., Montel-Hagen, A., Van Handel, B., Kerényi, M.A., Sasidharan, R., Rubbi, L., Fujiwara, Y., Pellegrini, M., Orkin, S.H., Kurdistani, S.K., Mikkola, H.K., 2015. Scl binds to primed enhancers in mesoderm to regulate hematopoietic and cardiac fate divergence. EMBO J. 34, 759–777. doi:10.15252/embj.201490542

Ornitz, D.M., Itoh, N., 2015. The Fibroblast Growth Factor signaling pathway. WIREs Dev Biol 4, 215–266. doi:10.1002/wdev.176

Osada, S.I., Wright, C.V., 1999. Xenopus nodal-related signaling is essential for mesendodermal patterning during early embryogenesis. Development (Cambridge, England) 126, 3229–40.

Pandur, P., Sirbu, I.O., Kuhl, S.J., Philipp, M., Kuhl, M., 2013. Islet1-expressing cardiac progenitor cells: a comparison across species. Development genes and evolution 223, 117–29. doi:10.1007/s00427-012-0400-1

Pant, V., Quintás-Cardama, A., Lozano, G., 2012. The p53 pathway in hematopoiesis: lessons from mouse models, implications for humans. Blood 120, 5118–5127. doi:10.1182/blood-2012-05-356014

Parameswaran, M., Tam, P.P., 1995. Regionalisation of cell fate and morphogenetic movement of the mesoderm during mouse gastrulation. Developmental genetics 17, 16–28. doi:10.1002/dvg.1020170104

Paranjpe, S.S., Veenstra, G.J.C., 2015. Establishing pluripotency in early development. Biochimica et Biophysica Acta (BBA) - Gene Regulatory Mechanisms 1849, 626–636. doi:10.1016/j.bbagrm.2015.03.006

Parisi, S., D'Andrea, D., Lago, C.T., Adamson, E.D., Persico, M.G., Minchiotti, G., 2003. Nodal-dependent Cripto signaling promotes cardiomyogenesis and redirects

the neural fate of embryonic stem cells. The Journal of cell biology 163, 303–14. doi:10.1083/jcb.200303010

Patient, R.K., McGhee, J.D., 2002. The GATA family (vertebrates and invertebrates). Current opinion in genetics & development 12, 416–22.

Pawani, H., Bhartiya, D., 2013. Pluripotent stem cells for cardiac regeneration: Overview of recent advances & emerging trends. Indian J Med Res 137, 270–282.

Payne, D.M., Rossomando, A.J., Martino, P., Erickson, A.K., Her, J.H., Shabanowitz, J., Hunt, D.F., Weber, M.J., Sturgill, T.W., 1991. Identification of the regulatory phosphorylation sites in pp42/mitogen-activated protein kinase (MAP kinase). EMBO J. 10, 885–892.

Pérez-Pomares, J.M., González-Rosa, J.M., Muñoz-Chápuli, R., 2009. Building the vertebrate heart - an evolutionary approach to cardiac development. Int. J. Dev. Biol. 53, 1427–1443. doi:10.1387/ijdb.072409jp

Perrimon, N., Pitsouli, C., Shilo, B.-Z., 2012. Signaling Mechanisms Controlling Cell Fate and Embryonic Patterning. Cold Spring Harb Perspect Biol 4, a005975. doi:10.1101/cshperspect.a005975

Peterkin, T., Gibson, A., Patient, R., 2009. Common genetic control of haemangioblast and cardiac development in zebrafish. Development 136, 1465–1474. doi:10.1242/dev.032748

Piccolo, S., 2008. p53 Regulation Orchestrates the TGF-β Response. Cell 133, 767–769. doi:10.1016/j.cell.2008.05.013

Piccolo, S., Agius, E., Leyns, L., Bhattacharyya, S., Grunz, H., Bouwmeester, T., De Robertis, E.M., 1999. The head inducer Cerberus is a multifunctional antagonist of Nodal, BMP and Wnt signals. Nature 397, 707–10. doi:10.1038/17820

Piepenburg, O., Grimmer, D., Williams, P.H., Smith, J.C., 2004. Activin redux: specification of mesodermal pattern in Xenopus by graded concentrations of endogenous activin B. Development 131, 4977–4986. doi:10.1242/dev.01323

Porath, J., Flodin, P., 1959. Gel filtration: a method for desalting and group separation. Nature 183, 1657–1659.

Powers, S.E., Taniguchi, K., Yen, W., Melhuish, T.A., Shen, J., Walsh, C.A., Sutherland, A.E., Wotton, D., 2010. Tgif1 and Tgif2 regulate Nodal signaling and are required for gastrulation. Development (Cambridge, England) 137, 249–59. doi:10.1242/dev.040782

Pownall, M.E., Tucker, A.S., Slack, J.M., Isaacs, H.V., 1996. eFGF, Xcad3 and Hox genes form a molecular pathway that establishes the anteroposterior axis in Xenopus. Development (Cambridge, England) 122, 3881–92.

Pratilas, C.A., Hanrahan, A.J., Halilovic, E., Persaud, Y., Soh, J., Chitale, D., Shigematsu, H., Yamamoto, H., Sawai, A., Janakiraman, M., Taylor, B.S., Pao, W., Toyooka, S., Ladanyi, M., Gazdar, A., Rosen, N., Solit, D.B., 2008. Genetic Predictors of MEK Dependence in Non–Small Cell Lung Cancer. Cancer Res 68, 9375–9383. doi:10.1158/0008-5472.CAN-08-2223

Qian, L., Huang, Y., Spencer, C.I., Foley, A., Vedantham, V., Liu, L., Conway, S.J., Fu, J., Srivastava, D., 2012. In vivo reprogramming of murine cardiac fibroblasts into induced cardiomyocytes. Nature 485, 593–598. doi:10.1038/nature11044

Ramsdell, A.F., 2005. Left–right asymmetry and congenital cardiac defects: Getting to the heart of the matter in vertebrate left–right axis determination. Developmental Biology 288, 1–20. doi:10.1016/j.ydbio.2005.07.038

Rana, A.A., Roper, S.J., Palmer, E.A., Smith, J.C., 2011. Loss of Xenopus tropicalis EMSY causes impairment of gastrulation and upregulation of p53. N Biotechnol 28, 334–341. doi:10.1016/j.nbt.2010.10.010

Rankin, S.A., Gallas, A.L., Neto, A., Gomez-Skarmeta, J.L., Zorn, A.M., 2012. Suppression of Bmp4 signaling by the zinc-finger repressors Osr1 and Osr2 is required for Wnt/beta-catenin-mediated lung specification in Xenopus. Development (Cambridge, England) 139, 3010–20. doi:10.1242/dev.078220

Reifers, F., Bohli, H., Walsh, E.C., Crossley, P.H., Stainier, D.Y., Brand, M., 1998. Fgf8 is mutated in zebrafish acerebellar (ace) mutants and is required for maintenance of midbrain-hindbrain boundary development and somitogenesis. Development 125, 2381–2395.

Reifers, F., Walsh, E.C., Leger, S., Stainier, D.Y., Brand, M., 2000. Induction and differentiation of the zebrafish heart requires fibroblast growth factor 8 (fgf8/acerebellar). Development (Cambridge, England) 127, 225–35.

Reissmann, E., Jörnvall, H., Blokzijl, A., Andersson, O., Chang, C., Minchiotti, G., Persico, M.G., Ibáñez, C.F., Brivanlou, A.H., 2001. The orphan receptor ALK7 and the Activin receptor ALK4 mediate signaling by Nodal proteins during vertebrate development. Genes Dev. 15, 2010–2022. doi:10.1101/gad.201801

Reiter, J.F., Alexander, J., Rodaway, A., Yelon, D., Patient, R., Holder, N., Stainier, D.Y., 1999. Gata5 is required for the development of the heart and endoderm in zebrafish. Genes Dev. 13, 2983–2995.

Reiter, J.F., Verkade, H., Stainier, D.Y., 2001. Bmp2b and Oep promote early myocardial differentiation through their regulation of gata5. Developmental biology 234, 330–8. doi:10.1006/dbio.2001.0259

Ricciardi, M.R., Scerpa, M.C., Bergamo, P., Ciuffreda, L., Petrucci, M.T., Chiaretti, S., Tavolaro, S., Mascolo, M.G., Abrams, S.L., Steelman, L.S., Tsao, T., Marchetti, A., Konopleva, M., Del Bufalo, D., Cognetti, F., Foà, R., Andreeff, M., McCubrey, J.A., Tafuri, A., Milella, M., 2012. Therapeutic potential of MEK inhibition in acute myelogenous leukemia: rationale for “vertical” and “lateral” combination strategies. J. Mol. Med. 90, 1133–1144. doi:10.1007/s00109-012-0886-z

Ringshausen, I., O’Shea, C.C., Finch, A.J., Swigart, L.B., Evan, G.I., 2006. Mdm2 is critically and continuously required to suppress lethal p53 activity in vivo. Cancer Cell 10, 501–514. doi:10.1016/j.ccr.2006.10.010

Rivlin, N., Brosh, R., Oren, M., Rotter, V., 2011. Mutations in the p53 Tumor Suppressor Gene Important Milestones at the Various Steps of Tumorigenesis. Genes & Cancer 2, 466–474. doi:10.1177/1947601911408889

Roberts, A.B., Sporn, M.B., 1993. Physiological actions and clinical applications of transforming growth factor-beta (TGF-beta). Growth factors (Chur, Switzerland) 8, 1–9.

Roger, V.L., 2013. Epidemiology of Heart Failure. Circulation Research 113, 646–659. doi:10.1161/CIRCRESAHA.113.300268

Rogers, K.W., Schier, A.F., 2011. Morphogen gradients: from generation to interpretation. Annu. Rev. Cell Dev. Biol. 27, 377–407. doi:10.1146/annurev-cellbio-092910-154148

Roos-Hesselink, J.W., Kerstjens-Frederikse, W.S., Meijboom, F.J., Pieper, P.G., 2005. Inheritance of congenital heart disease. Neth Heart J 13, 88–91.

Rosa, A., Spagnoli, F.M., Brivanlou, A.H., 2009. The miR-430/427/302 family controls mesendodermal fate specification via species-specific target selection. Dev. Cell 16, 517–527. doi:10.1016/j.devcel.2009.02.007

Ross, S., Hill, C.S., 2008. How the Smads regulate transcription. The International Journal of Biochemistry & Cell Biology 40, 383–408. doi:10.1016/j.biocel.2007.09.006

Rossant, J., 1996. Mouse mutants and cardiac development: new molecular insights into cardiogenesis. Circulation research 78, 349–53.

Rossi, A., Kontarakis, Z., Gerri, C., Nolte, H., Hölper, S., Krüger, M., Stainier, D.Y.R., 2015. Genetic compensation induced by deleterious mutations but not gene knockdowns. Nature. doi:10.1038/nature14580

Saga, Y., Hata, N., Kobayashi, S., Magnuson, T., Seldin, M.F., Taketo, M.M., 1996. MesP1: a novel basic helix-loop-helix protein expressed in the nascent mesodermal cells during mouse gastrulation. Development 122, 2769–2778.

Saga, Y., Hata, N., Koseki, H., Taketo, M.M., 1997. Mesp2: a novel mouse gene expressed in the presegmented mesoderm and essential for segmentation initiation. Genes Dev. 11, 1827–1839.

Saga, Y., Miyagawa-Tomita, S., Takagi, A., Kitajima, S., Miyazaki, J. i, Inoue, T., 1999. MesP1 is expressed in the heart precursor cells and required for the formation of a single heart tube. Development 126, 3437–3447.

Sah, V.P., Attardi, L.D., Mulligan, G.J., Williams, B.O., Bronson, R.T., Jacks, T., 1995. A subset of p53-deficient embryos exhibit exencephaly. Nat. Genet. 10, 175–180. doi:10.1038/ng0695-175

Saka, Y., Hagemann, A.I., Piepenburg, O., Smith, J.C., 2007. Nuclear accumulation of Smad complexes occurs only after the midblastula transition in Xenopus. Development 134, 4209–4218. doi:10.1242/dev.010645

Saka, Y., Hagemann, A.I., Smith, J.C., 2008. Visualizing protein interactions by bimolecular fluorescence complementation in Xenopus. Methods, Visualization of molecular processes in cells using fluorescence imaging 45, 192–195. doi:10.1016/j.ymeth.2008.06.005

Sakata, H., Maeno, M., 2014. Nkx2.5 is involved in myeloid cell differentiation at anterior ventral blood islands in the Xenopus embryo. Development, growth & differentiation 56, 544–54. doi:10.1111/dgd.12155

Sakuma, R., Ohnishi Yi, Y., Meno, C., Fujii, H., Juan, H., Takeuchi, J., Ogura, T., Li, E., Miyazono, K., Hamada, H., 2002. Inhibition of Nodal signalling by Lefty mediated through interaction with common receptors and efficient diffusion. Genes Cells 7, 401–412.

Samuel, L.J., Latinkić, B.V., 2009. Early Activation of FGF and Nodal Pathways Mediates Cardiac Specification Independently of Wnt/β-Catenin Signaling. PLoS ONE 4, e7650. doi:10.1371/journal.pone.0007650

Sander, J.D., Joung, J.K., 2014. CRISPR-Cas systems for editing, regulating and targeting genomes. Nat Biotech 32, 347–355. doi:10.1038/nbt.2842

Sasai, N., Yakura, R., Kamiya, D., Nakazawa, Y., Sasai, Y., 2008. Ectodermal Factor Restricts Mesoderm Differentiation by Inhibiting p53. Cell 133, 878–890. doi:10.1016/j.cell.2008.03.035

Sater, A.K., Jacobson, A.G., 1989. The specification of heart mesoderm occurs during gastrulation in Xenopus laevis. Development 105, 821–830.

Schier, A.F., 2009. Nodal morphogens. Cold Spring Harbor perspectives in biology 1, a003459. doi:10.1101/cshperspect.a003459

Schier, A.F., 2003. Nodal signaling in vertebrate development. Annu. Rev. Cell Dev. Biol. 19, 589–621. doi:10.1146/annurev.cellbio.19.041603.094522

Schlessinger, J., Plotnikov, A.N., Ibrahimi, O.A., Eliseenkova, A.V., Yeh, B.K., Yayon, A., Linhardt, R.J., Mohammadi, M., 2000. Crystal structure of a ternary FGF-FGFR-heparin complex reveals a dual role for heparin in FGFR binding and dimerization. Mol. Cell 6, 743–750.

Schmid, P., Lorenz, A., Hameister, H., Montenarh, M., 1991. Expression of p53 during mouse embryogenesis. Development 113, 857–865.

Schmierer, B., Hill, C.S., 2007. TGF[beta]-SMAD signal transduction: molecular specificity and functional flexibility. Nat Rev Mol Cell Biol 8, 970–982. doi:10.1038/nrm2297

Schneider, V.A., Mercola, M., 2001. Wnt antagonism initiates cardiogenesis in Xenopus laevis. Genes & Development 15, 304–315. doi:10.1101/gad.855601

Schoenwolf, G.C., Garcia-Martinez, V., Dias, M.S., 1992. Mesoderm movement and fate during avian gastrulation and neurulation. Dev. Dyn. 193, 235–248. doi:10.1002/aja.1001930304

Schohl, A., Fagotto, F., 2002. β-catenin, MAPK and Smad signaling during early Xenopus development. Development 129, 37–52.

Schoppy, D.W., Ruzankina, Y., Brown, E.J., 2010. Removing all obstacles. Cell Cycle 9, 1313–1319.

Schultheiss, T.M., Burch, J.B., Lassar, A.B., 1997. A role for bone morphogenetic proteins in the induction of cardiac myogenesis. Genes & development 11, 451–62.

Scott, I.C., 2012. Life before Nkx2.5: cardiovascular progenitor cells: embryonic origins and development. Curr. Top. Dev. Biol. 100, 1–31. doi:10.1016/B978-0-12-387786-4.00001-4

Sebolt-Leopold, J.S., 2008. Advances in the development of cancer therapeutics directed against the RAS-mitogen-activated protein kinase pathway. Clin. Cancer Res. 14, 3651–3656. doi:10.1158/1078-0432.CCR-08-0333

Sebolt-Leopold, J.S., Herrera, R., 2004. Targeting the mitogen-activated protein kinase cascade to treat cancer. Nat Rev Cancer 4, 937–947. doi:10.1038/nrc1503

Sell, S., 2013. Stem Cells Handbook. Springer Science & Business Media.

Shaner, N.C., Campbell, R.E., Steinbach, P.A., Giepmans, B.N.G., Palmer, A.E., Tsien, R.Y., 2004. Improved monomeric red, orange and yellow fluorescent proteins derived from Discosoma sp. red fluorescent protein. Nat Biotech 22, 1567–1572. doi:10.1038/nbt1037

Sharpe, P., Mason, I., 2009. Molecular Embryology: Methods and Protocols, Second edition. ed. Humana Press.

Shaul, Y.D., Seger, R., 2007. The MEK/ERK cascade: From signaling specificity to diverse functions. Biochimica et Biophysica Acta (BBA) - Molecular Cell Research, Mitogen-Activated Protein Kinases: New Insights on Regulation, Function and Role in Human Disease 1773, 1213–1226. doi:10.1016/j.bbamcr.2006.10.005

Shen, M.M., 2007. Nodal signaling: developmental roles and regulation. Development (Cambridge, England) 134, 1023–34. doi:10.1242/dev.000166

Shi, Y., Massague, J., 2003. Mechanisms of TGF-beta signaling from cell membrane to the nucleus. Cell 113, 685–700.

Shi, Y., Wang, Y.-F., Jayaraman, L., Yang, H., Massagué, J., Pavletich, N.P., 1998. Crystal Structure of a Smad MH1 Domain Bound to DNA: Insights on DNA Binding in TGF-β Signaling. Cell 94, 585–594. doi:10.1016/S0092-8674(00)81600-1

Shifley, E.T., Kenny, A.P., Rankin, S.A., Zorn, A.M., 2012. Prolonged FGF signaling is necessary for lung and liver induction in Xenopus. BMC Developmental Biology 12.

Shimizu, K., Gurdon, J.B., 1999. A quantitative analysis of signal transduction from activin receptor to nucleus and its relevance to morphogen gradient interpretation. Proceedings of the National Academy of Sciences 96, 6791–6796. doi:10.1073/pnas.96.12.6791

Shook, D.R., Majer, C., Keller, R., 2004. Pattern and morphogenesis of presumptive superficial mesoderm in two closely related species, Xenopus laevis and Xenopus tropicalis. Dev. Biol. 270, 163–185. doi:10.1016/j.ydbio.2004.02.021

Simões, F.C., Peterkin, T., Patient, R., 2011. Fgf differentially controls cross-antagonism between cardiac and haemangioblast regulators. Development 138, 3235–3245. doi:10.1242/dev.059634

Sissman, N.J., 1970. Developmental landmarks in cardiac morphogenesis: comparative chronology. The American journal of cardiology 25, 141–8.

Sive, H.L., Grainger, R.M., M., H.R., 2000. Early Development of Xenopus laevis: A Laboratory Manual. Cold Spring Harbor Laboratory Press.

Skirkanich, J., Luxardi, G., Yang, J., Kodjabachian, L., Klein, P.S., 2011. An essential role for transcription before the MBT in Xenopus laevis. Dev Biol 357, 478–491. doi:10.1016/j.ydbio.2011.06.010

Slack, J.M., Darlington, B.G., Gillespie, L.L., Godsave, S.F., Isaacs, H.V., Paterno, G.D., 1990. Mesoderm induction by fibroblast growth factor in early Xenopus development. Philos. Trans. R. Soc. Lond., B, Biol. Sci. 327, 75–84.

Slack, J.M., Forman, D., 1980. An interaction between dorsal and ventral regions of the marginal zone in early amphibian embryos. Journal of embryology and experimental morphology 56, 283–99.

Slack, J.M.W., 1991. From Egg to Embryo: Regional Specification in Early Development. Cambridge University Press.

Smith, J.C., Howard, J.E., 1992. Mesoderm-inducing factors and the control of gastrulation. Dev. Suppl. 127–136.

Smith, J.C., Price, B.M., Van Nimmen, K., Huylebroeck, D., 1990. Identification of a potent Xenopus mesoderm-inducing factor as a homologue of activin A. Nature 345, 729–731. doi:10.1038/345729a0

Smith, J.C., Price, B.M.J., Green, J.B.A., Weigel, D., Herrmann, B.G., 1991. Expression of a xenopus homolog of Brachyury (T) is an immediate-early response to mesoderm induction. Cell 67, 79–87. doi:10.1016/0092-8674(91)90573-H

Smith, J.C., Watt, F.M., 1985. Biochemical specificity of Xenopus notochord. Differentiation 29, 109–115.

Smith, S.J., Kotecha, S., Towers, N., Latinkic, B.V., Mohun, T.J., 2002. XPOX2-peroxidase expression and the XLURP-1 promoter reveal the site of embryonic myeloid cell development in Xenopus. Mechanisms of Development 117, 173–186. doi:10.1016/S0925-4773(02)00200-9

Smith, S.J., Mohun, T.J., 2011. Early cardiac morphogenesis defects caused by loss of embryonic macrophage function in Xenopus. Mechanisms of development 128, 303–15. doi:10.1016/j.mod.2011.04.002

Smith, W.C., McKendry, R., Ribisi, S., Harland, R.M., 1995. A nodal-related gene defines a physical and functional domain within the Spemann organizer. Cell 82, 37–46.

Sonntag, K.-C., Simantov, R., Björklund, L., Cooper, O., Pruszak, J., Kowalke, F., Gilmartin, J., Ding, J., Hu, Y.-P., Shen, M.M., Isacson, O., 2005. Context-dependent neuronal differentiation and germ layer induction of Smad4-/- and Cripto-/- embryonic stem cells. Mol. Cell. Neurosci. 28, 417–429. doi:10.1016/j.mcn.2004.06.003

Spemann, H., Mangold, H., 1924. Induction of embryonic primordia by implantation of organizers from a different species. Archiv für Mikroskopische Anatomie und Entwicklungsmechanik 100, 599–638.

Stalsberg, H., DeHaan, R.L., 1969. The precardiac areas and formation of the tubular heart in the chick embryo. Developmental biology 19, 128–59.

Stenger, J.E., Mayr, G.A., Mann, K., Tegtmeyer, P., 1992. Formation of stable p53 homotetramers and multiples of tetramers. Mol. Carcinog. 5, 102–106.

Sun, X., Meyers, E.N., Lewandoski, M., Martin, G.R., 1999. Targeted disruption of Fgf8 causes failure of cell migration in the gastrulating mouse embryo. Genes & development 13, 1834–46.

Sun, Y., Dong, Z., Nakamura, K., Colburn, N.H., 1993. Dosage-dependent dominance over wild-type p53 of a mutant p53 isolated from nasopharyngeal carcinoma. The FASEB Journal 7, 944–50.

Sun, Y., Hegamyer, G., Cheng, Y.J., Hildesheim, A., Chen, J.Y., Chen, I.H., Cao, Y., Yao, K.T., Colburn, N.H., 1992. An infrequent point mutation of the p53 gene in human nasopharyngeal carcinoma. Proc Natl Acad Sci U S A 89, 6516–6520.

Tadros, W., Lipshitz, H.D., 2009. The maternal-to-zygotic transition: a play in two acts. Development 136, 3033–3042. doi:10.1242/dev.033183

Tafvizi, A., Huang, F., Leith, J.S., Fersht, A.R., Mirny, L.A., van Oijen, A.M., 2008. Tumor suppressor p53 slides on DNA with low friction and high stability. Biophys. J. 95, L01-3. doi:10.1529/biophysj.108.134122

Takahashi, S., Yokota, C., Takano, K., Tanegashima, K., Onuma, Y., Goto, J., Asashima, M., 2000. Two novel nodal-related genes initiate early inductive events in Xenopus Nieuwkoop center. Development 127, 5319–5329.

Takebayashi-Suzuki, K., Funami, J., Tokumori, D., Saito, A., Watabe, T., Miyazono, K., Kanda, A., Suzuki, A., 2003. Interplay between the tumor suppressor p53 and TGFβ signaling shapes embryonic body axes in Xenopus. Development 130, 3929–3939. doi:10.1242/dev.00615

Tandon, P., Showell, C., Christine, K., Conlon, F., 2012. Morpholino Injection in Xenopus, in: Peng, X., Antonyak, M. (Eds.), Cardiovascular Development, Methods in Molecular Biology. Humana Press, pp. 29–46.

Tararbit, K., Lelong, N., Thieulin, A.-C., Houyel, L., Bonnet, D., Goffinet, F., Khoshnood, B., 2013. The risk for four specific congenital heart defects associated with assisted reproductive techniques: a population-based evaluation. Hum Reprod 28, 367–374. doi:10.1093/humrep/des400

Tashiro, S., Sedohara, A., Asashima, M., Izutsu, Y., Maéno, M., 2006. Characterization of myeloid cells derived from the anterior ventral mesoderm in the Xenopus laevis embryo. Dev. Growth Differ. 48, 499–512. doi:10.1111/j.1440-169X.2006.00885.x

Tchang, F., Gusse, M., Soussi, T., Méchali, M., 1993. Stabilization and expression of high levels of p53 during early development in Xenopus laevis. Dev. Biol. 159, 163–172. doi:10.1006/dbio.1993.1230

Thisse, B., Thisse, C., 2005. Functions and regulations of fibroblast growth factor signaling during embryonic development. Developmental Biology 287, 390–402. doi:10.1016/j.ydbio.2005.09.011

Thomas, P.S., Kasahara, H., Edmonson, A.M., Izumo, S., Yacoub, M.H., Barton, P.J., Gourdie, R.G., 2001. Elevated expression of Nkx-2.5 in developing myocardial conduction cells. Anat. Rec. 263, 307–313.

Thomsen, G., Woolf, T., Whitman, M., Sokol, S., Vaughan, J., Vale, W., Melton, D.A., 1990. Activins are expressed early in Xenopus embryogenesis and can induce axial mesoderm and anterior structures. Cell 63, 485–493. doi:10.1016/0092-8674(90)90445-K

Tian, J., Yam, C., Balasundaram, G., Wang, H., Gore, A., Sampath, K., 2003. A temperature-sensitive mutation in the nodal-related gene cyclops reveals that the floor plate is induced during gastrulation in zebrafish. Development 130, 3331–3342.

Tojo, M., Hamashima, Y., Hanyu, A., Kajimoto, T., Saitoh, M., Miyazono, K., Node, M., Imamura, T., 2005. The ALK-5 inhibitor A-83-01 inhibits Smad signaling and epithelial-to-mesenchymal transition by transforming growth factor-β. Cancer Science 96, 791–800. doi:10.1111/j.1349-7006.2005.00103.x

Toledo, F., Wahl, G.M., 2006. Regulating the p53 pathway: in vitro hypotheses, in vivo veritas. Nat. Rev. Cancer 6, 909–923. doi:10.1038/nrc2012

Tonissen, K.F., Drysdale, T.A., Lints, T.J., Harvey, R.P., Krieg, P.A., 1994. XNkx-2.5, a Xenopus Gene Related to Nkx-2.5 and tinman: Evidence for a Conserved Role in Cardiac Development. Developmental Biology 162, 325–328. doi:10.1006/dbio.1994.1089

Tsang, M., Dawid, I.B., 2004. Promotion and Attenuation of FGF Signaling Through the Ras-MAPK Pathway. Sci. Signal. 2004, pe17-pe17. doi:10.1126/stke.2282004pe17

Turner, N., Grose, R., 2010. Fibroblast growth factor signalling: from development to cancer. Nature reviews. Cancer 10, 116–29. doi:10.1038/nrc2780

Ueno, S., Weidinger, G., Osugi, T., Kohn, A.D., Golob, J.L., Pabon, L., Reinecke, H., Moon, R.T., Murry, C.E., 2007. Biphasic role for Wnt/beta-catenin signaling in cardiac specification in zebrafish and embryonic stem cells. Proceedings of the National Academy of Sciences of the United States of America 104, 9685–90. doi:10.1073/pnas.0702859104

Uochi, T., Takahashi, S., Ninomiya, H., Fukui, A., Asashima, M., 1997. The Na+, K+-ATPase α subunit requires gastrulation in the Xenopus embryo. Development, Growth & Differentiation 39, 571–580. doi:10.1046/j.1440-169X.1997.t01-4-00004.x

van Boxtel, A.L., Chesebro, J.E., Heliot, C., Ramel, M.-C., Stone, R.K., Hill, C.S., 2015. A Temporal Window for Signal Activation Dictates the Dimensions of a Nodal Signaling Domain. Dev. Cell 35, 175–185. doi:10.1016/j.devcel.2015.09.014

Vidarsson, H., Hyllner, J., Sartipy, P., 2010. Differentiation of human embryonic stem cells to cardiomyocytes for in vitro and in vivo applications. Stem Cell Rev 6, 108–120. doi:10.1007/s12015-010-9113-x

Vilar, J.M.G., Jansen, R., Sander, C., 2006. Signal processing in the TGF-beta superfamily ligand-receptor network. PLoS Comput. Biol. 2, e3. doi:10.1371/journal.pcbi.0020003

Villiard, É., Brinkmann, H., Moiseeva, O., Mallette, F.A., Ferbeyre, G., Roy, S., 2007. Urodele p53 tolerates amino acid changes found in p53 variants linked to human cancer. BMC Evolutionary Biology 7, 180. doi:10.1186/1471-2148-7-180

Vincent, J.P., Gerhart, J.C., 1987. Subcortical rotation in Xenopus eggs: an early step in embryonic axis specification. Dev. Biol. 123, 526–539.

Vizán, P., Miller, D.S.J., Gori, I., Das, D., Schmierer, B., Hill, C.S., 2013. Controlling long-term signaling: receptor dynamics determine attenuation and refractory behavior of the TGF-β pathway. Sci Signal 6, ra106. doi:10.1126/scisignal.2004416

Vliet, P.V., Wu, S.M., Zaffran, S., Pucéat, M., 2012. Early cardiac development: a view from stem cells to embryos. Cardiovascular Research 96, 352–362. doi:10.1093/cvr/cvs270

Vogelstein, B., Lane, D., Levine, A.J., 2000. Surfing the p53 network. Nature 408, 307–310. doi:10.1038/35042675

Vogt, J., Traynor, R., Sapkota, G.P., 2011. The specificities of small molecule inhibitors of the TGFss and BMP pathways. Cellular signalling 23, 1831–42. doi:10.1016/j.cellsig.2011.06.019

Wallingford, J.B., Seufert, D.W., Virta, V.C., Vize, P.D., 1997. P53 activity is essential for normal development in Xenopus. Current Biology 7, 747–757. doi:10.1016/S0960-9822(06)00333-2

Walmsley, M., Cleaver, D., Patient, R., 2008. Fibroblast growth factor controls the timing of Scl, Lmo2, and Runx1 expression during embryonic blood development. Blood 111, 1157–1166. doi:10.1182/blood-2007-03-081323

Walters, M.J., Wayman, G.A., Christian, J.L., 2001. Bone morphogenetic protein function is required for terminal differentiation of the heart but not for early expression of cardiac marker genes. Mechanisms of development 100, 263–73.

Wang, H., Hao, J., Hong, C.C., 2011. Cardiac induction of embryonic stem cells by a small molecule inhibitor of Wnt/β-catenin signaling. ACS Chem. Biol. 6, 192–197. doi:10.1021/cb100323z

Wang, J., Greene, S.B., Martin, J.F., 2011. BMP signaling in congenital heart disease: new developments and future directions. Birth defects research. Part A, Clinical and molecular teratology 91, 441–8. doi:10.1002/bdra.20785

Wang, R.N., Green, J., Wang, Z., Deng, Y., Qiao, M., Peabody, M., Zhang, Q., Ye, J., Yan, Z., Denduluri, S., Idowu, O., Li, M., Shen, C., Hu, A., Haydon, R.C., Kang, R., Mok, J., Lee, M.J., Luu, H.L., Shi, L.L., 2014. Bone Morphogenetic Protein (BMP) signaling in development and human diseases. Genes & Diseases 1, 87–105. doi:10.1016/j.gendis.2014.07.005

Wang, S.E., Narasanna, A., Whitell, C.W., Wu, F.Y., Friedman, D.B., Arteaga, C.L., 2007. Convergence of p53 and transforming growth factor beta (TGFbeta) signaling on activating expression of the tumor suppressor gene maspin in mammary epithelial cells. J. Biol. Chem. 282, 5661–5669. doi:10.1074/jbc.M608499200

Warkman, A.S., Krieg, P.A., 2007. Xenopus as a model system for vertebrate heart development. Seminars in cell & developmental biology 18, 46–53. doi:10.1016/j.semcdb.2006.11.010

Wiedemann, M., Trueb, B., 2000. Characterization of a novel protein (FGFRL1) from human cartilage related to FGF receptors. Genomics 69, 275–9. doi:10.1006/geno.2000.6332

Wolf, M.J., Rockman, H.A., 2008. Drosophila melanogaster as a model system for genetics of postnatal cardiac function. Drug discovery today. Disease models 5, 117–123. doi:10.1016/j.ddmod.2009.02.002

Wolpert, L., Tickle, C., Arias, A.M., 2015. Principles of Development. Oxford University Press.

Wright, J.D., Lim, C., 2007. Mechanism of DNA-binding loss upon single-point mutation in p53. J. Biosci. 32, 827–839.

Wright, J.D., Noskov, S.Y., Lim, C., 2002. Factors governing loss and rescue of DNA binding upon single and double mutations in the p53 core domain. Nucleic Acids Res 30, 1563–1574.

Wu, G., Chen, Y.-G., Ozdamar, B., Gyuricza, C.A., Chong, P.A., Wrana, J.L., Massagué, J., Shi, Y., 2000. Structural Basis of Smad2 Recognition by the Smad Anchor for Receptor Activation. Science 287, 92–97. doi:10.1126/science.287.5450.92

Wu, M.Y., Hill, C.S., 2009. TGF-β Superfamily Signaling in Embryonic Development and Homeostasis. Developmental Cell 16, 329–343. doi:10.1016/j.devcel.2009.02.012

Xin, M., Olson, E.N., Bassel-Duby, R., 2013. Mending broken hearts: cardiac development as a basis for adult heart regeneration and repair. Nat. Rev. Mol. Cell Biol. 14, 529–541. doi:10.1038/nrm3619

Xu, C., Liguori, G., Adamson, E.D., Persico, M.G., 1998. Specific arrest of cardiogenesis in cultured embryonic stem cells lacking Cripto-1. Dev. Biol. 196, 237–247. doi:10.1006/dbio.1998.8862

Xu, C., Liguori, G., Persico, M.G., Adamson, E.D., 1999. Abrogation of the Cripto gene in mouse leads to failure of postgastrulation morphogenesis and lack of differentiation of cardiomyocytes. Development (Cambridge, England) 126, 483–94.

Yamagishi, H., Yamagishi, C., Nakagawa, O., Harvey, R.P., Olson, E.N., Srivastava, D., 2001. The combinatorial activities of Nkx2.5 and dHAND are essential for cardiac ventricle formation. Dev. Biol. 239, 190–203. doi:10.1006/dbio.2001.0417

Yanai, I., Peshkin, L., Jorgensen, P., Kirschner, M.W., 2011. Mapping gene expression in two Xenopus species: evolutionary constraints and developmental flexibility. Dev. Cell 20, 483–496. doi:10.1016/j.devcel.2011.03.015

Yang, X., Dormann, D., Munsterberg, A.E., Weijer, C.J., 2002. Cell movement patterns during gastrulation in the chick are controlled by positive and negative chemotaxis mediated by FGF4 and FGF8. Developmental cell 3, 425–37.

Yatskievych, T.A., Ladd, A.N., Antin, P.B., 1997. Induction of cardiac myogenesis in avian pregastrula epiblast: the role of the hypoblast and activin. Development (Cambridge, England) 124, 2561–70.

Yeo, C., Whitman, M., 2001. Nodal signals to Smads through Cripto-dependent and Cripto-independent mechanisms. Molecular cell 7, 949–57.

Yeo, C.-Y., Chen, X., Whitman, M., 1999. The Role of FAST-1 and Smads in Transcriptional Regulation by Activin during Early Xenopus Embryogenesis. J. Biol. Chem. 274, 26584–26590. doi:10.1074/jbc.274.37.26584

Zacchi, P., Gostissa, M., Uchida, T., Salvagno, C., Avolio, F., Volinia, S., Ronai, Z. 'ev, Blandino, G., Schneider, C., Del Sal, G., 2002. The prolyl isomerase Pin1 reveals a mechanism to control p53 functions after genotoxic insults. Nature 419, 853–857. doi:10.1038/nature01120

Zaffran, S., Frasch, M., 2002. Early signals in cardiac development. Circulation research 91, 457–69.

Zhang, H., Bradley, A., 1996. Mice deficient for BMP2 are nonviable and have defects in amnion/chorion and cardiac development. Development (Cambridge, England) 122, 2977–86.

Zhang, J., Houston, D.W., King, M.L., Payne, C., Wylie, C., Heasman, J., 1998. The role of maternal VegT in establishing the primary germ layers in Xenopus embryos. Cell 94, 515–524.

Zhang, X.-H., Tee, L.Y., Wang, X.-G., Huang, Q.-S., Yang, S.-H., 2015. Off-target Effects in CRISPR/Cas9-mediated Genome Engineering. Mol Ther Nucleic Acids 4, e264. doi:10.1038/mtna.2015.37

Zhang, Y., Chang, C., Gehling, D.J., Hemmati-Brivanlou, A., Derynck, R., 2001. Regulation of Smad degradation and activity by Smurf2, an E3 ubiquitin ligase. Proc. Natl. Acad. Sci. U.S.A. 98, 974–979. doi:10.1073/pnas.98.3.974

Zhao, Y., Zhang, Z.Y., 2001. The mechanism of dephosphorylation of extracellular signal-regulated kinase 2 by mitogen-activated protein kinase phosphatase 3. The Journal of biological chemistry 276, 32382–91. doi:10.1074/jbc.M103369200

Zheng, H., You, H., Zhou, X.Z., Murray, S.A., Uchida, T., Wulf, G., Gu, L., Tang, X., Lu, K.P., Xiao, Z.-X.J., 2002. The prolyl isomerase Pin1 is a regulator of p53 in genotoxic response. Nature 419, 849–853. doi:10.1038/nature01116

Zorn, A.M., Wells, J.M., 2007. Molecular basis of vertebrate endoderm development. Int. Rev. Cytol. 259, 49–111. doi:10.1016/S0074-7696(06)59002-3